

**LOW COST VERTICAL AXIS WIND ENERGY HARVESTING SYSTEM USING
SUPERCAPACITORS FOR RURAL MALAYSIA**

MD SHAHRUKH ADNAN KHAN

Thesis submitted to the University of Nottingham for the degree of Doctor of

Philosophy

Supervisor: Dr. Rajprasad Kumar Rajkumar

May 2016

ABSTRACT

Numerous countries worldwide are conscious about the fact that the past and current trends of energy system are not sustainable and a solution needs to be drawn to protect the world energy from a drastic falling. One of the sources that can replace the current trend is surely wind energy that momentously depends on the availability of the wind resource. For a typical horizontal axis wind turbine to run and generate power, a wind speed of at least 5 m/s is required. Countries like Malaysia have less than 5m/s average wind speed. Another predicament is that these regions face unsteady multi-directional winds making HAWT totally incompatible in such areas. The vertical axis wind turbine on the other hand is appropriate for such regions due to its ability to capture wind energy at any direction. Also, the use of Neodymium magnets for suspension at the bottom surface assist attaining nearly zero friction (Maglev), could be of help improving the output efficiency. Conventional generators now-a-days have been replaced with Permanent Magnet Synchronous Generator (PMSG). Although a number of researches in the area of VAWT and PMSG are carried through separately, few attempts were taken to build a system that work efficiently at low wind speed. Moreover, there is another gap in research for an off-grid standalone energy harvesting device incorporated with low wind Maglev VAWT.

This thesis provides a platform for a novel innovative approach towards an off-grid energy harvesting system (EHS) for Maglev VAWT. This EHS basically a Supercapacitor based hybrid battery charging energy harvesting device. Rural areas in countries like Malaysia where grid connection is not always available, this standalone system there can make a difference for small scale electronic devices. In this thesis, a complete

simulation analysis is done for all 3 types of PMSG connected to VAWT and result was compared. This novel comparison showed that 5-phase is a better performer both in high and low speed comparing with 3-phase and dual stator. Moreover, although at high speed dual stator provides better power efficiency than 3-phase, at low wind, output power performance in 3-phase surpasses that of dual stator. At low wind, even though 5-phase PMSG shows better performance in low wind speed, 3-Phase PMSG was chosen for low maintenance cost, light weight and less complicated design. With the variation of design parameters under low wind speeds, two configurations were optimized for rural Malaysia in terms of low speed, high power and output torque. First configuration was a 1.5KW 220V 20 Pole AFPMSG adopted to a Maglev based VAWT having radius and height of 1m and 2.6m respectively. The other configuration presents a 200W 12V 16 Pole AFPMSG attached to Maglev VAWT of 14.5cm radius and 60cm of height. Later weight to Power Ratio is applied subsequently and the second configuration has been proved to be more cost-effective. The proposed system was also compared with existing models in rural Malaysia for cost-efficiency. A prototype version of the low cost optimized system is built up in lab for open circuit performance and with satisfactory findings, design is sent for fabrication. Upon arrival, the optimized system is implemented into the energy harvesting circuit and field testing is carried to observe the performance. The energy harvesting circuit shows better efficiency in charging battery in all aspects comparing to direct charging of battery regardless of with or without converter. Sufficient groundwork and results have been laid out in this thesis to deliver the necessary development and framework for further improvements. Based on analysis and results carried out in this thesis, all feasibility studies and information are provided for the next barrier.

PUBLICATIONS

Journal

1. 'Feasibility Study of a Novel 6V Supercapacitor based Energy Harvesting Circuit Integrated with Vertical Axis Wind Turbine for Low Wind Areas', International Journal of Renewable Energy Research (Thomson Reuters), Vol. 6, no 3, 2016.
2. 'A LabVIEW based Real Time GUI for Switched Controlled Energy Harvesting Circuit for Wind Power Application', IETE Journal of Research, Taylor & Francis.
Status: Accepted on 19/09/2016.
3. 'A Novel Approach towards Introducing Supercapacitor based Battery Charging Circuit for Off-grid Low Voltage Maglev VAWT', International Journal of Control Theory and Application, Vol. 9(5), pp 369-375, 2016.
4. 'Cost-effective Design Fabrication of a Low Voltage Vertical Axis Wind Turbine', International Journal of Control Theory and Application, Vol. 9(6), pp 2827-2833, 2016.
5. 'Optimization of Multi-Pole Three Phase Permanent Magnet Synchronous Generator for low speed Vertical Axis Wind Turbine', Applied Mechanics and Materials, Vol. 446-447, pp 704-708, 2014.
6. 'A Comparative Analysis of Three- phase, Multi-phase and Dual Stator Axial PMSG for Vertical Axis Wind Turbine', Applied Mechanics and Materials, Vol. 446-447, pp 709-715, 2014.
7. 'Comprehensive Review on the Wind Energy Technology', International Journal of Control Theory and Application, Vol. 9(6), pp 2819-2826, 2016.
8. 'Optimization of Multi-Pole Permanent Magnet Synchronous Generator based 8 Blade Magnetically Levitated Variable Pitch Low Speed Vertical Axis Wind Turbine', Applied Mechanics and Materials, Vol. 492, pp 113-117, 2014.
9. 'Performance analysis of 20 Pole 1.5 KW Three Phase Permanent Magnet Synchronous Generator for low Speed Vertical Axis Wind Turbine', Journal of Energy and Power Engineering, Vol. 5, pp. 423-428, July 2013.

Conference

'Performance analysis of a 20 Pole 1.5KW Three Phase Permanent Magnet Synchronous Generator for low speed Vertical Axis Wind Turbine', 5th Asia-Pacific Power and Energy Engineering Conference, APPEE2013, July 12-14, Beijing, China.

Acknowledgement

I would like to express my gratitude to my supervisor **Dr. Rajprasad Rajkumar**. I am deeply indebted to him for his guidance, supervision and never ending support throughout my entire research period.

I would also like to thank **Dr. Rajparthiban Rajkumar** and **Dr. CV Aravind** for giving me simulating suggestions and technical advice throughout the entire period of time. Special thanks goes to my moderator **Dr. Amin Malek** who assessed my work and gave me constant encouragement.

I have furthermore to thank MOSTI to fund our research project. Moreover, I would like to show gratitude to the UNMC faculty of Engineering for giving me the opportunity to work under UNMC.

Furthermore, I would also like to acknowledge, with much appreciation, the crucial role of my wife, **Ainun Kamal (Civil Engineer; Director, AK Associates)**, for her constant motivation and support.

Most importantly, I would like to mention my mother, **Selima Shahnaz (Geologist; Deputy General Manager, Petrobangla, BAPEX)**, for her infinite ocean of love towards me and my father, **Adil Yar Khan (Civil Engineer; Managing Director, Dakhin Hawa PVT. Ltd.)**, for his never ending constant blessings and prayers. And I have no word to express my gratefulness to the Almighty to finish my thesis.

Dedication

This thesis is dedicated to my eldest daughter **Late Aeesha Safreen Khan**. She passed away in March 4, 2015 at the age of 2 months.

Table of Contents

Abstract	i
Publications	iii
Acknowledgements	iv
Dedication	v
Table of Contents	vi
List of Tables	ix
Acronyms	x
Chapter 1 Introduction	
1.1 Introduction	1
1.2 Problem Statement	6
1.3 Research Objectives	7
1.4 Research Scope	7
1.5 Research Overview	10
1.6 Thesis Contribution	11
1.7 Thesis Organization	12
Chapter 2 Literature Review	
2.1 Wind Turbine Classes with an emphasize on VAWT	14
2.1.1 HAWT	15
2.1.2 VAWT	16
2.1.2.1 Darrieus Turbine	17
2.1.2.2 Savonius Turbine	19
2.1.2.3 Hybrid VAWT	20
2.2 21 st Century and Present Situation	21
2.3 Wind Turbine Performance Parameters	26
2.3.1 Bet's Elementary Theory	26
2.3.2 Tip Speed Ratio	31
2.3.3 Angle of Attack	32
2.3.4 Pitch Angle	33
2.3.5 Blade Design	33
2.3.6 Pitch Control and Yaw Control	33
2.4 Generator details with an Emphasize on PMSG	35
2.4.1 Asynchronous Generator	35
2.4.2 Synchronous Generator	37
2.4.3 PMSG	40
2.5 Wind System: Trends and Concepts	44

2.5.1	Fixed Speed Concept	45
	Variable Scale with Partial Power Converter	45
	Variable Scale with Full Scale Power Converter	46
2.6.	Energy Harvesting System	47
2.6.1	Battery	47
2.6.2	Supercapacitor	48
2.6.3	Hybrid Energy Storage System	51
Chapter 3 Methodology		57
3.1	Design and Simulation of VAWT	59
3.1.1	VAWT Mathematical Model	59
3.1.2	Simulink Model	60
3.1.2	Analysis of Simulink Model	61
3.2	Design and Simulation of AFPMSG	61
3.2.1	Mathematical Model of PMSG	62
3.2.2	Modelling in Simulink	70
3.2.3	Parameter Details	76
3.3	Optimization of PMSG based VAWT	77
3.3.1	Modelling	80
3.3.2	Parameter Designing	83
3.4	Low Cost System Optimization for Rural Malaysia	84
3.5	Laboratory Prototype of VAWT	90
3.5.1	Hardware Architecture	91
3.5.2	Data Collection	94
3.5.3	Experimental setup	97
3.6	Energy Harvesting Circuit	98
3.6.1	System Architecture	99
3.6.2	Hardware Designing	101
3.6.3	Energy Harvesting Control System	112
3.6.4	Software Architecture	115
Chapter 4 Result and Discussion		
4.1	Design and Simulation of VAWT	121
4.1.1	Comparing the Simulation Data with theoretical Value	121
4.1.2	Simulation of VAWT under different parameter	123
4.2	Design and Simulation of AFPMSG	129
4.3	Optimization of PMSG based VAWT for Rural Malaysia	135
4.3.1	Optimization of VAWT for low wind speed	135
4.3.2	Optimization of PMSG for VAWT	142
4.4	Low Cost System Optimization for Rural Malaysia and Design fabrication	143
4.5	Laboratory prototype of Maglev VAWT adopted to PMSG	149
4.6	Energy Harvesting Circuit	153
4.6.1	Part 1: For Wind Speed 5m/s	155
4.6.2	Part 2: Wind Speed 4m/s	163

4.6.3	Part 3: Wind Speed 3m/s	169
4.6.4	Overall Summary and Efficiency Comparison	175
4.6.5	Battery Charging- 5.5V to 6V	176
4.6.6	Theoretical Analysis of Battery Charging via Supercapacitor Cycle	178
Chapter 5 Conclusion		
5.1	Conclusion	180
5.2	Future Work	188
References		191
Appendix		200

List of Table

Table Number		Name of the Table	Page
Table 2.1	:	Design and Performance Parameter Identification of Wind Turbine	35
Table 2.2	:	Comparison of Different Battery Types	48
Table 3.1	:	PMSG Design Parameters	76
Table 3.2	:	Existing Wind Turbine in Malaysia- Case 1 Configuration	78
Table 3.3	:	Existing Wind Turbine in Malaysia- Case 2 Configuration	78
Table 3.4	:	Existing Wind Turbine in Malaysia- Case 3 Configuration	78
Table 3.5	:	Existing Wind Turbine in Malaysia- Case 4 Configuration	79
Table 3.6	:	Existing Wind Turbine in Malaysia- Case 5 Configuration	79
Table 3.7	:	VAWT & PMSG Parameter Configuration for optimization	83
Table 3.8	:	Cost Analysis- Case 1 Configuration and Overall Cost	86
Table 3.9	:	Cost Analysis- Case 2 Configuration and Overall Cost	87
Table 3.10	:	Cost Analysis- Case 3 Configuration and Overall Cost	87
Table 3.11	:	Cost Analysis- Case 4 Configuration and Overall Cost	88
Table 3.12	:	Cost Analysis- Case 5 Configuration and Overall Cost	88
Table 3.13	:	Cost Analysis- Proposed System Configuration and Overall Cost	89
Table 3.14	:	System configuration for Energy Harvesting Circuit	99
Table 4.1	:	Efficiency comparison of PMSG Output Power at Different Wind Speed	131
Table 4.2	:	PMSG Output Power efficiency comparison for minimum and maximum number of pole	133
Table 4.3	:	Optimized VAWT Design Configuration	135
Table 4.4	:	Optimized System Design Configuration 1	146
Table 4.5	:	Optimized System Design Configuration 2	146
Table 4.6	:	Weight to Power Ratio	147
Table 4.7	:	Cost Analysis of Current Existing System in Rural Malaysia in Comparison with Proposed Turbine	148
Table 4.8	:	Energy Harvesting System Open Circuit Performance	153
Table 4.9	:	Charging Battery (from 4.2V to 5V) through Supercap at 5m/s Wind Speed	162
Table 4.10	:	Efficiency Comparison among Case A, Case B and Case C at 5m/s	162
Table 4.11	:	Charging Battery (from 4.2V to 5V) through Supercap at 4m/s Wind Speed	168
Table 4.12	:	Efficiency Comparison among Case A, Case B and Case C at 4m/s	168
Table 4.13	:	Charging Battery (from 4.2V to 5V) through Supercap at 3m/s Wind Speed	174
Table 4.14	:	Efficiency Comparison among 'Case A', 'Case B' and 'Case C' at 3m/s	174
Table 5.1	:	Summary of results	183

Acronyms

VAWT	:	Vertical Axis Wind Turbine
HAWT	:	Horizontal Axis Wind Turbine
PMSG	:	Permanent Magnet Synchronous Generator
AFPMSG	:	Axial Flux Permanent Magnet Synchronous Generator
RFPMG	:	Radial Flux Permanent Magnet Synchronous Generator
TFPMG	:	Transverse Flux Permanent Magnet Synchronous Generator
AOA	:	Angle of Attack
Supercap	:	Supercapacitor
Maglev	:	Magnetic Levitation
PM	:	Permanent Magnet
TSR	:	Tip Speed Ratio
WPR	:	Weight to Power Ratio
WTG	:	Wind Turbine Generator
ESR	:	Equivalent Series Ratio

CHAPTER 1

INTRODUCTION

1.1 Introduction

We are breathing in an era that is currently facing several threats in terms of energy security. It is a known fact that sooner or later our non-renewable energy sources are going to be depleted; which are the earth minerals and fossil fuels (coal, petroleum and natural gas) [1]. We can sense the obvious consequence of this change that drives us towards the renewable energy options. According to the executive summary of Global Status Report of 2015 by Renewable Energy Policy Network, Renewable energy, dominated by wind, solar and hydro power, takes around 58.5% of net additions to global power capacity in 2014, with noteworthy increase in all regions [2]. Figure 1.1 gives an idea about the total wind power capacity from 2004 to 2014. As it can be seen, wind energy produces 370GW out of 657 GW of total renewable power at the end of 2014 which is 56% of the total renewable power excluding hydro energy. Figure 1.1 also illustrates that total wind energy capacity in the world has increased from 318 GW (end of 2013) to 370 GW (end of 2014) which indicates a momentous boost of 16%.

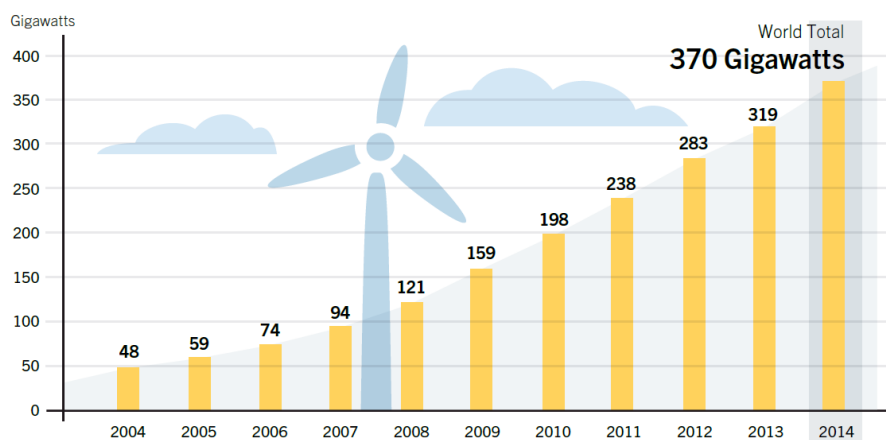


Figure 1.1: Wind Global Power Capacity from 2004 to 2014

Wind energy is emerging in different number of locations, and new markets continued to expand in Africa, Asia, and Latin America [3]. Asia captured the largest market of wind power for the last few years. A noteworthy increase in wind power global capacity can be marked each year and predominantly for the last year, 51GW was added making the total of the wind power to be 370GW.

Since wind global power capacity has been increasing each year significantly, plentiful researches in the field of wind energy harvesting have been conducted frequently. However, many of the current options have their own limitations such as require wider area to install, difficult to implement in rural area, high costing, real time maintenance and so on. Apart from solar power, batteries are often used in replace of energy sources when electric grids are not available. Despite batteries being small and easily used, batteries are impractical due to their short cycle life, low power density and it tends to degrade at low temperature [4, 5].

Therefore, there is a need of an alternative way to harvest energy where it is easily accessible and available most of the time. This brings up the idea and interest of harvest energy through Super Capacitor based hybrid system. Current environment demand to have small, autonomous and energy harvesting in wind power for off grid system.

Areas found around the equatorial regions tend to have low wind speeds. For example, Malaysia currently has an average wind speed of 2-3 m/s, with higher wind velocity in the east coast of west Malaysia [6]. For a typical horizontal axis wind turbine to run and generate power, a wind speed of at least 5 m/s is required [7]. A speed that is less than 5 m/s is not sufficient to turn the turbine. Another predicament is that

these regions face unsteady multi-directional winds making HAWT totally incompatible in such areas. In contrast, vertical axis wind turbine (VAWT) is capable of rotating at low wind speed and capturing wind from various directions, making it more suitable to be implemented in Malaysia. Another major advantage of VAWT is that it can be installed closely together in a position so that each turbine counter rotates with respect to each other. This causes the turbine to rotate in the same direction, resulting in better wind flow hence improving overall turbine performance [8].

Also, the use neodymium magnets for suspension at the bottom surface assist attaining less friction, which helps counter the low wind speed problem [7]. Conventional generators can be replaced with Permanent Magnet Synchronous Generator (PMSG) using multi-pole stator arrangement. The multi-pole stator arrangement can be configured to generate high voltage at low revolution, and high current at faster speeds. The stator is designed to produce negligible cogging torque therefore causing the generator to start up and cut-in at low speeds to produce high current [9]. One significant advantage of PMSG is that it is much lighter, smaller in size, and uses less constructional material so lowering cost and hub size [7-9].

Presently, wind turbines with Permanent Magnet Synchronous Generator (PMSG) are getting popular in the industry for being able to attain maximum power output along with reduction in the overall size of the wind turbine [10-11]. It is also lightweight, robust, does not require external dc excitation and has a high current to torque ratio [12-15]. Besides, PMSG has been drawing attention over the years for its gearless construction hence eliminates the possibility of having moving contacts which leads to higher efficiency reducing operation and maintenance costs [16-17].

Coming back to VAWT which is eligible to handle low wind speed, an innovative method of designing it is to implement magnetic levitation (Maglev) [18-19]. Developing a wind turbine by replacing the conventional mechanical bearing with maglev has become an eye opener for its ability to eliminate mechanical friction between the rotor and stator [18-19]. Marc T. Thompson showed in his work at 2009 that bearing could be replaced with Magnetic Levitation [19]. He also stated in his IEEE paper that using Neodymium magnets, the blades would be attached to the generators in a frictionless motion [20]. Another few advantages of maglev is high efficiency, no noise pollution, low maintenance, small in size and reduced power loss [19-21]. In the year of 2012, Nirav Patel from Lakehead University, Canada and M. Nasir Uddin described in their work that use of axial flux permanent magnet (AFPM) generator with dual rotor incorporated with maglev increases the efficiency of the Savonius VAWT [22]. This design has proven to greatly reduce the friction between rotor and stator, thus cutting down on maintenance cost and improving life span. Another research by Liu S, Bian Z, Li D and Zhao W referred in [19] successfully reduces the damping of VAWT using maglev design resulting in stable rotation with low wind speed. Further study still needs to be done to develop maglev wind turbine for commercial use.

In order for wind turbines to achieve low wind speed with high efficiency, there is still lack of research being done on the effects of combining both maglev VAWT and PMSG systems together for off-grid system. This thesis finds the lacking of research in the wind power energy in low speed that works for energy harvesting for off-grid system. Our study brings the supercapacitor based hybrid energy harvesting for first time into the off-grid low wind power application. As stated before, Malaysia has low wind

speed due to its geographical location. Moreover, implementing wind power and connecting it to grid system is not possible for most of the rural areas in Malaysia. But, the use of electronics and battery charging devices have never been in demand but now. A need of an alternative way to harvest energy, therefore, is required where it is easily accessible and available. Thus, these places require an off-grid energy harvesting turbine being able to work in low wind. Yet again, the batteries cannot be charged directly through the turbine as low wind turbines would not be able to generate sufficient amount of voltage to charge up a battery. In addition, a constant voltage source is required for battery charging which is not possible for varying wind speed. This brings up the idea and interest of harvest energy through Super Capacitor based hybrid system for low voltage output turbines. Having compared Supercapacitors with conventional capacitors, Supercapacitors have huge value of capacitance and thus having higher energy density.

An in depth investigation of the problem, proposed solution and implementation were carried through on a step by step analysis. A thorough study on Vertical Axis Wind Turbine connected to a Maglev Permanent Magnet Synchronous Generator in low wind speed for energy harvesting has been conducted in the thesis. A novel Maglev Vertical Axis Wind Turbine adopted in Permanent Magnet Synchronous generator was put through in experiment. Simulation was performed followed by lab prototype investigation. Next part was the fabrication which was then put in the field for testing for different wind parameters. Finally, energy harvesting circuit was brought into the experiment and efficiency was tested.

1.2 Problem Statement

Malaysia has low wind speeds due to its geographical location, and its dense urban areas. Malaysia averages wind speeds of 2-3m/s, which is not favourable to wind power technology. Horizontal axis has dominated large scale wind turbines throughout the world predominantly but it operates at 5m/s and above, which does not work for Malaysian wind conditions. As conventional energy sources are depleting, it is vital to source for alternative power generating method. Factoring in the rapid development of electronic devices with increasing complexity, the desire for power has never been higher as consumers spend more time on their devices but are often constrained by limited battery charge. Moreover, no off-grid wind energy harvesting device has yet been implemented for low wind speed. There are many rural areas in countries like Malaysia where electricity cannot reach to mass people in each and every aspect of life. Implementing wind power and connecting it to grid system are not possible for most of the places. Therefore, places like those require an off-grid energy harvesting turbine system under ambient conditions that work well in low wind speed. There has been a lack of research in the field of wind turbine when it comes to low wind off-grid standalone system. In addition, energy harvesting through off-grid low wind turbine system has yet been practically implemented. There has been a significant gap in ‘energy harvesting’, ‘off-grid VAWT system’ and ‘low wind speed’ in terms of research being made for bringing them together. Countries like Malaysia demand to have standalone system charge up their devices or use small scale electronic device in a greener way while industrial sectors can diversify their energy options and be less dependent on a single energy source for their equipment.

1.3 Research Objective

- 1.** Simulation and performance analysis of Vertical Axis Wind Turbine in low wind speed, to investigate the effect of different design parameters on turbine mechanical torque and power.
- 2.** Simulation and performance analysis of different types of Axial Flux Permanent Magnet Synchronous Generator for low wind Vertical Axis Turbine.
- 3.** To design a cost-effective, optimized Maglev based VAWT system adopted to a 3-Phase Axial Flux PMSG for Rural Malaysia.
- 4.** Evaluation of the developed system and comparison of it with current existing models in rural Malaysia in terms of cost analysis.
- 5.** To come up with an efficient, off-grid energy harvesting hybrid system by using battery and Supercapacitor bank for a low voltage Maglev based VAWT that can perform well in low wind speed.

1.4 Research Scope

Recent revolutionary advances in technology are creating better future for countries with low wind speeds like Malaysia and also changing the face in wind technology. The most significant technological advancement is the use of magnetic levitation (Maglev) in Vertical Axis Wind Turbine (VAWT) wind turbine. Using very powerful neodymium magnets, the VAWT can be levitated without the use of bearing, reducing frictional losses and lower start up speed. This type of turbine is expected to produce power at speed as low as 2-3m/s. Also, powerful Permanent Magnet (PM) generators can be used that can produce high power output, and no attractive force in the machines

makes it turn at low wind speeds. Together with PM generators and direct drive coupling, there is no need for bearing and gears hence possibly it will be reducing power loss in the system making it turn at low wind speed. The blade can be designed to maximise the wind capture ability. With this VAWT, more power can be produced at lower cost than horizontal wind turbines, and more importantly it requires less space when compared to its equivalency in solar power. Incorporating this technology, VAWT can be installed in building rooftops and tower and can be ideal for low wind speed urban countries like Malaysia so reducing the burden on fossil fuels. Last but not the least, implementing a hybrid energy harvesting system into VAWT, rather a load powered by battery, will surely bring a change in off-grid low speed wind power sector.

The motivation for this thesis is to incorporate a novel design of a small vertical axis wind turbine (VAWT) to provide power source to charge batteries for energy storage. This design of VAWT uses magnetic levitation concept, making it gearless and lightweight which result in significant reduction in friction and start-up wind speed. The charges generated are desired to be stored in a lead acid battery. The charges generated from the turbine are not constant because it depends highly on the wind speed. Therefore, Supercapacitor bank followed by a boost converter can be used to provide a constant current supply to charge the battery through discharging the Supercapacitor; thereby, able to lengthen the life cycle of the battery. Since Supercapacitors are able to hold charges for a long time, hence it will not deplete its charges comparing to normal capacitors. A comparison could be shown between

direct charging and through Supercapacitor Bank in terms of efficiency and the result should be discussed further.

A control system using Arduino would be implemented to control the charging and discharging circuit so that the system is able to perform efficiently. On top of that, DAQ could be used that would interface with laptop through LabVIEW based GUI for data acquisition. This system would be built in such a way so that it could be used in almost any place having a wind speed as low as 3-4 m/s. For instance, it can be installed on the rooftop houses to produce own energy to power up small electronic devices. This greatly will help to reduce the utility cost. In addition to that, this concept is able to provide a better quality of life for people in rural areas where electricity generation is still a big concern. East Malaysia, having a higher average wind speed, particularly is more suitable to have a wind farm. Hence, it has better chance to produce even more electricity. Implementing an off-grid energy harvesting system for low wind speed countries like Malaysia would certainly open the door of ample opportunities. Wind energy is no doubt a reliable alternative source of energy in Malaysia and it can help to conserve the environment for future generations.

The entire research has mildly been affected by few factors. There were few limitations of the developed system. Due to budget and time constrain, Finite Element Analysis of turbine blades and Computational Fluid Dynamics for magnet positioning could not be implemented. In addition, vibration test using CFD was also not implemented due to the same reason. Therefore, the simulation scale was limited to Simulink only.

1.5 Research Overview

Diagram 1.2 shows the overall system flowchart summarising most of the concepts discussed in the previous sections.

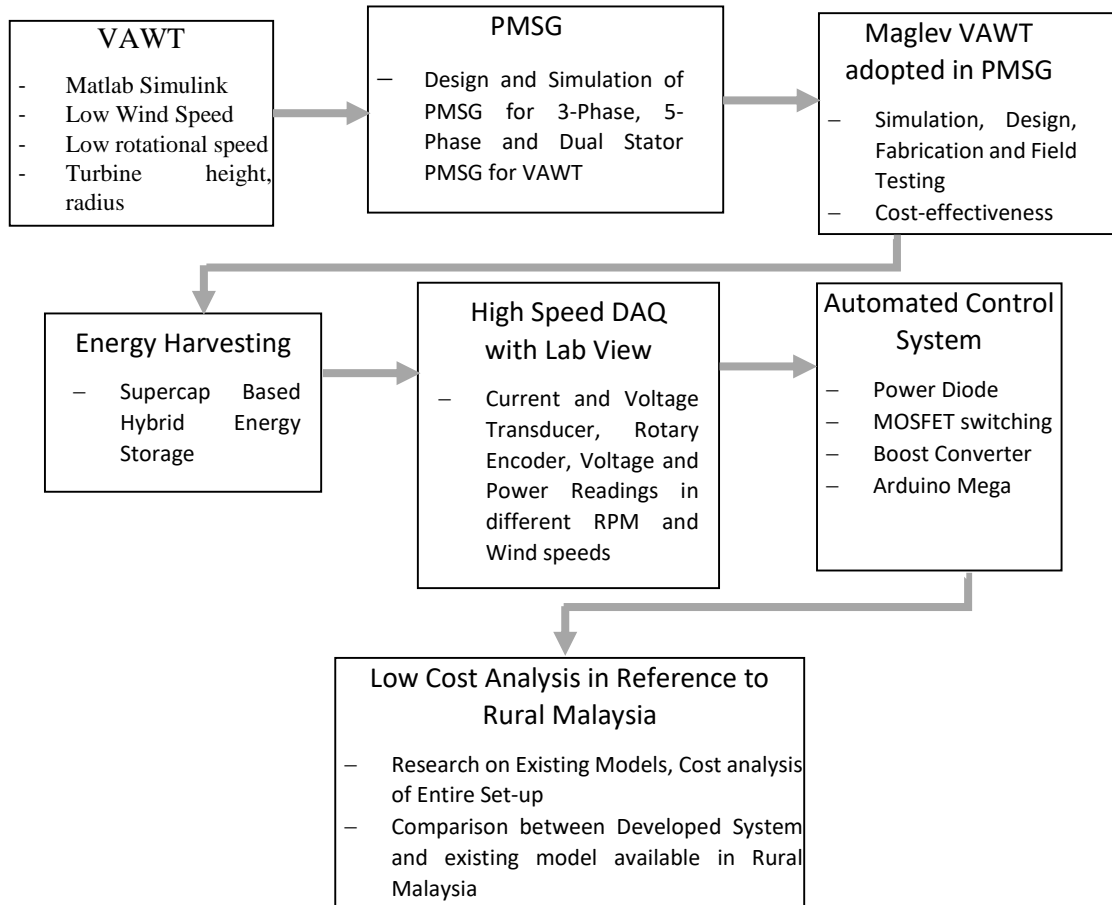


Figure 1.2: Block Diagram of overall system

In this research, a complete simulation analysis is done for VAWT under different parameter configurations. Subsequently, modelling was done for 3 types of Axial Flux PMSG. After comparing the simulation result, 3 phase PMSG was chosen for the system. Next, VAWT was connected with 3-Phase PMSG and the entire system was modelled in Simulink. With the variation of design parameters under low wind speeds, two configurations were optimized in terms of low speed, high power and output torque. A prototype version of the low cost optimized system was built up in lab for

open circuit performance and with satisfactory findings, design is sent for fabrication. Upon arrival, the optimized system is implemented into the energy harvesting circuit and field testing is carried to observe the performance. Lastly, the developed system was compared with the existing models in respect to rural Malaysia and the novel outcomes of our stand alone system was discussed.

1.6 Thesis Contribution

Previous work in the field of ‘PMSG adopted Maglev VAWT’ and ‘energy harvesting’ was mostly carried out on separate field. Only a few studies concentrated to make an attempt to build a system together that work more efficiently at low wind speed. This thesis fills up the gap in research for an off-grid standalone energy harvesting device incorporated with 3-Phase PMSG adopted to Maglev VAWT that can perform in low speed. Simulation was carried out for VAWT at first, followed by the adaptation of 3-Phase PMSG into the system. This includes a dq axis reference frame modelling by Park Transformation for 3-phase, 5-phase and Dual Stator PMSG in VAWT platform. Comparison of 3 types Axial Flux PMSG in VAWT platform has not been previously performed. The optimization section takes 2 configurations in which ‘Weight to Power Ratio’ is applied to find out the relative cost-efficient configuration. Again, not many cases have applied this technique in wind power energy.

A full phase complete system analysis was made, starting from optimization of the design, cost-efficiency calculation, followed by a laboratory prototype design before sending the simulation design for fabrication. Very few cases in wind history dealt with

such full scale experiment for off-grid VAWT system. If energy harvesting is brought into the system, no case will be found to have such set-up for low wind speed. Hence, not only this thesis proposes a novel idea of bringing the three different fields together namely “Low speed Maglev VAWT”, “3types of Axial Flux PMSG” and “Low Voltage Supercab based energy harvesting device” but also it gives an optimized performance for better charging efficiency. A novel optimized Maglev based VAWT for rural Malaysia has been proposed in this research together with an innovative Supercapacitor based battery charging circuit. This novel standalone system has specially been designed to work under low wind speed and this idea has not yet been implemented. It has a promising aspect in low wind countries like Malaysia. Last but not the least, this sets the stage for future improvements to the developed techniques and also serves as catalyst for future research in the area of wind power and energy harvesting technology.

1.7 Thesis Organization

Chapter 2: *Literature Review* – This chapter reviews some of the related work in the area of wind energy, power generation and energy harvesting together with few definitions of the related terms and functions of the equipment used in this thesis.

Chapter 3: *Methodology* – This chapter is divided by 6 parts. 1st two parts present the simulation analysis, followed by the optimization of the system. 4th part deals with cost-efficiency whereas the next part presents prototype version of optimized system. Lastly, in part 6, the turbine is implemented into energy harvesting circuit.

Chapter 4: *Results and Discussion* – The results of the hardware implementation are stated as well as simulations of various experimental setups. Discussions on each set

of results are also provided here. Comparison between different setups have also been given. This part also consists of 6 parts synchronized with the methodology chapter.

Chapter 5: *Conclusion and future work* – Conclusion is presented here in which major accomplishments and achievements of research objectives are summarised. The possibilities for future work and improvements to be carried out will also be discussed.

Chapter 2

Literature Review

This chapter reviews some of the most important literature that has been done on particular areas covered in this thesis. The emphasis is placed on reviewing literature in wind power history, types of wind turbine, generator and it's classes associated with various wind turbines, energy harvesting circuits and power electronics with their definitions and functions those are made use in this thesis. Furthermore, turbine classification, history behind it, types of generator used in wind technology are also brought to attention focusing on the trend.

The main idea of this section is to get the overview of the gradual development towards wind power technology that has happened in a step by step process. At the same times, all the research that have been carried through in recent years along with the novel published ideas as journals, articles have been reviewed in brief in a sequential manner. This chapter tries to give a clear idea on the preliminary stage of wind energy followed by its gradual progress and perfection together with the latest innovation and research work carried by the scientists and engineers.

2.1. Wind Turbine Classes with an Emphasize on VAWT

Wind turbines mainly are of two types which are horizontal axis wind turbine (HAWT) and vertical axis wind turbine (VAWT) (Figure 2.1). For low wind speed area and places where wind direction change frequently, VAWT is favoured. This section describes the

turbine types and classes, advantages and disadvantages of each class and focus of the thesis in accordance with its objectives.

Is it important to note that since no FEA (Finite Element analysis) of the blade, CFD (computational fluid dynamics) and no other aero-dynamical analysis have been done in this thesis, therefore, the aerodynamics of the lift based Vertical Axis Wind Turbine together with the other types of VAWT are not explained in details in this thesis for the simplicity.

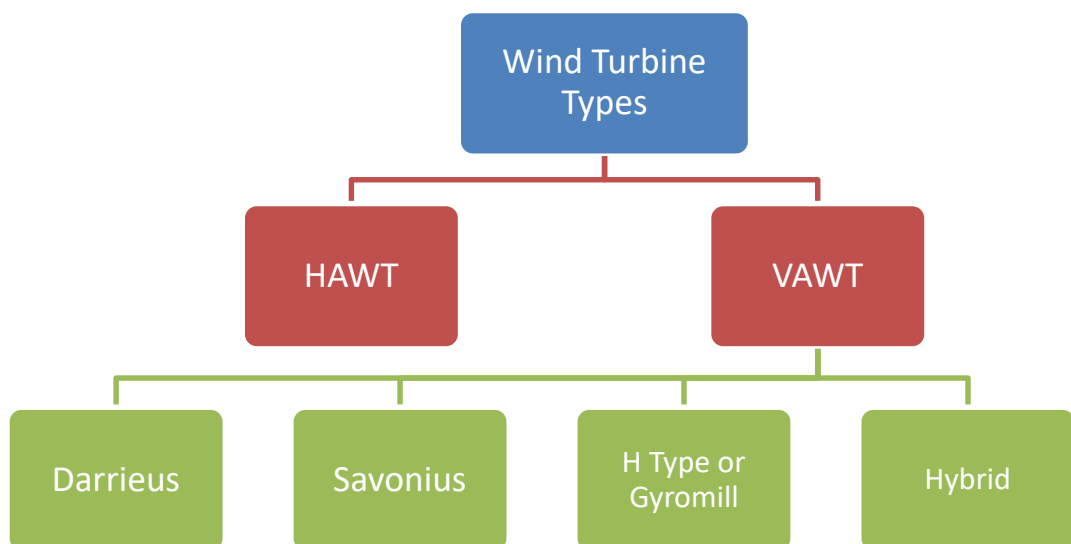


Figure 2.1: Block Diagram- Wind Turbine Classes

2.1.1. HAWT

The Horizontal axis wind turbine has its rotor's axis of rotation parallel to the ground (Figure 2.2). They are generally used as commercial grid-connected wind turbines. They are mostly made of three or two blades that designed to catch energy from the wind. The blade aerofoil is designed in a way such that a higher pressure point is generated at the lower side of the blade as the wind passes over it. The difference in pressure between the upper and lower sides of the blade results in an aerodynamic lift. And because the blades are restricted to a centre point, the aerodynamic lift

results in a rotary movement about the horizontal axis [23-25]. The main advantages are high generating capacity, better efficiency, versatile control system such as yaw mechanism and variable pitch blade capacity. There are also disadvantages such as requiring tall tower to capture large amount of wind energy, consistent noise, killing of birds and so on. It also needs higher maintenance due to its interference with radio, TV transmission and radar [52]. Also for low and multi directional wind, HAWT is not capable of producing power for low and multi directional wind areas [23-25].

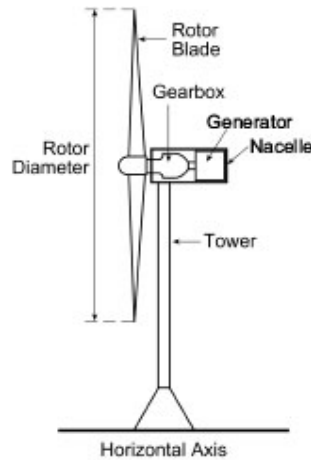


Figure 2.2: HAWT [25]

2.1.2. VAWT

The vertical axis wind turbine (VAWT) rotates around vertical axis perpendicular to the ground. Figure 2.3 is a typical VAWT that shows its components. It can be with (Variable gear) or without gearbox (fixed gear). The control system and the generator generally installed at the base of the turbine. In turbulent conditions with gusty winds (rapid changes in wind direction) in urban environments, VAWT will generate more electricity despite its lower efficiency. Also, the VAWT is designed to operate near the

ground where wind power is lower and produce drag on the blades as they rotate. In short, the VAWT is good for a low-wind turbulent environment [31].

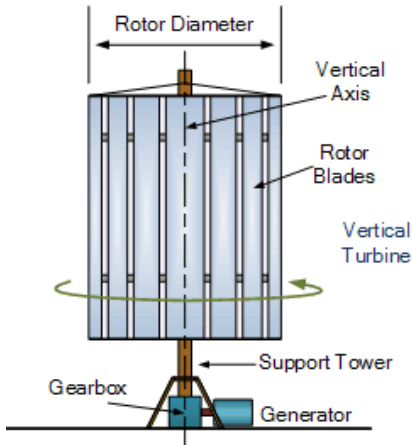
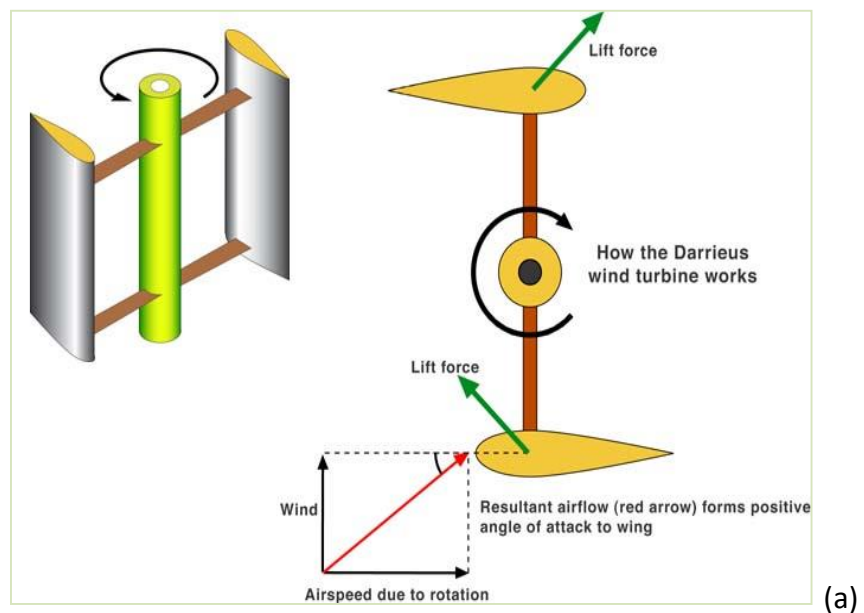


Figure 2.3: Configuration of a typical VAWT

2.1.2.1. Darrieus Turbine

The Darrieus wind turbines as shown in Figure 2.4 are lift-type which was invented by a French engineer, Georges Darrieus. Curve-bladed Darrieus turbines are better in performance because of their lower bending stress compared to a straight bladed Darrieus turbine. However, straight blades are preferable due to its simplicity in design [26-27].



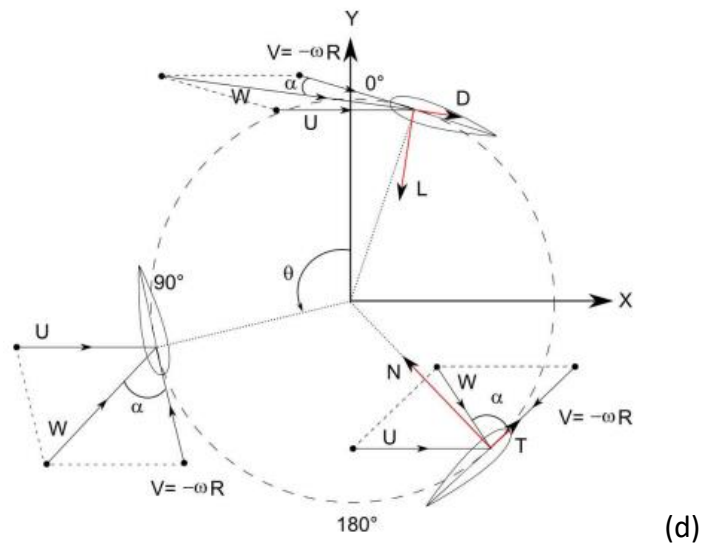
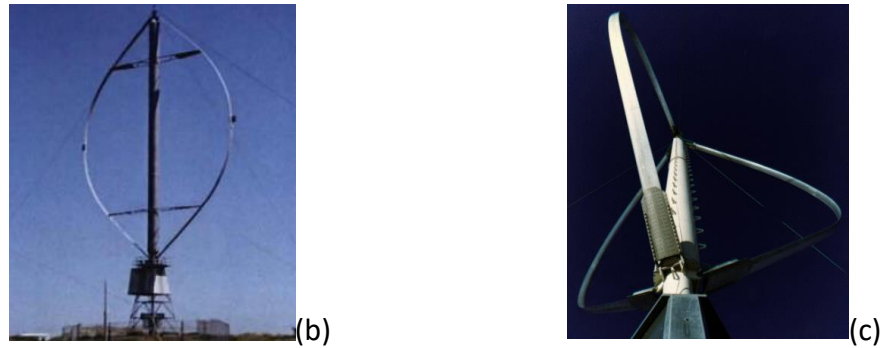


Figure 2.4: Darrieus Turbine-a: Lift Based Turbine; b: 2-bladed Darrieus; c: 3-bladed Darrieus; d: forces that act on turbine [26-30]

The original version of the Darrieus design indicates symmetrical arrangement of aerofoils that has zero rigging angle. Rigging angle is the set-up angle of the aerofoil relative to the structure on which they are mounted. In VAWT, arrangement is equally effective regardless of multi wind direction [29]. When the Darrieus rotor is spinning, the aerofoils are moving forward through the air in a circular path. This creates an airflow relative to the blade. This airflow is added- to the wind vector wise resulting a varying small positive angle of attack to the blade. As the aerofoils are arranged symmetrically and the rigging angle is zero, despite of the change in angle of attack due to the movement of aerofoil, generated force is still obliquely in the direction of

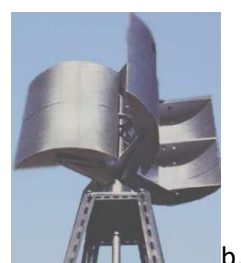
rotation. The energy arising from the torque and speed of the turbine are generally extracted from an electrical generator which can be of few kinds. The Darrieus design uses much more expensive material in blades and it is not self-starting. [26-29]

2.1.2.2. Savonius Turbine

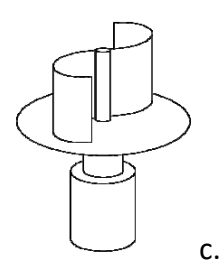
The Savonius wind turbine was invented by a Finnish engineer, Sigurd Savonius (Figure 2.5). This drag-type turbine is said to have the simplest design among all VAWT where the blade looks like an "S" shape or a scoop. The wind that blows at the outer scoop of the blade causes the drag from the inner scoop to increase which eventually produces more torque and lower cut-in speed. It helps the turbine to start rotating with low wind speed. Thus, the Savonius turbine, even though having a lower efficiency compared to Darrieus, is preferred compared to Darrieus due to its ability to self-start, its high starting torque, low operating speed and low maintenance [22] [26]. Savonius vertical-axis machines are good at pumping water and similar kind of work but are not generally used for grid connection. It can also be used for other high torque, low rpm applications [30] [32].



a.

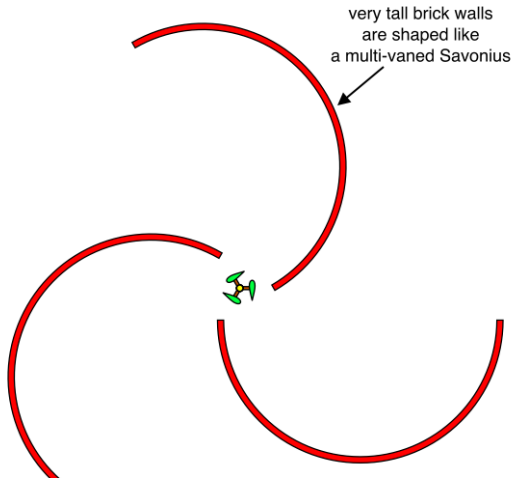


b.

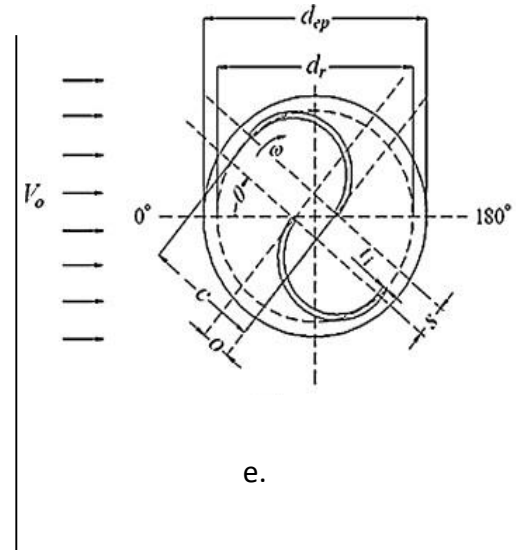


c.

the actual turbine is in the center, and it is any kind of VAWT (including a Savonius)

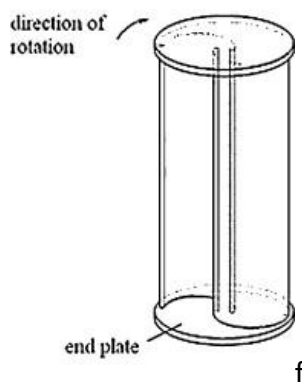


Stationary Savonius Turbine

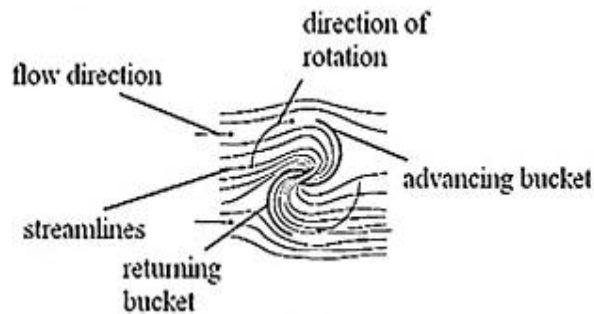


e.

d.



f.



g.

Figure 2.5: Savonius Turbine (a, b), structure (c, f), aerodynamics (d, e, g) [22] [26][30][32]

2.1.2.3.H Type and Hybrid

The H-Darrieus turbine is also addressed as Giromill. It is an enhanced design of the Darrieus rotor that offers higher efficiency. The Giromill is designed to be self-controlling in all wind speeds [28] [31]. Another advantage is that it can reach its optimal rotational speed, shortly after the cut-in-wind speed [33-34]. Figure 2.6 is the

example of H-Darrieus rotor turbine. The Giromill could have been ideal in large-scale electricity production but due to its earlier design failures and lower blade efficiency, not enough researches have been made to develop the turbine further.



Figure 2.6: H Type VAWT



Figure 2.7: Hybrid VAWT

Hybrid VAWTs are the subtypes of VAWT which have been designed over the years. In order to diminish the limitations of each type of VAWT, new turbines have been implemented on the basis of the previous designs. Figure 2.7 is the example of Hybrid VAWT. As it can be seen, the design has adopted both the Darrieus and Savonius's concept. In the current market, this hybrid combination of Darrieus and Savonius have gathered much popularity. They have features including self-starting, low wind level and multi-directional [27].

2.2. 21st Century and Present Situation

Although there are a lot of activities going on towards the offshore wind energy, the development process was still very slow. But from the beginning of 21st century, the offshore deep blue wind technology has gained new inspiration. From the starting of 21st century, within 6 years of time, 21 offshore plants had been built in different countries namely Denmark, Sweden, Ireland, Germany and Netherlands [35]. By the end of 2006, installed capacity of offshore project in the entire world reached 798.2

MW [33]. Around time there were couple of famous projects which have to be mentioned- East China Bridge in Shanghai generating electricity of around 100MW, Shanghai Fengxian Nanhui Offshore Wind Power and Cixi Wind Power at sea in Zhejiang. European countries, America and other countries such as China also have been progressing firmly. China had constructed 59 wind farms by 2005 including 1883 turbine generator. They produced 1266 MW of Power in 2005 making sure to be one of the top 10 global wind energy producers [36].

In the year of 2009, I. Paraschivoiu, O. Trifu and F. Saeed had done some more works on H- Darrieus Wind Turbine. Later their work was published in the ‘International Journal of Rotating Machinery’ in the year of 2009. They proposed a method of calculating the optimal variation of the pitch angle of the blade of the turbine which would increase the torque speed at its maximum level at some rated conditions. The prototype was built having a rated power of 7KW. A specific code (CAARDAAV) was used with an optimizer which was based on genetic algorithm in order to get the optimal variation of the pitch angle of the straight bladed turbine. A range of pitch variation was optimized in a low wind case and an overall gain of around 30% was achieved in the annual production of energy [37].

In 2010, Ming-Hung Hsu came up with a solution for the dynamic problems related to the blades of the wind turbines. His solution dealt with radial basis function. The concept was that the dynamic problems could be represented by partial differential equations which he transformed into discrete eigenvalue matrix in his work. After running the simulation, the result achieved from the transferred matrix was that the

blade shaft speed controlled the 1st frequency of the wind turbine whereas this rotational speed could not able to vary the 2nd, 3rd or 4th frequency of the blade [38].

S.Eriksson, H. Bernhoff and M. Leijon from Sweden published their work in “Advance in Power Electronics” in August, 2011 on a unique Direct Drive Permanent Magnet Generator adapted to a Vertical Axis Wind Turbine. The design had been successfully constructed and results from the simulation were analysed. The generator had a very low reactance thereby causing a low voltage drop in generator side. Moreover, the pitch control was successfully replaced by the electrical control. The generator performed successfully with a high efficiency for the whole operation period and it showed a high torque capability. The system was later installed in Sweden having a rated power of 200KW [39].

The Northern side of the world has good wind energy but still development of wind power has not yet been observed that much due to couple of major problems until 2011. Among them, icing on the turbine blade is the main obstacle. In average 20% power loss occurred annually due to this problem. To overcome it, not much of steps were taken. In 2011, Muhammad S. Virk, Matthew C. Homola, Per J. Nicklasson from Narvik University College carried out a numerical study on a horizontal axis wind turbine (5MW) about the atmospheric ice accretion. The result was achieved using Computational Fluid Dynamics. For both of the conditions of rime and glaze ice, five different sections in the blades were taken into consideration for numerical analysis. Moreover, several atmospheric temperatures were used to simulate the rate and shape of accreted ice. The result indicated that both the blade size and relative section velocity of the blade affected ice growth. Near the root section, the icing was less. In

the blade section, from centre to top, significant change in icing was noticed with the variation in atmospheric temperature. Furthermore, the result also proved that the icing could be managed by optimizing the geometric design parameters [40].

In the same year in China, Li Yan, Chi Yuan, Han Yongjun, Li Shengmao and Tagawa Kotaro from Northeast Agricultural University carried out research on Vertical Axis Wind Turbine blade airfoil. Using Computational Fluid Dynamics Technique, the simulation result of static aerodynamic performance of icing blade was analysed. The research indicated the icing on blade forced drag to be enlarged causing poor blade performance. The ice accretion was proportional to the variation of water flow flux and wind speed [41].

In recent years, Micro-Wind Energy has made a lot of impact due to its low speed operation along with low power applications resulting cost reduction and simplicity. For example, Massimiliano, Marcello and Gianpaolo from Italy designed a simple, effective and low cost Micro-Wind Energy Conversion System in 2011 that gathered several attentions. It used a Permanent Magnet Synchronous Generator, boost converted, and Voltage Oriented Controller were used. The system performed a reliable operation at the maximum power. It also showed a promising quick response with variable wind speeds. It had low losses and almost zero reactive power exchanged with the power grid. In comparison with a conventional wind turbine of same maximum power range and with the same average wind speed, it could generate twice the energy produced by the generator [42]. In Canada, Md. Arifujjaman from the University of New Brunswick also did some research on modelling and simulation of grid connected permanent magnet generator based on small wind energy

conversion system. He presented a mathematical modelling and control strategy for the system similar to the previous one. A unique controller was design that used to vary the duty cycle that changed boost controller output voltage and current giving the maximum power to the grid. The control system also decreased the system parameter dependence and made the system less complicated [43]. In the same year he together with M.T. Iqbal and J.E. Quacoe wrote an article on development of an isolated small wind turbine emulator. It was based on a separately excited DC motor. It was implemented to justify the performance of control method. By performing the turbine at optimal tip-speed ratio, highest power draw was made certain. This emulator system can be helpful for additional study and research on a micro wind turbine system providing at the same time a test bed to look into different new control strategy [44].

Meanwhile, in November 2, 2010, Ciprian Nemes and Florin Munteanu from Technical University of Iasi, Romania published an article on development of reliability model for wind farm power generation. The main aim of the paper was to measure the power distribution of the farm. The system was implemented in North-East of Romania. The article showed an analytical approach to estimate the power generation of a wind farm with varying wind speed. With Monte Carlo simulations, the results were made sure to be validated and the probabilistic functions of simultaneously running of wind turbine were calculated [45].

2.3 Wind Turbine Performance Parameters

A major role to influence the performance of a turbine in terms of generating torque, power and energy is affected and played by a few special terms, definitions and sectors. In this section, these performance parameters will be discussed.

2.3.1. Betz's Elementary Theory [33] [37] [46]

Since wind turbines cannot convert all the energy into work, there should be a loss. The efficiency is not very satisfactory unlike the other turbines. The information about the maximum energy that we can get from the turbine is got from Betz's elementary theory which came up with a power co-efficient concept.

The expression of kinetic energy of an air where mass, m , moving with a velocity, v , is:

$$E = \frac{1}{2} m v^2 (Nm) \quad (1)$$

Considering a certain cross-sectional area, A , from figure 2.8, if the air passes through volume V with a velocity v , the so-called volume flow, \tilde{V} , is:

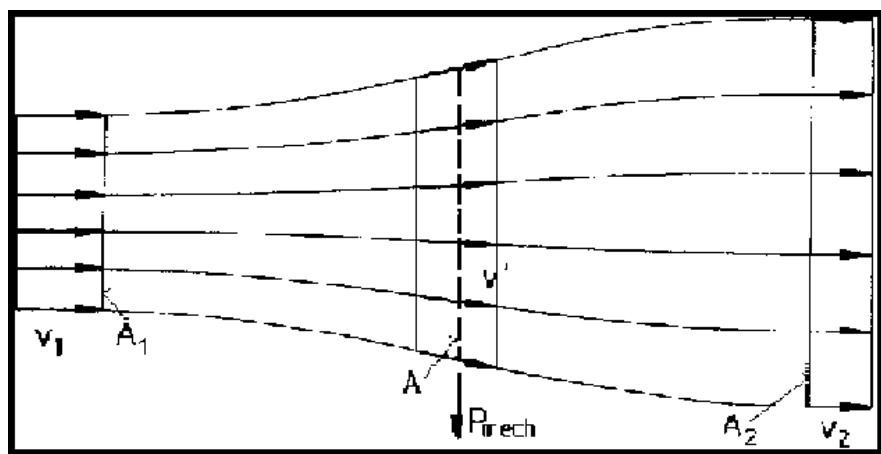


Figure 2.8: Flow conditions due to the extraction of mechanical energy from a free-stream air flow, according to the elementary momentum theory

$$\tilde{V} = v \cdot A \text{ (m}^3/\text{s)}(2)$$

The mass flow with the air density ρ is:

$$\dot{m} = \rho v A \left(\frac{kg}{s}\right) (3)$$

For the moving air for that cross sectional area, the kinetic power (P) would be:

$$P = \frac{1}{2} \dot{m} v^3$$

$$\text{or, } P = \frac{1}{2} \rho v^3 A (w)(4)$$

Kinetic energy contained in the wind stream must be extracted to convert to mechanical energy. To be precise, the flow velocity behind the wind energy converter must decrease with an unchanged mass flow. Nevertheless, reduced velocity means the same mass flow must pass through a widening of the cross-section at the same time. Hence, it is essential to consider the conditions in front of and behind the converter.

From the figure 2.8, v_1 is the un-delayed free-stream wind velocity with cross sectional area of A_1 before it reaches the converter, whereas v_2 is the flow velocity behind the converter with cross sectional area of A_2 .

Hence the mechanical energy the air stream before and after the converter:

$$P = \frac{1}{2} \rho A_1 v_1^3 - \frac{1}{2} \rho A_2 v_2^3 = \frac{1}{2} \rho (A_1 v_1^3 - A_2 v_2^3) \text{ (W)}(5)$$

Maintaining the mass flow (continuity equation) requires that:

$$\rho A_1 v_1 = \rho A_2 v_2 \quad (\text{Kg/s}) (6)$$

Thus,

$$P = \frac{1}{2} \rho A_1 v_1 (v_1^2 - v_2^2) \quad (W)(7)$$

Or

$$P = \frac{1}{2} \dot{m} ((v_1^2 - v_2^2)) \quad (W)(8)$$

From this equation it follows that, power would have to be at its maximum when v_2 is zero, namely when the air is brought to a complete standstill by the converter. However, this result does not make sense physically. If the outflow velocity v_2 behind the converter is zero, then the inflow velocity before the converter must also become zero, implying that there would be no more flow through the converter at all. As could be expected, a physically meaningful result consists in a certain numerical ratio of v_2/v_1 where the extractable power reaches its maximum. This requires another equation expressing the mechanical power of the converter. The mechanical power of the converter needs to be expressed by a different equation. The force which the air exerts on the converter can be expressed using the law of conservation of momentum:

$$F = \dot{m} (v_1 - v_2) \quad (N)(9)$$

The amount of force exerted by the converter on the air flow must be neutralised by an equal amount of thrust produced in accordance with the principle- 'action equals reaction'. The air mass at air velocity v' present in the plane of flow of the converter is being pushed by the thrust. Below presented is the power required for this:

$$P = F v' = \dot{m} (v_1 - v_2) v' \quad (W)(10)$$

Hence, the mechanical power extracted from the air flow can be derived from the energy difference before and after the converter, as well as, from the thrust and the flow velocity. Equating both the expressions gives:

$$\frac{1}{2} \dot{m}((v^2_1 - v^2_2) = \dot{m}(v_1 - v_2)v' \quad (11)$$

$$\text{Where, } V' = \frac{1}{2}(v_1 - v_2) \quad (\text{m/s}) \quad (12)$$

Thus, the arithmetic mean of v_1 and v_2 is equal to the flow velocity through the converter as shown:

$$V' = \frac{v_1 + v_2}{2} \quad (\text{m/s}) \quad (13)$$

The mass flow thus becomes:

$$\dot{m} = gA v' = \frac{1}{2} gA(v_1 + v_2) \quad (\text{kg/s}) \quad (14)$$

The mechanical power output of the converter can be expressed as:

$$P = \frac{1}{4} gA(v^2_1 - v^2_2)(v_1 + v_2) \quad (15)$$

In order to provide a reference for this power output, it is compared with the power of the free-air stream which flows through the same cross-sectional area A , without mechanical power being extracted from it. This power was:

$$P_o = \frac{1}{2} g v_1^3 A \quad (W) \quad (16)$$

The ratio between the mechanical power extracted by the converter and that of the undisturbed air stream is called the “power coefficient” C_p :

$$C_p = \frac{P}{P_o} = \frac{\frac{1}{4} gA(v^2_1 - v^2_2)(v_1 + v_2)}{\frac{1}{2} g v_1^3 A} \quad (17)$$

Re arranging:

$$C_p = \frac{P}{P_o} = \frac{1}{2} \left| 1 - \left(\frac{v_2}{v_1} \right)^2 \right| \left| 1 + \frac{v_2}{v_1} \right| \quad (18)$$

The power coefficient, therefore, depends only on the ratio of air velocities as it is the ratio of the mechanical power extracted to the power confined in the air stream.

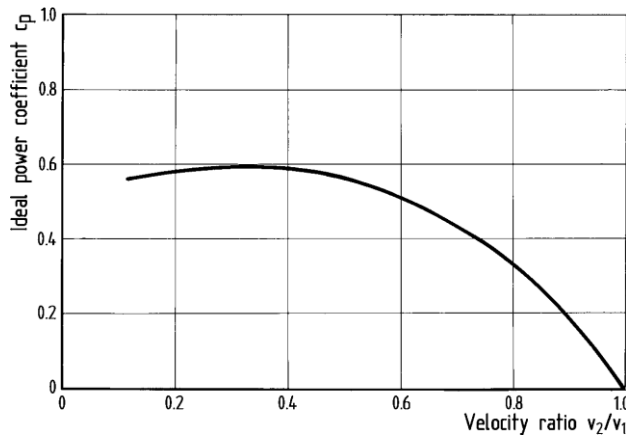


Figure 2.9 (a): Power coefficient versus the flow velocity ratio of the flow before and after the energy converter

With $v_2/v_1=1/3$ the maximum ideal power coefficient becomes: $c_p = 0.593$. This is also known as 'Betz factor'. Hence the flow velocity,

$$v' = \frac{2}{3} v_1 \quad (19)$$

And the required reduced velocity,

$$v_2 = \frac{1}{3} v_1 \quad (20)$$

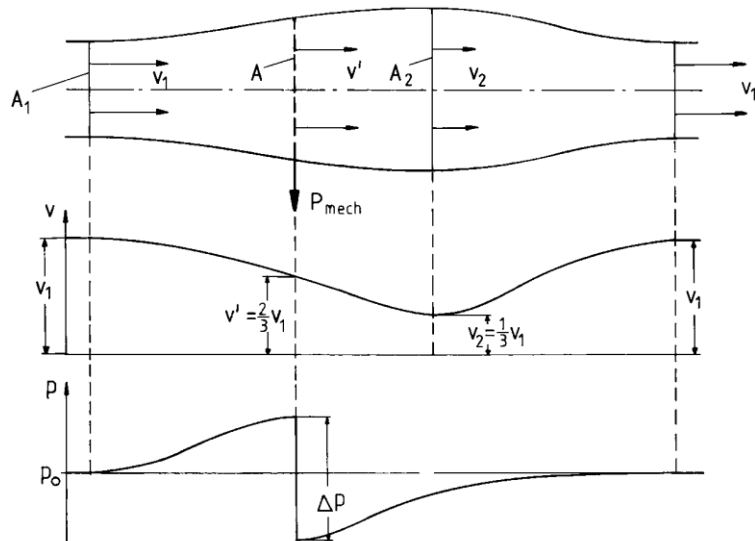


Fig 2.9 (b): Flow conditions of the stream through an ideal disk-shaped energy converter with the maximum possible extraction of mechanical power

The diagram above shows the flow condition through the wind energy converter in details – flow velocity and static pressure are indicated along with the flow lines. When air flows through the turbine its velocity is reduced to minimum at the exit point. Moreover, due to pressure equalization the increased static pressure in the converter is reduced to the ambient pressure just before it exits the converter. We must understand that ideal and frictionless conditions are assumed for the basic relationships. However, the power coefficient value is lower than the ideal cases in real life situations.

2.3.2. Tip Speed Ratio

The rotating converter of the turbine, a rotor, creates a rotating motion which is addressed as the rotational speed of the turbine or the rotor speed. This angular velocity is basically the tangential velocity of the rotor blade tip. Tip Speed ratio, λ ,

given in the following equation, is determined by this rotor speed in relation to the wind velocity.

$$\text{Tip Speed Ratio, } \lambda = \frac{U}{V_w} = \frac{\text{Tangential Velocity of the Rotor Blade Tip, } U}{\text{Speed of the Wind, } V_w} = \frac{wr}{V_w} \quad [21]$$

Where, V_w is wind speed (m/s), u is velocity of the rotor tip (m/s), r is the rotor radius (m), and ω the angular velocity (rad/s) [46].

The power coefficient directly depends on the ratio between the energy components from the rotating motion and the motion of the air stream. Thus, it depends on Tip Speed Ratio. A higher tip speed ratio, or TSR, results in high shaft rotational speed needed for efficient operation to produce more electricity [46] [47].

2.3.3. Angle of Attack

The angle of attack is an important parameter in shaping the performance of the turbine blades for power generation. With a view to having a good lift force, the relative wind should hit the blade at a proper angle which is called the angle of attack. The amount of force generated from an aerofoil depends greatly on the angle that it makes with the direction of the relative wind (figure 2.10a) [48] [49].

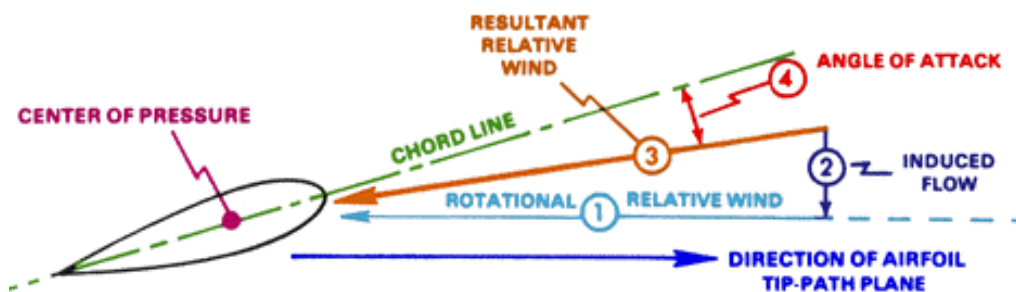


Figure 2.10 (a): Angle of Attack on turbine aerofoil

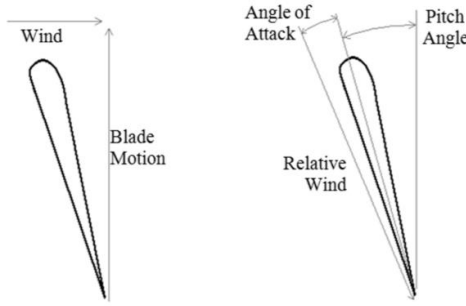


Figure 2.10 (b): Pitch angle of the aerofoil in relative to angle of attack

2.3.4. Pitch Angle

Figure 2.10 (b) shows the pitch angle of a blade aerofoil. Pitch angle maintains a uniform rotor speed under different wind conditions to accomplish optimum power from the turbine. Even a small increase or decrease in the pitch angle can make huge changes on the power output of the wind turbine [49] [50].

2.3.5. Blade Design

As far as the rotor blade designing concerns, aerodynamic forces, lifts and drags are the fundamental factor. There could be 2 –bladed, 3-bladed and multi-bladed turbines. The details of blade design have not been covered in this thesis rather it focuses towards the simulation and design of Maglev vertical axis turbine for popular multi-bladed system and synchronise the result with energy harvesting circuit to get optimal output for low wind speed.

2.3.6. Pitch control and Yaw Control

The pitch control system a subsystem of the wind turbine and it is quite expensive. It is located and operates inside the hub where it rotates around their radial axis as wind velocity changes during operation. The pitch control is a system that changes the angle

of attack by pitching the blades in order to produce more power. There are mainly two types of control system- hydraulic and electromechanical. Pitch control is expensive, it has many maintenance and mechanical issues and they are quite complicated [51-52]. For multi directional low wind off-grid system, pitch control is not preferred. This thesis studies fixed pitch VAWT without having a variable pitch control system. For electromechanical there are issues with the batteries.

The yaw system guides the turbine towards the wind. The system consists of a bearing, motor and drive. This mechanism is controlled by an automatic controller with the wind sensors placed on the hub. Generally, the yaw system is applicable for HAWT. As VAWT is capable of generating power regardless of wind direction, yaw mechanism is not needed to implement there.

Following table identifies the design parameters and performance parameters of wind turbine. ‘Cut-in’ and ‘Cut-off’ wind speed range should be determined in order to make sure whether the turbine will work under low or high wind speed. Turbine height, radius, blade number and pitch angles are the main design parameters whereas mechanical torque and mechanical power are the performance factors which would be analysed. For Vertical Axis Wind Turbine, the turbine gives maximum efficiency in Null pitch angle [null pitch angle]. In this research, a prototype was built in which the turbine blade pitch angle was varied to make sure at null pitch, the developed VAWT produces maximum power.

Table 2.1: Design and Performance Parameter Identification of Wind Turbine

Design Parameter	Performance parameter
<ul style="list-style-type: none"> • Wind Speed (m/s) • Turbine Height (m) • Turbine Radius (m) • Pitch Angle 	<ul style="list-style-type: none"> • Mechanical Torque (Nm) • Mechanical Power (P)

2.4. Generator details with an emphasize on PMSG

A generator converts mechanical energy to electrical energy. A prime mover is required to rotate the generator shaft with the mechanical energy extracted from the wind, which is, in our thesis, the VAWT. The generator applies Faraday's law of electromagnetic induction. The law says that current is produced when a moving magnetic field is passing over a stationary coil (conductor). There are basically two kinds of generator: DC and AC. DC generators are not preferred for wind turbine because of high maintenance requirements due to brushes and it also requires DC-AC inverters. Coming back to AC generator, they are mainly of two types: The Asynchronous (induction) and synchronous [53]. Each of the generator has its own classes and types. This part of the thesis briefly describes the generators used in wind turbine mentioning their advantages and disadvantages. It also states the type of generator that is used in this system and the reason behind it.

2.4.1. Asynchronous Generator

Asynchronous generators are also known as Induction generators. This type of generator produces electrical power when the rotor turns faster than synchronous speed. Synchronous speed is the rate of rotation of the magnetic field on the stator. Since the speed of the rotor never matches the synchronous speed, hence it is

addressed as asynchronous. Here, a separate electrical source needs to provide the external current that produces the magnetizing flux resulting current into rotor and their interaction produces voltage at the stator. The excitation current, its magnitude and frequency is determined by a closed loop control system.

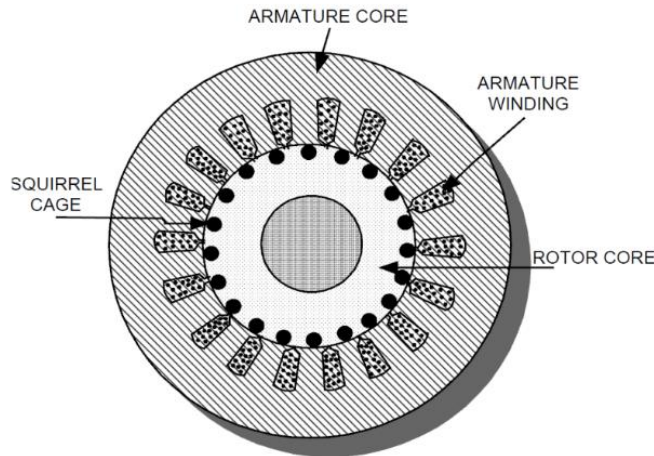


Figure 2.11: A cross section of an asynchronous generator

A close loop control system varies the excitation current and the frequency of it so that constant voltage can be fed to the generator regardless of the variations of speed and load current. Figure 2.11 shows a cross section of an induction generated that has its squirrel cage type rotor. Generally, induction generators are of three kinds- A) Doubly Fed Induction Generator, B) Wound Rotor Induction Generator, C) Squirrel Cage Induction Generator [54] [55].

2.4.2. Synchronous Generator

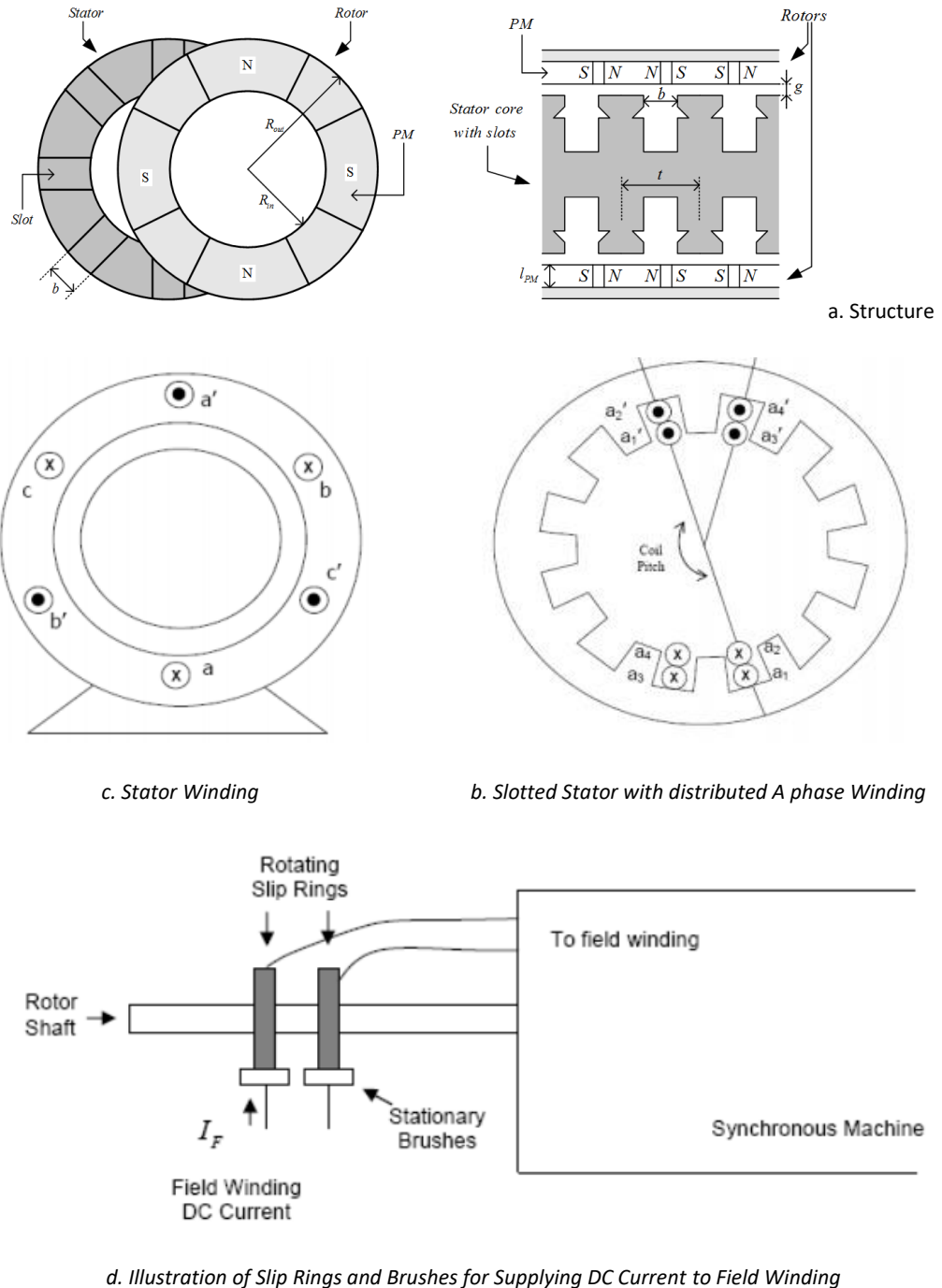


Figure 2.12 (a, b, c, d): Synchronous machine configuration

A three-phase synchronous machine consists of a rotating cylinder called the rotor and a stationary housing called the stator as shown in Figure 2.12(a). Generally, the rotor position is inside and the stator is outside. A shaft rotates through the rotor and bearing helps the shaft to be in order. A three-phase synchronous generator requires

three identical coils of wire. Each of the coil can have several turns. These coils are placed in the stator slots. Figure 2.12 (b) represents one of the three phase windings. This winding is also addressed as armature. The angular distance between the sides of a turn is called the coil pitch whereas the distribution of the turns is termed as coil breadth. Each of the phase coil is separated by 120° from its adjacent phase. Figure 2.12 (c) shows the three stator phases a, b and c. Dot indicates the current to be coming out of the page whereas cross indicates current going into the page. The rotor contains the field winding that produces the magnetic field needed to generate a voltage. As it can be seen in figure 2.12 (d), the end connections of the field winding are connected to two copper rings with carbon brushes. The brushes are mounted on the rotor shaft. This ring is called slip ring. The DC exciting field current is produced normally by a DC voltage source through the slip ring. The maintenance is not as costly as DC generator. The induced voltage produced by each phase coil has the same frequency, magnitude and has a displacement by 120° in phase [53-56].

The rotor speed, n , of a synchronous machine is given by the following equation:

$$n = \frac{120f}{p} \quad (22)$$

Where, f = frequency of the rotary field, grid frequency for grid connection (in Hz); p = number of pole pairs,

In terms of rotor configuration, synchronous generators are of two types: the salient pole and non-salient pole. Salient pole rotor is used mostly in low speed applications whereas the non-salient pole (wound/cylindrical rotor) are for high speed applications.

2.4.2.1. Salient pole rotor

These are synchronous generators that are mostly used in situations where the rotor is required to rotate at a slow pace to extract maximum power. It is generally constructed with a large number of poles [57]. The stator having a laminated iron core with slots. According to figure 2.13, phase windings are placed into the slots [58] [59]. The external dc current is provided through the slip rings and brushes. It has ability to run at low speed while extracting maximum power. Typical application for salient pole rotors are low speed hydraulic applications [58].

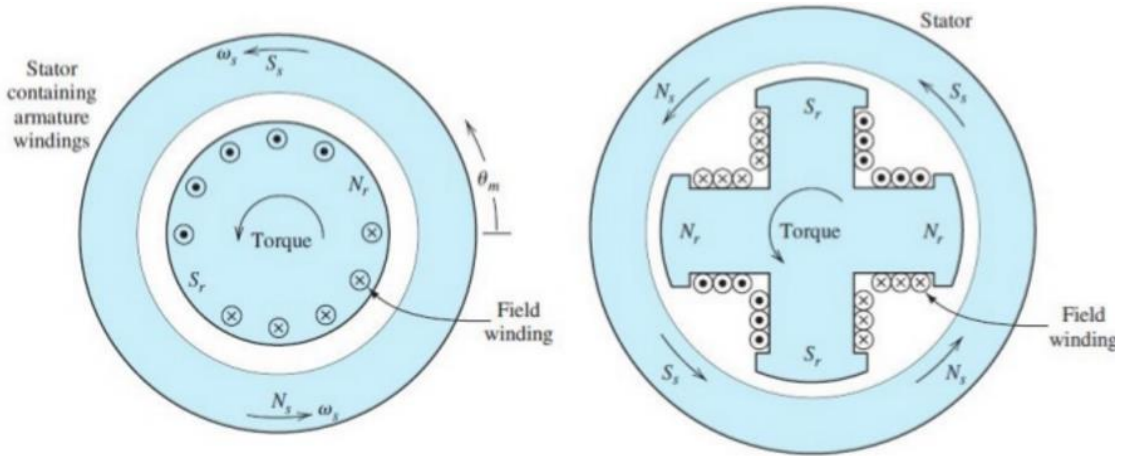


Figure 2.13: Salient Pole rotor and Non-Salient Pole

2.4.2.2. Wound/cylindrical rotor synchronous generators

Mostly used for high speed applications, non-salient or wound or cylindrical rotor provides efficient power at high rotor speed. Generally, it has fewer poles than salient machine. Forged iron core rotor is installed on the shaft and insulated copper bars are placed in the slots. At low speed condition, it is incapable to provide efficient power; thus making it impractical for this project [57] [59].

2.4.2.3. A comparison between Salient Pole and Non Salient Pole

(wound/cylindrical) Machine [57-59]

<i>Salient Pole Machine</i>	<i>Non Salient Pole Machine</i>
<ol style="list-style-type: none">1. Consist of large diameter and short axial length, excessive windage losses.2. Low speed operation, typical speed 100-375RPM. More number of pole up to 60. Cheaper compared to Wound rotor.3. Flux distribution is not uniform due to the presence of salient poles, hence emf waveform generated is not good compared to cylindrical machine	<ol style="list-style-type: none">1. Consist of smaller diameter and longer axial length, less windage losses.2. High speed operation, typical speed 1500-3000 rpm. Less number of pole, generally 4-6. Expensive compared to Salient pole.3. Nearly sinusoidal flux distribution around the periphery, therefore gives a better emf waveform than salient pole machine

2.4.3. Permanent Magnet Synchronous Generators

Permanent magnet synchronous generator (PMSG) belongs to the synchronous generator type having the same principle. A set of permanent magnets produce the magnetic field instead of external source. As magnets being used as field provider, it is less bulky and is best suited for low wind speeds. The advantages are many including elimination of copper losses, simpler construction without slip rings, lower weight and size resulting higher power density and efficiency. Here, the higher power density

indicates reduced mass at a given power, i. e. the construction happens to be more compact. [60-64]

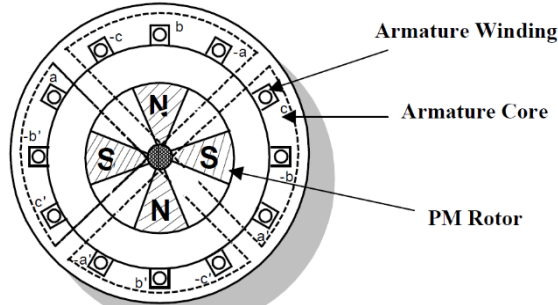


Figure 2.14: A cross section of a permanent magnet synchronous generator [2]

Figure 2.14 represents a cross sectional area of a PMSG [65] whereas figure 2.15 [56] shows a simple surface mounted PMSG with the basic structure. It has a complete magnetic flux circuit, half N-pole and half S-pole, the magnetic flux travels from the rotor surface through the air gap, the magnetic silicon steel in the stator, the air gap and then back to the rotor to form a complete closed-loop.

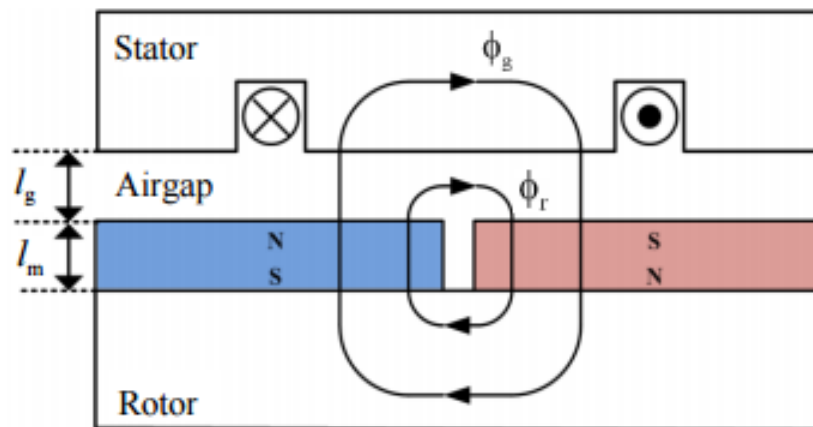


Figure 2.15: Schematic diagram of permanent-magnet synchronous generator (PMSG): magnetic flux path.

The permanent magnet synchronous generators could either be surface mounted (exterior) or embedded (interior) permanent magnet generator. The surface mounted generator has its magnets placed over the surface of the rotor while the embedded has an interior permanent magnet [66]. Based on the manner of flux propagation across the generator air gap, the PM generators are classified as radial, axial and transverse which are defined as follows [61-63].

2.4.3.1. Radial flux permanent magnet:

This type of PMSG has its permanent magnets radically placed on the rotor, making the magnetic flux propagated at a radial direction (Figure 2.16) [63]. These types are preferred for direct drive wind turbines. Gluing the magnets on the surface of the rotors is the simplest way to implement this system [63-67].

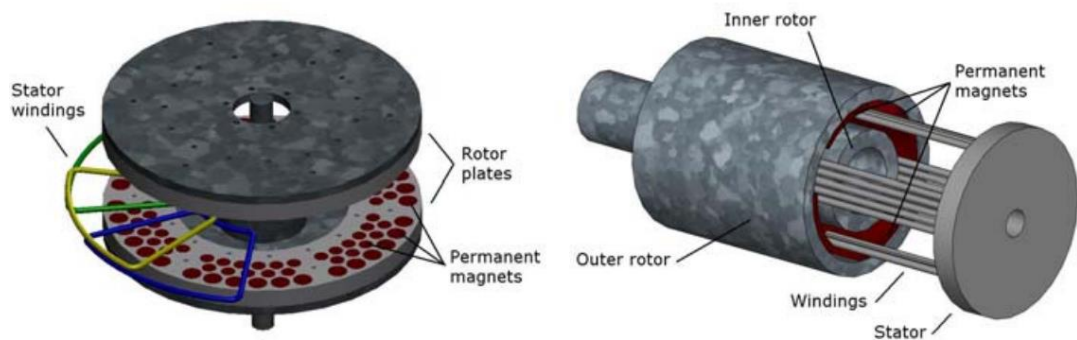


Figure 2.16: Basic configuration of Axial Flux PMSG and Radial Flux PMSG

2.4.3.2. Axial Flux Permanent Magnet

These types have its magnetic flux propagating at an axial direction from the magnets. These ones are best suited for low wind speed applications. Figure 2.16 and 2.17 show example of AFPM. Axial Flux PMSG can be of 3 types namely 3-Phase, 5-Phase and

Dual Stator in which 3-Phase is the least complicated and cost effective among three.

[66-68]

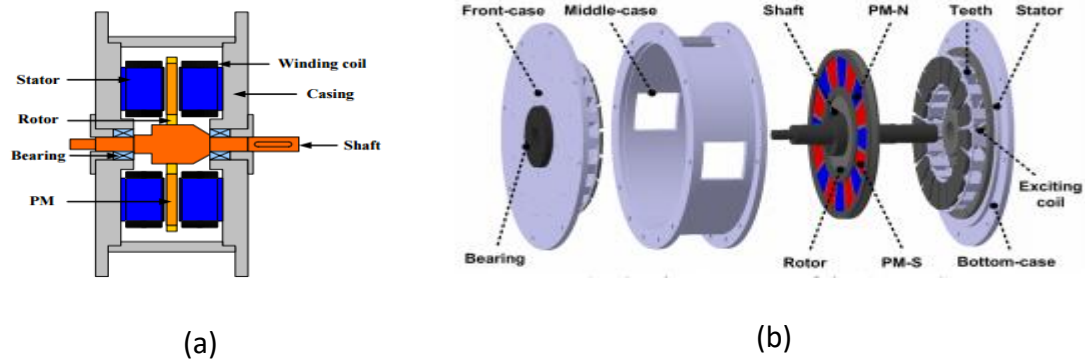


Figure 2.17: Cross Section View of Axial Flux PMSG (a); Structure of AFPMSG (b)

2.4.3.3. Transverse Flux Permanent Magnet

The transverse permanent magnet generator has its flux propagating a perpendicular angle to the motion of the rotor [69-71].in this system, the direction of magnetic flux is perpendicular with the direction of the rotational rotor. There is a few configurations of this system. Fig 2.18 [69] shows the configuration of a surface-mounted transverse-flux PMSG. A transverse flux PM (TFPM) machine is a synchronous machine in nature, and it will function in a manner similar to any other PMSG in principle.

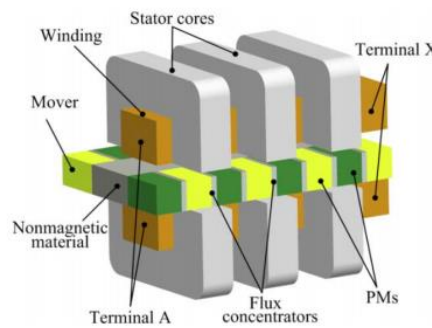


Figure 2.18: Typical Transverse Flux PMSG structure of a U-shaped Stator Core

In comparison, axial flux design offers high torque and power density values that are suitable for low speed applications. If radial is used, it requires a step down or step up gear boxes to reach the desired rotational speed for the driven machinery. The transverse permanent magnet generator is no more in use because of its complexity and maintenance problem. Due to this, axial flux permanent magnet generator will be better suited for this work [69-76].

2.5. Wind Turbine System: Trends and Concepts

This section will deal with the classification of wind turbine as well as the trend of use of different types of turbine in accordance with time. The general classification of turbine deals with rotor speed. It can be divided into two categories namely fixed speed, limited variable speed and variable speed. Since the variable speed wind turbines use the power converter, on the basis of it, turbines can be subdivided into another two categories namely partial scale and full scale power electronic converter. Leaving the motor speed aside, variable speed wind turbines can be divided into another two subcategories in terms of power converter- partial scale power convert and full scale power converter [76-79]. There is also direct drive, single stage geared and multi-stage gear concept. In terms of generator used, it can be classified into electrically excited synchronous generator, permanent magnet synchronous generator and Squirrel Cage induction generator. Among these three, permanent magnet synchronous generator can be sub divided considering its flux direction and these are radial flux, axial flux and transversal flux. The details of the classifications are mentioned in brief as follow. [72-75]

2.5.1. Fixed speed concept

This turbine worked with a multiple stage gearbox with Squirrel Cage Induction generator. Normally it is directly connected to grid with a transformer. Since induction generator operates in the range of synchronous speed, this system is called fixed speed wind generator system. In the period between 1980 and 1999, this concept was being applied. This is called the conventional concept since it was one of the oldest systems in terms of wind turbine. It was very popular on that period to many Danish manufacture companies. The advantages of this system are robustness, cheap and stability in terms of control system. However, speed is not variable and cannot be controlled. And because of the speed being fixed, any fluctuation in wind results straight in torque variation. As a result, there is a stress in gearbox, aerofoils and generator. It is also necessary for the system to have a three stage gearbox which is very inconvenient in nature. [76, 78] [79-83]

2.5.2. Variable speed concept with a partial-scale power converter

This system relates either to a Wound Rotor or doubly fed Induction generator with a variable speed wind turbine. In the rotor circuit, a partial scale power converter is used. This system is also addressed as Double Fed Induction generator. The rotor relates to a power converter whereas the stator is connected straight to the grid. The power converter varies the frequency of rotor resulting changing of rotor speed supporting a vast speed range. In need of a multistage gearbox, heat dissipation from gearbox friction, regular maintenance of partial scale converter and gearbox, strong protection of power electronic converter and high torque loads on drive train because of large stator peak current are the disadvantages of this system. [77-81]

2.5.3. Variable speed direct-drive concept with a full-scale power converter

In this system, through a full-scale power converter, the system is connected to the grid. It can be used for off-grid system as well. The difference between this system to geared drive system is the speed of the rotor. In this case, generator rotates in a slow speed since it is connected straight to the turbine rotor hub. The low speed results high torque. For direct drive, this low speed and high torque needs of multi poles requiring large diameter for putting extra number of poles. However, the simplicity of drive train, good reliability and efficiency with the absence of gearbox is the good sides of this system. It has an advantage against partial scale converter of performing smooth grip connection. Direct-drive generators used here can be divided into two categories namely electrically excited synchronous generator and permanent magnet synchronous generator. [77-79]

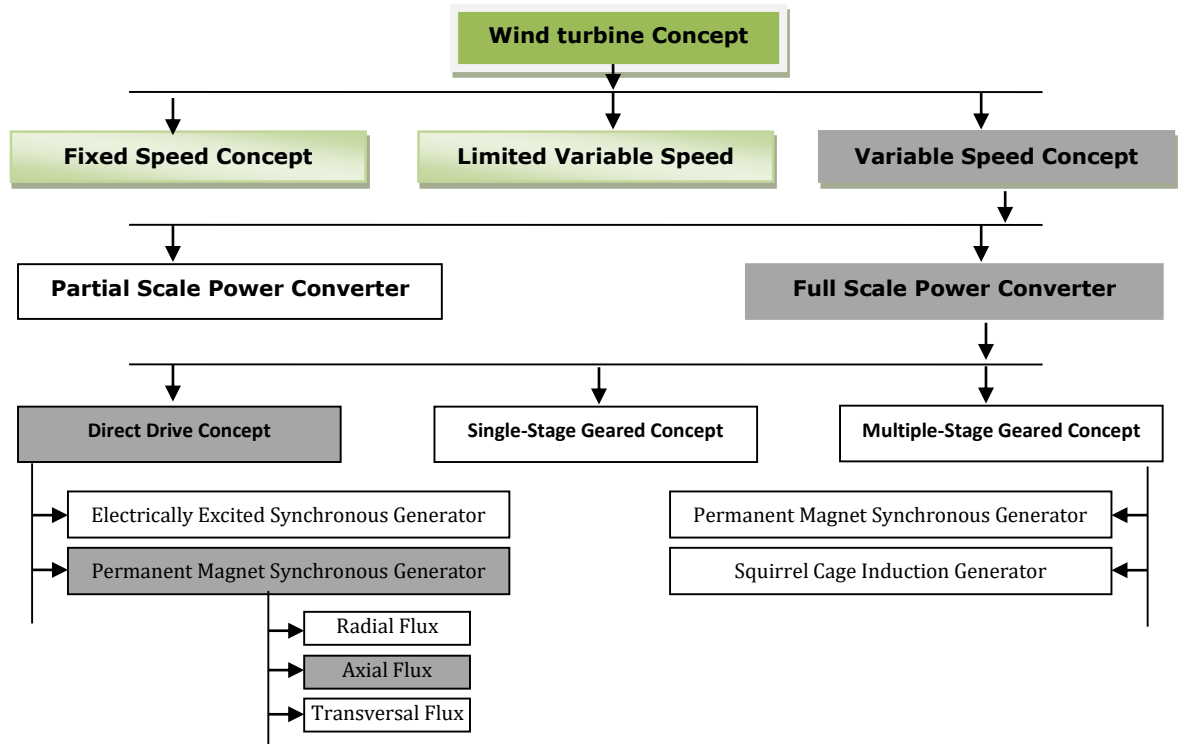


Figure 2.19: A block diagram of wind turbine classification

2.6. Energy Harvesting System

Wind power fluctuates and therefore adversely impacts power systems. Integration of energy storage systems (ESS) into wind farms is a promising solution to manage wind power. For near-to-midterm (seconds to minutes) power management, the most commonly implemented storage technologies in a wind farm are battery energy storage system (BESS), advanced capacitors and supercapacitors, flywheel energy storage (FES), and superconducting magnetic energy storage (SMES). The power and energy ranges of the four technologies are projected in Figure 2.20 [64]. The battery technology provides a high energy capacity but low power, while on the other end the supercapacitor has a high power capacity but is short in duration. The flywheel and SMES fall somewhere in the middle. None of the four single ESS technologies fit themselves well into the wind application requirement.

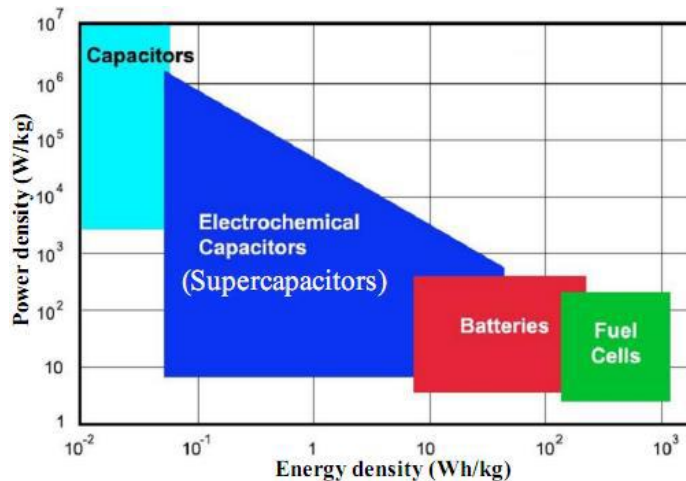


Fig. 2.20. Power vs Energy ranges for different Energy Harvesting Technology

2.6.1. Battery

Batteries have already been widely used since decades ago and still a popular energy storage system up until today. There are many variations of batteries present today either non-rechargeable or rechargeable with different types such as lithium-ion, lead-

acid, nickel-metal-hydride and many more. Overall, batteries have high energy densities, low self-discharge rate and costs less when compared to supercapacitors. Though widely used, there are still many negative factors affecting the batteries. These are temperature, slow charging time, low power density and short life cycle [58]. The characteristics of different batteries are tabulated in Table 2.2 [83-87].

Table 2.2 Comparison of different battery types

<i>Type of battery</i>	<i>Lead-acid</i>	<i>Nickel-cadmium (Nicd)</i>	<i>Nickel-metal hybrid (NiMH)</i>	<i>Lithium-ion (Li-ion)</i>
<i>Cycle life</i>	500-800	2000-2500	500-1000	1000-10000
<i>Cycle Efficiency (%)</i>	70-90	70-90	66	>90
<i>Self-discharge per day (%)</i>	0.1-0.3	0.2-0.6	0.5-1	0.1-0.3
<i>Energy Density (Wh/kg)</i>	30-50	50-75	60-80	100-250
<i>Power density (W/kg)</i>	75-300	150-300	250-1000	250-340

2.6.2. Supercapacitor

Electric double-layer capacitors (EDLCs), ultracapacitors, electrochemical capacitors or supercapacitors are able to store charges more than a thousand times compared to an electrolytic capacitor. Supercapacitors are normally rated in Farads (F) whereas the basic electrolytic capacitors are rated in microfarads (μF). The ability of

supercapacitors to store a large amount of charges is because of its very small distance between the electrode layers separating the charges which results in a larger electrode plate surface area [88].

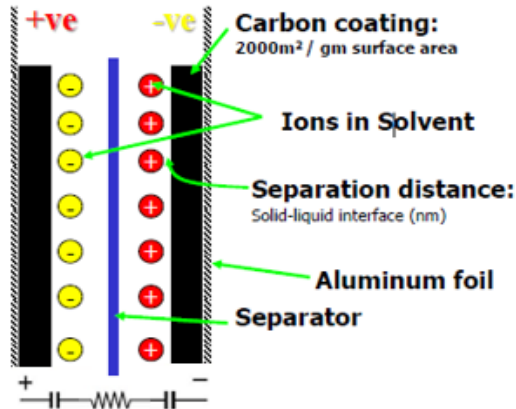


Figure 2.21: Model of a supercapacitor.

Supercapacitors have started to gain attention and are widely used for energy storage in the recent years especially in the renewable energy sector. The advantages such as fast charging time, unlimited life cycle, low equivalent series resistance (ESR), robust and high power density makes it attractive and have been used to replace battery in a number of applications [89]. However, supercapacitors are greatly affected by temperature as an increase in temperature will produce negative effects to the electrolyte in the supercapacitor, thus reduces the lifespan. Charge balancing of supercapacitors has always been an issue and it is important to minimise it in order to improve the performance and reliability. Linzen *et. al.* [90] analysed a few of existing charge balancing circuits and presented their pros and cons. By placing passive resistors across each capacitor, there is a high power loss from the resistors which causes this circuit to be inefficient. Implementing active switched resistors to allow current to bypass when the supercapacitors are fully charged adds additional costs to

the circuit. Another concept of using DC-DC converters across two supercapacitors on the other hand results in high efficiency as no other losses occur besides from the converters itself. However, this circuit requires a large amount of components which adds to the cost. Zener diode placed across each supercapacitor can also be used where the voltage will be constant when supercapacitor and Zener voltage are balanced but this circuit also causes high power losses (Fig. 2.22).

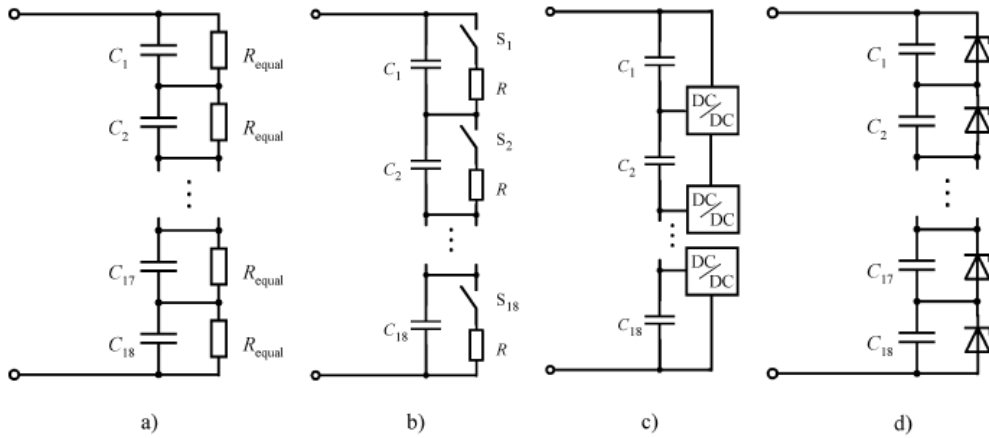


Figure 2.22: Various types of charge balancing circuit. (a) Passive resistor (b) Active switched resistor (c) DC-DC converter (d) Zener diode [90]

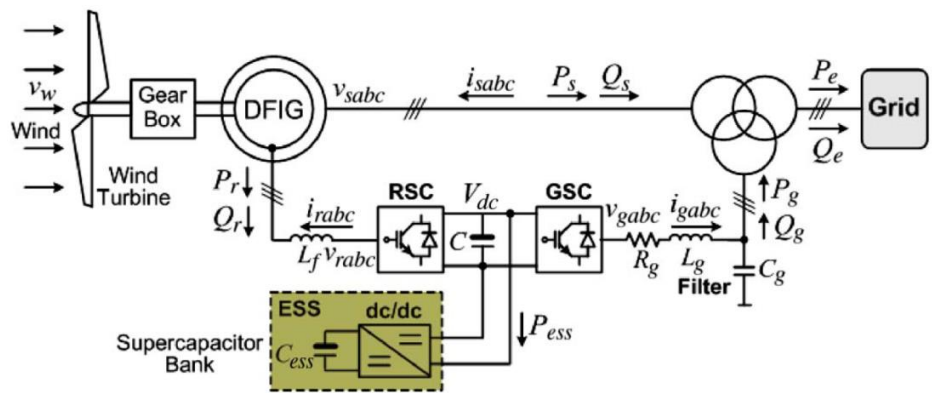


Figure 2.23: Configuration of a DFIG wind turbine equipped with a supercapacitor ESS connected to a power grid [91].

Liyan Qu, Wei Qiao in the year of 2011 proposed a novel two-layer constant power control (CPC) scheme for a wind farm equipped with doubly fed induction generator (DFIG) wind turbines [91], where each WTG is equipped with a supercapacitor energy storage system (ESS) (Fig. 2.23). The CPC consists of a high-layer wind farm supervisory controller (WFSC) and low-layer WTG controllers. The ESS serves as either a source or a sink of active power to control the generated active power of the DFIG wind turbine. Results have shown that the proposed CPC scheme enabled the wind farm to effectively participate in unit commitment and active power and frequency regulations of the grid [91-92]. The proposed system and control scheme provides a solution to help achieve high levels of penetration of wind power into electric power grids. Output power of Wind Turbine fluctuates constantly, which may cause grid frequency variations, and impose a high risk on system stability. In order to smooth power output of wind turbine, the proposed system was used. By using a Supercapacitor based energy storage, the effects of frequency fluctuation and deviation on system during fault condition was minimized. This was one of the early examples of using Supercapacitors in wind turbine. However, our research deals with off-grid wind energy harvesting; therefore, Lian Qu's model cannot be used. Moreover, our research aims to charge a DC battery through whereas Lian Qu worked with 3 Phase grid connection.

2.6.3. Hybrid Energy Storage System (HESS)

Battery and supercapacitors are used together to form a hybrid system. As discussed earlier, battery and supercapacitor has their own advantages and disadvantages. The Ragone plot in Figure 2.20 shows that supercapacitors have high power density but low energy density whereas batteries have low power density and high energy

density. Besides, battery also has higher ESR which results in high internal loss, thus less efficient compared to supercapacitors. Therefore, both devices are often integrated so that they can complement each other. This system known as hybrid energy storage system (HESS) are widely used now in order to prolong the lifespan of each device and improve standalone systems [93]. As an example, Babazadeh *et. al.* [94] implemented a HESS system into a PMSG wind turbine with a large variable wind speed between 6 – 21 m/s. The HESS system helps to smoothen and regulate the output caused by peaks generated due to variation in the wind speed by using a control system to disconnect the battery from wind turbine. This successfully proved that the battery life is able to last longer as the battery experiences lesser stress. Currently available electric vehicle (EV) such as Tesla Model S, Toyota Prius and Chevrolet Volt use only battery banks and do not employ HESS. The average urban driving patterns that require rapid discharging of battery banks when accelerating and charging of banks when decelerating will reduce the battery banks' lifespan, thus supercapacitors are beneficial in this case. Since supercapacitors are able to charge and discharge at a fast rate, it is able to provide a boost of power during acceleration and absorbs power during regenerative braking [95] [96].

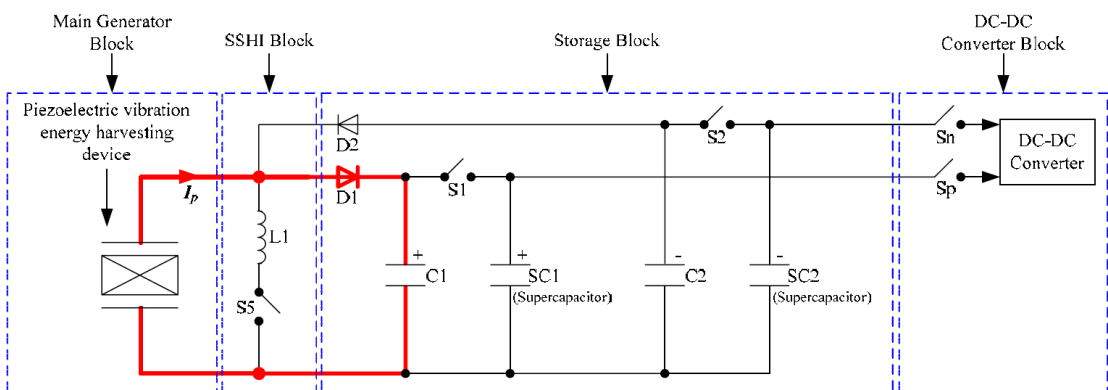


Figure 2.24: Energy harvesting circuit of showing current flowing in the positive half cycle [97].

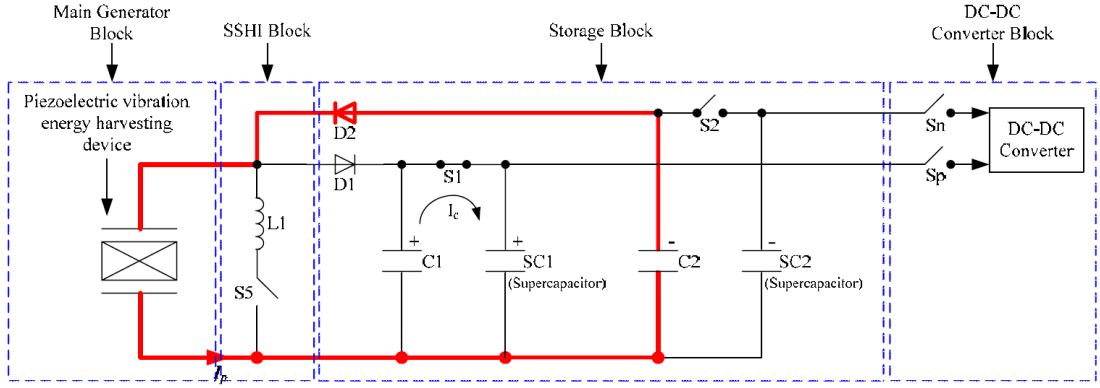


Figure 2.25: Energy harvesting circuit of showing current flowing in the negative half cycle [97].

In 2010, Worthington [97] proposed a novel circuit that combines the SSHI technique with a charge pump tyre circuit which will be connected to a load capacitor directly to harvest energy. This allows the capacitor to act as a reservoir that will be disconnected when fully charged and then discharged it to a load. Experiment results showed that this idea is capable of harvesting three times more amount of energy compared to the usual bridge rectifier circuit. It also has an advantage of being able to collect charge during the whole AC cycle from the PT as shown in Figure 2.24 and Figure 2.25 [97].

Most common methodologies use two storage banks directly connected in parallel [98] and a bidirectional DC/DC converter interfacing two storage banks (Figure 2.26) below [98-99].

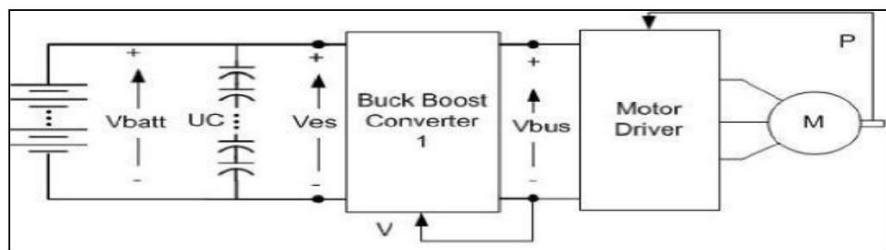


Figure 2.26: Conventional Hybrid Energy harvesting circuit

One of the problems of establishing the hybrid storage system is the different voltage level of Supercapacitor and battery bank. The most common way of coupling the two storage device is to connect them in parallel. Although this way of harvesting energy maintains the same voltage in both the storage banks but however it restricts the power delivered by the Supercapacitor. M.E. Glavin, Paul K.W. Chan (2008) inspected the role of an electronic control unit in a battery supercapacitor hybrid energy storage system under different load conditions with the aid of various sensors [100-101]. Here, the DC/DC converter permits the Supercapacitor to supply extra power required by the load. However, in low wind speed, it will not be possible for the turbine to charge a hybrid storage system where both the Supercapacitors and battery are connected in parallel. Because at low wind speed, the turbine rotates at a very low RPM resulting a low output voltage at the generator terminal which is not sufficient to charge the hybrid storage in parallel configuration.

Having compared with previous models, in which Tankari used a 4.5KW PMSG [102], Abbey as well as L. QU used a 1MW induction generator [103-104]; this research adopts a small VAWT scale connected to a PMSG making it as a portable standalone system. Also areas with low wind does not require a system that includes a generator of Mega Watt range. Coming back to the energy harvesting circuit, this investigation discovers a novel hybrid circuit with a combination of a battery and Supercapacitor bank. In 2010, Worthington proposed a novel circuit that combines the Synchronous Switched Harvesting technique which was connected to a load capacitor directly to harvest energy [105]. This allowed the capacitor to act as a reservoir that would be disconnected when fully charged and then would discharge to a load. The circuit was connected with a charge pump tire circuit [105]. Experiment results showed that this

idea was capable of harvesting three times more amount of energy compared to the usual bridge rectifier circuit. However, this idea has not yet been implemented into off-grid wind energy sector. Although Lee [106] implemented a hybrid energy harvesting storage in 2008 for wind power application, it was meant for grid connection and again was of high power range. Hence, it was impossible for the energy storage system to be implemented for off-grid system. This study brings the supercapacitor based hybrid energy harvesting for first time into the off-grid low wind power application. A supercapacitor bank is used in this experiment that charges up from the turbine and discharges through the battery with the use of power electronics.

Batteries have relatively high energy density comparing to Supercapacitors; however, it does not have the characteristics of Supercapacitors- instantaneous charging and discharging. Even though batteries can store more energy but it requires longer time to discharge and recharge. Moreover, batteries require constant voltage for charging. If the current exceeds battery rating, it may get heated up and also voltage fluctuation reduces life span of the battery. In order to give a constant voltage from the generator, a DC/DC converter has to be used. However, the internal voltage drops in DC/DC converter together with low voltage at generator output do not make a Vertical Axis Wind Turbine worthy of charging a battery in low wind speed. Therefore, this research proposes a balancing circuit which introduces Supercapacitor to act as a buffer between the turbine and a battery. Supercapacitor would get charged up from the turbine and discharge through the battery in two separate process by using MOSFET control switching system. This novel idea does not include a DC/DC converter in the Turbine-Supercapacitor part avoiding the voltage drop across the converter. Rather,

the turbines charges the Supercapacitor directly and after getting charged up, the Supercapacitor gets isolated from the turbine by the help of MOSFET switching and charges the battery through a DC/DC converter by self-discharging. In this way, even a small voltage of 3-4V can charge up a 6V/12V battery. In this research, the proposed hybrid Supercapacitor based battery charging circuit has been implemented into a Vertical Axis Wind Turbine in low wind speed and compared with direct charging of battery from turbine with or without a DC/DC converter. Lastly, the proposed system has also been compared with current existing systems of rural Malaysia in terms of cost-effectiveness.

Chapter 3

Methodology

This Chapter consists of 6 parts. First two parts consist of design and simulation of VAWT and PMSG respectively. Third part brings the first two sections together and describes the entire simulation process of VAWT adapted to PMSG. Part 4 includes low cost optimization of the entire VAWT system for rural Malaysia. Part 5 describes the design and experimental set-up of a Laboratory prototype of a Maglev Based VAWT. Part 6 explains the energy harvesting circuit and the control system of it. Part 7 brings the energy harvesting circuit into two different Maglev based VAWT having separate configuration. This part details the overall system set-up, control theory and data collection process for both the system. Figure 3.1 presents the data flow block diagram of this part.

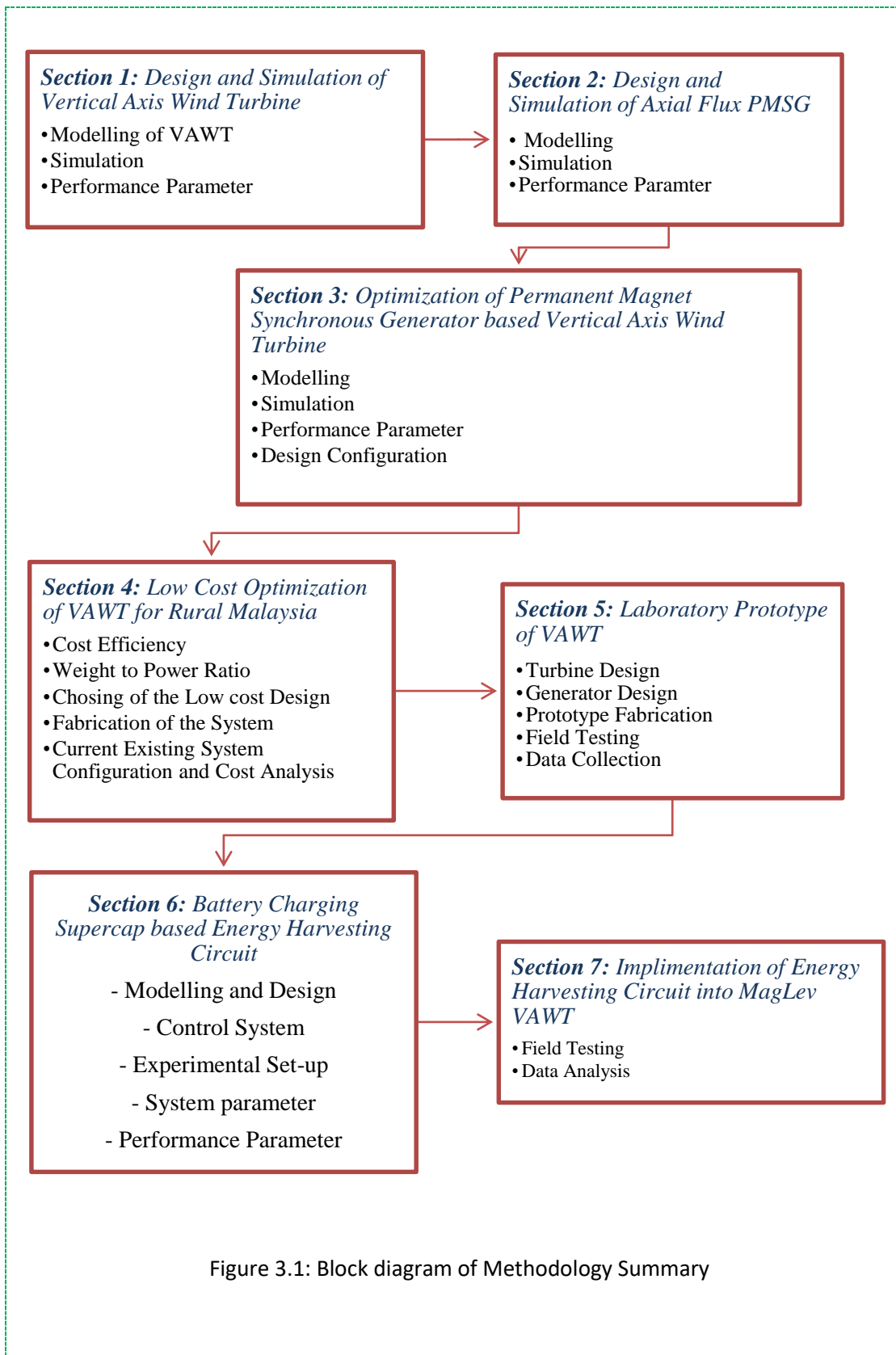


Figure 3.1: Block diagram of Methodology Summary

3.1. Design and Simulation of Vertical Axis Wind Turbine

The first part of methodology includes the design and simulation process of Vertical Axis Wind Turbine. First, VAWT theoretical equations had been studied and implemented in Matlab/Simulink for modelling. The analysis of design parameters followed by performance parameters was given. The observation and further study were kept for “Result & Discussion” chapter. Following is the process flow chart of this sub-methodology chapter.

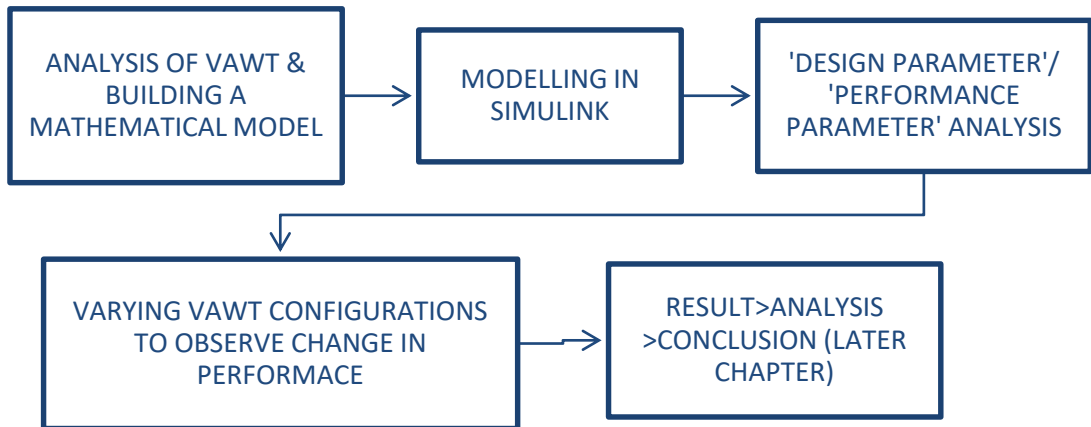


Figure 3.2: Process Flow Chart of Section 3.1

3.1.1 VAWT Mathematical Model:

From the section 2.3 under the chapter of Literature Review and taking in consideration of reference [121-127], the aerodynamic equations of the turbine are given by the equation stated below [107-113]:

$$P_m = C_p(\lambda) \frac{1}{2} \rho A U_w^3 \quad (3.1)$$

$$\lambda = \frac{\omega_m R}{U_w} C_p \quad (3.2)$$

$$T_m = \frac{P_m}{\omega_m} \quad (3.3)$$

$$A = 2RH \quad (3.4)$$

Here, A is the turbine rotor cover area in meter square (m^2), ρ is the air density, U_w is the wind speed in meter per second (ms^{-1}), C_p is the power coefficient of the wind turbine, λ is the tip-speed ratio, ω_m is the rotor angular speed in $rads^{-1}$, R is turbine radius in meter (m) and H is turbine height in meter (m).

To generate mechanical torque and power, the turbine depends on its physical parameters which in this case are wind speed, height and radius of the turbine. Also tip speed ratio and power co-efficient also play an important role. As discussed earlier, the tip speed ratio is the ratio of the blade tip speed to the wind stream upstream of the rotor. Based on the tip speed ratio, the power coefficient which is the amount of energy taken from the wind can be calculated by using a universal equation [113]:

$$C_p(\lambda, \beta) = C_1 \left(\frac{C_2}{\lambda_i} - C_3 \beta - C_4 \right) e^{-\frac{C_5}{\lambda_i}} + C_6 \quad (3.5)$$

The coefficients c1 to c6 are: c1 = 0.5176, c2 = 116, c3 = 0.4, c4 = 5, c5 = 21 and c6 = 0.0068 [113] [114]; where β is the pitch angle and is angle at which the wind hits the blades. The maximum value of C_p (0.48) is achieved for $\beta = 0$ degree.

3.1.2 Simulink/ Matlab Model:

The equations stated above were implemented in SIMULINK. Simulink is a block diagram environment integrated with MATLAB for simulation and Model-Based Design. MATLAB, version 7.9.0.529 (R2009b), was used to model the system. Figure 3.3 shows the VAWT model developed in SIMULINK.

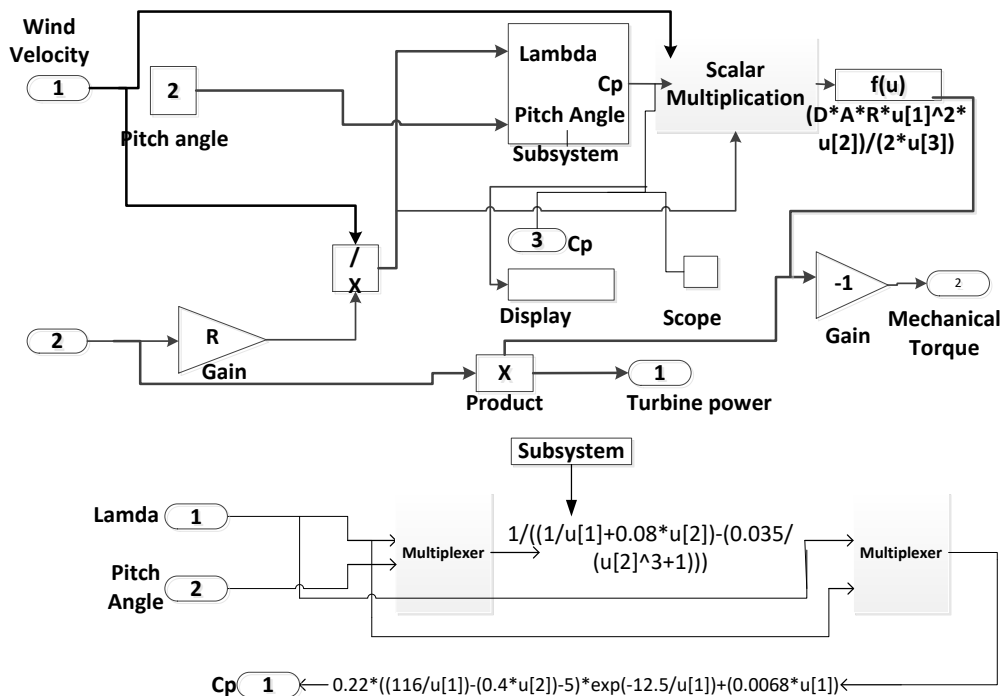


Figure 3.3: Turbine SIMULINK model

3.1.3 Analysis of the Model:

To observe the performance of VAWT, the turbine characteristics is simulated for various changes in parameters such as change in the radius, height, turbine speed, tip speed ratio while maintaining a fixed wind speed unless stated otherwise to observe the change in output torque, rotational speed and generated power.

3.2. Design and Simulation of Axial Flux Permanent Magnet Synchronous Generator

In this section, all three kinds of axial type Multi-Pole Permanent Magnet Synchronous Generators (PMSG) namely ‘Three-phase’, ‘Five Phase’ and ‘Double Stator’ PMSG have been modeled and then compared in order to get an optimal system.

'MATLAB/Simulink' had been used to model and simulate the wind turbine system together with all the three types Permanent Magnet Generators.

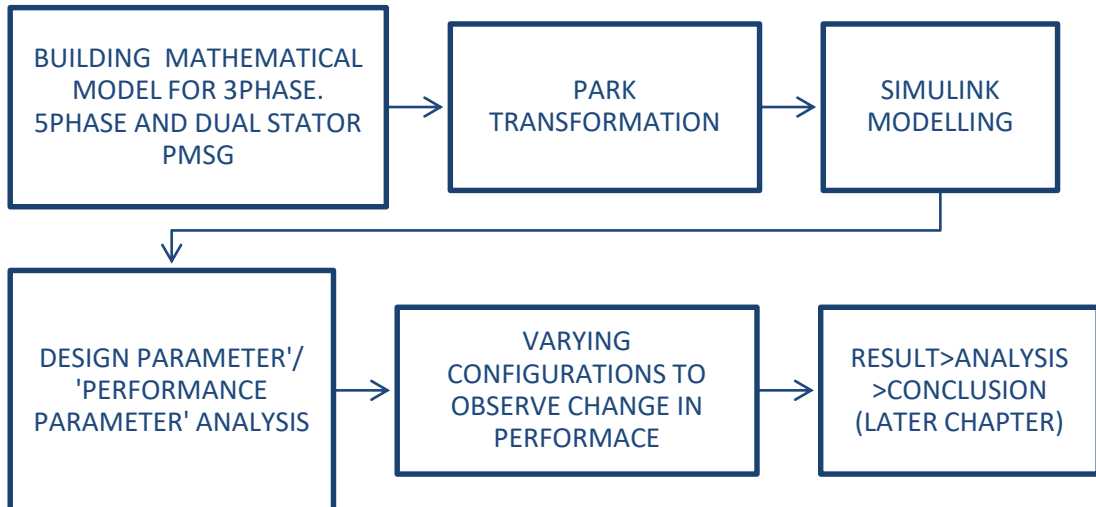


Figure 3.4: Process Flow Chart of Section 3.2

3.2.1. Mathematical model of PMSG

3.2.1.1. 'Park Transformation' and 'Swings Equation'

Park transform is a vector representation of AC circuit of multi-phase models in a ' dq axis' reference coordinates. The $dq0$ Park's transformation was 1st introduced by R.H. Park in 1929 and this mathematical transformation helps to simplify the analysis of different types of synchronous machines. By applying Park's transformation, the AC quantities are transformed to DC quantities which is much easier to model in Simulink. For PMSG DQ axis reference frame, the positive q -axis is aligned with the magnetic axis of the permanent magnet whereas the positive d -axis leads the positive q -axis by 90 degrees. The entire simulation of 3-phase, 5-phase and Dual Stator PMSG were

designed in terms of park transformation analysis. Equation (3.6) and (3.7) represents the Park Transform; where f can be of current (I), voltage (V) or flux (λ) [112-115].

$$\begin{bmatrix} f_q \\ f_d \\ f_0 \end{bmatrix} = [T_{qd0}] \begin{bmatrix} f_a \\ f_b \\ f_c \end{bmatrix} \quad (3.6);$$

Whereas T_{qd0} is the “abc-dq0 Transformation Matrix” which is expressed as follows:

$$[T_{qd0}(\theta_q)] = \frac{2}{3} \begin{bmatrix} \cos \theta_q & \cos(\theta_q - \frac{2\pi}{3}) & \cos(\theta_q + \frac{2\pi}{3}) \\ -\sin \theta_q & -\sin(\theta_q - \frac{2\pi}{3}) & -\sin(\theta_q + \frac{2\pi}{3}) \\ \frac{1}{2} & \frac{1}{2} & \frac{1}{2} \end{bmatrix} \quad (3.7);$$

Here, θ_q is the angular position of the rotor. The relationship between ‘dq’ reference frame and ‘abc’ axis coordinates on which equation 3.7 has been stated is given in the following figure 3.5. This transformation matrix was described by R.H. Park (1933) in his “Two Reaction Theory of Synchronous Machines” [114-116].

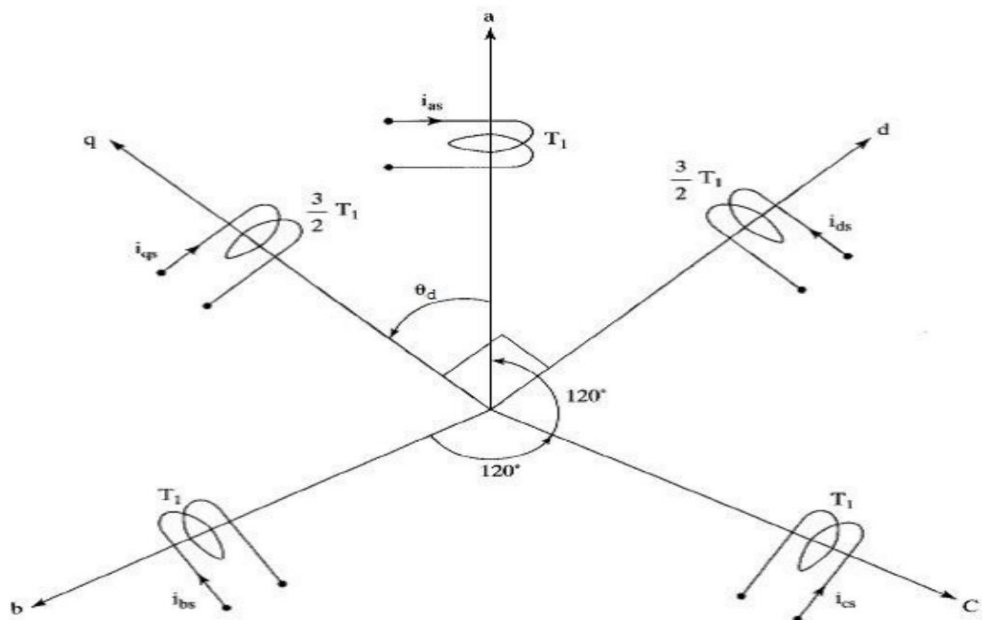


Figure 3.5: Park Transformation

After analysis and modelling under dq reference frames, ‘Park Inverse Transformation’ is used to convert back to the previous system in order to get the original phase results. The inverse transform is given below; where θ_q is the angular position of the rotor [115].

$$\left[T_{qd0}(\theta_q) \right]^{-1} = \begin{bmatrix} \cos \theta_q & -\sin \theta_q & 1 \\ \cos\left(\theta_q - \frac{2\pi}{3}\right) & -\sin\left(\theta_q - \frac{2\pi}{3}\right) & 1 \\ \cos\left(\theta_q + \frac{2\pi}{3}\right) & -\sin\left(\theta_q + \frac{2\pi}{3}\right) & 1 \end{bmatrix} \quad (3.8)$$

Equation (3.9) and (3.10) are recognized as ‘Swings Equation’. Associating with the ‘Park Transform’, it explains the physical features of a turbine. This equation describes how a common drive shaft of the turbine drives the generator rotor acting as the coupling element between the turbine and generator.

$$J \frac{d^2\theta}{dt^2} = T_m - T_e = T_a \quad (3.9);$$

$$T_a = \frac{dw_e}{dt} \quad (3.10)$$

Here, J is the total moment of inertia of the rotor mass in kgm^2 , T_m is the mechanical torque supplied by the turbine in Nm, T_e is the electrical torque output of the generator in Nm, w_e is the mechanical speed of the rotor in radian/sec and θ is the angular position of the rotor in radian.

The electromagnetic power P_e is the power that is developed or seen at the stator end of a generator and it is given by the expression shown below:

$$P_e = T_e \times W \quad (3.11)$$

Where T_e is the electromagnetic torque at the stator and W is the angular speed of the generator. The electromagnetic power describes the power density that the generator has at a particular point in time. The generators P_e are investigated at a low and optimal wind speed.

3.2.1.2. Three Phase Permanent Magnet Synchronous Generator

The analysis of the three phase permanent magnet synchronous generator was done using a quadrature dq equivalent circuit reference frame, in which the q-axis was 90° ahead of the d-axis with respect to the direction of rotation. Voltage, current and electromagnetic torque for a PMSG in the d-q axis synchronous rotational frame had then been expressed as following (equation 3.11-3.18) [116-117]:

$$V_q = -(R_s + pL_q)i_q - w_e L_d i_d + w_e \lambda_m \quad (3.12.a);$$

$$V_d = -(R_s + pL_d)i_d + w_e L_q i_q \quad (3.12.b);$$

$$L_d = L_{ds} + L_{ls} \quad (3.13);$$

$$L_q = L_{qs} + L_{ls} \quad (3.14);$$

$$\frac{di_d}{dt} = \frac{-R_s i_d}{L_d} + \frac{w_e L_q i_q}{L_d} - \frac{V_d}{L_d} \quad (3.15);$$

$$\frac{di_q}{dt} = \frac{-R_s i_q}{L_q} - \frac{w_e L_d i_d}{L_q} + \frac{\lambda_0 w_e}{L_q} - \frac{V_q}{L_q} \quad (3.16);$$

$$w_e = p w_m \quad (3.17);$$

$$T_e = 1.5p((L_d - L_q)i_d i_q + i_q \lambda_0) \quad (3.18);$$

Here, L_d , L_q and L_{ds} , L_{qs} are the inductances and leakage inductances (H) of d and q axis respectively; L_s is the stator leakage inductance; i_q , i_d and V_q , V_d are the stator currents and voltages; R_s is the stator resistance in ohms (Ω); λ_o is the magnetic flux in Weber (Wb); W_e is the electrical rotating speed (rad/s); p is the number of poles and T_e indicates the electromagnetic torque.

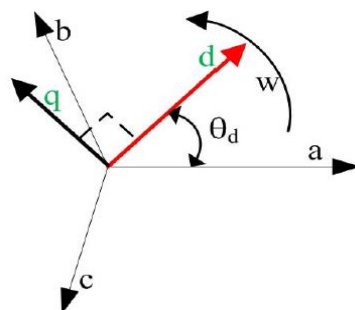


Figure 3.6: Park Transformation dq frame reference

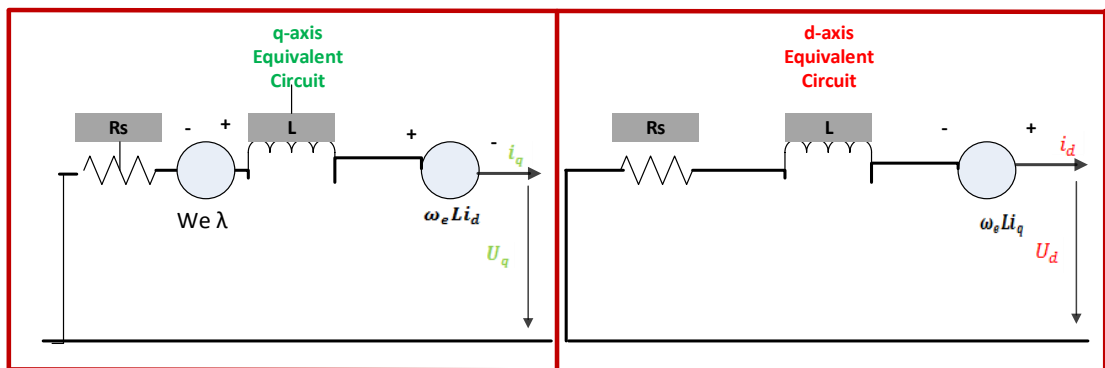


Figure 3.7: Q and D axis equivalent circuit respectively

Figure 3.6 shows the reference frame of Park Transformation whereas Figure 3.7 represents the equivalent circuit for d and q axis reference based on equation 3.12 (a) and 3.12 (b). U_q and U_d represent the q and d axis reference voltage respectively.

3.2.1.3. Multi-phase or 5 phase permanent magnet generator

The multi-phase has more slots on its stator to occupy more than 3 phase windings [118]. It is known to offer a more power density and better efficiency. The mathematical model included a multiple-reference-frame. The physical quantities of the five phase generator were transformed into two rotating reference frames namely $d1q1$ and $d2q2$. The $d1q1$ frame serves as the fundamental quantity operating at the synchronous speed while the $d2q2$ acts as the third order harmonics of the system operating at three times the synchronous speed. The transformation is given in the following set of equation (3.19-3.27). The electromagnetic torque of the generator is given by equation (3.28) where P_n is the number of poles [118-121].

$$T_{qd0}(\theta_q) = \frac{2}{5} \begin{vmatrix} \cos \theta & \cos(\theta - \frac{2\pi}{5}) & \cos(\theta - \frac{4\pi}{5}) & \cos(\theta + \frac{2\pi}{5}) & \cos(\theta - \frac{2\pi}{5}) \\ -\sin \theta & -\sin(\theta - \frac{2\pi}{5}) & -\sin(\theta - \frac{4\pi}{5}) & -\sin(\theta + \frac{4\pi}{5}) & -\sin(\theta + \frac{2\pi}{5}) \\ \cos 3\theta & \cos 3(\theta - \frac{2\pi}{5}) & \cos 3(\theta - \frac{4\pi}{5}) & \cos 3(\theta + \frac{4\pi}{5}) & \cos 3(\theta + \frac{2\pi}{5}) \\ -\sin 3\theta & -\sin 3\theta(\theta - \frac{2\pi}{5}) & -\sin 3\theta(\theta - \frac{4\pi}{5}) & -\sin 3\theta(\theta + \frac{4\pi}{5}) & -\sin 3\theta(\theta + \frac{2\pi}{5}) \\ \frac{1}{2} & \frac{1}{2} & \frac{1}{2} & \frac{1}{2} & \frac{1}{2} \end{vmatrix} \quad (3.19);$$

$$V_{d1} = R_s i_{d1} - w_e L_{q1} i_{q1} + L_{d1} \frac{di_{d1}}{dt} \quad (3.20);$$

$$V_{q1} = R_s i_{q1} + w_e (L_{d1} i_{d1} + \lambda_{m1}) + L_{q1} \frac{di_{q1}}{dt} \quad (3.21);$$

$$V_{d2} = R_s i_{d2} - 3w_e L_{q2} i_{q2} + L_{d2} \frac{di_{d2}}{dt} \quad (3.22);$$

$$V_{q2} = R_s i_{q2} + 3w_e (L_{d2} i_{d2} + \lambda_{m2}) + L_{q2} \frac{di_{q2}}{dt} \quad (3.23);$$

$$\frac{di_{d1}}{dt} = \frac{-R_s i_{d1}}{L_{d1}} + \frac{w_e L_{q1} i_{q1}}{L_{d1}} + \frac{V_{d1}}{L_{d1}} \quad (3.24);$$

$$\frac{di_{q1}}{dt} = \frac{-R_s i_{d2}}{L_{d2}} - \frac{w_e (L_{d1} i_{d1} + \lambda_{m1})}{L_{q1}} + \frac{V_{q1}}{L_{q1}} \quad (3.25);$$

$$\frac{di_{d2}}{dt} = \frac{-R_s i_{d2}}{L_{d2}} + \frac{3w_e L_{q2} i_{q2}}{L_{d2}} + \frac{V_{d2}}{L_{d2}} \quad (3.26);$$

$$\frac{di_{q2}}{dt} = \frac{-R_s i_{q2}}{L_{q2}} - \frac{3w_e (L_{d2} i_{d2} + \lambda_{m2})}{L_{q2}} + \frac{V_{q2}}{L_{q2}} \quad (3.27);$$

$$T_C = \frac{5}{2} P_n (\lambda_{m1} i_q + \lambda_{m2} i_{q2}) \quad (3.28)$$

Here, subscripts $d1, q1, d2, q2$ refer to the five phase quantities of Park Transformation dq frame; $i_{q1}, i_{d1}, i_{q2}, i_{d2}$ and $V_{q1}, V_{d1}, V_{q2}, V_{d2}$ are the stator currents and voltages corresponding to the rotating reference frame, L_{d1}, L_{q1} and L_{d2}, L_{q2} are inductances(H) of the generator on the $d1q1$ and $d2q2$ axis respectively, R_s is the stator resistance in ohms(Ω), λ_1 and λ_2 are the permanent magnetic flux in (Wb).

3.2.1.4. Double stator permanent magnet generator

As the name implies, it has two stators operating with one rotor. It is much preferable to a single stator construction due to its high torque rating [120]. The dual stator configuration is to have two sets of three phase stator windings. Figure 3.8 shows the 2 sets of dq axis frame for Dual Stator PMSG.

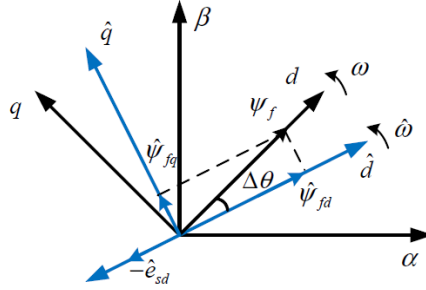


Figure 3.8: dq frame reference of Park Transformation for Dual Stator PMSG

All the physical parameters of the two windings will be made the same for the analysis.

Equations (3.28-3.21) are the Park Transformed dq axis frame representation.

$$u_{sd1} = -R_s i_{sd1} - L_{sd} \frac{di_{sd1}}{dt} + \omega_s L_{sq} i_{sq1} \quad (3.28)$$

$$u_{sq1} = -R_s i_{sq1} - L_{sq} \frac{di_{sq1}}{dt} - \omega_s L_{sd} i_{sd1} + \omega_s \Psi_f \quad (3.29);$$

$$u_{sd2} = -R_s i_{sd2} - L_{sd} \frac{di_{sd2}}{dt} + \omega_s L_{sq} i_{sq2} \quad (3.30);$$

$$u_{sq2} = -R_s i_{sq2} - L_{sq} \frac{di_{sq2}}{dt} - \omega_s L_{sd} i_{sd2} + \omega_s \Psi_f \quad (3.31);$$

$$T_e = \frac{3p_n}{2} [-\Psi_f (i_{sq1} + i_{sq2}) + (L_{sd} - L_{sq})(i_{sd1} i_{sq1} + i_{sd2} i_{sq2})] \quad (3.32);$$

Equations (3.28-3.31) represent voltage equations to 1st and 2nd set of three phase winding respectively where $usd1$, $usd2$, $usq1$, $usq2$, $isd2$, $isd2$, $isq1$, $isq2$ are the voltages and currents of two sets winding respectively. Here, R_s is the stator resistance, L_{sd} and L_{sq} are the inductance components in the d - and q -axis, Ψ_f is rotor flux produced by permanent magnet and ω_s is the rotor electrical angular speed [122]. The electromagnetic torque (T_e) of the generator is given by equation (3.32) where P_n is the number of poles [122].

3.2.2. Modelling in SIMULINK

The mathematical models of each type of generator were implemented in SIMULINK.

Inverse Park Transform function is applied at the end of the model to bring back the original frame to get the terminal data. Figure 3.9 shows the process flow method for building up the model. Figure 3.10, 3.11(a) and 3.11(b) represent the ‘Mask Model’ of 3-phase, 5-Phase and Dual Stator PMSG respectively whereas figure 3.13 shows the entire Simulink model.

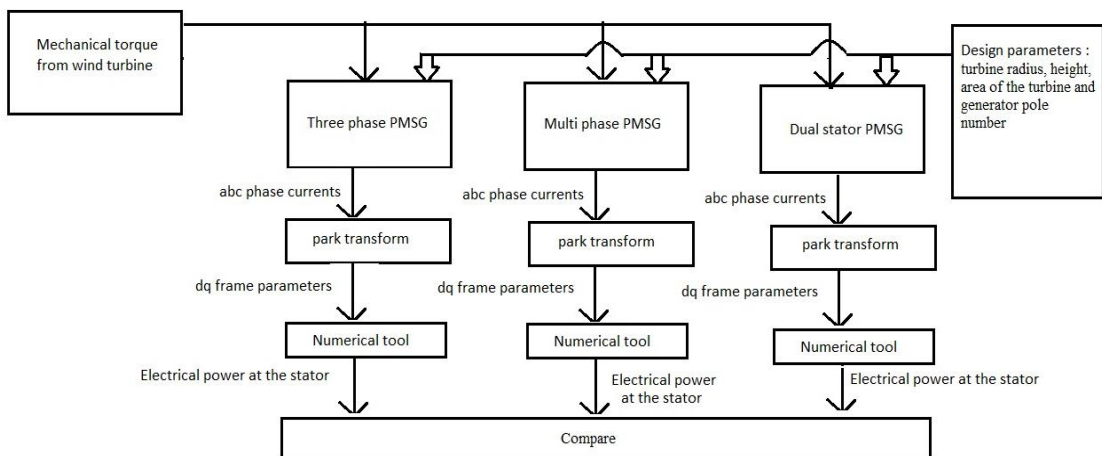


Figure 3.9: Process flow chart of SIMULINK Modelling

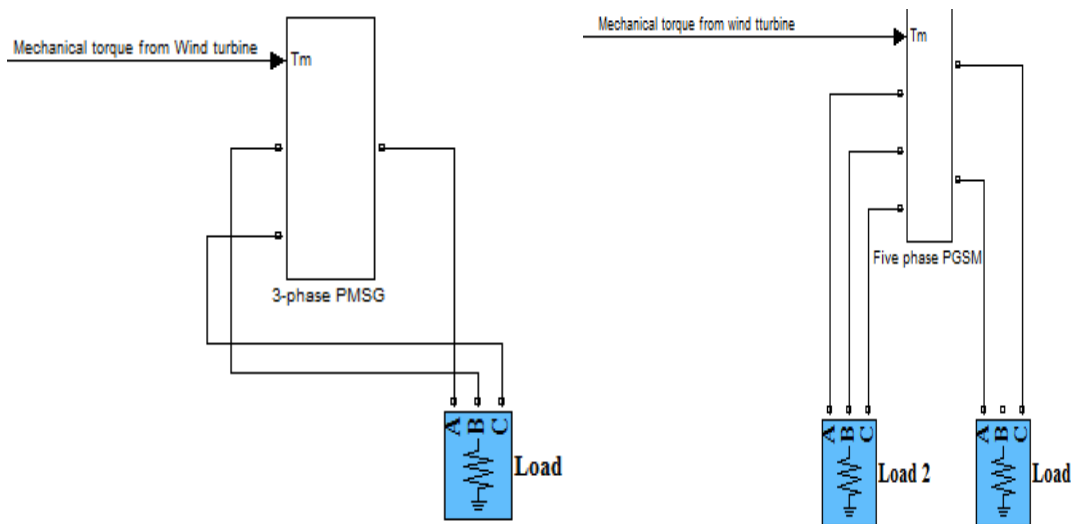


Figure 3.10: Mask Model of 3-Phase PMSG

Figure 3.11 (a): Mask Model of 5-Phase PMSG

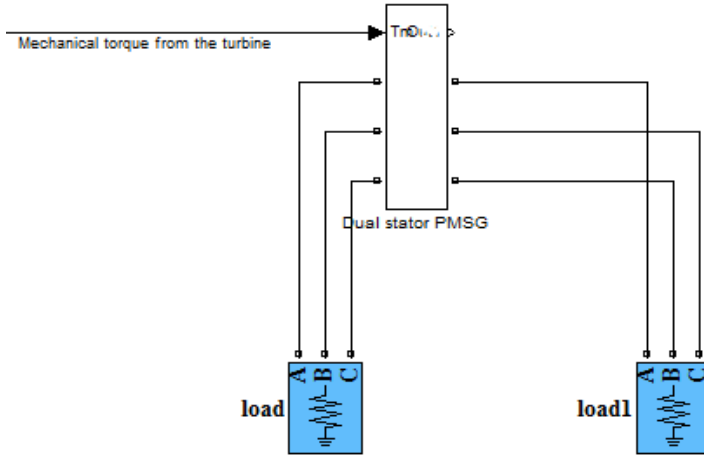
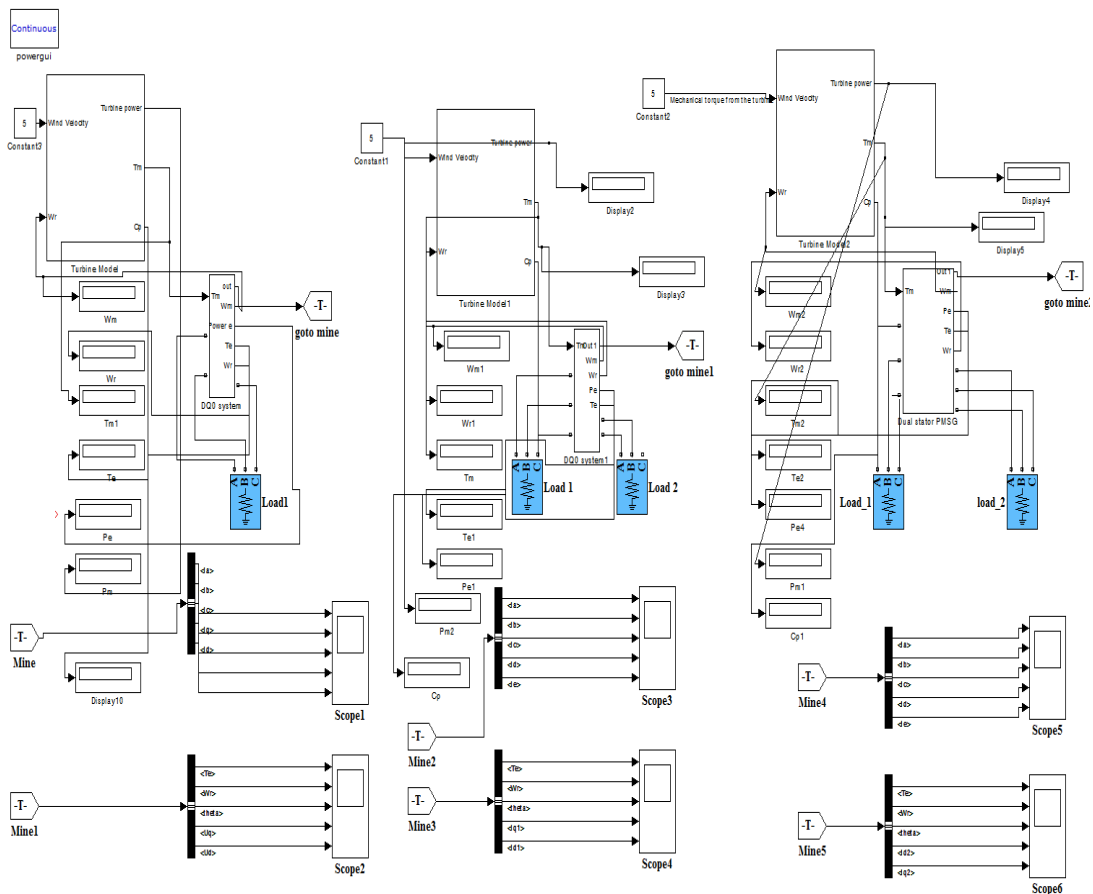


Figure 3.11(b): Mask Model of Dual Stator PMSG



3.12: Matlab Simulation of 3-Phase, 5-Phase and Dual Stator PMSG for VAWT

3.2.2.1. Simulation under Mask inside details:

The mechanical torque produced by the wind turbine is received by the generator model as an input. As it can be seen in figure 3.13, for the 3 Phase PMSG, the

mechanical torque from the wind turbine serves as an input. Based on equations, mentioned above earlier, and the electrical rotating speed used in those equations, the dq reference currents I_d and I_q were constructed. For dq-abc transformation of the currents, the theta from the swing's equation was used. Then abc current was fed to a load. Inside a closed loop operation, the acquired voltage, across each phase of the load, later converted to V_d and V_q which were fed back into the I_d and I_q formulation design. In the same way, for 5-phase, the mechanical torque from the wind turbine was put into the swing's equation subsystem. The abcde currents were fed to a load as it can be observed from figure 3.14. By using voltage measurement blocks, the voltage across each phase of the load was obtained, the value of which was then converted to dqd2q2 reference frames to be fed back into the currents formulation design. Subsequently, the design of 3 Phase was identical to that of Dual Stator but two stators shared one rotor in this case (Figure 3.15). For each of the stator, the abcde current was fed to the load and the voltage across each phase of the load was converted to V_d and V_q to be fed back into the I_d and I_q formulation design.

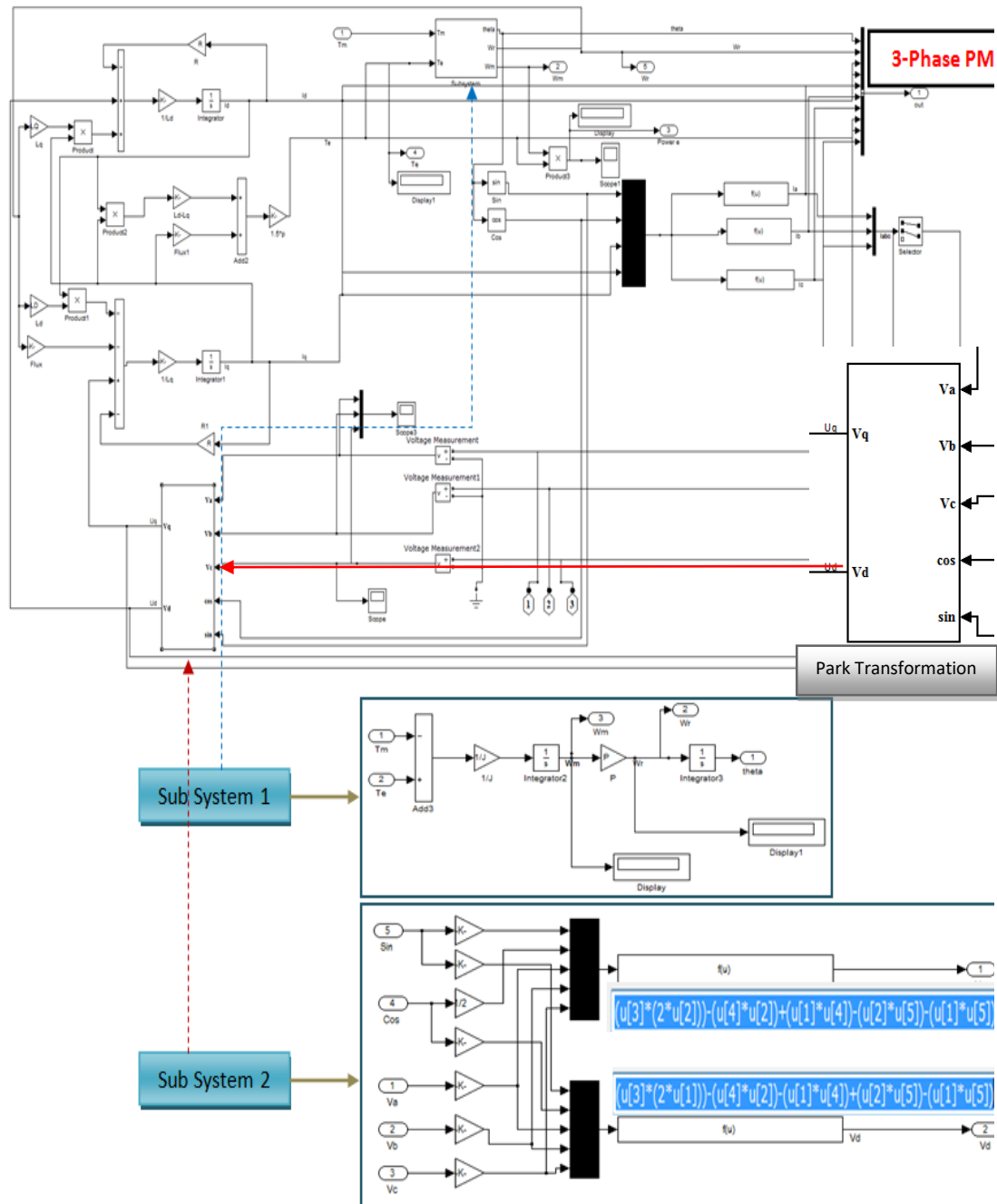


Figure 3.13: Under Mask SIMULINK details of 3-Phase PMSG

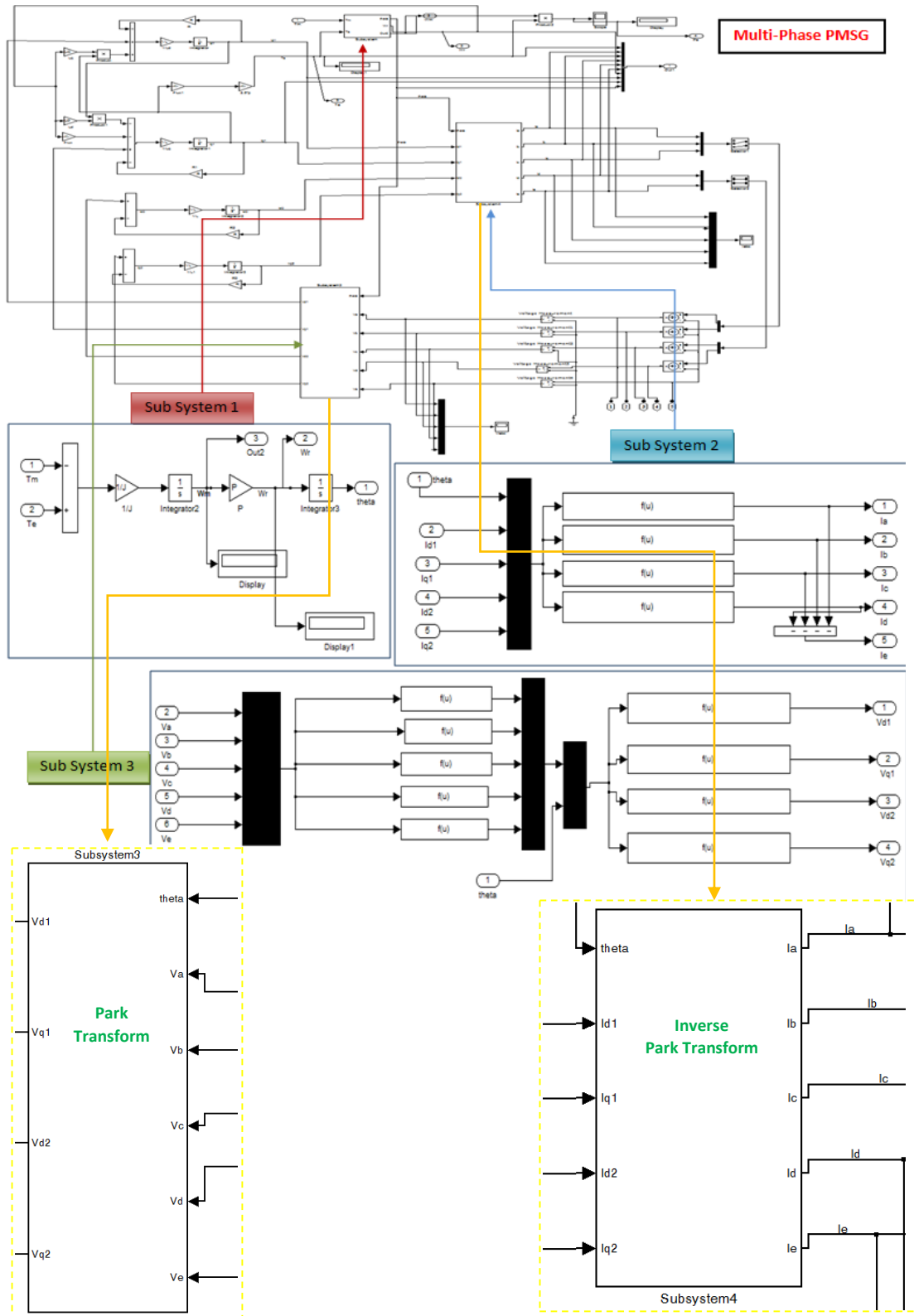


Figure 3.14: Under Mask SIMULINK details of 5-Phase PMSG

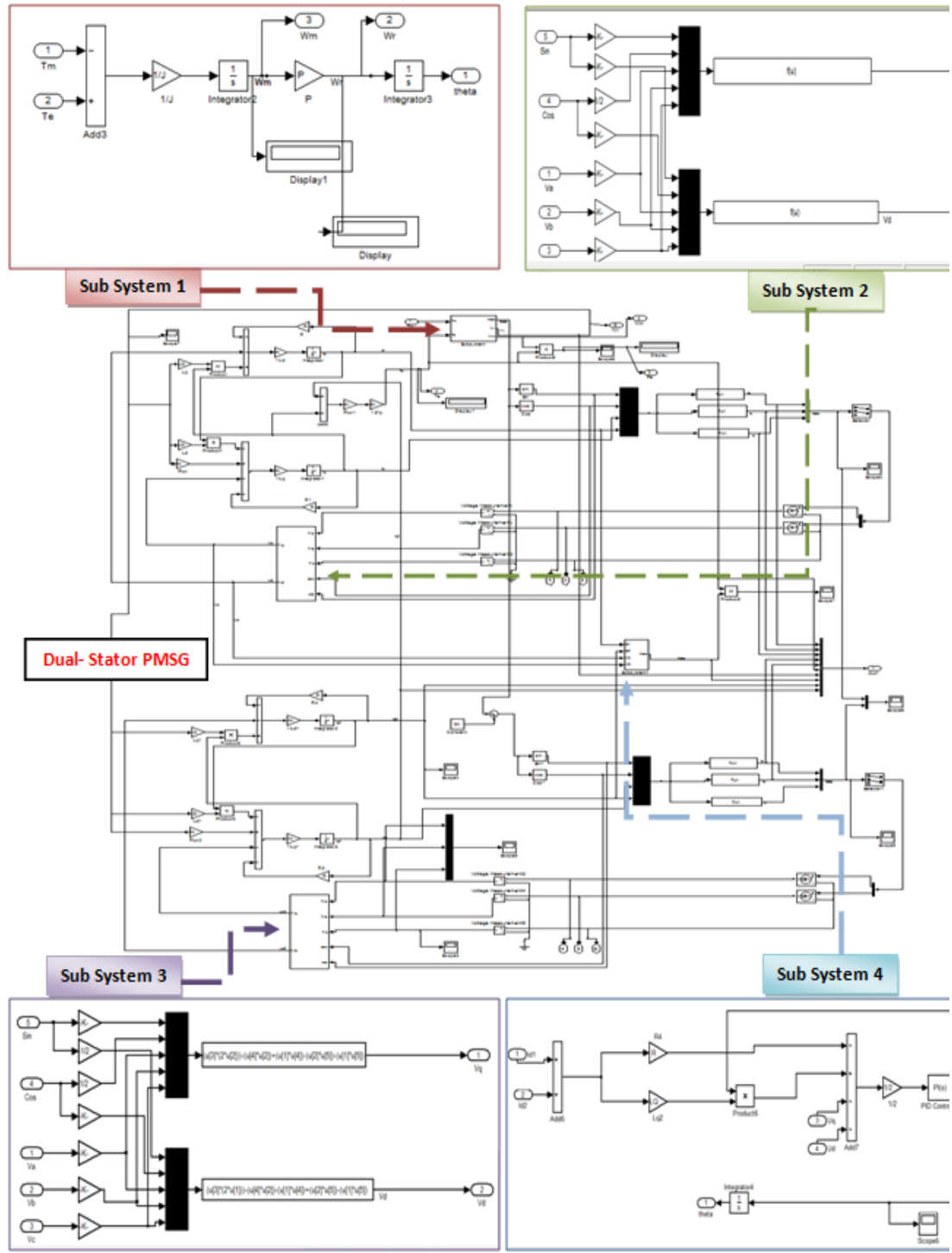


Figure 3.15: Under Mask SIMULINK details of Dual Stator PMSG

3.2.3. Parameter Details

In order to make the system less complicated, PMSG stator resistance, stator inductance, PMSG flux linkage were considered to be same value although in the practical system it may not be same always. Having been done with the Research conducted on previous works in this field [123-127], VAWT and PMSG parameter configuration is given in the following table.

Table 3.1: PMSG Design Parameters

Parameter Value	3 phase PMSG	5 phase PMSG	Dual stator PMSG
VAWT Radius	1.5m	1.5m	1.5m
VAWT Area	2.25m ²	2.25m ²	2.25m ²
Air density	1. 225 kg/m ³	1. 225 kg/m ³	1. 225 kg/m ³
PMSG Stator Resistance	0.435 Ω	0.435 Ω	0.435 Ω
PMSG Stator Inductance	0.199 H	0.199 H	0.199 H
PMSG Flux linkage	0.07 Wb	0.07 Wb	0.07 Wb
PMSG Mass Inertia	0.089 kgm ²	0.089kgm	0.089 kgm ²
Nominal Frequency	60Hz	60Hz	60Hz
PMSG Pole Number	4	4	4
PMSG Load	10KW	10KW	10KW

As different parameter configurations can be observed from table 3.1, the load on the generator was fixed at 10KW. In order to compare all the three types of PMSG generator, a higher rated output power was chosen. For low rated power load, generator output might not vary sufficient enough for all three types. Therefore,

generator load was chosen as 10KW. Here, wind speed was varied as external input and turbine radius, height, area and generator pole, friction factor were changed one by one keeping the others fixed. Rotational speed, torque and power had been achieved, tabulated and graphically analysed. On the other hand, the voltage and current drawn by the generator were also collected for further analysis. PMSG Friction factor is related with Maglev. Implementing Maglev in the system will reduce the friction factor to almost zero. Therefore, friction factor also varied as an implementation of Maglev to observe the voltage and power efficiency.

3.3. Optimization of Permanent Magnet Synchronous Generator based Vertical Axis Wind Turbine

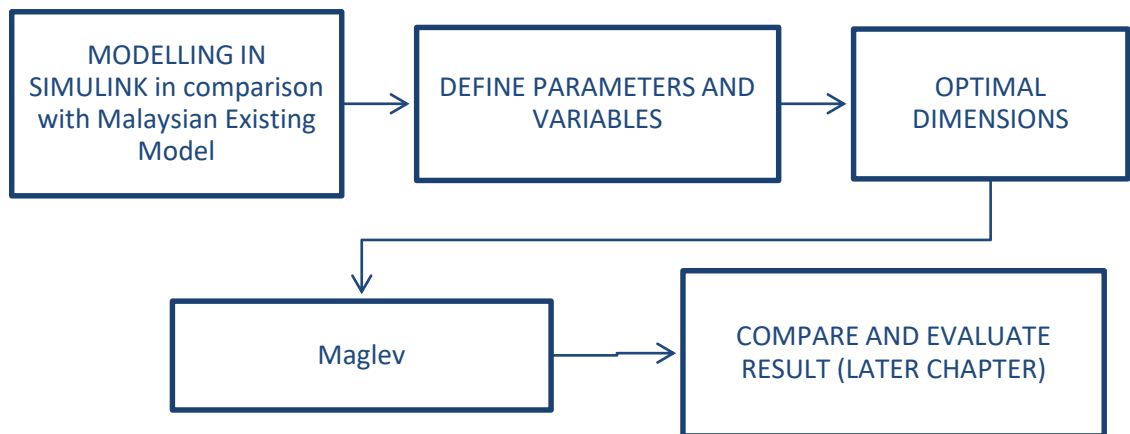


Figure 3.16: Process Flow Chart of Section 3.2

Existing Wind Turbines in Malaysia

Table 3.2: Case 1 Configuration [128]

Location	Turbine Type	Turbine Height (m)	Turbine Diameter (m)	Generator type	Generator Drive	Generator Power rating (W)
Shah Alam	3 Bladed H Type VAWT	2.14	0.5	PMSG	Direct Drive	700

Table 3.3: Case 2 Configuration [129]

Year	Location	Turbine Type	Turbine Height (m)	Turbine Diameter (m)	Generator type	Generator Drive	Generator Power rating (W)
2013	Kuala Terengganu	VAWT	1.5	0.5	PMSG	Direct Drive	1000

Table 3.4: Case 3 Configuration [130]

Year	Location	Turbine Type	Turbine Height (m)	Turbine Diameter (m)	Generator type	Generator Drive	Generator Power rating (W)
2015	Johor Baru	Savonius VAWT	1.5	1	PMSG	Step Up Gearbox	2000

Table 3.5: Case 4 Configuration [131]

Year	Location	Turbine Type	Turbine Height (m)	Turbine Diameter (m)	Generator type	Generator Drive	Generator Power rating (W)
2007	Pulau Perenthian	HAWT	Unknown	Unknown	Unknown	Step Up Gearbox	100k

Table 3.6: Case 5 Configuration [132]

Year	Location	Turbine Type	Turbine Height (m)	Turbine Diameter (m)	Generator type	Generator Drive	Generator Power rating (W)
2012	Penang	VAWT	10	1	PMSG	Fixed Drive	2000

This section focuses on developing an optimal system of Vertical Axis Wind Turbine (VAWT) for low wind speed. After observing the current available system configurations in Malaysia, it was obvious that most of the turbines used Permanent Magnet Direct Drive generator. Therefore, PMSG was used in Simulink to get the optimized result. Turbine height was varied from 1m to 2.6m in different models in the above case examples whereas the diameter was from 0.5m-1m. Therefore, in simulation, a set of height and radius starting from as low as 0.5m was taken. After studying the performance analysis of the turbine parameters for speeds less than 5 m/s, a realistic model was designed in Matlab/ Simulink that could produce suitable torque for low wind condition.

The turbine design parameters such as the radius, height and wind speed were varied to observe the change in generator output voltage and power; and based on that, an

optimal design for Permanent Magnet Synchronous Generator was proposed that can be observed in the result section.

The simulation results were performed with Permanent Magnet Synchronous Generator applying the optimized turbine parameters and were compared accordingly for error calculation. Lastly, future possibility of improvement and the limitations had been proposed to develop the system further.

3.3.1. Modelling

At first, the mathematical formulas of VAWT and PMSG had been put into the design in SIMULINK for both VAWT and PMSG. As far as the turbine concerns, radius, wind speed, area, the power coefficients and pitch angles were made to be the variables whereas turbine mechanical speed, output torque and power were taken as turbine output. Next, three phase Axial Flux PMSG was designed and in the same way simulation was performed for different values of turbine mechanical torque and RPM whereas on the other hand, load voltage, current and power were taken as the output of the generator.

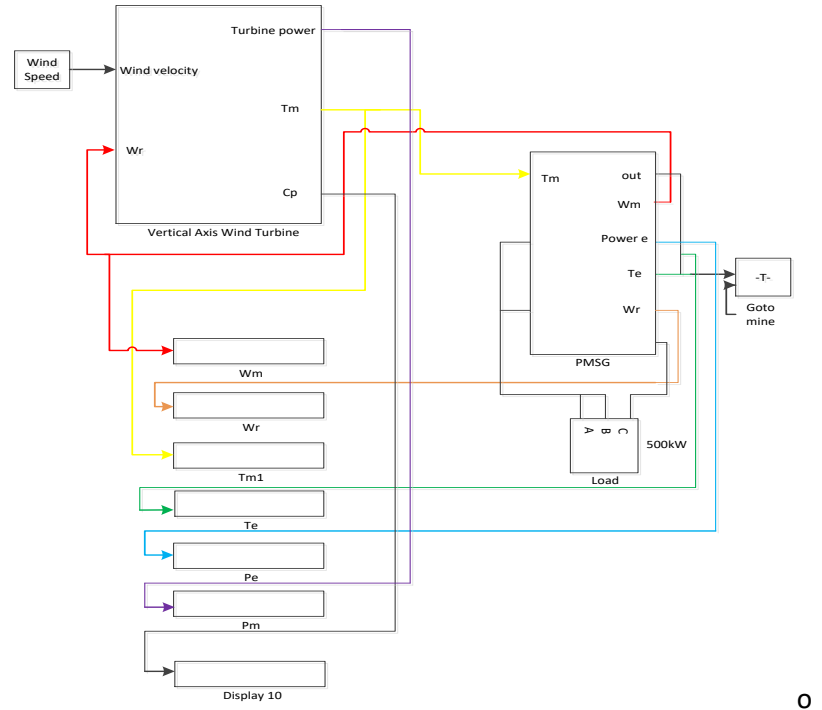


Figure 3.17: Block Diagram of overall simulation model designing

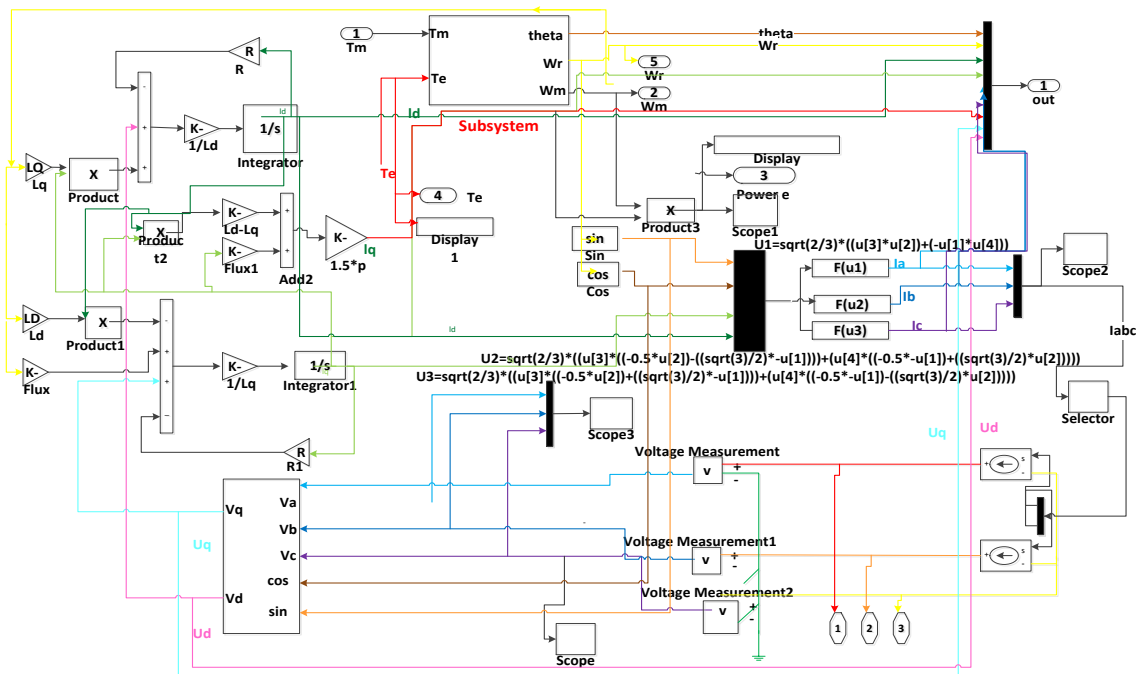


Figure 3.18.a: Modelling of PMSG

The generator mask model, as shown in the figure 3.18.a, takes the mechanical torque generated by the wind turbine as an input and gives out the *abc* phase currents and voltages. The variables used in this model are d axis equivalent inductance L_d in Henry,

q axis equivalent inductance L_q in Henry the stator resistance R_s in Ohms and λ_0 the flux of the permanent magnetic in Wb.

Based on the equations in the previous section [Equation 3.12 – 3.18], the model blocks were designed. Park transform and the swings equations subsystems were essential in the design; they form the backbone of the entire blocks setting. The figure below shows the under the mask look of the 3 phase permanent magnet synchronous generator.

The mechanical torque from the wind turbine serves as an input to the swing's equation subsystem where Equation 3.9 and 3.10 were implemented in order to get the angular position of the rotor (θ) and the electrical rotating speed of the generator (W_e). Figure 3.18.b is the subsystem for implementing the Swing's Equation.

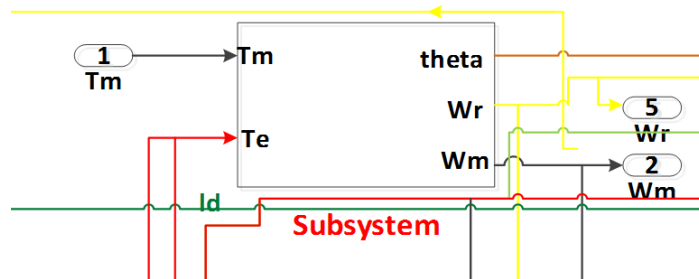


Figure 3.18.b: Modelling of PMSG, Subsystem for Swing Equation

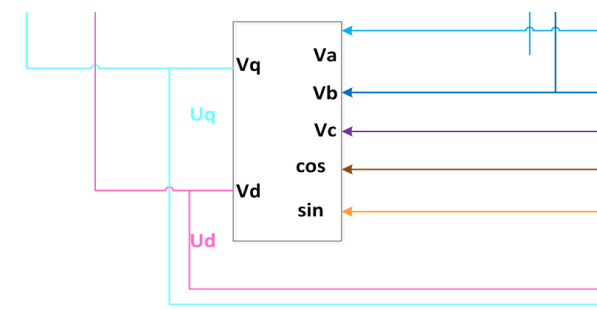


Figure 3.18.c: Modelling of PMSG

The dq reference currents I_d and I_q were achieved implementing Equation 3.15 – 3.16. The theta from the swings equation is used for $abc-dq$ transformation as described by Equation 3.6-3.8. Figure 3.18.c shows the Park Transformation subsystem in Simulink. The generator *output* current is fed to a load which is located outside the mask model (Figure 3.17). The entire cycle is confined in a closed loop continuous operation.

3.3.2. Parameter Designing

Table 3.7: VAWT & PMSG Parameter Configuration for optimization

<i>Model</i>	<i>Parameter Name</i>	<i>Value</i>
VAWT	<i>Air Density</i>	1.225kg/m ³
	<i>Pitch Angle</i>	0
	<i>Cp</i>	0.4412
	<i>Wind Speed</i>	2m/s-7m/s
	<i>Turbine Height</i>	Varying
	<i>Turbine Radius</i>	Varying
PMSG	<i>Stator Phase Resistance</i>	14 ohm
	<i>Inductance (d,q)</i>	0.8mH
	<i>Flux Linkage</i>	0.175V.s
	<i>Inertia</i>	0.089J
	<i>Nominal Frequency</i>	50Hz

The stator resistance of the PMSG was taken as 15Ω ; the inductance was taken as $0.8mH$; the flux linkage of magnet was 0.175 Wb and mass inertia was considered to be 0.089 kg/m^2 . Research had been made on previous works conducted in this field and for the sake of simulation these values were taken as a standard basis [123-128] [133-134]. It is important to note that the Stator Phase Resistance, Inductance, Flux Linkage etc. are not the optimized value for this experiment; rather this set of value, based on previous work, was chosen to apply in all three types of generators in order

to see which type gives the best output. The objective was to observe the change in output power and torque and set turbine radius and height as well as generator rated power, voltage and pole pair.

3.4. Low Cost System Optimization for Rural Malaysia

This sub-chapter discussed the two system configuration in brief and came up with a low cost system which was then sent for fabrication.

A simple but effective ‘Weight to Power Ratio’ technique was used here.

‘Weight to Power Ratio’ is commonly applied to power sources in order to find out the relative cost effective but yet efficient unit or design being compared to a second unit or design. It simultaneously represents efficiency and cost-effectiveness together and indicates which design is better in terms of percentage. [135] [136]

It is important to note that this model tells a relative cost effective scenario in terms of ‘Kg/W’ or ‘ m^2/s^3 ’. It is a measurement of relative cost-effective performance of any engine, motor, generator or power source. It is also used as a measurement of efficiency of a system as a whole, in here, which is the weight (m) of the entire system (PMSG adopted to VAWT) being divided by the PMSG rated output power (P).

It is noteworthy to mention that in ‘Weight to Power Ratio’, ‘Weight’ in this context means ‘Mass’ (m). Weight is the colloquial term often used instead of mass and since then ‘Weight to Power Ration’ has been conventionally used. [135-137]

Physical Interpretation:

$$WPR = \frac{m}{P} \quad (3.33)$$

$$\begin{aligned} \sim \frac{m}{\left(\frac{W}{t}\right)} &= \frac{m}{\left(\frac{FS}{t}\right)} = \frac{m}{\left(\frac{ma \cdot S}{t}\right)} = \frac{m \cdot t}{m \cdot a \cdot s} = \frac{m \cdot t}{\left(m \cdot \frac{v}{t} \cdot S\right)} \\ &= \frac{m \cdot t^2}{m \cdot v \cdot S} = \frac{m \cdot t^2}{\left(m \cdot \frac{S}{t} \cdot S\right)} = \frac{t^3}{S^2} \end{aligned}$$

$$\sim \frac{kg}{W} = mnt^3/m^2$$

$$\text{Efficiency, } \eta = \frac{WPR_1 - WPR_2}{WPR_1} \times 100 \% \quad (3.34)$$

After applying the cost effective technique in the two configurations achieved from the simulation, the better model, in terms of low costing, was sent for fabrication. Lastly, the configuration was also compared with the current existing wind turbines of Malaysia. The brief description of the wind turbines found in rural Malaysia in operation is given as follows:

Cost Analysis of different existing Vertical Axis Wind Turbine Models in Rural Malaysia

Case 1- System configuration and Cost Analysis of H Type VAWT in Shah Alam [128]

Since 2007, in Shah Alam, a 3 bladed H type Vertical Axis Wind Turbine has been operational. The turbine was developed by A. Hossain, A.K.M.P Iqbal, M. Afrin and M. Mazian. A belt power transmission system was used which was designed at the

Thermal Laboratory of Faculty of Engineering, University Industri Selangor. With a diameter of 0.5m and height of 2.1336m, the turbine cost was USD253. The generator capacity was 700W. The price of the generator was not mentioned; however in Alibaba.com, the price of 700W PMSG was stated around USD840. Together with the generator the overall price of the turbine with belt power transmission was roughly USD1093. However, the turbine was not able to perform less than 6m/s.

Table 3.8: Case 1 Configuration and Overall cost

Inventor	Year	Location	Turbine Type	Turbine Height (m)	Turbine Diameter (m)	Generator type	Generator Drive	Generator Power rating (W)	Overall Cost (USD)
A. Hossain, A.K.M.P Iqbal, M. Afrin	2007	Shah Alam	3 Bladed H Type VAWT	2.14	0.5	PMSG	Direct Drive	700	1093

Case 2- System configuration and Cost Analysis of Savonius VAWT in Kuala Terengganu [129]

A. Albani and M. Z. Ibrahim (2013) developed a Vertical Axis Savonius wind turbine which was in operation at Kuala Terengganu. The diameter of the turbine was 0.5m whereas the height of the turbine was 1.5m. A 1KW Permanent Magnet Synchronous Generator was Chosen for the turbine. The turbine was designed to work in low wind speed and it could work under 4m/s wind speed. The cost of the turbine was 250USD. The turbine used to produce 2.4W in 4m/s. The overall cost including the 1KW Permanent Magnet Generator was 1780USD.

Table 3.9: Case 2 Configuration and Overall cost

Inventor	Year	Location	Turbine Type	Turbine Height (m)	Turbine Diameter (m)	Generator type	Generator Drive	Generator Power rating (W)	Overall Cost (USD)
A. Albani, M. Z. Ibrahim	2013	Kuala Terengganu	VAWT	1.5	0.5	PMSG	Direct Drive	1000	1780

Case 3- System configuration and Cost Analysis of Savonius VAWT in Johor Baru [130]

A.S.M.F Aljen and A. Maimun proposed a small current electric turbine system in Johor Baru which could possibly be implemented in rural areas and islands in Malaysia. The developed 4 bladed vertical axis wind turbine was based on Savonius rotor and a 2KW Permanent Magnet Generator was used in their design. The system weighted 57Kg. The diameter of the turbine was of 1m and the height was 1.5m. The turbine used a speed up gearbox that weighted 11kg. In Alibaba, the price of the entire system without the gearbox is more than USD2500. The Cut-in speed of the turbine was 3m/s.

Table 3.10: Case 3 Configuration and Overall cost

Inventor	Year	Location	Turbine Type	Turbine Height (m)	Turbine Diameter (m)	Generator type	Generator Drive	Generator Power rating (W)	Overall Cost (USD)
A.S.M.F Aljen, A. Maimun	2015	Johor Baru	Savonius VAWT	1.5	1	PMSG	Step Up Gearbox	2000	2500

Case 4- System configuration and Cost Analysis of VAWT in Pulau Perenthian [131]

In 2007, Malaysian Government along with Kuala Terengganu's State Government under Joint Venture Partnership established a project in Pulau Perenthian to integrate power supply. The project includes setting up two wind turbine, one Solar Panel, one Generator and a battery. Both the wind turbine units were of 100KW each and were only operational above 6m/s. The estimated cost was for installing a 100KW turbine was more than USD180000.

Table 3.11: Case 4 Configuration and Overall cost

Inventor	Year	Location	Turbine Type	Turbine Height (m)	Turbine Diameter (m)	Generator type	Generator Drive	Generator Power rating (W)	Overall Cost (USD)
State Govt.	2007	Pulau Perenthian	HAWT	Unknown	Unknown	Unknown	Step Up Gearbox	100k	180k

Case 5- System configuration and Cost Analysis of VAWT in Nibong Tebal, Penang [132]

M.E. Al, N. Mohammed and N.H. Hariri installed a low wind speed turbine in Nibong Tebal, Penang in the year of 2012. The turbine was rated 2KW and the height was 10m. It was operational at 6.1m/s and the estimated cost was USD2500. It was located at the Engineering campus in University Sains Malaysia and was operational for 2 years.

Table 3.12: Case 5 Configuration and Overall cost

Inventor	Year	Location	Turbine Type	Turbine Height (m)	Turbine Diameter (m)	Generator type	Generator Drive	Generator Power rating (W)	Overall Cost (USD)

M. Mohammed, N.H. Hariri	2012	Penang	VAWT	10	1	PMSG	Fixed Drive	2000	2500
--------------------------------	------	--------	------	----	---	------	----------------	------	------

Configuration of Proposed VAWT System 1 and Cost Analysis

The 1st proposed optimized system of this research includes a 3 bladed VAWT with 1.5KW Permanent Magnet Synchronous generator with Maglev implementation. The height of the turbine was 2.6m whereas the diameter was 1m. The fabrication cost was in total USD1500.

Configuration of Proposed VAWT System 2 and Cost Analysis

The proposed optimized system of this research includes a 9 bladed VAWT with 200W Permanent Magnet Synchronous generator with Maglev implementation. The height of the turbine was 0.6m whereas the diameter was 0.29m. The fabrication cost was in total USD310.

Table 3.13: Proposed System Configuration and Overall cost

Inventor	Year	Location	Turbine Type	Turbine Height (m)	Turbine Diameter (m)	Generator type	Generator Drive	Generator Power rating (W)	Overall Cost (USD)
Proposed System 2	2016	UNMC, Selangor	3 Bladed VAWT	2.6	1	PMSG	Direct Drive	1500	1500
Proposed System 2	2016	UNMC, Selangor	Hybrid VAWT	0.6	0.29	PMSG	Direct Drive	200	310

The cost analysis comparison table with optimized proposed configuration is given in the result chapter.

3.5. Laboratory Prototype of Vertical Axis Wind Turbine

The aim of this section is to observe, before sending the original hardware design for fabrication, whether the impact of the design parameter is synchronizing with simulation result or not. Figure 3.16 shows the process flowchart of this section. It presents a VAWT, designed using magnetic levitation (Maglev), adopted to a Permanent Magnet Synchronous Generator (PMSG). A lab prototype of VAWT was built which was run at low wind speed of around 3 to 5 meter per second. The bearing was replaced by Neodymium Magnet to avoid the friction which in turns reduces the losses and increase the efficiency. A Prototype version of PMSG was built which could generate voltage from the turbine even in low rotational speed. Suitable turbine blade angle was also determined using trial and error method. The aim of this section is to observe whether the impact of the design parameter is synchronizing with the performance wise before sending the original design for fabrication.

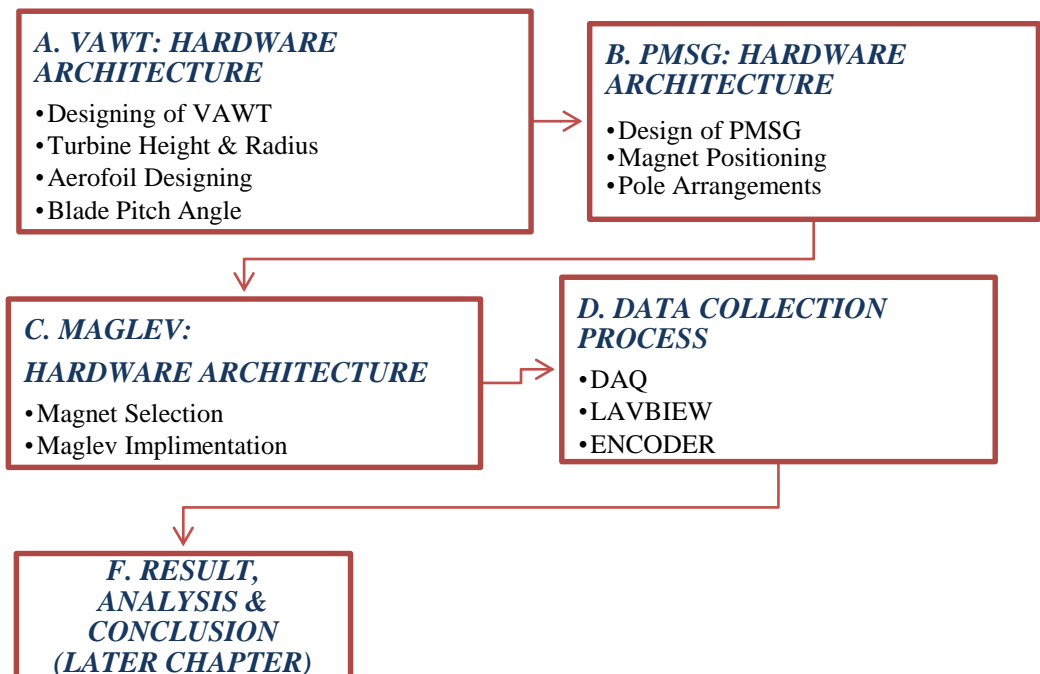


Figure 3.19: Block diagram of Methodology Summary

3.5.1. Hardware Architecture

3.5.1.1. VAWT Design-

The design of VAWT included eight half-oval shape blades as aerofoil attached in between a drum set (figure 3.20). Direction of the blades are set in such a way so that the pitch angle can be varied from 0 to 180 degree (Figure 3.21). All the blades were placed in a circular shape at a same distance with the curve of the drum set. The whole wind turbine was made of plastics material providing a light weight and low cost (figure 3.22). The length of the blade, that was also the height of the turbine, was 60cm, the aerofoil chord diameter was 6.5cm and the radius of the turbine was 14.5cm. The shaft, passing through the centre of the surface from the bottom to the top, was made of wood.

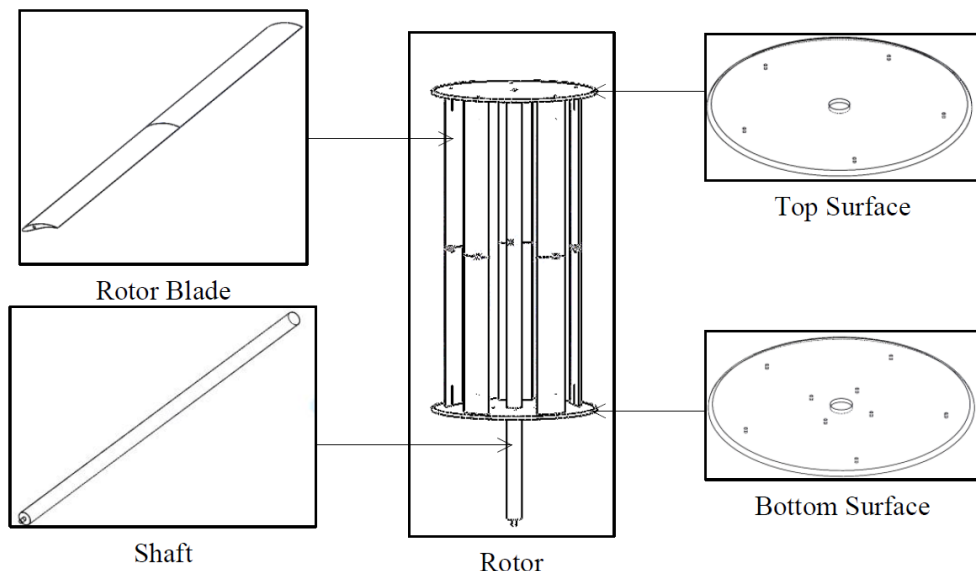


Figure 3.20: Hardware Architecture- Design of VAWT



Figure 3.21: Hardware Architecture- VAWT Blade angle control



Figure 3.22: Hardware Architecture- Prototype of VAWT

3.5.1.2. 3-Phase PMSG design:

Synchronous Generator was used for the system. The magnetic poles were varied from 2 to 8 poles and they were attached to a stainless steel casing. Three phases of permanent magnet synchronous generator is use for transferring the kinetic energy to electrical energy. The PM was designed with 2, 4 and 8 poles respectively. The magnetic poles were placed diagonally to each other and they were glued with epoxy on the inner sides of the casing. Stainless steel was used as a casing to avoid corrosion.

Figure 3.23 shows the arrangements of the magnetic poles attached to the casing whereas Figure 2.24 shows the pole arrangements inside PMSG.

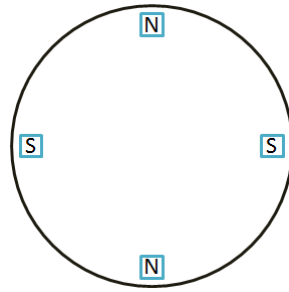


Figure 3.23 (a): 4 poles Arrangements

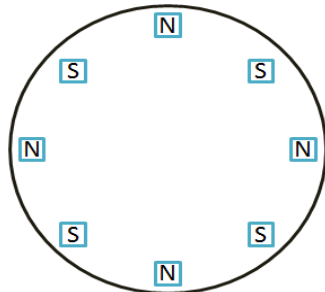


Figure 3.23 (b): 8 poles Arrangements

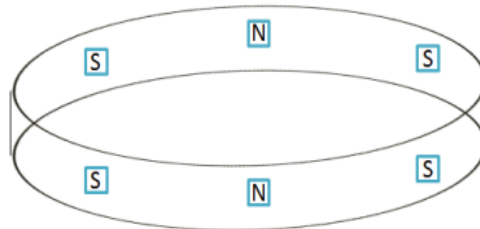


Figure 3.23 (c): Side View of PMSG



Figure 3.24 (a): Magnet poles glued with
epoxy on stainless steel casting



Figure 3.24 (b): 4 Poles 3-Phase PMSG

3.5.1.3. MagLev Implementation with Neodymium Magnet:

The Neodymium NX8CC-N42 magnets were used for the Magnetic Levitation. These magnets were nickel plated to enhance and protect the magnet itself. Two magnets having the same poles faced to each other to create a repelling force, thus can levitate the whole turbine without attaching it with the shaft reducing the friction loss

of the system. Figure 3.25 and 3.26 show the magnets which were placed in the shaft of vertical axis wind turbine.

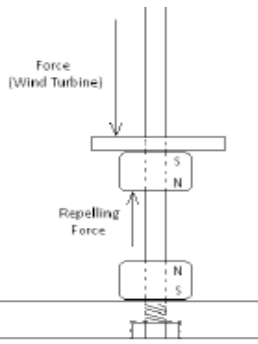


Figure 3.25: MAGLEV
arrangements

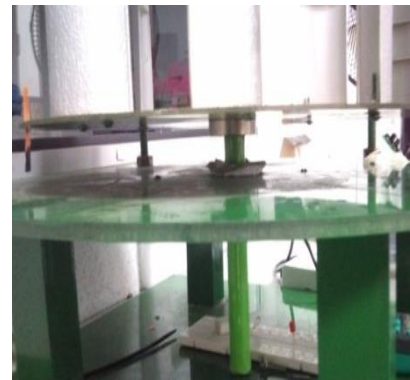


Figure 3.26: Maglev implementation

This maglev technology, served as a useful replacement for ball bearings reducing friction loss to almost as negligible to null. Here Maglev was implemented between the rotating shaft of the turbine blades and the base of the wind turbine system (figure 3.25).

3.5.2. Data Collection Process

Two standing fans were used to give wind speed to the wind turbine. While the wind turbine was spinning, the generator used to produce an AC output voltage which was measured by multimeter. The set-up included a rotary encoder kit (RE08A) followed by NI-USB 6212 Driver which was connected to a laptop. The rotary encoder kit had a 5V power supply from NI-USB 6212 Driver while NI-USB 6212 Driver had power supply from laptop/computer. RE08A is a rotary encoder kit which can convert the data of rotary motion into a series of electrical pulses which is read by controller. When one specific end of the turbine detects one rotation of the turbine, the LED sensor will be turned off and the signal will be sent to NI-DAQ driver which is used for data acquisition (DAQ). LAB View Signal express 2011 program collects the signal from NI-

DAQ driver and gives a digital input. The RPM will then be calculated from the interval of two complete rotations of the turbine. The system was then experimented with some other parameters, giving different speed of wind turbine for rotating and different angle of blades. All the readings were taken down and recorded.

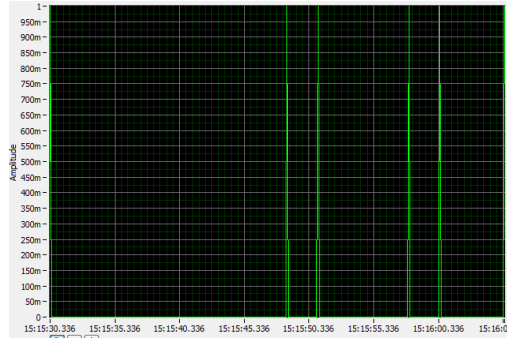


Figure 27: Time interval recording

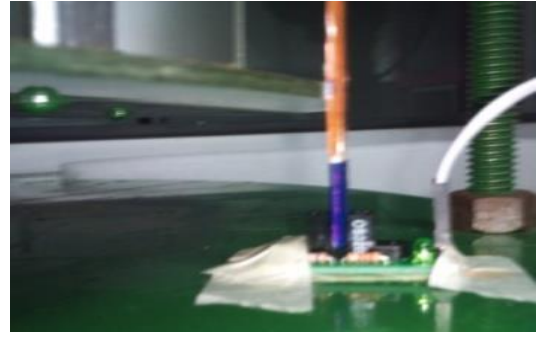


Figure 28: Rotary Encoder Kit (sensor)

Angular Speed of the turbine was measured with the equations below:

The time interval and the number of revolute by the wind turbine are recorded and then calculating to the revolution per second.

$$\text{rev/s} = \frac{\text{number of turns of wind turbine revolute}}{\text{time interval}} \quad (3.33)$$

It is converting to revolution per minute,

$$\text{rpm} = \frac{\text{rev}}{\text{s}} * 60 \quad (3.34)$$

However, it is changing to angular velocity, ω , (radian per second)

$$\text{angular velocity, } \omega = \frac{\text{rev}}{\text{s}} * 60 \quad (3.35)$$

$$\text{linear velocity, } V (\text{m/s}) = \omega r \quad (3.36)$$

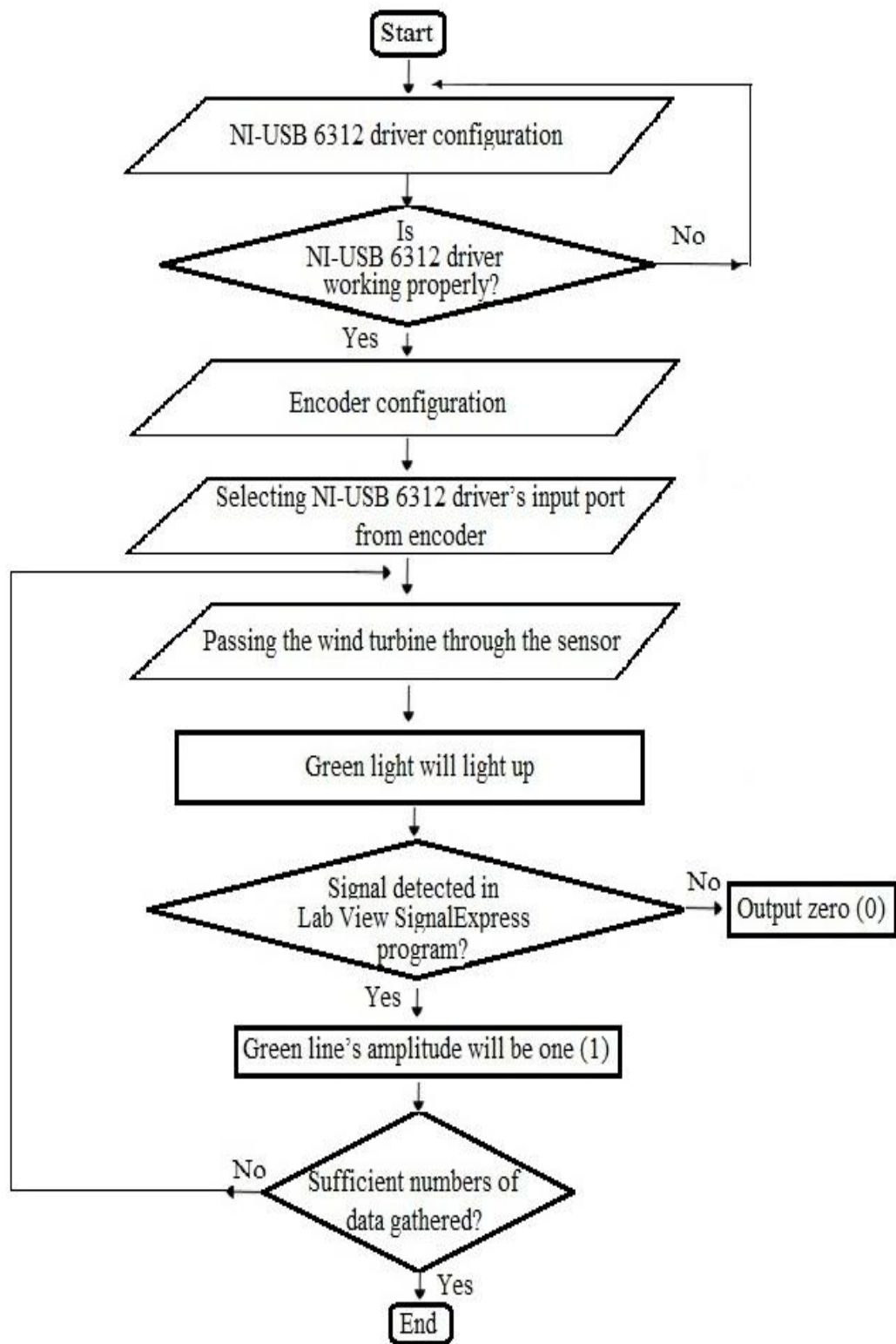


Figure 3.29: Flowchart for data collection from encoder procedure

3.5.3. Experimental set-up

Figure 3.30 explains the overall working process of the laboratory set-up in-brief.

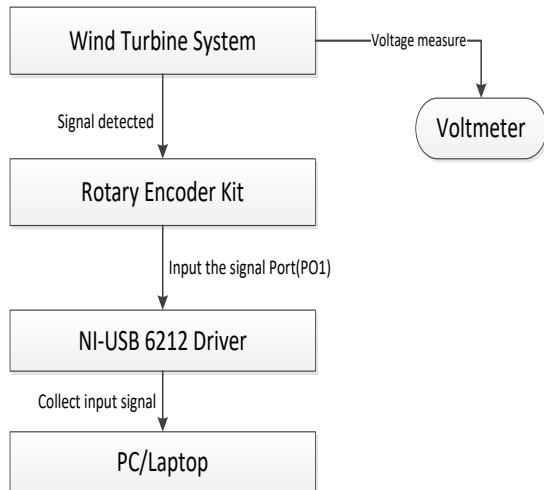


Fig. 3.30 Overall hardware setup for the system.

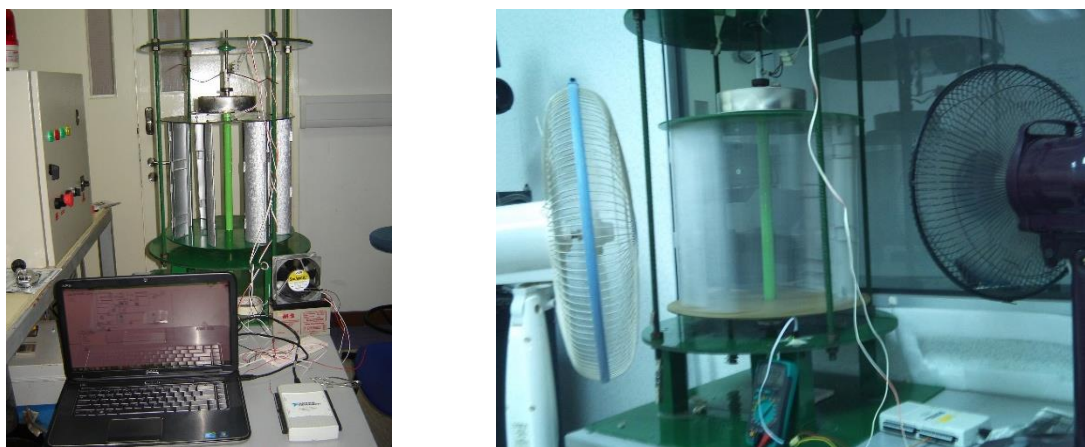


Figure 3.31: Experimental Set-up

Figure 3.31 shows the experimental set-up where the turbine was being rotated with external fans and open circuit voltage was measured by a multimeter. Encoder was passing the signal to Labview through DAQ.

3.6. Energy Harvesting Circuit

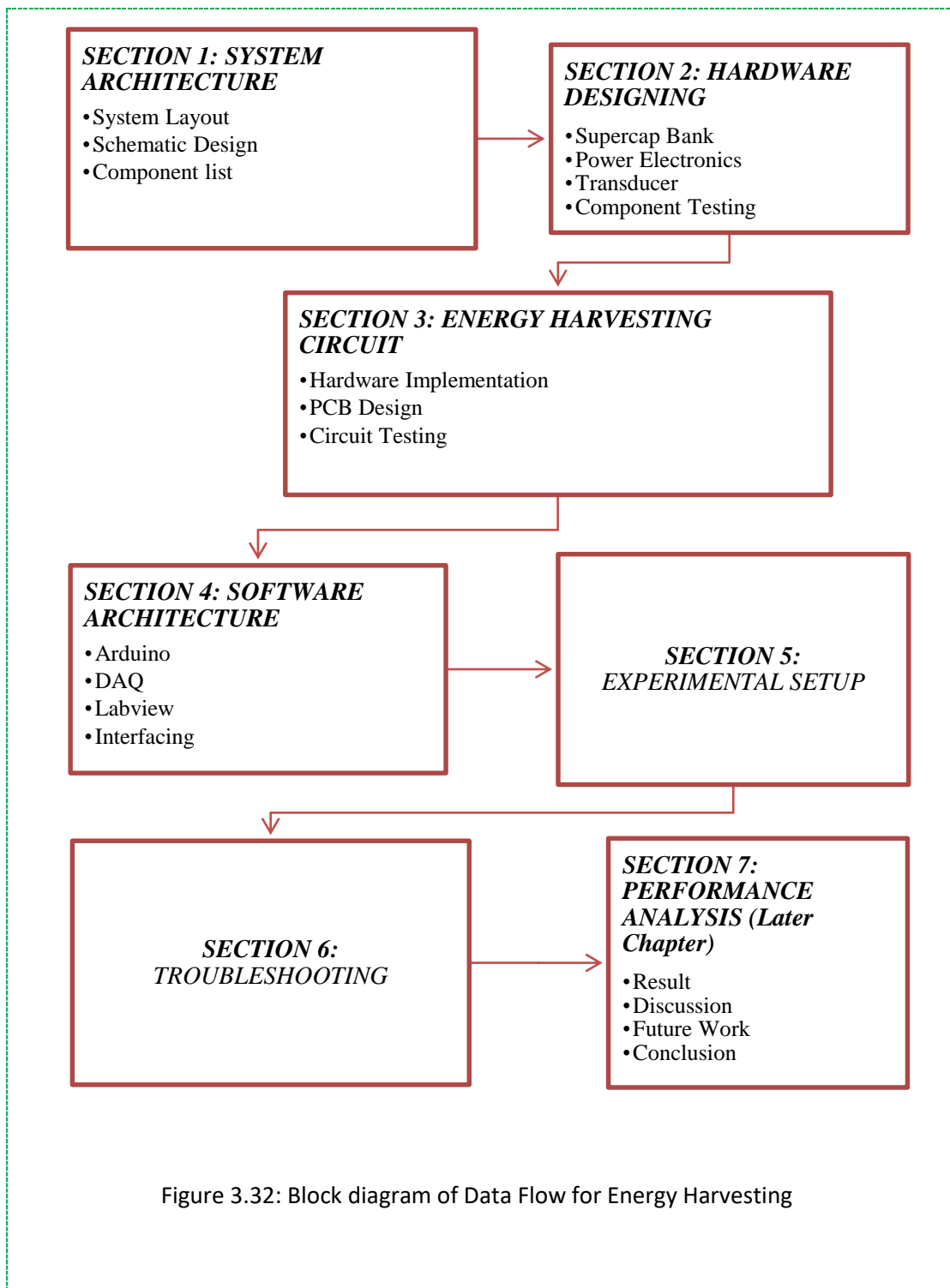


Figure 3.32: Block diagram of Data Flow for Energy Harvesting

3.6.1. System Architecture

From the previous findings, the specifications of MagLev VAWT with PMSG that was chosen for the energy harvesting is given as follows:

Table 3.14: System configuration for Energy Harvesting Circuit

VAWT		
	Wind Speed	: 5 m/s
	Height	: 60 cm
	Radius	: 14.5 cm
	Number of blade	: 9
PMSG	Phase	: 3-Phase
	Rated Power	: 200W
	Rated Voltage	: 12V
	Diameter	: 16cm
Top net weight		: 12.5kg
Generator Open Circuit performance	Open Circuit Voltage	: <ul style="list-style-type: none"> • 8V (Wind Speed 5m/s) • 6.5V (Wind Speed 4m/s) • 3.5V (Wind Speed 3m/s)

As discussed in the literature review, battery and supercapacitors are used together to form a hybrid system. For our circuit, such hybrid energy harvesting device was considered. It was deliberated previously that battery has higher ESR comparing to Supercapacitor which results in high internal loss, thus less efficient compared to supercapacitors. In addition, voltage coming from the generator of turbine is not

constant, wind dependent and may fluctuate. Therefore, a combination of supercapacitor and battery is needed to be employed. Moreover, it can be observed from table 3.14, the highest open circuit voltage ranges from 3.5V to 8V for our low wind speed configuration. As far as low voltage concerns, for batter selection, we are left with two choices; either to work with a battery 6V or 12V. Since we are dealing with low voltage, stepping up a low voltage input to 12V, that has a minimum range of 3V, will result the small amount of current to be stepped down in even smaller amount. With a view of the facts stated above, it was decided to use a 6V battery that has to be charged by the turbine. A Supercapacitor bank were to be placed before the battery which would be charged up by taking the voltage generated from the turbine and subsequently would be discharged through the battery. Since the battery needs a constant voltage for charging up, the system needs of a DC DC boost converter in between the Supercapacitor Bank and Battery give a constant stepped up voltage to the battery while the Supercapacitor bank is being discharged. The field testing was limited to laboratory.

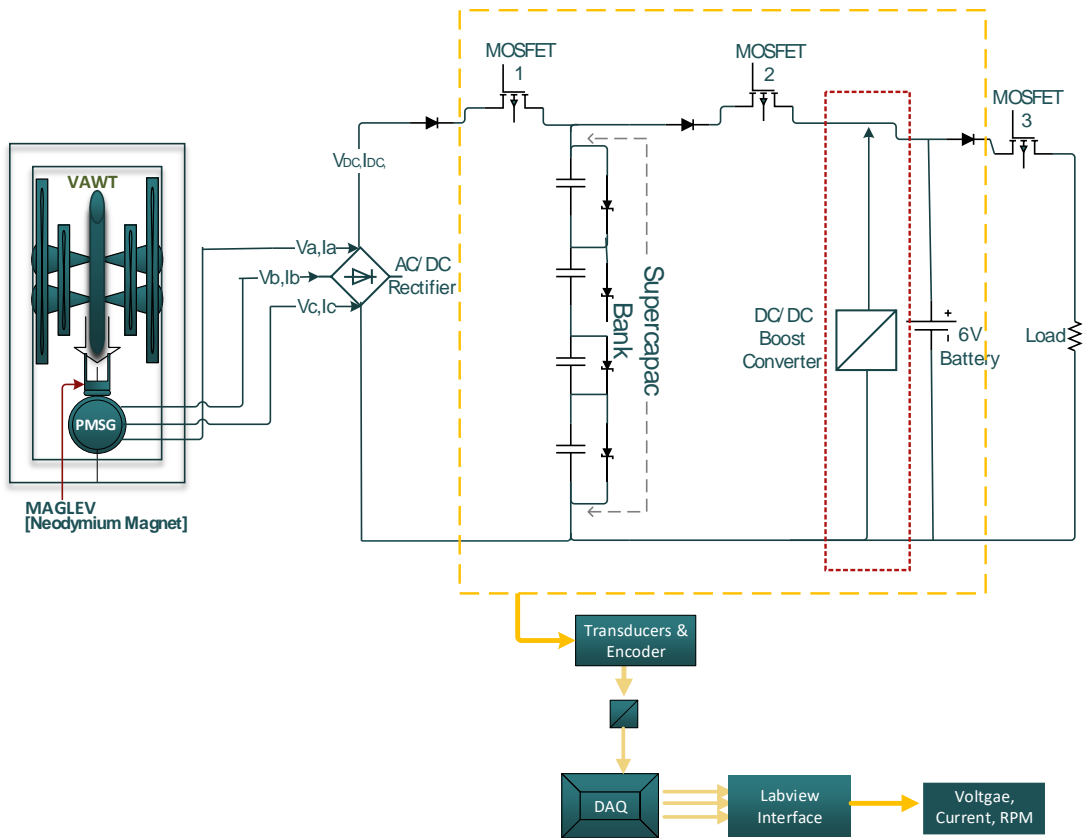


Figure 3.33: Schematic Diagram of System Architecture of Energy Harvesting system

The above is the schematic diagram of the system architecture. Few LED lights along with a 434Ohm resistor were put as loads to discharge the battery.

3.6.2. Hardware Designing

3.6.2.1. Selection of Supercapacitor Bank

As a part of the hybrid energy harvesting, supercapacitors were used to store the charges initially generated by the turbine. In this project, to form a supercapacitor bank, four supercapacitors of 35F each, manufactured by Cooper Bussmann with voltage rating of 2.7 V were placed in a series connection.

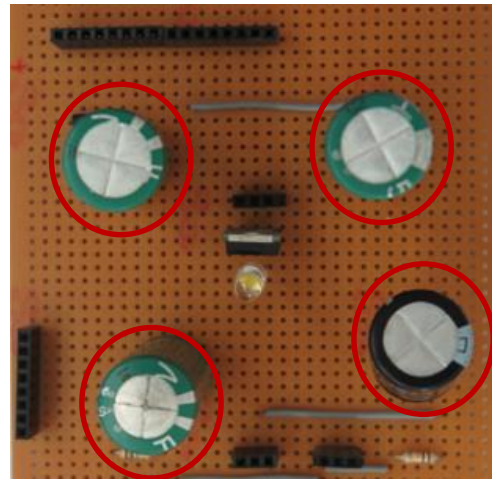


Figure 3.34: Configuration of Supercapacitors on Stripboard

When four supercapacitors are linked in series, total operating voltage, V_t :

$$V_t = V_1 + V_2 + V_3 + V_4 = 2.7 \times 4 = 10.8V$$

When four supercapacitors are linked in series, total capacitance, C_{total} ,:-

$$\begin{aligned} C_{total} &= \frac{1}{\frac{1}{C_1} + \frac{1}{C_2} + \frac{1}{C_3} + \frac{1}{C_4}} \\ &= \frac{1}{\frac{1}{35} + \frac{1}{35} + \frac{1}{35} + \frac{1}{35}} = 8.76F \end{aligned}$$

As a result, a supercapacitor bank with 8.75F capacitance and voltage rating of 10.8V was assembled.

3.6.2.2. Selection of Rechargeable Battery:

There are many variations of batteries present today. Choosing the other part of hybrid energy storage, either non-rechargeable or rechargeable, with different types; such as lithium-ion, lead-acid, nickel-metal-hydride and several more, can be confusing. Comparing to supercapacitors, batteries generally have high power densities, low self-discharge rate and costs less. There are still many negative factors

affecting the batteries such as temperature, slow charging time, low energy density and short life cycle even though they are widely used [136].

Although there were a few better batteries found in the research but they were excluded from the list due to the cost-effectiveness and maintenance difficulties. For example, as a result of additional protection circuit requirement, Li-Ion batteries was omitted; even though have high efficiency and cycle life. Considering all the facts, because of having the optimum characteristics, lead-acid battery remained as the best choice. Throughout this project, a 6 V (3.2AH/20HR), 3 cells, lead-acid battery (figure 3.35), manufactured by Yokohama, was chosen.



Figure 3.35: 6V Yokohama Lead Acid Battery

3.6.2.3. DC-DC Boost Converter

As per the schematic diagram of hardware architecture, a DC DC Boost Converter was used in the system to give a constant voltage of 7.5V to the 6V battery. The “LT1303” micro-power step-up high efficiency DC/DC converter was chosen as they were ideal for use in small, low-voltage battery operated systems. An adjustable version of LT1303 is LT1303 which can supply an output voltage up to 25V. The circuit diagram of LT1303 converter is shown in Figure 3.36.

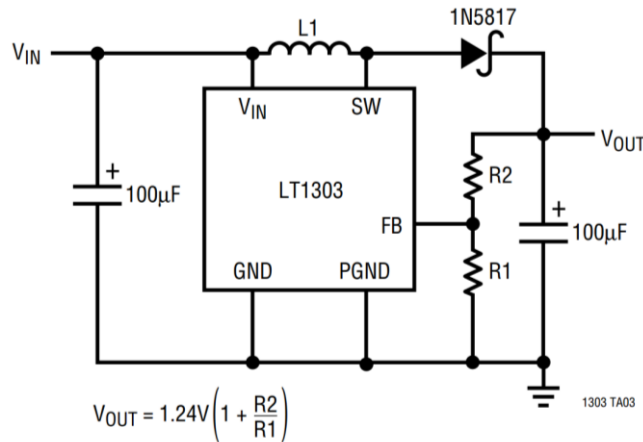


Figure 3.36: Circuit Diagram of LT1303

As suggested in the diagram, an inductor, L_1 of value $10\mu H$ and capacitors $100\mu F$ were connected. Since the constant charge cycle of the battery ranges from 7.4V-7.5V, it was therefore set to 8.18V. The voltage was expected to drop down by 0.6V-0.7V after the load connection, therefore the output at DC DC converter was set as little high. The ratio of resistors R_1 and R_2 was set in order to achieve the desired output. The output voltage can be calculated as shown:

$$V_{OUT} = 1.24 \left(1 + \frac{560K}{100k}\right)$$

$$= \underline{\underline{8.18 \text{ V}}}$$

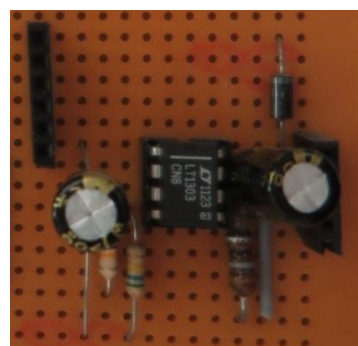


Figure 3.37: Configuration of LT1303CN8 on Stripboard

By setting the $R_1 = 100k$ and $R_2 = 560k$, a constant output voltage of 8.18V can be produced at V_{out} with the minimum input voltage, V_{IN} , as low as 3.5V. For testing purpose, a power supply was used to input different voltage to study the performance of the converter.

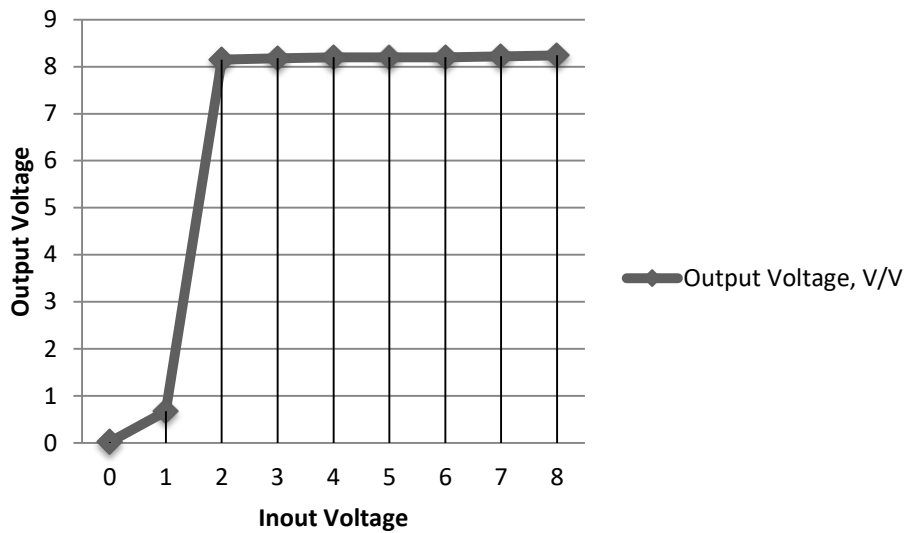


Figure 3.38: Analysis of converter output voltage for a set of input

3.6.2.4. Switches/ MOSFETs:

To control the charging and discharging algorithm of the supercapacitors bank and rechargeable battery, two N-channel MOSFETs were used to act as a switching circuit in this project. In order to verify the suitability and validity of the use of N-channel MOSFET several tests had been carried out. When a PWM pulse with amplitude of 1V was connected to the gate to source; the MOSFET was off. On the other hand, when a 4.8V PWM pulse was applied to the gate to source, it can be seen from figure 3.39 (b) that the MOSFET was switched on. In this project, a 5V PWM was used from Arduino to turn on the MOSFET and 0V to turn off.

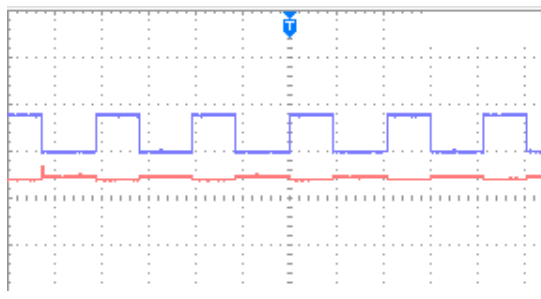


Figure 3.39 (a): Analysis of MOSFET when it is turned off using Oscilloscope

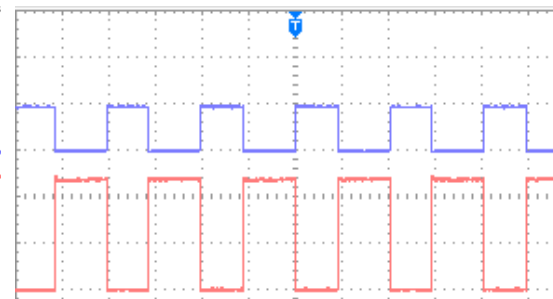


Figure 3.39 (b): Analysis of MOSFET when it is turned on using Oscilloscope

3.6.2.5. Transducers

A vital role in monitoring the physical quantities of an electrical circuit is played by the transducers or sensing circuits. Aiming to provide a corresponding output efficiently and controlled decisions and adjustments, the converted electrical or optical signal obtained from sensing parameters are fed into a microprocessor. The current and voltage transducers used in the system are as follows.

- *Current Sensing Circuit:*

Current monitoring is a fundamental technique in many electronics systems. A sense resistor is placed on the high side, located in between the supply voltage and load, for a high-side current sensing circuit as shown in figure 3.40 (a). For a low-side sensing (figure 3.40 (b)), a sense resistor is placed on the low-side, which is connected to the load and grounded on the other side [138-140]. A high-side current sensing is preferred if the generated current from the wind turbine is basically the measured current flowing through the load [139] [140]. Therefore, for our energy harvesting circuit, a high-side current sensor was chosen.

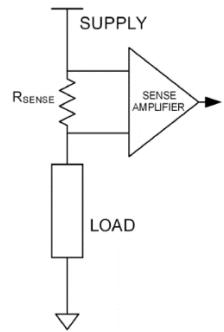


Figure 3.40 (a): High-side Current Sensing Circuit Configuration

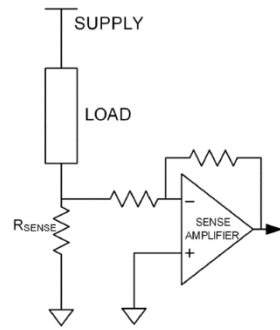


Figure 3.40 (b): Low-side (right) Current Sensing Circuit Configuration

Here, a low offset high-side current monitor, namely ZXCT 1022, was used to read the value of current. The circuit diagram and the stripboard form are shown in figure 3.41 (A) and 3.41 (b) respectively. It is noteworthy to remark that value of R_{sense} was set to the 0.1Ω and V_{out} was connected to the analog input pin of the Arduino microprocessor. The actual current flow in the load was measured using a Multimeter and recorded to observe the accuracy.

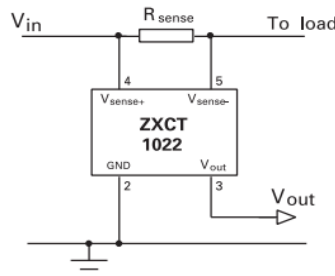


Figure 3.41 (a): ZXTT Current Sensor Pin configuration and Circuit diagram

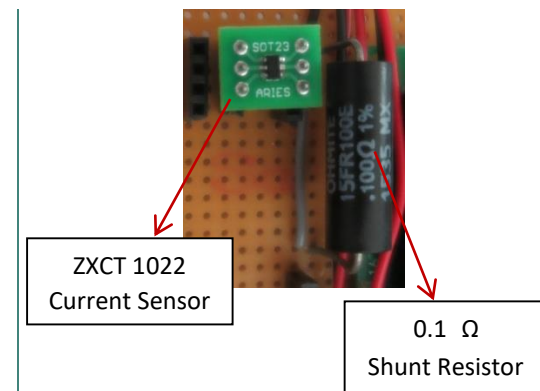


Figure 3.41 (b): Configuration of Current Sensing Circuit on Stripboard

Percentage of Error: Actual Current Vs Measured Current

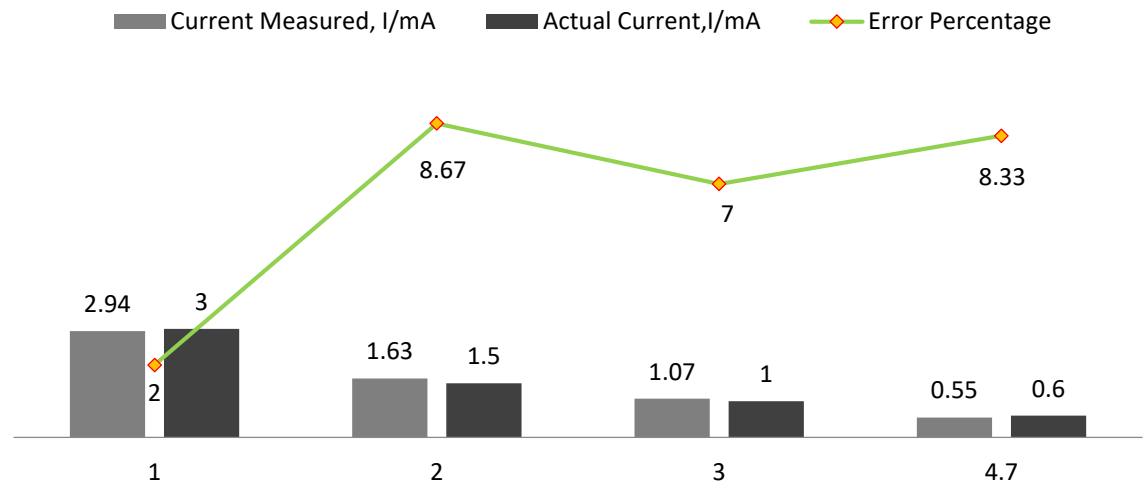


Figure 3.42: Accuracy of Current Transducer

Result shows a highest 8.67% fluctuation from the original value. Now it was high percentage of error if higher amount of current was supposed to be measured. But since throughout the process, a very low amount of current (mA range) would be dealt with, the error percentage would not matter a little for the project.

- Voltage Sensing Circuit:

To sense the voltage input into a circuit, a voltage sensing circuit was used. A simple voltage divider circuit was structured to detect the voltage in this project. The signal is then processed and sends into the microcontroller as shown in figure 3.43.

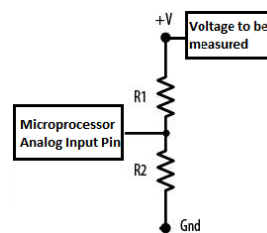


Figure 3.43 (a): Voltage Sensing Circuit

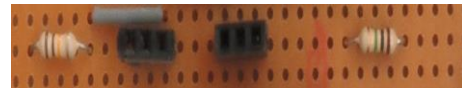


Figure 3.43 (b): Configuration of Voltage Sensing Circuit on Stripboard

The ratio of R_1 and R_2 resistors should be a complete number so that the calibration in the coding would be accurate to create an error-free voltage divider. Here, R_1 and R_2 were set to be $10\text{k}\Omega$ and $100\text{k}\Omega$ respectively which were considerably large enough to prevent current flow into the circuit. Again Multimeter was used to check the accuracy of the circuit. Highest fluctuation measured was 0.93% making the circuit good enough for the system.

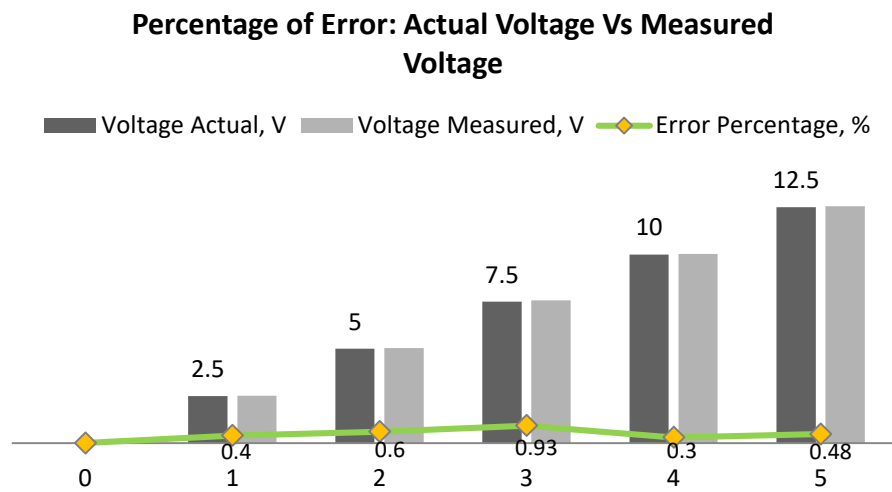


Figure 3.44: Accuracy of Voltage Transducer

3.6.2.6. Rotary Encoder

To measure the rotational speed of the wind turbine, a rotary encoder (figure 3.45a) was used for this project. As presented in figure 3.45b, it was installed at the base of the turbine. It could sense the rotation and send the signal to Labview through DAQ. Simple digital binary signals of on and off was being used there. It sent logic high

whenever the marked turbine blade cuts through the encoder; or else logic low. To count the number of logic high per minute, counter was used in labview.

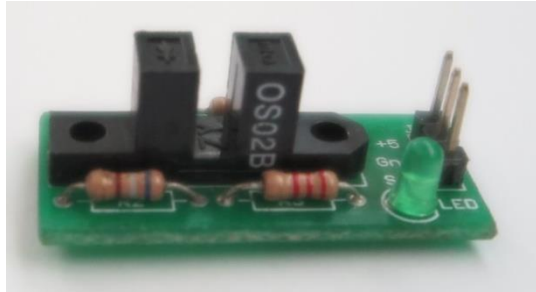


Figure 3.45 (a): Rotary Encoder RE08A



Figure 3.45 (b): Rotary Encoder Installed
on Wind Turbine

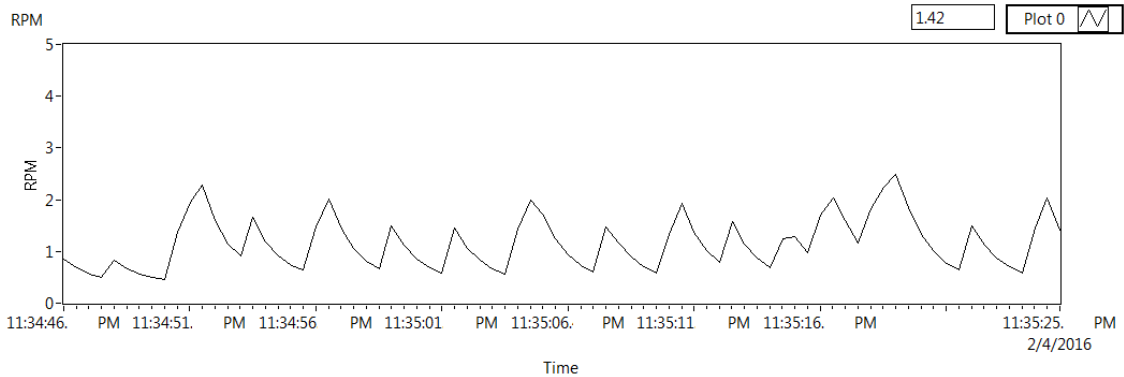


Figure 3.46: Rotary Encoder using LabVIEW

Figure 3.46 is an example of calculation of RPM from the labview. While the turbine was rotating, encoder counted 15 spikes or logic high (15 complete rotation) in 40 seconds and calculated RPM as follows:

$$\text{Revolution per minute, RPM} = \frac{15 \times 60}{39} = 23 \text{ RPM}$$

3.6.2.7. Anemometer

In this project, an anemometer, shown in figure 3.47, was used to measure the wind speed. The measurements obtained from this particular device were in miles

per hour (mph). Hence, the conversion of units from mph to m/s was required as shown.



Figure 3.42: Anemometer

3.6.2.8. Liquid Crystal Display (LCD)

In this project, for displaying of the power and most importantly the current flowing through the load a ‘16x2 LCD’ screen was used. LCD screen had to be connected to Arduino.



Figure 3.43: LCD Screen Displays the Load Current and Power Consumption

Figure 3.43 displays the LCD screen of current and power consumed under a specific load condition. A series of DC LED lights with 1kOhm resistor were used as load so that the battery could discharge though it.

3.6.3. Energy Harvesting Control System

In this energy harvesting system, switching circuit plays a vital role. Two N-channel MOSFETs namely, P36NF06L, with the aid of Arduino UNO microprocessor, were used in this project to create the switching condition in energy harvesting circuit. A LED was placed in parallel to the gate-source pin of the MOSFET for testing purpose.

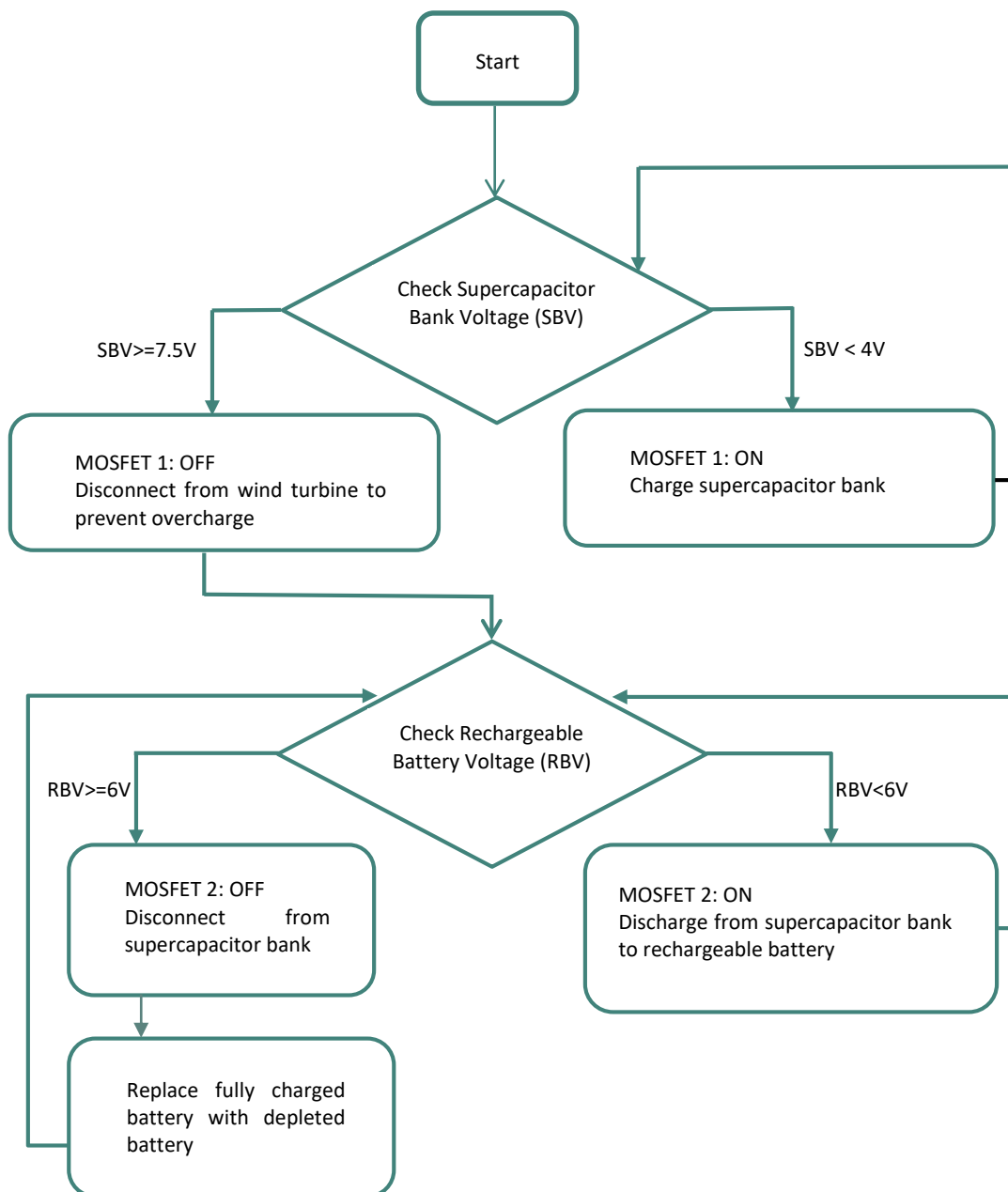


Figure 3.44: Flow Chart of Energy Harvesting Control Algorhythm

The indication of the MOSFET being turned on was figured by the LED. The decision-making switching algorithm flow chart is illustrated in figure 3.44. MOSFET 3 is all time turned off unless stated otherwise. It is significant to declare that even though the MOSFET 3 does not have any role in the control system, it is put in the circuit if battery needed to discharge to the load manually. Therefore unless stated otherwise, MOSFET3 will be considered as an open circuit all the time.

3.6.3.1. Condition 1- Charging Supercapacitor from Wind Turbine Circuit

Figure 3.45 shows the supercapacitor charging circuit. This condition occurs when V_{Supercap} was less than 4V. MOSFET 1 was turned on so that the wind turbine could charge up the supercapacitor bank. In this period of time, MOSFET 2 was turned off which basically isolated the battery from the Supercap.

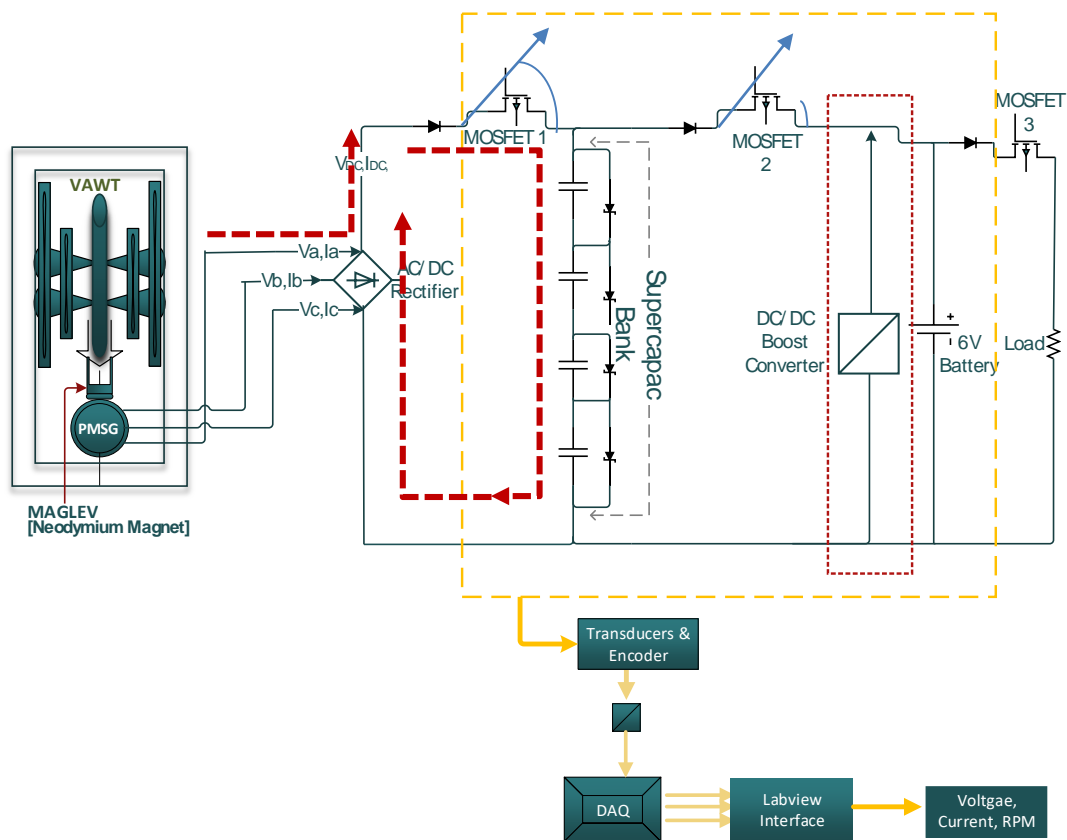


Figure 3.45: Charging Supercap from VAWT

3.6.3.2. Condition 2: Discharging Supercapacitor Bank to Rechargeable Battery

This condition occurs when V_{Supercap} is greater or equal to 7.5V, MOSFET 1 then was turned off to prevent overcharging from the wind turbine, while MOSFET 2 was turned on. At this point of time, the rechargeable battery was charged up to the battery rated voltage, 6V. MOSFET 1 would be switched on again as soon as the voltage of supercapacitor dropped to 4V (Fig. 3.46).

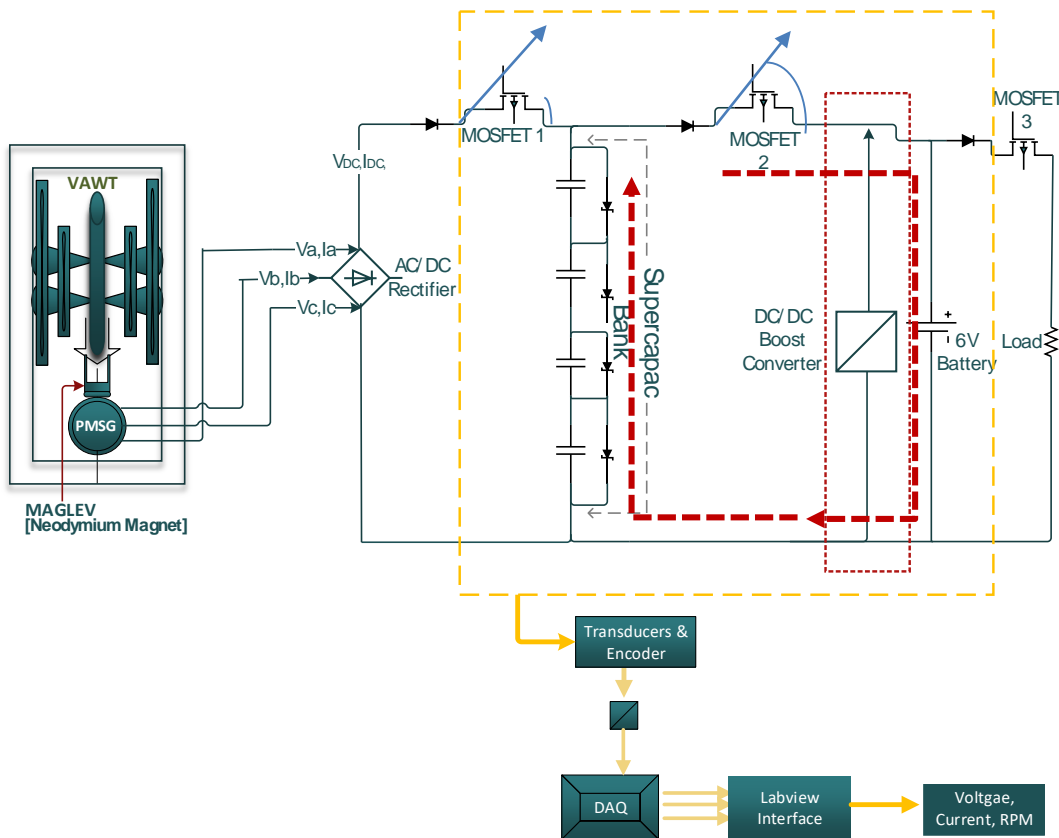


Figure 3.46: Charging Battery from Supercap

Until the battery was charged up to 6V, the charging and discharging process would be continued. The MOSFETs placements in the stripboard of the energy harvesting circuit was given in figure 3.47. Two LEDs are put aligned with the bias voltage. To indicate its logic high close circuit status, LED would light on whenever the MOSFET was turned on and vice versa.

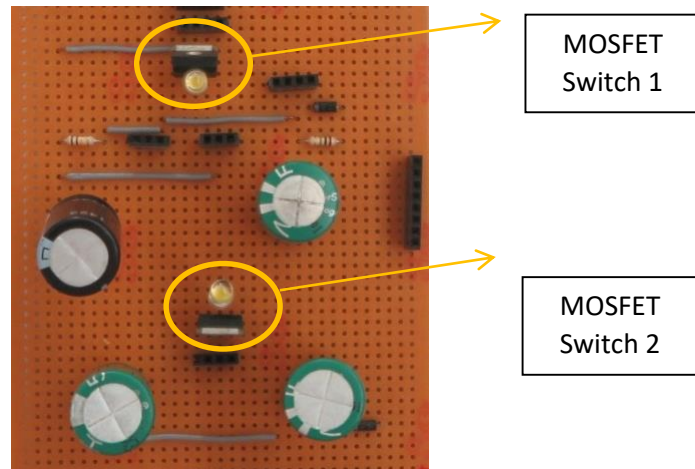


Figure 3.47: Configuration of Switching Circuit on Stripboard

3.6.4. Software Architecture

3.6.4.1. Sensing Circuit

```

int volt_batt;
float voltage_batt;

void setup(){
  Serial.begin(9600);
}

void loop(){
  volt_batt = analogRead(A0);
  voltage_batt = volt_batt*(5.0*11/1023);
}
  
```

Figure 3.48: Sensing Circuit Coding in Arduino IDE

As it can be seen in figure 3.48, the setup function was used to activate the serial communications, at 9600 bits per second, between Arduino Board and computer. In the main loop, a variable namely *volt_batt* was declared to store the resistance value. The function *analogRead* was used to get the resistance value and fed into the Arduino microprocessor. A *float* type variable (*voltage_battery*) was formed to store the value

ranging from 0-1023 obtained from the resistance value, the corresponding value of voltage could be converted using the following equation:

$$voltage_batt = volt_batt \times 5.0 * 11 / 1023 \quad [\frac{R_1}{R_1+R_2} = \frac{10k}{10k+100K} = \frac{1}{11}],$$

The same concept was applied to the current sensing circuit. Since $V = IR$, the voltage value obtained was divided by the resistance value to the corresponding magnitude of current drawn in the circuit.

3.6.4.2. Energy Harvesting Control System

```

if (voltage_cap >= 7.5)
{
    digitalWrite(MOSFET1,LOW);
    digitalWrite(MOSFET2,HIGH);
}

else if (voltage_cap < 4)
{
    digitalWrite(MOSFET1,HIGH);
    digitalWrite(MOSFET2,LOW);
}

```

Figure 3.49: Switching Circuit Coding in Arduino IDE

Simply by setting the conditions of switching algorithm in an “if” statement, the switching circuit could be coded, after obtaining the desired voltage values as featured in figure 3.49.

The basic working principle of this part of code is very simple. A signal “LOW” corresponding to 0V was sent to the Arduino digital pin assigned to “MOSFET 1”. As soon as the voltage across the supercapacitor bank exceeded 7.5V, MOSFET1 would be switched off to prevent overcharging. A signal “HIGH” which equals to 5V was sent to Arduino digital pin “MOSFET 2” at the same time and the rechargeable battery then

would be charged up by supercapacitor bank. Now, a signal “HIGH” would be sent to one of the Arduino digital pins assigned “MOSFET 1” as soon as the voltage across supercapacitor bank would smaller than 4V. A signal “LOW” equivalent to 0V was sent to Arduino digital pin assigned to “MOSFET 2” at the same time. This charging and discharging of supercapacitor bank algorithm repeated simultaneously until battery becomes fully charged.

3.6.4.3. DAQ & Labview

Data acquisition was implemented using NI-6212 device (figure 3.50). The graphical user interface (GUI) for this project was created using LabVIEW. A user friendly GUI enabled the user to be able to monitor and analyze data. Figure 3.51 shows the block diagram of Labview interface whereas the front panel GUI of the LabView is shown in figure 3.52 and 3.53(a). The parameters that can be monitored from this GUI are the supercapacitor and battery voltage, current drawn by the Supercap while charging, current drawn by the battery while the Supercap being discharged and the rotational speed of the turbine through the encoder. The data from the graph could also be exported to Excel. This enabled user to keep track and acknowledge the current status of the system (figure 3.53b).



Figure 3.50: NI USB- 6212 DAQ

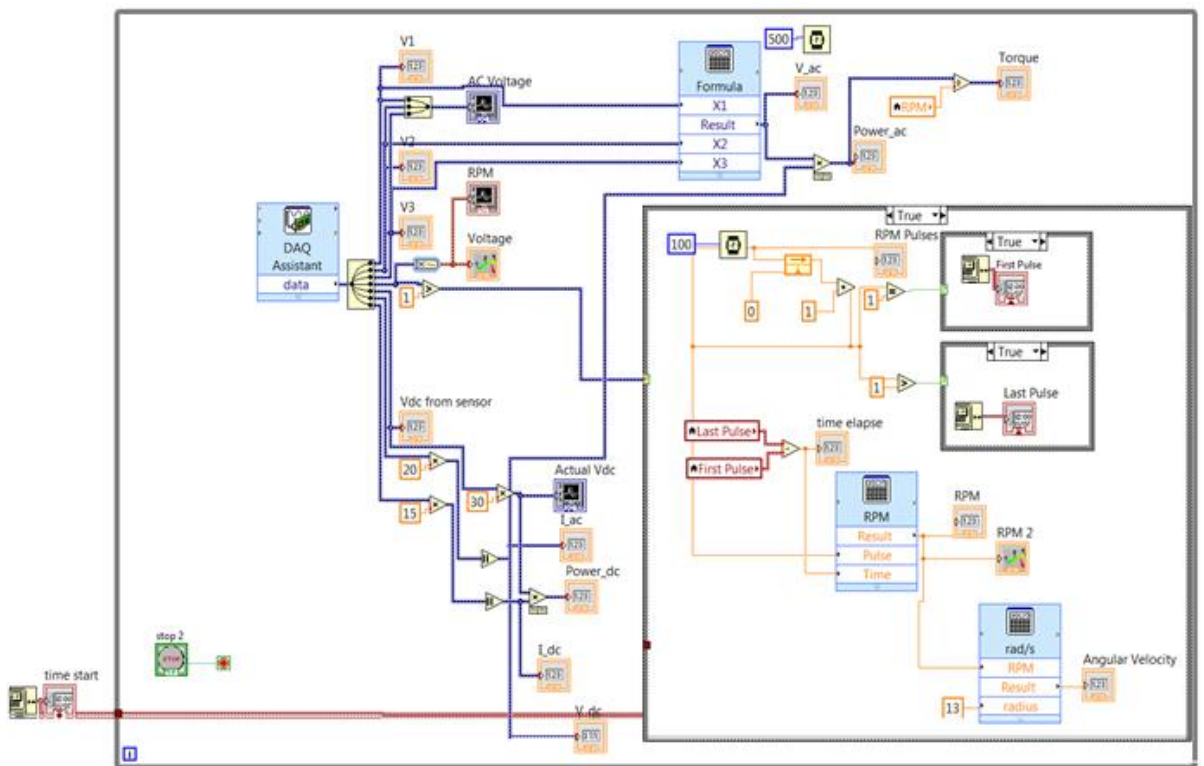


Figure 3.51: LabVIEW Block Diagram

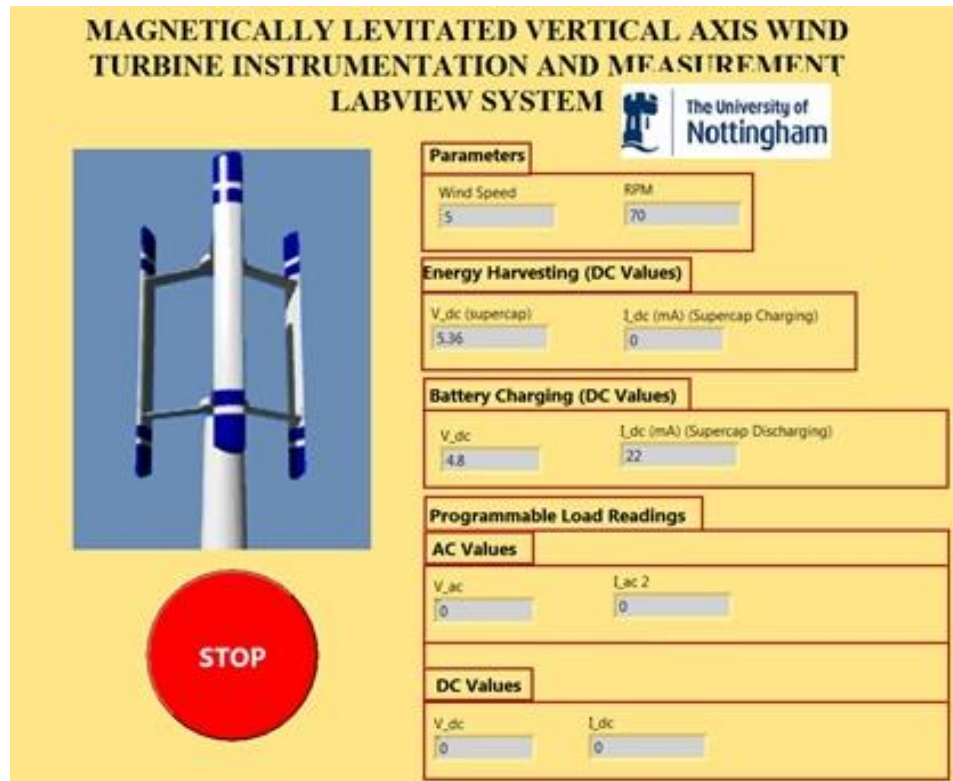


Figure 3.52: Front Panel of LabVIEW GUI Design

A	B	C	D	E	F	G	H	I	J
Time	Supercapacitor 1	Time	Supercapacitor 2	Time	Supercapacitor 3	Time	Supercapacitor 4	Time	Battery
2 8:00:01 AM	1.7717	8:00:01 AM	1.1286	8:00:01 AM	0.0851	8:00:01 AM	0.0751	8:00:01 AM	4.3092
3 8:00:02 AM	1.7717	8:00:03 AM	1.1311	8:00:03 AM	0.0876	8:00:03 AM	0.0776	8:00:03 AM	4.3167
4 8:00:03 AM	1.7692	8:00:06 AM	1.1361	8:00:06 AM	0.0876	8:00:06 AM	0.0776	8:00:06 AM	4.3167
5 8:00:04 AM	1.7692	8:00:08 AM	1.1386	8:00:08 AM	0.0876	8:00:08 AM	0.0776	8:00:08 AM	4.3167
6 8:00:05 AM	1.7717	8:00:09 AM	1.1386	8:00:09 AM	0.0876	8:00:09 AM	0.0751	8:00:09 AM	4.3167
7 8:00:06 AM	1.7717	8:00:11 AM	1.1436	8:00:11 AM	0.0851	8:00:11 AM	0.0776	8:00:11 AM	4.3167
8 8:00:07 AM	1.7717	8:00:12 AM	1.1411	8:00:12 AM	0.0876	8:00:12 AM	0.0751	8:00:12 AM	4.3167
9 8:00:08 AM	1.7692	8:00:14 AM	1.1461	8:00:14 AM	0.0876	8:00:14 AM	0.0776	8:00:14 AM	4.3167

Figure 3.53 (a): Data exported to Excel spreadsheet from LabVIEW

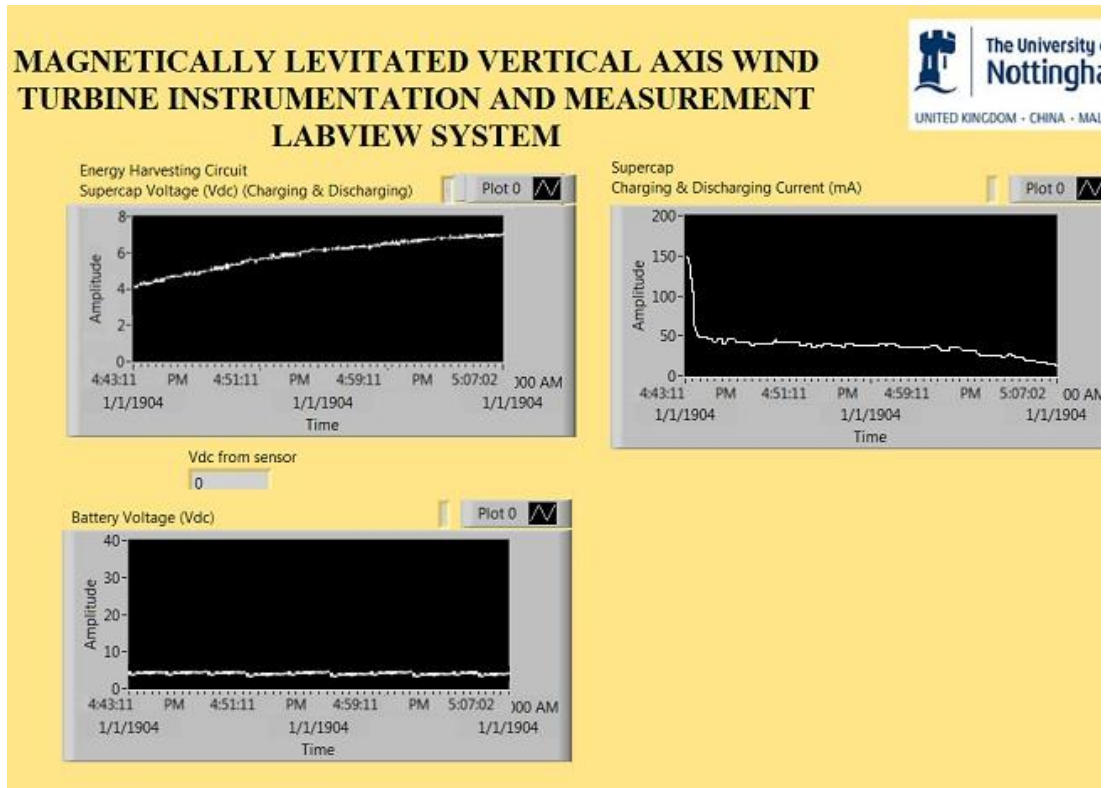


Figure 3.53 (b): LabVIEW Graph Panel GUI Design

3.6.4.4. Experimental setup

Figure 3.54 and 3.55 illustrate the energy harvesting circuit built and the experimental set-up of it respectively. The field testing was carried in the Research Building, Block N, University of Nottingham Malaysia Campus.

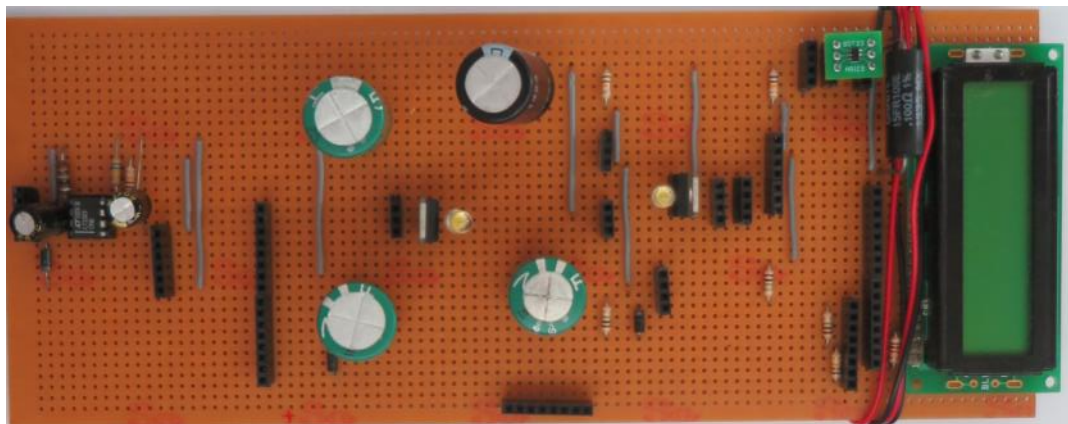


Figure 3.54: Energy Harvesting Circuit Built on Stripboard

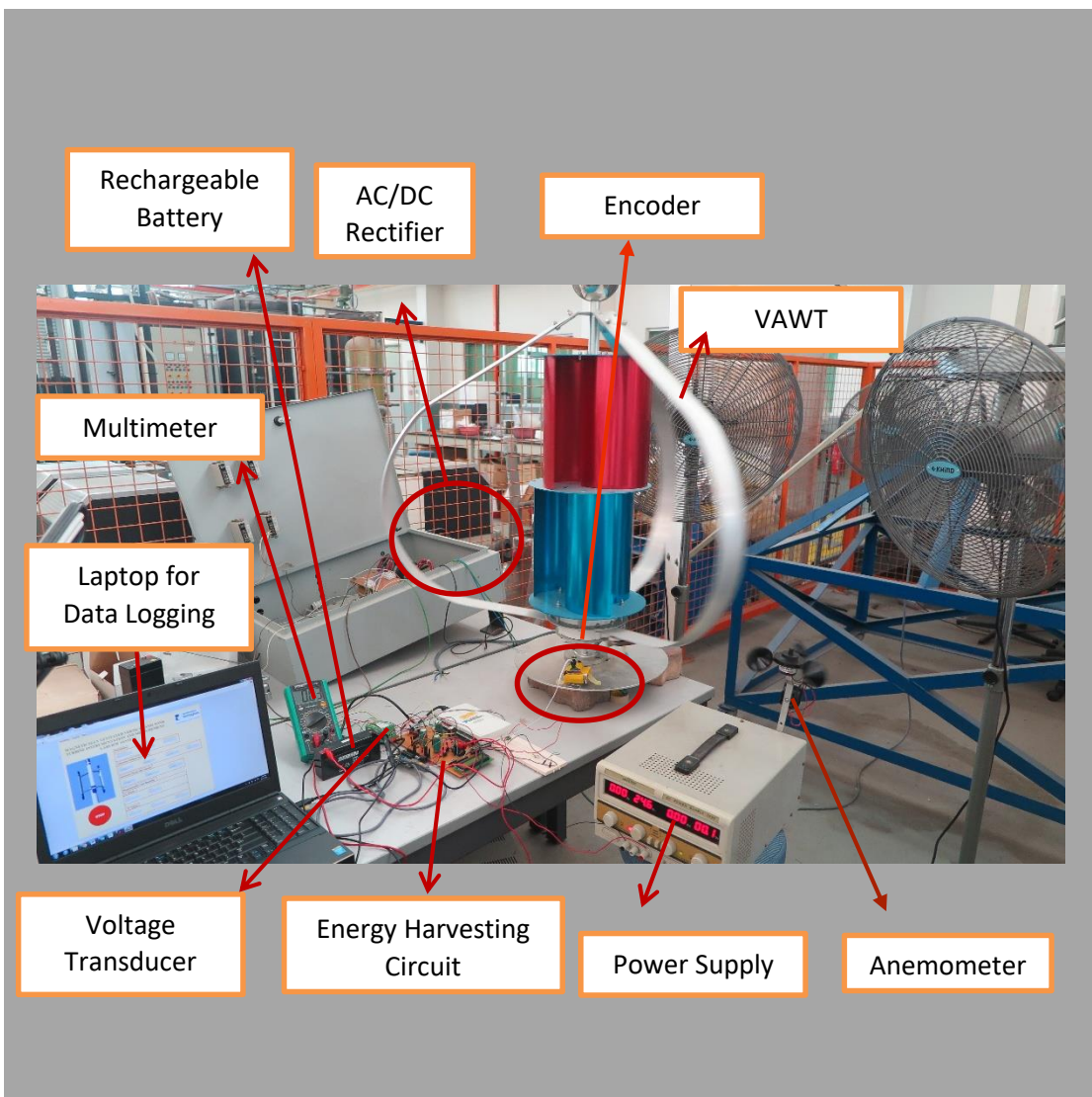


Figure 3.55: Experimental Setup for the Integrated System

Chapter 4

Results and Discussion

‘Results and Discussion’ chapter consists of 6 parts. First two parts provides simulation result of VAWT and PMSG respectively. Third part brings the first two sections together and gives entire simulation data of VAWT connected to PMSG which is analysed further in comparison with rural Malaysian existing model. Part 4 includes low cost optimization of the entire VAWT system for rural Malaysia. Here, configuration of few existing wind turbine models is given with an overall cost for each model. Later, our proposed system is compared in terms cost wise. Part 5 provides the results of experimental set-up of a Laboratory prototype of a Maglev Based VAWT. Part 7 makes available the battery charging result through the energy harvesting circuit into three separate configurations and concludes the chapter with efficiency comparison of energy harvesting circuit with direct charging of the battery from turbine.

4.1. Design and Simulation of Vertical Axis Wind Turbine

4.1.1. Comparing the Simulation Data with theoretical value

At first a simulation was made to compare the result with theoretical value using equations taken from mathematical model in the methodology. A set of values namely ‘Air Density’ of 1.23 kg/m^3 , ‘Pitch Angle’ of 0, ‘Power Co-efficient’ of 0.4412 was taken in consideration. Simulation was performed under the wind speed of 5m/s.

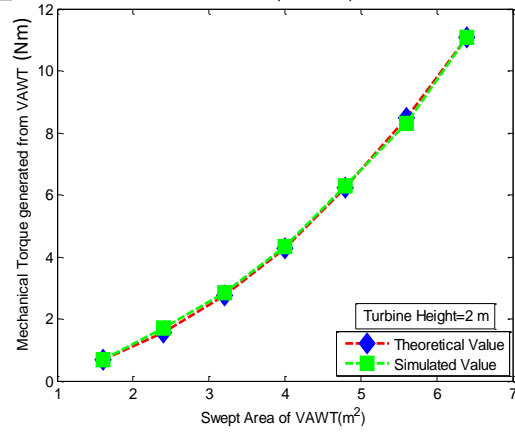


Figure 4.1: ‘Mechanical Torque’ vs ‘Swept Area’ for a given height of 2m

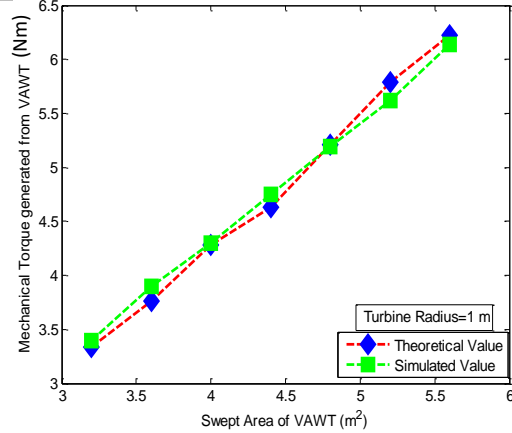


Figure 4.2: ‘Mechanical Torque’ vs ‘Swept Area’ for a given radius of 1m

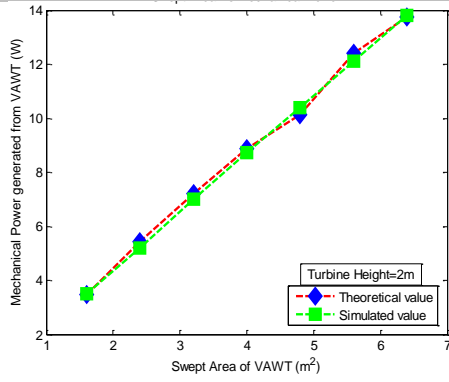


Figure 4.3: ‘Mechanical Power’ vs ‘Swept area’ for a given height of 2m

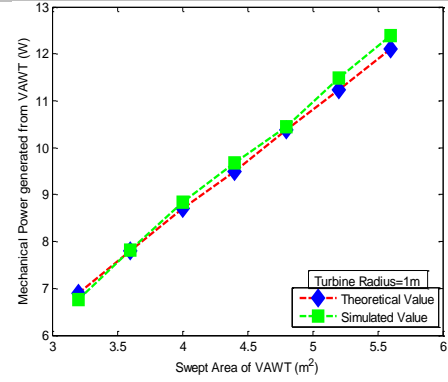


Figure 4.4: ‘Mechanical Power’ vs ‘Swept Area’ for a given radius of 1m

Figure 4.1 and 4.2 represent the torque generated by the turbine under different swept areas. As discussed in 3.1.1 earlier, the ‘Swept Area’ depends on the height and radius of the turbine. As such, figure 4.1 takes different radius in consideration to get different ‘Swept Area’ values keeping the height as a constant whereas figure 4.2 does the opposite. Figure 4.3 and 4.4 indicate the mechanical power generated by the turbine under the same configurations. The theoretical value and the simulation results were approximately same. The maximum difference observed while calculating the Mechanical Torque of the turbine for a given radius of 1m. Here, for a

Swept Area of 5.25m^2 , the theoretical value of the mechanical torque was 5.7Nm whereas the simulation gives 5.62Nm ; which gives the maximum tolerance of 1.4% which can be negligible. This certainly proved the design of the turbine created in ‘Matlab’ to be realistic enough to work with.

4.1.2. Simulation of VAWT under different Parameter

This section carries the simulation of the system under different design parameter to observe the change made at the output. The analysis is done based on a required power output of 5KW. The parameters ‘Air Density’ of 1.23 kg/m^3 , ‘Pitch Angle’ of 0, ‘Power Co-efficient’ were fixed at 1.23 kg/m^3 , 0, and 0.4412 respectively as per standard value [121] [142] unless stated otherwise. Wind speed was considered as 5m/s unless stated otherwise. By changing the design parameters of the turbine such as radius, height, wind speed and pitch angle; the turbine performance parameter such as mechanical torque, power, Swept Area, TSR (Tip Speed Ratio), rotational speed were changed. Therefore, to understand how each parameter affects the output of the turbine, the parameters have been analysed through plots. Only one parameter was varied at a time to observe the change in the output unless stated otherwise.

It is important to note that in the 1st part of the simulation, only the change in turbine output power is being observed under one variable at a time. While one variable is being changed, others have to be kept as constant. This is applicable in other parts of simulation as well unless stated otherwise. Figure 4.5 shows the mechanical power generated from the turbine under different heights. Since, the height was being changed, the radius had to be fixed at a certain value. Here, for a typical average scale of VAWT, the radius was fixed at 0.5m [145]. It can be observed that the height of the

turbine is directly proportional to the power generated from the turbine. Since height here is the combination of the turbine height and the distance from ground to the base of the turbine, naturally the output power will greatly depend on it. Keeping the height fixed at 1000m, it can be seen from figure 4.6 and 4.7, the turbine power increased with the increase of turbine radius. However, after a certain level, turbine cannot cope up with the increasing radius unless the height of the turbine is also increased in a proportion. Although theoretical study and simulation result will not indicate this scenario, however, this is obvious as the radius of the turbine should not be greater than the height of it. Otherwise the turbine will be off-balance and efficiency will decrease. But when it comes to increase the height, turbine power will keep increasing regardless the radius of the turbine being fixed at a certain point. This is the relationship between the power required, radius and height.

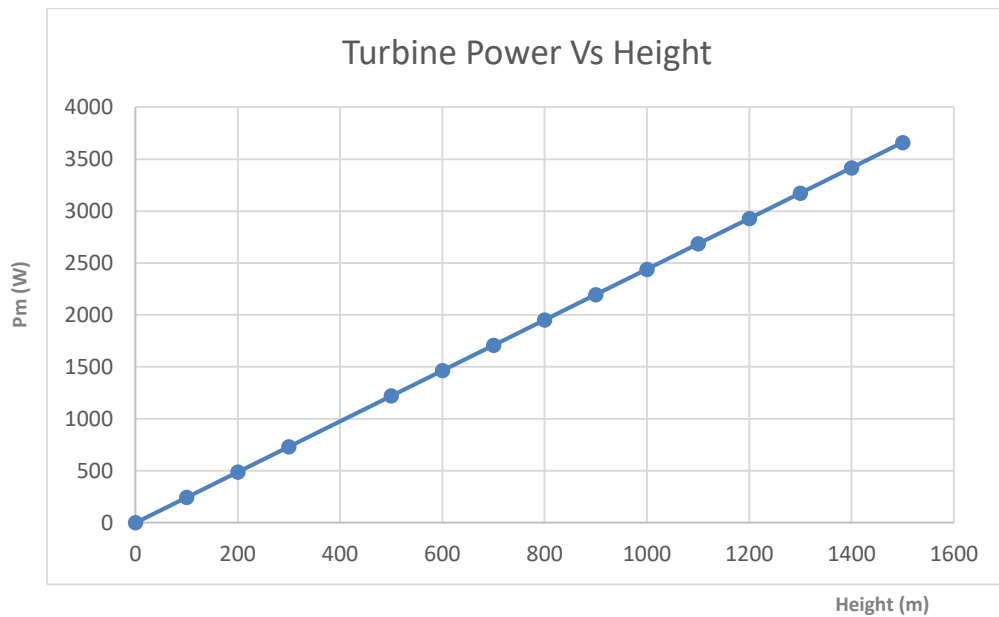


Figure 4.5: Turbine Power vs Height

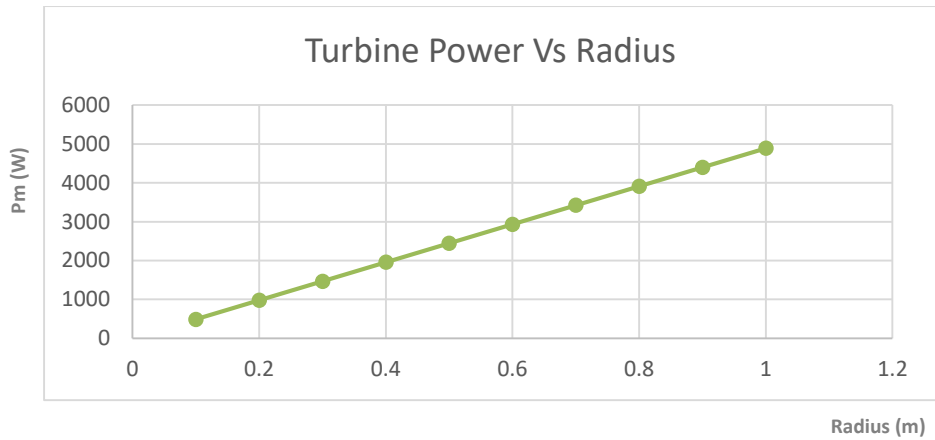


Figure 4.6: Turbine Power vs Radius

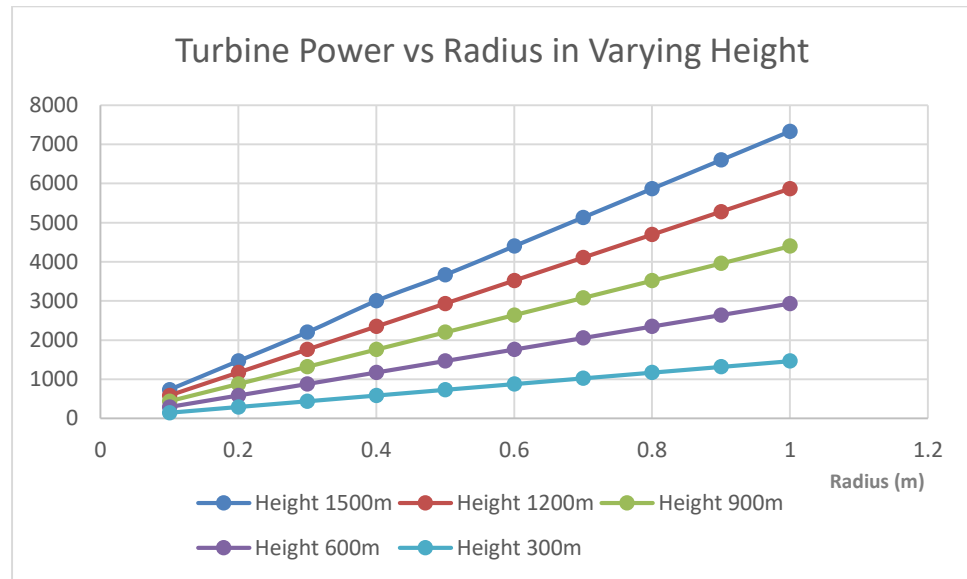


Figure 4.7: Turbine Power vs Radius under different heights

This is the relationship between the power required with varying radius under different heights. As it can be observed at minimum radius, varying height does not make a significant impact on turbine output power. Here, at 0.1m radius, turbine output power varies from 143 W to 746 W with an increase height from 300m to 1500m respectively. On the other hand, at 0.5m radius, turbine output power varies from 733 W to 3.67 KW with an increase height from 300m to 1500m respectively. Lastly, at maximum radius of 1m, turbine output power increases from 1.47 KW to 7.33 KW with an increase height from 300m to 1500m respectively.

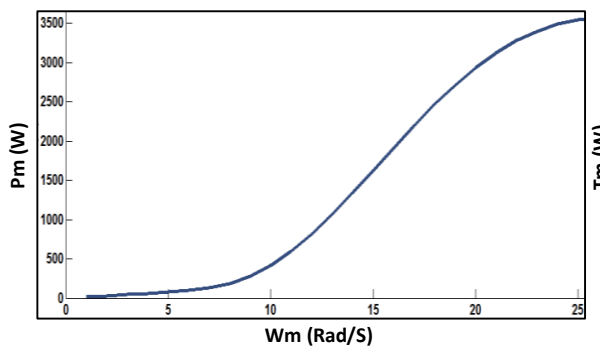


Figure 4.8: Power vs Rotational Speed

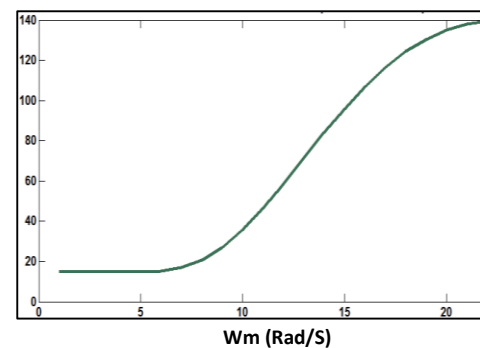


Figure 4.9: Torque vs Rotational Speed

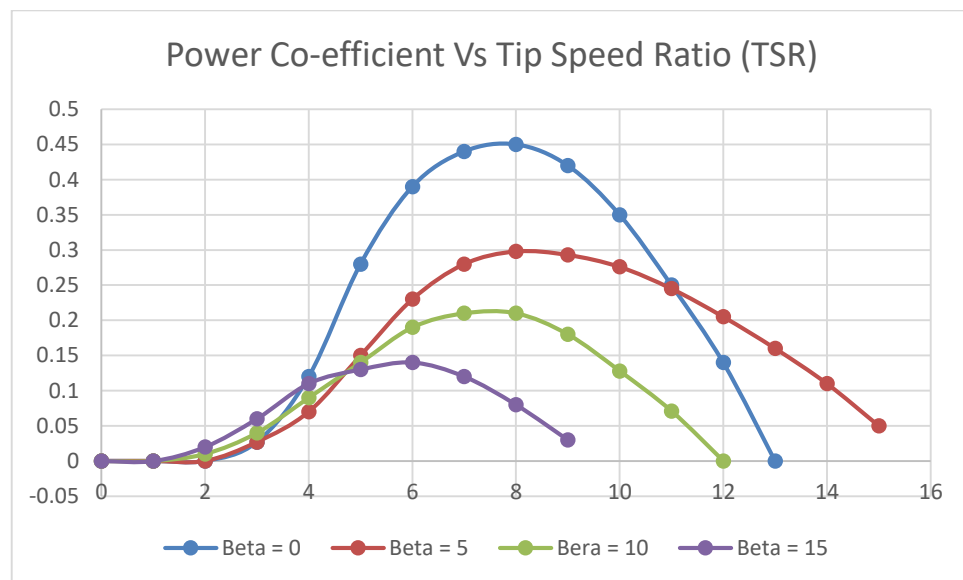


Figure 4.10.a: Turbine Power Co-efficient Vs TSR under different Pitch Angle

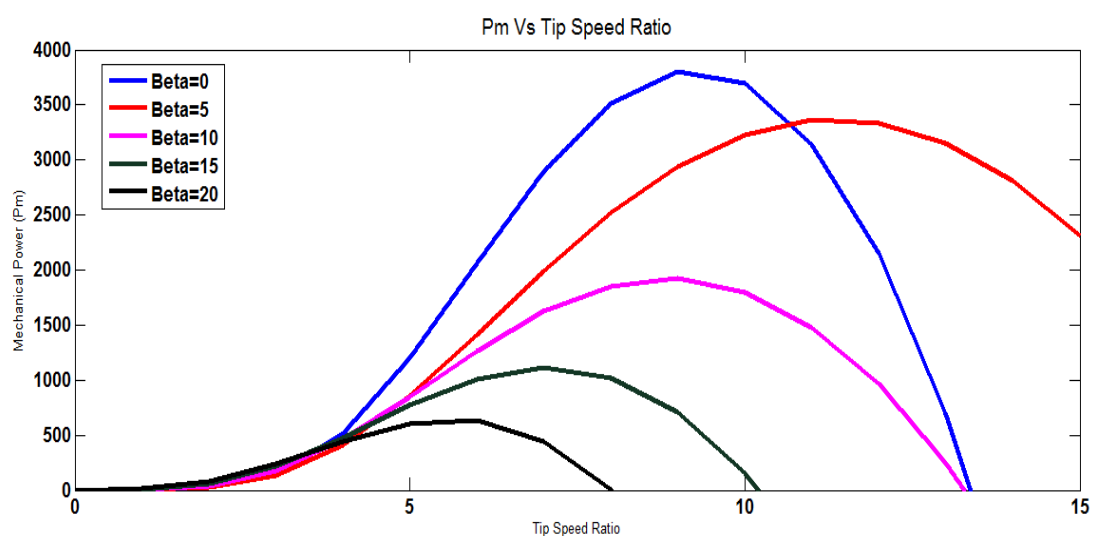


Figure 4.10.b: Turbine Power Vs TSR under different Pitch Angle

Figure 4.8 and 4.9 indicate that power along with the torque are increased with the increase of the rotor speed (Wm). At this situation, the radius and height of the rotor are kept constant as 1000m and 0.5m respectively. This shows that the torque produced by the wind turbine increases with increase in mechanical speed until maximum torque is achieved. Here, the mechanical speed affects the tip speed ratio and in turn affects the power coefficient.

Another simulation was carried to observe the power under various TSR (Tip Speed Ratio). The ‘Pitch Angle’ (Beta) was changed for each simulation and the result is graphically plotted in figure 4.10.a. It can be noticed that the power coefficient much depends on the tip speed ratio of the turbine. Generally, the Tip Speed Ratio should be high as it results in a high rotational speed. With the increase of Tip Speed Ratio, initially power co-efficient increases. However, after a certain point, a decrease in power co-efficient is noticed with increasing Tip Speed Ratio. This is because if the tip speed ratio is too low, the wind turbine is likely to slow down. The turbine becomes slow and it allows too much wind to pass through at very low tip speed ratio; therefore, cannot extract sufficient energy [21] [tip speed ratio]. On the other hand, if the tip speed ratio is too high, the turbine rotates very fast which does not extract optimal power from the wind and it is at risk of structural failure. Referring to figure 4.10.a, for null pitch angle ($\text{Beta} = 0$), power co-efficient became the highest which was 0.45. At that point, the Tip Speed Ratio was 8. It can be decided that at null pitch angle turbine power co-efficient becomes the highest. A study of the graph in figure 4.10.b indicates that the blade pitch angle also plays a vital role in turbine output. Since, power co-efficient directly proportional to the turbine power, it can also be concluded that null pitch angle produces the maximum amount of power. Lastly, as

derived earlier in section 2.3.1, the maximum power coefficient is 0.593 percent as per the Betz Limit. In practice however, obtainable values of the power coefficient ranges from 70% to 80% of Betz's actual limit which is 0.42-0.47 [tip speed ratio]. Similarly, in figure 4.10.a, the maximum power co-efficient was 0.45 drawn by a TSR of 8.

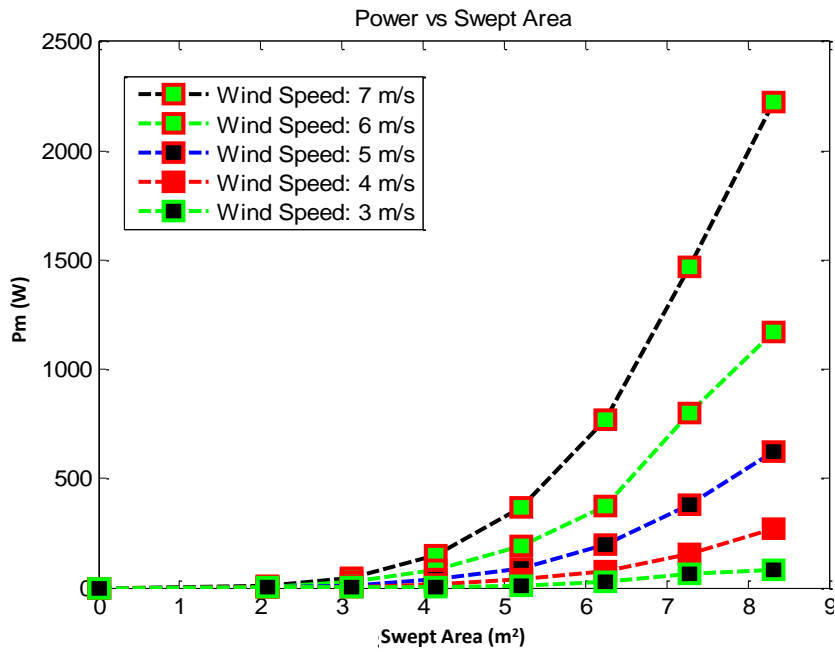


Figure 4.11: Turbine Power Vs Swept Area under various wind speeds

Lastly, the simulation was carried for various swept areas speeds to see the change in the power for different wind speeds. It was observed from figure 4.11 that at high wind, a slight increase in the swept area results bigger change in power. Therefore, any change in the radius or height will cause significant power variation at high speed and vice versa. At low wind speed such as 4 or 3 m/s, more efforts, meaning significant change in the turbine design in terms of radius and height will be needed to generate higher current and power.

4.2. Design and Simulation of Axial Flux Permanent Magnet Synchronous Generator

4.2.1. Varying the wind speed

This section presents the result of the 3 types Axial Flux PMSG simulation carried for 2 different wind speeds; - 3m/s, 8m/s

4.2.1.1. Wind Speed 3m/s



Figure 4.12: Current (A) from 3-phase PMSG 3 m/s wind speed (Peak 0.06A)

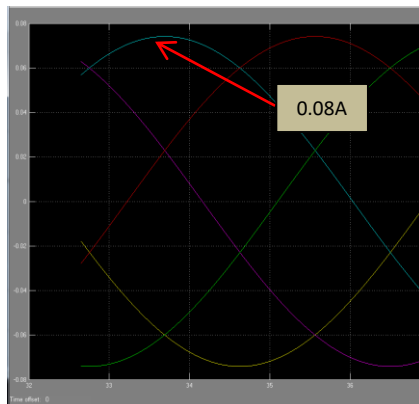


Figure 4.13: Current (A) from 5-phase PMSG 3 m/s wind speed (Peak 0.08A)

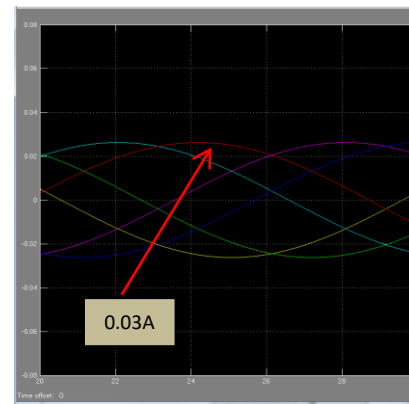


Figure 4.14: Current from Dual stator PMSG at 3 m/s wind speed (Peak 0.03A)

Figure 4.12, figure 4.13 and figure 4.14 indicate the AC current generated from all 3 types of generator whereas figure 4.15, 4.16 and 4.17 display the power generated from all 3 generators.

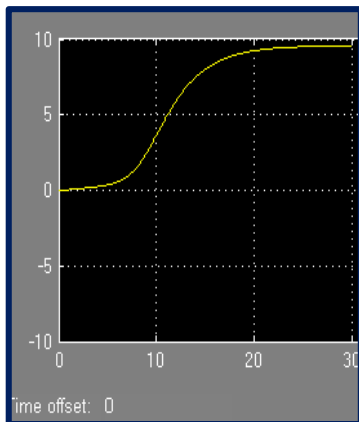


Figure 4.15: Three phase

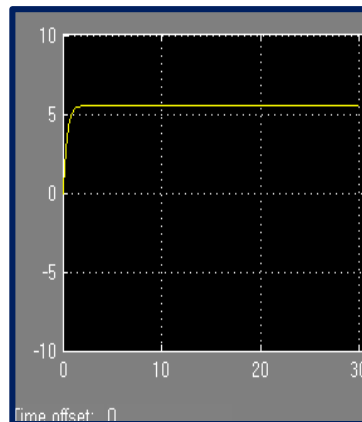


Figure 4.16: Multi phase

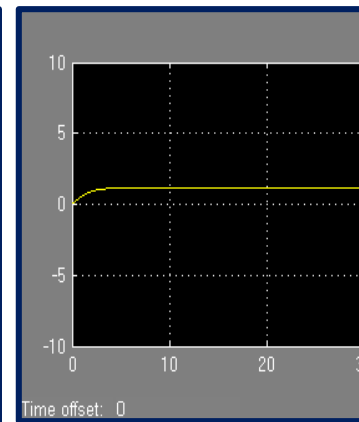


Figure 4.17: Dual stator

PMSG output Power

(Peak 5 W) at 3m/s

PMSG output power (Peak)

10 W) at 3m/s

PMSG output power

(peak 2W) at 3m/s

The above simulated result shows the current of the 3-phase, 5-phase and Dual Stator PGSM at a slow wind speed of 3m/s. The 3-phase PMSG current had an approximate peak value of 0.06A. The current of the 5-phase PMSG had a peak approximate value of 0.08A. This value was higher than both of the three phase PMGS current and dual stator PMSG current (0.03A). Dual Stator had the lowest amount of current.

Coming to the power generated by all the 3 types of PMSG, the multiphase or 5-phase PMSG has a higher electromagnetic power among three generators having a value of 10W. 3-phase PMSG followed with a value of 5W and Dual stator had the lowest among all having 2W. This showed that the multiphase had a more power density at lower speed than the other two generators.

4.2.1.2. Wind Speed 8m/s

Figure 4.18, figure 4.19 and figure 4.20 show the AC current generated from all 3 types of generator whereas figure 4.21, 4.22 and 4.23 indicate the power generated from all 3 generators.

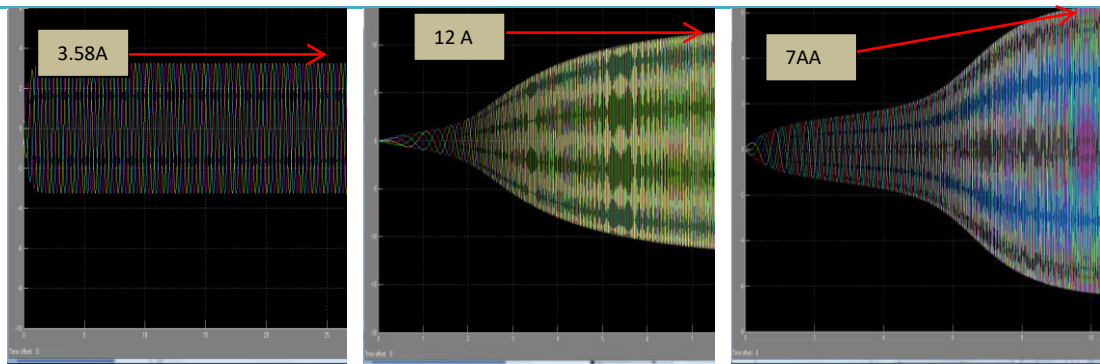


Figure 4.18: Current (A)
from 5-phase PMSG 8
m/s wind speed

Figure 4.19: Current (A)
from 5-phase PMSG 8
m/s wind speed

Figure 4.20: Current (A)
from 5-phase PMSG 8 m/s
wind speed

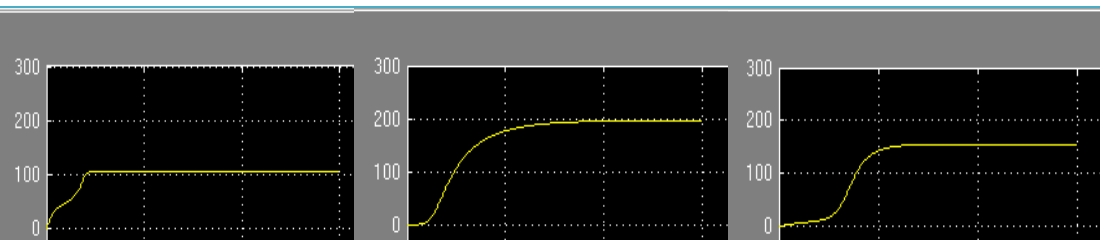


Fig. 4.21: 3-Phase PMSG
output Power (Peak
100W) at 8m/s

Fig. 4.22: 5- phase PMSG
output power (Peak
198W)at 8m/s

Fig. 4.23: Dual stator
PMSG output power
(peak 158W) at8 m/s

The peak value of the PMSG current reached 3.5A at 8m/s speed whereas 5-phase PMSGAt reached to a final value of 13A. However, the peak value of the Dual Stator PMSG current touched 7A surpassing that of the three phase generator but lower than that of the 5-phase generator at the same wind speed. As far as the power concerns, again 5-phase topped having power of 198W, followed by Dual Stator (158W). 3-Phase PMSG had the least amount of power (100W).

Table 4.1 Efficiency comparison of PMSG Output Power at Different Wind Speed

PMSG Types	Wind speed	
	3 m/s	8 m/s
Turbine Power (W) efficiency (Reference: 3- Phase PMSG)		
Dual stator PMSG	40% reduction	58% increase
5-Phase PMSG	99.9% increase	98% increase

At low wind speed, 5-phase PMSG was the most efficient among all having the double amount of power (100%) than 3-phase which was 5W (table 4.1). Surprisingly Dual stator showed significant reduction in efficiency of 40% comparing to 3-phase. An important observation to note down is that when the wind speed increased to 8m/s, 5-phase still holds the top but this time dual stator surpasses 3-phase with a 58% increase. This indicates that Dual Stator performs better than 3-phase in high wind. However, performance of Dual Stator decreases significantly even than of the 3-phase when wind speed becomes low. This is because at low wind, the turbine rotates so slow that it cannot go up to the Dual Stator's high rated RPM making the generator unworthy to use. Therefore, for low wind speed Dual Stator cannot be used as a primary option.

4.2.2. Varying the pole number

If higher number of poles were taken in consideration (Fig. 4.22) at a fixed wind speed of 5m/s, it could be monitored that with the increase of pole number, 5 Phase PMSG

responded the most with getting high power values followed by Dual Stator and 3 Phase respectively.

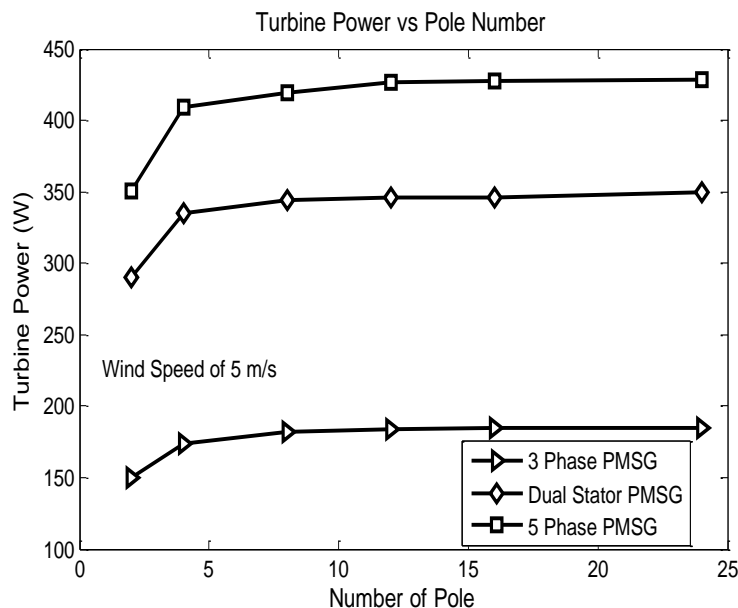


Figure 4.22: Number of Pole Vs Turbine Power for 3 Phase, 5 Phase and Dual Stator PMSG

Table 4.2. PMSG Output Power efficiency comparison for minimum and maximum number of pole

PMSG Types	Number of poles	
	24	2
	Turbine power (W) [Reference 5 phase PMSG]	
Dual stator PMSG	17.78% reduction	17.14% reduction
3 phase PMSG	45.71% reduction	48.28% reduction

According to table 4.2, when the number of poles was fixed at 24, turbine power reduced 17.78% from 5 Phase to dual stator for same configuration. For same number of poles, turbine power dropped down 45.71% for 3 Phase PMSG with respect to 5 Phase. While using 2 pole generator, 17.14% reduction in turbine power was noticed

for dual stator as far as 5 Phase is concerned. Lastly, 3 phase PMSG's turbine power reduced remarkably, 48.28%.

4.2.3. Varying the Rotational speed of the turbine

Keeping the wind speed fixed at 5m/s, the rotational area was varied to observe the change in generator output power. As turbine rotor speed or rotational speed is related to wind speed and TSR (Tip Speed Ratio), a fixed wind speed indicates a direct involvement of the rotor speed with TSR.

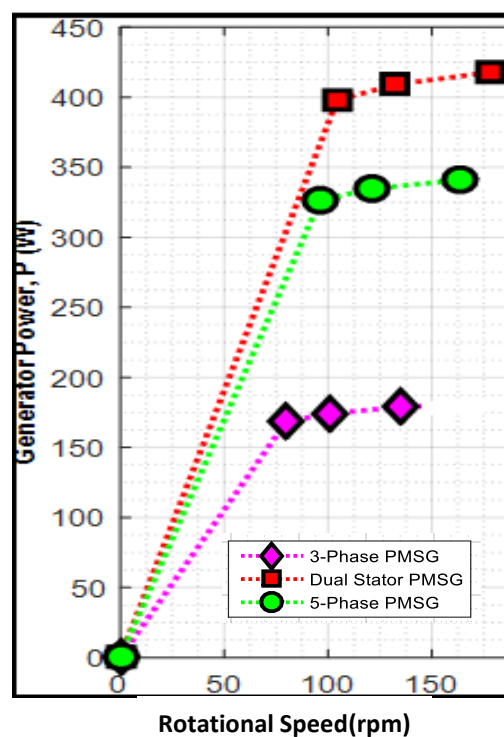


Figure 4.23: Generator Power Vs Turbine Rotational Speed

As it could be observed that at higher rotor speed (figure 4.23), power generation was also high. Leading from the front, 5-phase surpassed all in terms of power followed by Dual Stator. Again, 3-Phase had the lowest amount of power with the varying rotor speed. But it is important to mention that for a rotational speed less than 20rad/s (less than 190RPM), rotational speed is almost same in all the 3 types of generator. This is

an important observation as it tells us that for low speed system, all the 3 types of generator configuration will not differ much in terms of power.

4.3. Optimization of Permanent Magnet Synchronous Generator based Vertical Axis Wind Turbine for Rural Malaysia

4.3.1. Optimization of VAWT for low wind speed

VAWT Configuration:

2 configurations were selected after carefully analysing of simulation data. Following table 4.3 presents VAWT configurations followed by the justified analysis of it.

Table 4.3: Optimized VAWT Design Configuration

VAWT		
Configuration 1		
Wind Speed	:	Low Wind
Height	:	2.6m
Radius	:	1m
Number of blade	:	3
Pitch Angle	:	0
Power coefficient	:	0.4412
Air density	:	1.225kg/m ³
VAWT		
Configuration 2		
Wind Speed	:	Low Wind
Height	:	60 cm
Radius	:	14.5 cm

	Number of blade : 9
	Pitch Angle : 0
	Power coefficient : 0.4412
	Air density : 1.225kg/m ³

4.3.1.1. Simulation Analysis- Configuration 1

After designing the turbine, simulation was performed to get the mechanical torque and power from the turbine for different values of radius and height keeping one fixed at a time. To get the optimal turbine design parameters, 2 cases had been taken for consideration. The 1st one was to vary the radius keeping the height fixed and the 2nd one was the opposite of it.

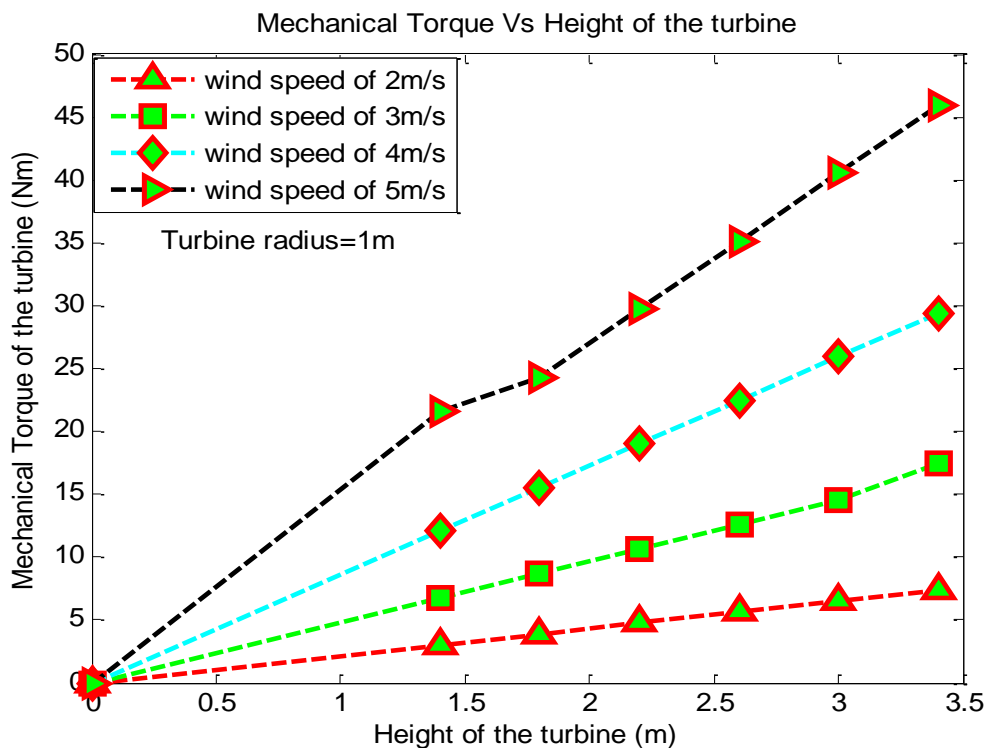


Figure 4.24: Torque generated for different heights of VAWT

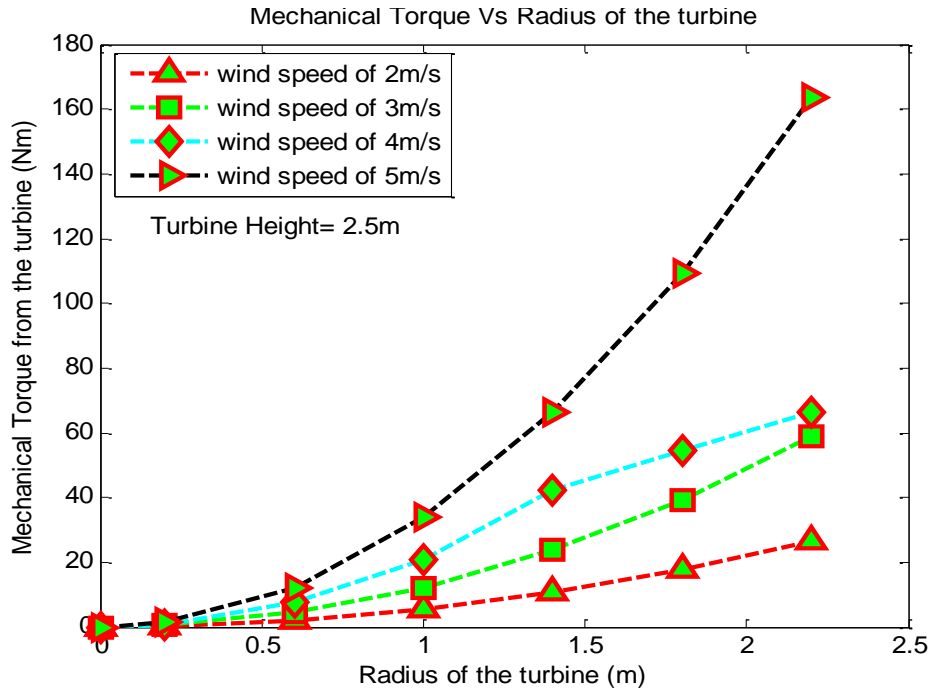


Figure 4.25: Torque generated for different radius values of VAWT

Figure 4.24 and 4.25 above show the mechanical torque generated for different heights of VAWT. Turbine radius was fixed at 1m and the swept area therefore varied according to the change of the height as observed in 4.1 section. Simulation was performed under different low wind speeds and the result shows good improvement on generated torque as soon as the height exceeded one meter. Figure 4.26 represents mechanical power data for different values of radius and heights. Wind speed was fixed at 2m/s in order to observe the low wind performance. Turbine height was fixed at 2m while running the simulation on radius and the radius was fixed at 1m while running the simulation on height. Simulation shows better understanding in terms of turbine power efficiency. To generate at least 7W in low wind, turbine height has to be minimum 1.6m. As far as turbine radius concerns, radius should at least be 0.8m. Any radius below 0.8m cannot be matched with more than 1.5m turbine height.

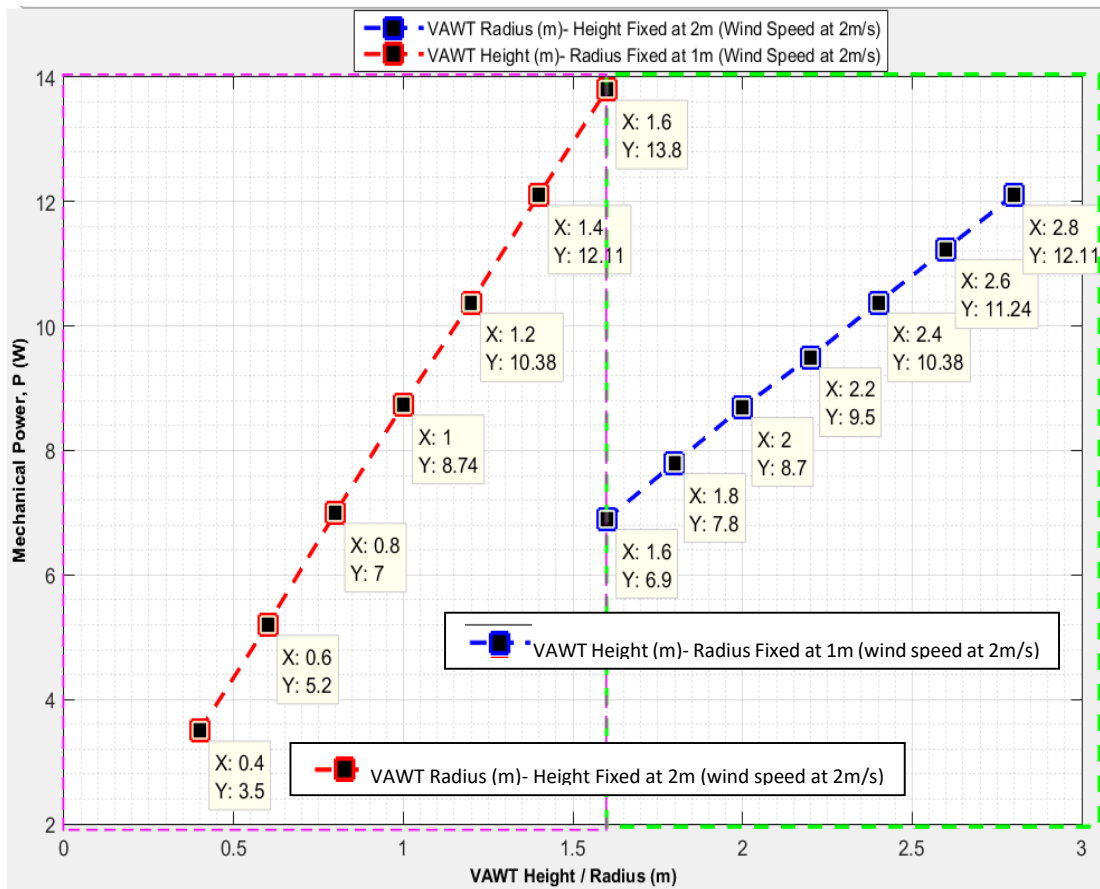


Figure 4.26: Mechanical Power for different radius/height of VAWT

After taking consideration of different values of turbine radius and height, it could be seen that at low wind speed, 0.8m-1.2m radius could be suitable for producing higher power and proper torque. Yet again, to have a realistic system, the radius of the turbine has been decided to fix at 1m. Following the same concept, it can be observed that the height between 2m-2.8m were suitable enough to produce good power and torque. Therefore, with respect to the turbine radius, the height of it was fixed at 2.6m.

4.3.1.2. Simulation Analysis- Configuration 2

A smaller version of configuration1 was created in this part. For cost efficiency, a small system was required, therefore further simulation was carried on and data was

graphically plotted. Figure 4.27 and 4.28 display the mechanical torque generated for different height and radius respectively under various wind speeds whereas figure 4.29 and figure 4.30 show power generated against the same parameters.

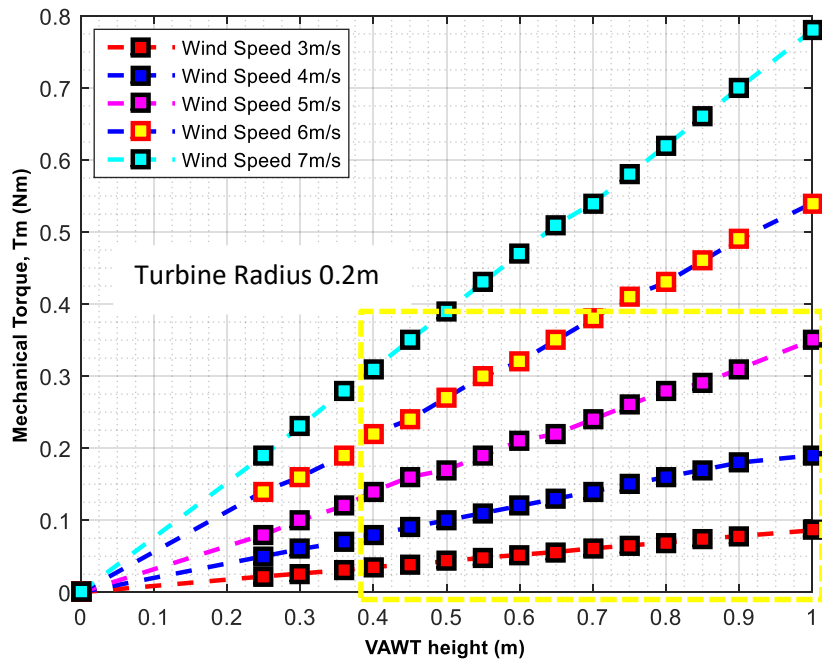


Figure 4.27: Torque generated for different heights under different wind speeds

While running the simulation for turbine power under different heights, radius was fixed at 0.2m (Figure 4.27). In such way, the swept area will vary with only the change of the turbine height. As it can be seen, the low torque generated in the low wind (2m/s-5m/s) improves with the gradual increase of the height from 0.4m onwards.

Similarly, while running the simulation for turbine power under different radius, height was fixed at 0.5m (Figure 4.28). In such way, the swept area will vary with only the change of the turbine radius. As it can be spotted, the low torque generated in the low wind (2m/s-5m/s) improves with the gradual increase of the radius from 0.2m onwards.

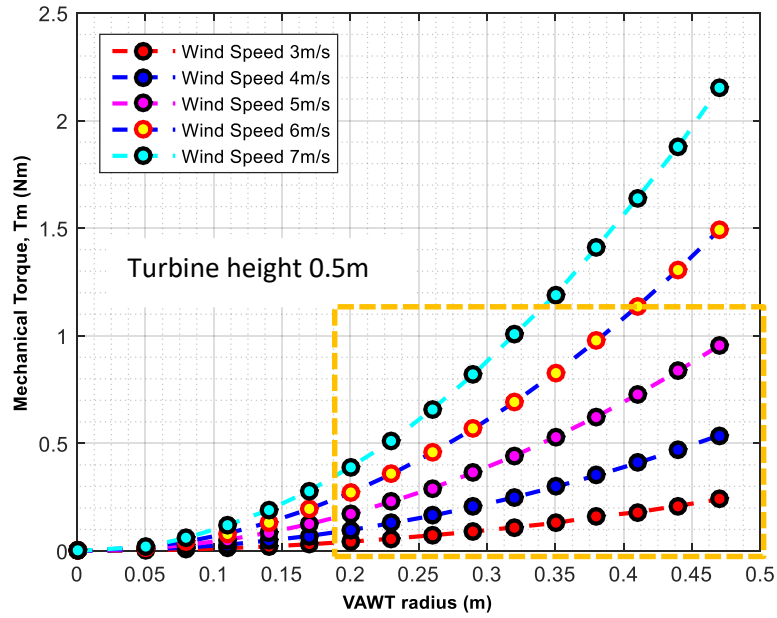


Figure 4.28: Torque generated for different heights under different wind speeds

Figure 4.29 and figure 4.30 represent mechanical power against height and radius simulation analysis respectively. The simulation style was same like before which was keeping the radius fixed at 0.2m while changing the height to different values and keeping the height fixed at 0.5m while changing the radius to different values. Simulation illustrates the same result as the torque vs turbine radius and height indicated. For low wind speed range of 3m/s to 5m/s, turbine height more than 0.4m improves the turbine power. Turbine power did not seem to be affected much by turbine radius in low wind speed. For a wind speed of 3m/s and 4m/s, the impact was almost negligible for increasing the radius. However, at wind speed 5m/s, simulation showed improvement in power with the changing radius starting from 0.1m although it was not very promising.

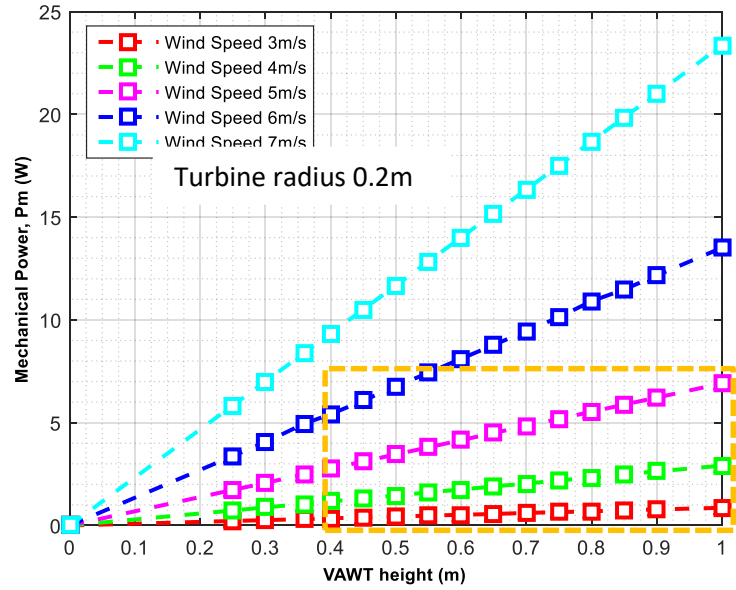


Figure 4.29: Power generated for different heights under various wind speeds

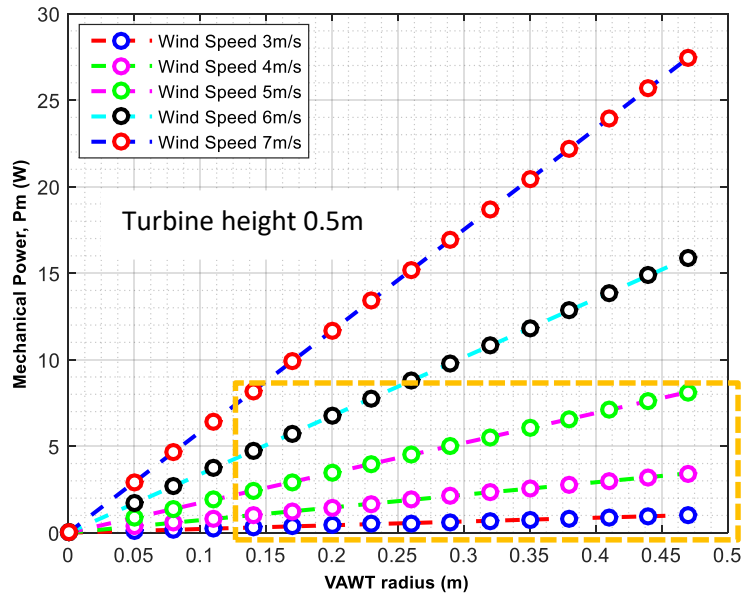


Figure 4.30: Power generated for different radius under various wind speeds

Figure 4.31 shows the mechanical power versus mechanical torque graphs. Swept Area of the turbine was varied with a fixed height of 0.5m. It can be observed that in low wind speed, the mechanical power fluctuates under 10W. Low torque and low

power, ranges from 1W-8W, are the characteristics while dealing with smaller range of turbine design parameters.

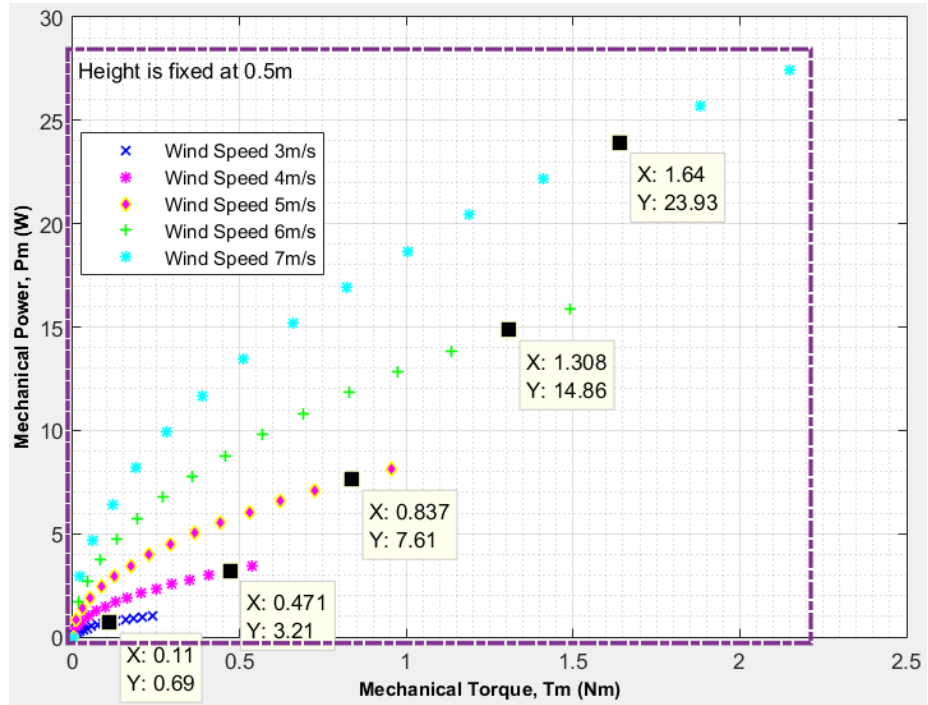


Figure 4.31: Power generated for different radius under various wind speeds

4.3.2. Optimization of PMSG for VAWT

The stator resistance, inductance at dq frame, flux linkage, mass inertia and pole pairs were varied to perform simulations and a set of realistic parameter values were fixed in which the voltage and current were sufficient enough to produce a good amount of power. Stator resistance was fixed at 14Ω , inductance at dq axis was considered to be 0.8mH , flux linkage was taken as 0.175 Wb/A , mass inertia was 0.089 J . Low wind speed was taken in consideration as it was varied from 3 to 7 m/s.

Since, it was decided to use 3-Phase PMSG for low wind VAWT, 3-Phase PMSG was being analysed further. The pole pair and friction factor was taken in consideration in depth and simulation was carried under varying mechanical torque. Figure 4.32 and figure 4.32 below represent the data collected from the simulation.

From section 4.1, it was analyzed that mechanical torque of the turbine directly depends on the design of it, precisely on turbine's height, radius and power coefficient. Here, figure 4.32 illustrates the effect of turbine torque on generator output power on various pole pairs. When the torque is high, number of pole played a vital role on generator power. As it can be seen, the generator power jumped from 548W to 3.6KW with change of the pole pair from 8 to 18. As far as low torque range concerns, it could be spotted that at a fixed torque of 5Nm, generator power increased from 6.6W to 24W for the same change in Pole Pair. Therefore, pole pair plays a vital role in generator performance regardless low or high wind range. Also to get high power output from the generator (around 1.5KW and above), minimum of 10-12 pole pair (20-24pole) should be chosen if possible. In low torque range, low wind speed makes the generator difficult to produce enough power. As it can be observed from the figure, for low torque, the rated output power from the generator could maximum be 500W.

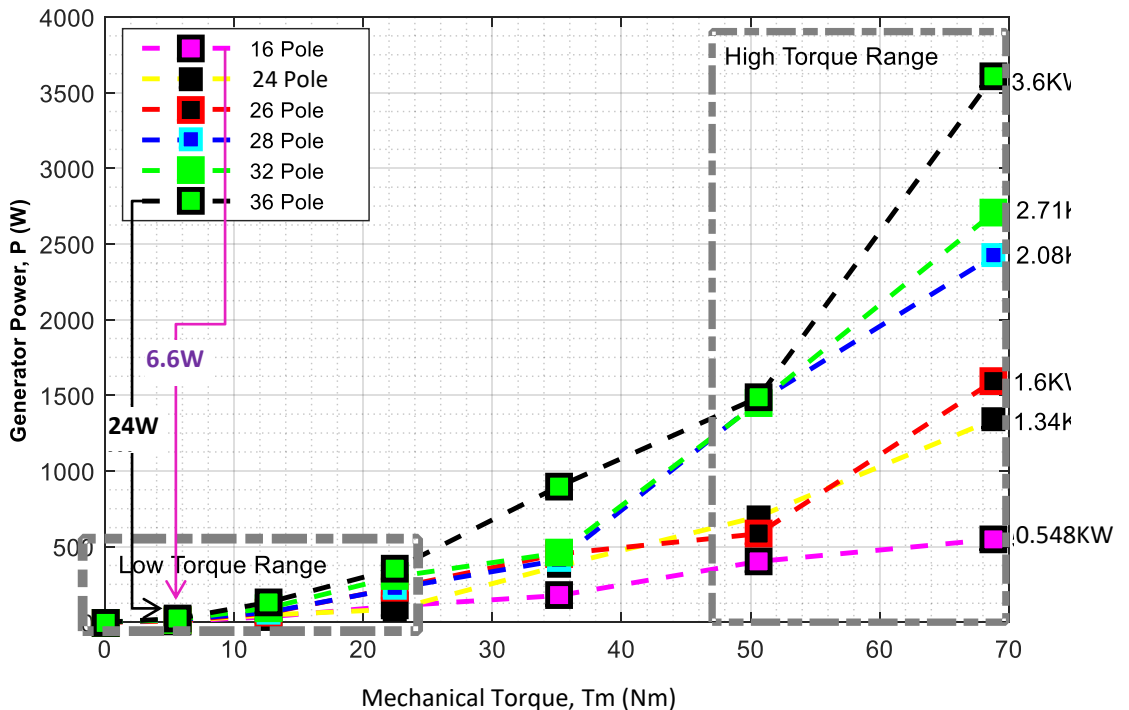


Figure 4.32: Generator Power Vs Mechanical Torque under Various Pole Number

With view of the facts achieved from the simulation result above, 2 configurations of the 3-Phase PMSG were fixed to match the two VAWT designs. For the first one, 3-Phase PMSG was rated as 1.5KW and to make a realistic system, it was decided to put 10 pole pairs in it. The second generator configurations were to be matched with the other VAWT design which would be the smaller version of the 1st one. Therefore, the low torque range power ratings (less than 500W) were to be considered according to the previous findings and for that a rated power of 200W was fixed as the generator output. The pole pair was decided to be 8 which makes the number of pole of the 3-phase PMSG to be 20.

It was said before that friction factor plays an important part on generator performance. It basically represents the friction in the bearing while being rotated with relative to the shaft. Since Maglev reduces the friction to almost zero in the

bearing by levitating the system with the repulsive force of the magnets, friction factor directly is related to Maglev. A minimal of friction factor hence may represent the Maglev implementation in the system.

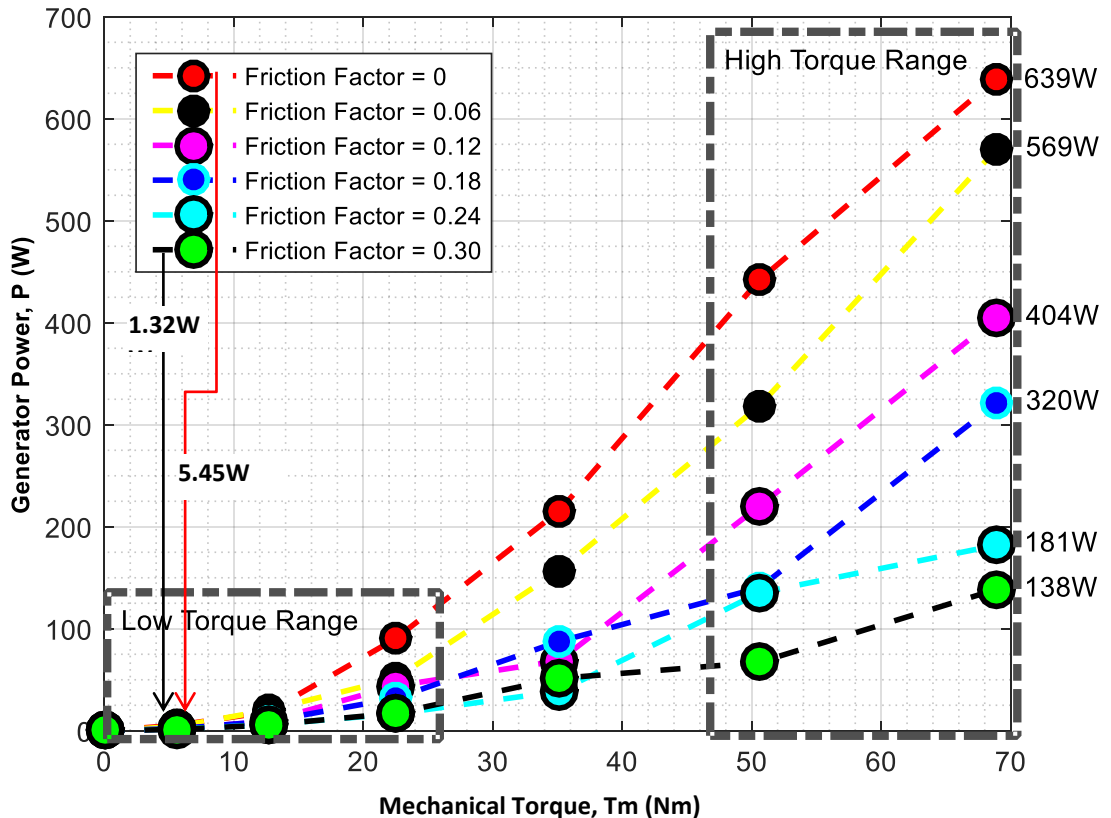


Figure 4.33: Generator Power Vs Mechanical Torque under different Friction Factor

Figure 4.33 demonstrates that not only at high torque range but also when the torque generated from the turbine is very low, implementation of Maglev can significantly increase the output power. Simulation showed a 0.3 reduction in the friction factor increases the output power from 1.32W to 5.45W at a mechanical torque of 5Nm. Hence, for low wind system, implementing Maglev makes noteworthy improvement in efficiency.

4.4. Low Cost System Optimization of Rural Malaysia and Design Fabrication

This part of the chapter compared the two configuration discussed earlier sent the relative cost effective design for fabrication. Following are the two proposed design details.

Table 4.4: Optimized System Design Configuration 1

VAWT			
	Height	:	2.6m
	Radius	:	1m
	Number of Blade	:	3
	Pitch Angle	:	0
PMSG			
	Phase	:	3-Phase
	Type	:	Axial Flux
	Rated Power	:	1.5KW
	Rated Voltage	:	220V
	Pole Pair	:	10
Top net weight			
		:	75KG

Table 4.5: Optimized System Design Configuration 2

VAWT			
	Height	:	60 cm
	Radius	:	14.5 cm
	Number of Blade	:	9
	Pitch Angle	:	0
Power Co-efficient			
		:	0.4412

PMSG		
Phase	:	3-Phase
Type	:	Axial Flux
Rated Power	:	200W
Rated Voltage	:	12V
Pole Pair	:	8
Diameter	:	16cm
Top net weight		
	:	12.5kg

According to equation 3.33 and 3.34,

$$WPR = \frac{m}{P}$$

$$\text{Cost efficiency, } \eta = \frac{WPR_2 - WPR_1}{WPR_2} \times 100 \%$$

Table 4.6: Weight to Power Ratio		
Weight to Power Ratio 1, WPR_1	:	0.05 Kg/W
Weight to Power Ratio 2, WPR_2	:	0.0625 Kg/W
Cost Efficiency, η	:	20%

Table 3.6 illustrates the ‘Weight to Power Ratio of the two design configuration. It is clear that the smaller design version is 20% cost effective relative to the first design due to its small weight scale. Also, this 200W, 12V 9 bladed rated system much compact comparing to the 1.5kW, 220V, 3 bladed turbine. As far as low wind and low torque concern, the voltage and power output will also be very low as per the simulation data. Also, the energy harvesting devices should take place in such areas

where on-grid turbines are not frequently available. Places like these, generally demand for a compact, low cost standalone system. Figure 4.7 shows the overall cost of different existing wind turbines in rural Malaysia with proposed turbine. It can be observed that only one existing turbine is operational at 3m/s. The rated output power is 2KW and the overall cost of the turbine is USD2500. The turbine is large in size having height and diameter of 1.5m and 1m respectively. For low cost, compact portable standalone system, the model is not suitable for small scale battery charging application. Also it costs almost 8 times higher than our proposed 200W 9 Bladed hybrid VAWT system (Configuration 2). Therefore, it was decided to send design configuration 2 for fabrication.

Table 4.7: Cost Analysis of Current Existing Wind Turbine in Rural Malaysia in Comparison with Proposed Turbine

	Year of installation	Location	Turbine Type	Turbine Height (m)	Turbine Diameter (m)	Generator type	Generator Power rating (W)	Overall Cost (USD)
Case Study 1	2007	Shah Alam [Cut-in Wind Speed 6m/s]	3 Bladed H Type VAWT	2.14	0.5	PMSG	700	1093
Case Study 2	2013	Kuala Terengganu [Cut-in Wind Speed 4m/s]	VAWT	1.5	0.5	PMSG	1000	1780
Case Study 3	2015	Johor Baru [Cut-in Wind Speed 3m/s]	Savonius VAWT	1.5	1	PMSG	2000	2500

Case Study 4	2007	Pulau Perenthian [Cut-in Wind Speed 6m/s]	HAWT	Unknown	Unknown	Unknown	100K	180000
Case Study 5	2012	Penang [Cut-in Wind Speed 6.1 m/s]	VAWT	10	1	PMMSG	2000	2500
Proposed System 2	2016	Selangor [Was not made Operational]	3 Bladed VAWT	2.6	1	PMMSG	1500	1500
Proposed System 2	2016	Selangor [Cut-in Wind Speed 3m/s]	Hybrid VAWT	0.6	0.29	PMMSG	200	310

4.5. Laboratory Prototype of Maglev VAWT adopted to PMSG

A Chinese Company was chosen for design fabrication. The company was requested to put Maglev in the system. They had also been asked to provide a data sheet for the system but generally data sheets were to be provided only after fabrication, not before that. Therefore, before ordering from the Chinese Company, in order to be assured that the design would work well in low wind speed, a lab prototype was built similar to the design configuration 2. The idea was to go for fabrication only if the lab prototype indicated good pattern of result.

The hardware architecture was described in the methodology chapter. The field testing results were given below. The turbine was tested under low wind speeds

ranging from 4m/s to 7m/s and the generator open circuit voltage was plotted against turbine rotational speed. Generator pole and turbine blade angle were changed to observe the impact on the output voltage. As discussed in the literature review, if the blade angle is kept at 0, it should cut maximum wind, thus it will rotate at a higher speed and produce larger voltage. On the other hand, when the blade angle is 90 degree, it will cut minimum wind and will produce minimum voltage. Figure 4.34 and 4.35 represent the open circuit PMSG output voltages under different rotational speeds. Figure 4.34 was made for 8 Pole PMSG whereas figure 4.35 was for 4 Pole PMSG. The PMSG was constructed with two pole configurations to observe whether the system output voltage improves with the increase number of pole.

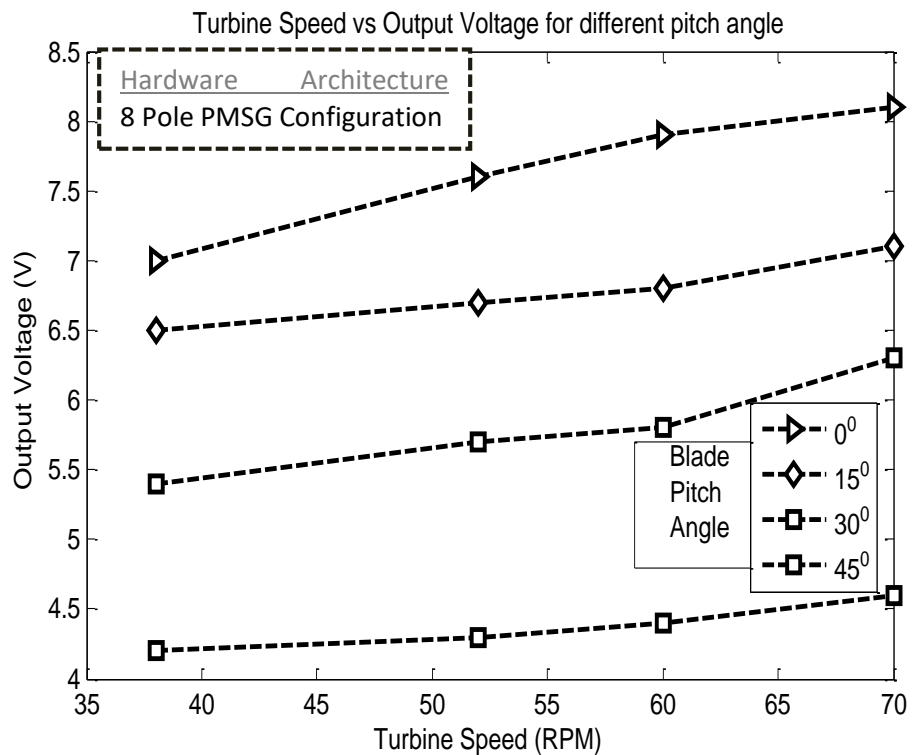


Figure 4.34: Generator Open Circuit Voltage vs VAWT speed under different pitch angle (8 pole)

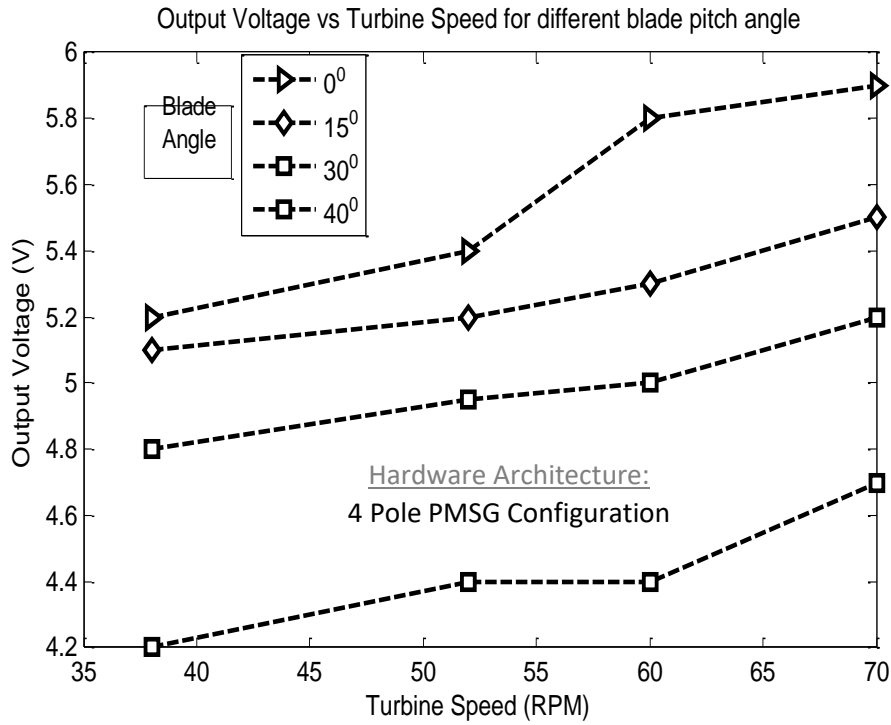


Figure 4.35: Generator Open Circuit Voltage vs VAWT speed under different pitch angle (4 pole)

Referring to figure 4.34, firstly, for 0 blade angle, open circuit voltage was 7V at 38 rpm (4m/s). Output voltage dropped down to 6.5 V when the blade angle was changed to 15 degree keeping the turbine's speed same. Output voltage was around 5.5 V and 4.2 V for 30 and 45 degree blade angle respectively, which clearly shows the reduction in voltage with respect to increasing blade angle. Again, at 52 rpm (5m/s), it could be observed that generated output voltage was 7.5 V for 0 degree blade angle. Then the voltage reduced to 6.6 V for 15 degree blade pitch. Voltage came down to 5.6 V for 30 degree and 4.3 V for 45 degree pitch angle. Output voltage followed the same sequence for 60 and 70rpm. In addition, when the turbine was being rotated at 70 rpm (7m/s), more than 8V was produced with 0 degree blade angle orientation.

Next, PMSG with 2 pole pair (4 Pole) was experimented (figure 4.35). Observations supported the same trend in the case of 4 pole pair generator. But here, lower output

voltage was observed compared to 4 pole pair generator for the similar conditions. For example, when the turbine speed was 38 rpm, output voltage was 5.2 V for 0 degree blade angle. Increasing the blade angle to 15, 30 and 45 degree reduced the output voltage to 5.1 V, 4.8 V and 4.2 V respectively. For all turbine speeds null blade angle provided the highest output voltage. For 8 pole permanent magnet generator, output voltage was maximum when the blade angle was null for all turbine speed. Generated output voltage started to reduce when we start to increase the blade angle, keeping the turbine speed same. As we increase the blade angle, the output voltage reduces and vice versa. By analyzing all the recorded values, it was concluded that, greater turbine speed, smaller pitch angle, higher number of poles give maximum voltage for the generator. Figure 4.36 and figure 4.37 focus the generator open circuit voltage at null pitch angle. Furthermore, at the lowest wind speed of 4m/s, the generator was still able to produce an open circuit voltage of 7V (figure 4.37). It was not possible to make a 16 pole configuration for the prototype but even with 8 pole configuration it showed good result overall. Therefore, it was decided that the prototype system made accordance with the 2nd configuration was good enough to produce low voltage at lower wind speeds.

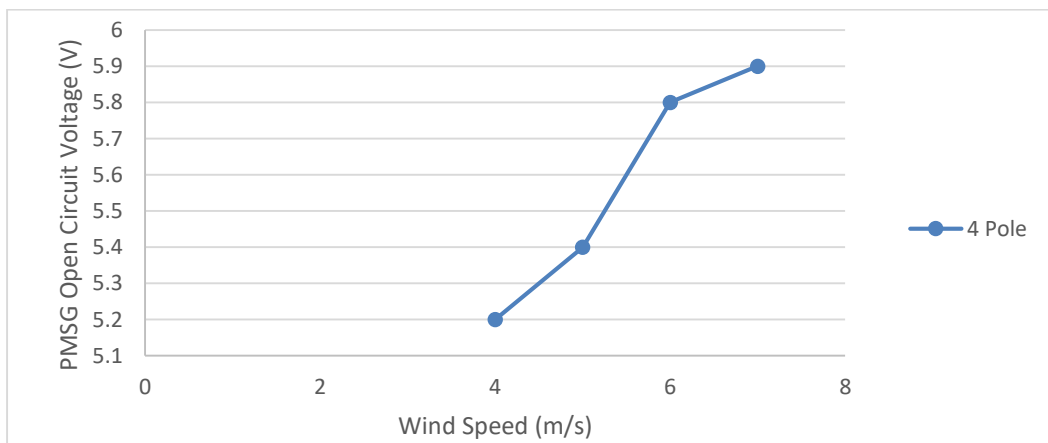


Figure 4.36: Prototype 3-phase 4 Pole PMSG Open Circuit Voltage for various wind speeds

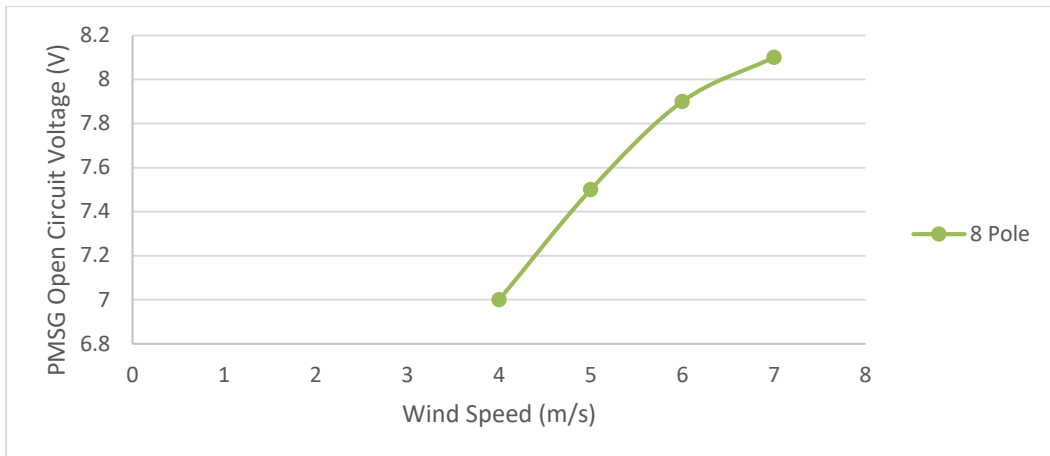


Figure 4.37: Prototype 3-phase 8 Pole PMSG Open Circuit Voltage for various wind speeds

4.6. Energy Harvesting

This section gives performance analysis of a Supercap (Superacitor) based energy harvesting battery charging device operated by the Maglev VAWT adopted to a 200W PMSG as per the configuration discussed previous which was sent for fabrication. Upon arrival of the turbine, system was set-up in the lab and field testing was performed to tabulate the data. Following table 4.8 recaptures the system configuration and the open circuit voltage taken in low wind speed.

Table 4.8: Energy Harvesting System Open Circuit Performance

VAWT		
Wind Speed		: 5 m/s
Height	:	60 cm
Radius		: 14.5 cm
Number of blade	:	9
PMSG		
Phase		: 3-Phase
Rated Power	:	200W
Rated Voltage		: 12V

	Diameter	:	16cm
Top net weight		:	12.5kg
Open Circuit Analysis	PMSG Open Circuit Voltage	:	<ul style="list-style-type: none"> • 8.5V (Wind Speed 5m/s) • 6.5 V (Wind Speed 4m/s) • 4.8 V (Wind Speed 3m/s)

This sub-chapter has two parts. First part includes 3 cases which have been compared for performance analysis. ‘Case A’ showed a battery of 6V, 3.2AH, which was charged from 4.2V to 5V through a DC DC converter followed by a series of 4 Supercapacitors (2.7V, 35F). ‘Case B’ and ‘Case C’ demonstrated the direct charging of the battery; where ‘Case B’ was experimented with the converter and ‘Case C’ was without converter. All the three cases were experimented in low wind speed that ranges between 6m/s to 3m/s. Second part of this section deals with the complete charging analysis. It is important to note that, although Supercapacitors have lower energy density comparing to the battery, the proposed novel energy harvesting circuit still capable of charging a battery which has higher energy density. This is because Supercapacitor bank used here charges the battery though its instantaneous charging and discharging cycle. It does not store the energy for long; rather as soon as the Supercapacitor bank gets fully charged by the turbine, it promptly discharges through the battery.

4.6.1. Part 1: For wind Speed = 5m/s

Case A: Energy Harvesting through Supercap

In this case, battery was charged through supercapacitor. Supercapacitors, being charged by the generator, discharged to battery. One entire charging and discharging process was considered as one cycle. For a wind speed of 5 m/s, 18 cycle was needed to charge the battery from 4.2V to 5V. Each cycle was for 27 minutes in which charging of Supercap took 25 minutes on average whereas discharging took 2minutes. 18 cycles, therefore, indicate 8.1 hours of total charging process of the battery.

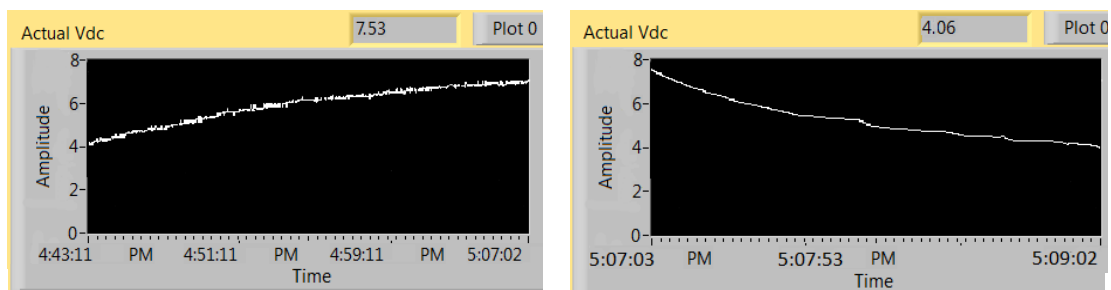


Figure 4.38: Labview GUI for Supercap Charging & Discharging

In reference with figure 4.35, diagrams given as follow illustrate the overall system process in details. Among them, figure 4.39 and figure 4.40 above represents the voltage analysis of one complete cycle. In figure 4.39 shows data, taken for four cycles, which were charged up to 7.5V from 4V. It took 25 minutes for one cycle to charge up and all the four cycles indicated the same pattern. On the other hand, figure 4.40 displays the discharging voltage of four cycles from 7.5V to 4V. Here, 2 cycles took 110 seconds and another two required 120 seconds. For calculation, on average, 2 minutes (120 Seconds) were taken in consideration for the discharging process.

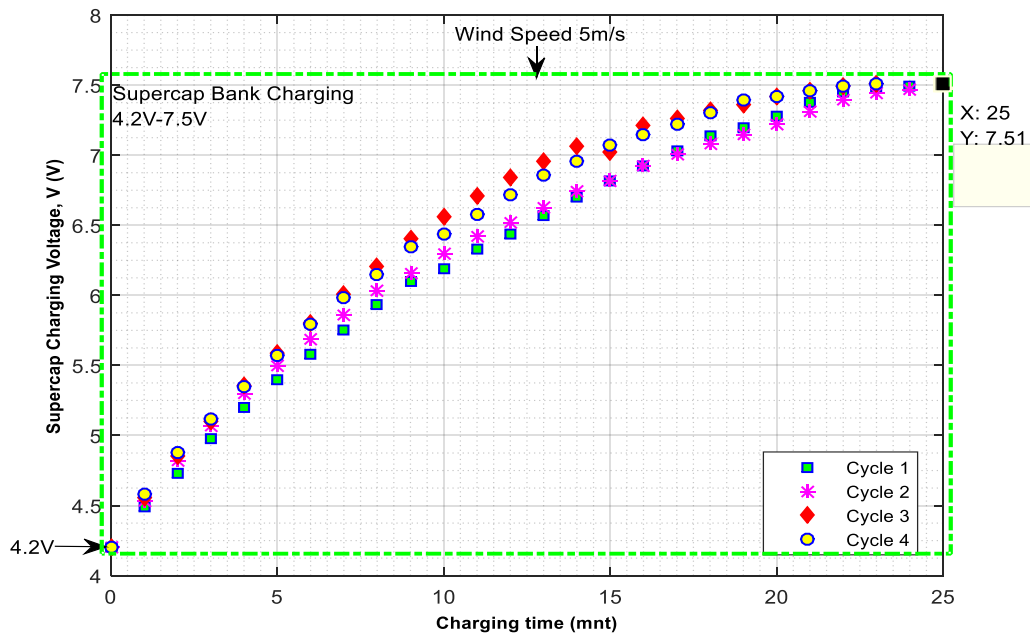


Figure 4.39: 'Supercap Charging Voltage' vs 'Time' for different charge cycle at Wind Speed 5m/s

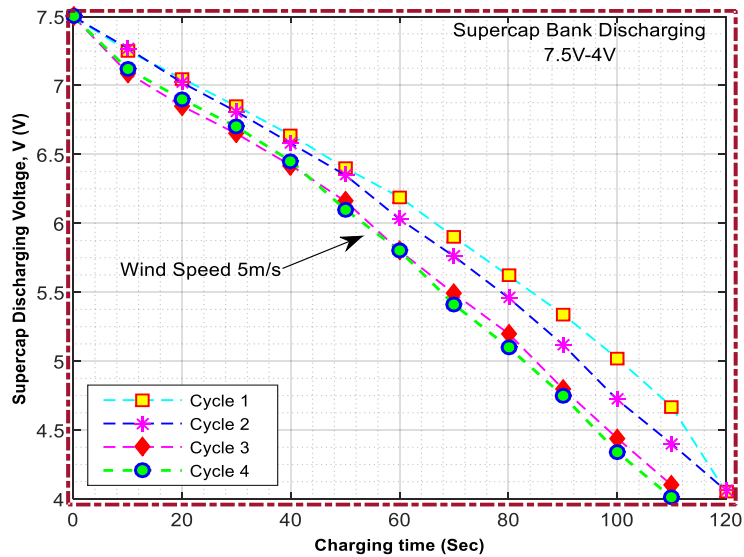


Figure 4.40: 'Supercap Discharging Voltage' vs 'Time' for different charge cycle at Wind Speed 5m/s

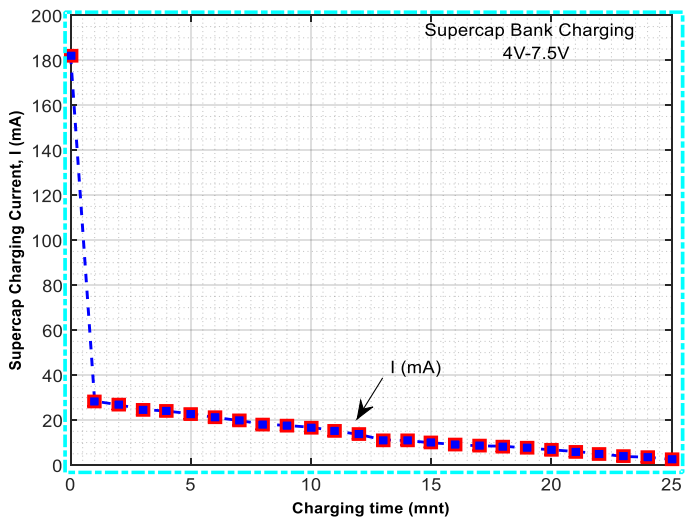


Figure 4.41: 'Supercap Charging Current' vs 'Time' at Wind Speed 5m/s

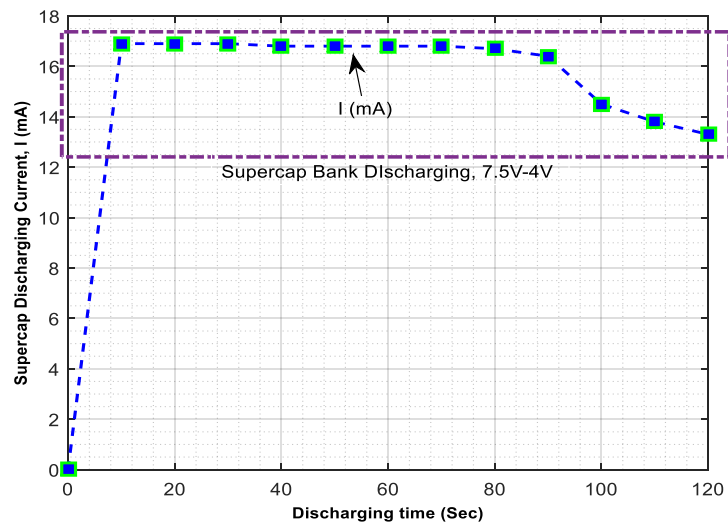


Figure 4.42: 'Supercap Discharging Current' vs 'Time' at Wind Speed 5m/s

Following two figures of 4.41 and 4.42 illustrate charging and discharging current of the Supercap. During the charging process, the peak current was 180mA at the starting time, followed by a sharp decline to 30mA and then a gradual slow decrease to 25mA. Therefore, the current drawn by the Supercap, for a wind speed of 5m/s, ranges between 30mA-25mA. Coming to the discharging process, Supercap Bank took only two minutes to discharge to the battery (from 7.5V to 4V) as stated earlier. The current drawn from the battery progressively slowed down to 12.5mA from 17.5mA.

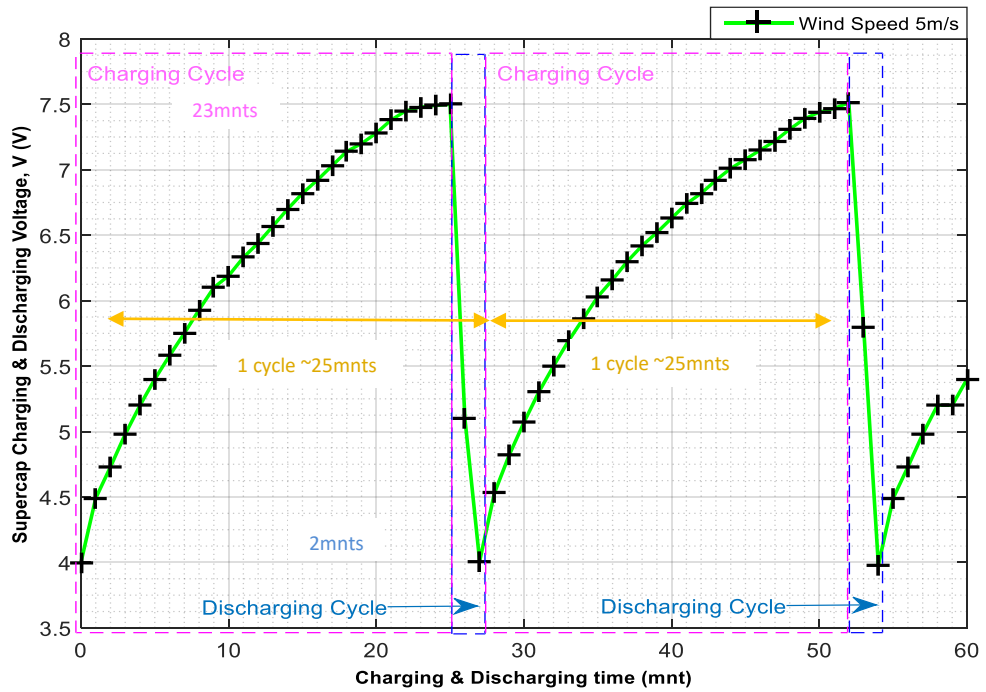


Figure 4.43: Supercap Charging & Discharging Voltage in respect of time at Wind Speed 5m/s

Figure 4.43 above gives Supercap charging and discharging voltage for 5m/s speed which was earlier observed in Labview GUI. One cycles required 25mnts to complete in which charging took 23 minutes and discharging took 2 minutes. Figure 4.44 and figure 4.45 point towards the increase of the battery voltage in respect to cycle and charging our respectively.

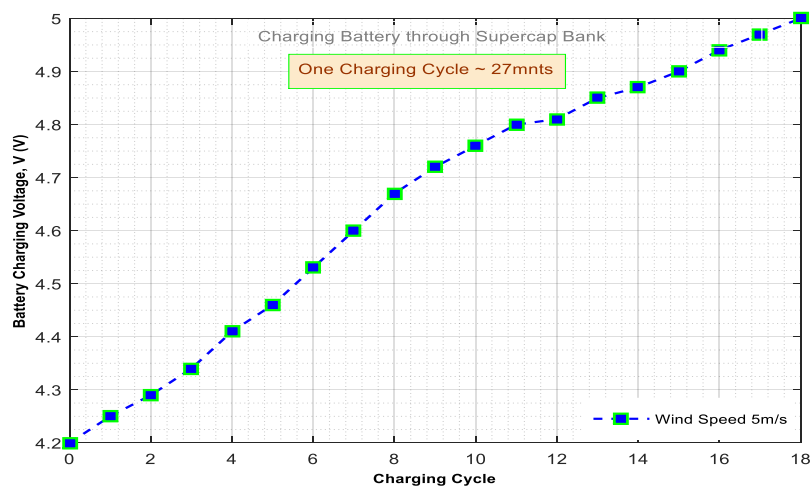


Figure 4.44: Battery Charging Voltage with respect to charge cycle for 5m/s Wind Speed

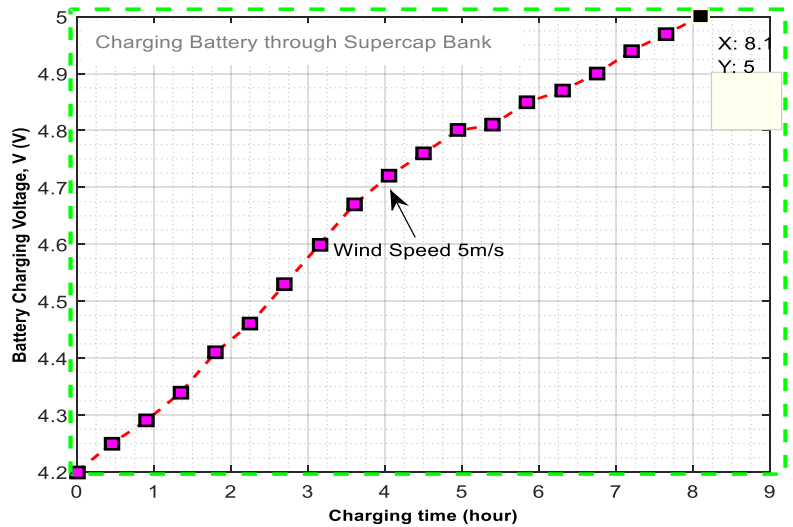


Figure 4.45: Battery Charging Voltage with respect to time for 5m/s Wind Speed

To sum it up, at 5m/s speed, Case 1 required 18 cycle of 27 minutes in order to charge the battery from 4.2V to 5V which was 8.1 hours in total.

Case B: Energy Harvesting without Supercap (with converter)

In this part, without the use of supercapacitors, turbine was fed to charge the battery through the converter. According to figure 4.46, it took almost 17.5 hours to reach its maximum value of 4.8V. After that the increase of the voltage was so less with respect to time, the value was not taken in consideration.

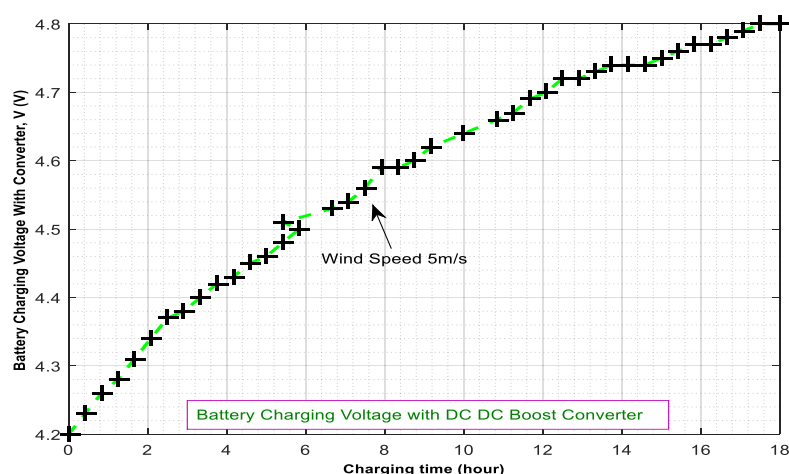


Figure 4.46: Battery Charging Voltage with respect to time for 5m/s Wind Speed (with converter)

Case C: Energy Harvesting without Supercap (without converter)

This part takes the converter out and connects the turbine directly with the battery.

As it can be observed from figure 4.47, this approach took less time (10 hours) than case B (direct charging via converter). However, the generator output voltage fluctuates and battery needs a steady constant voltage for charging up. Therefore, this method is not recommended and applying this method for a longer period will result damaging of the battery. Still results were gathered for the sake of comparison.

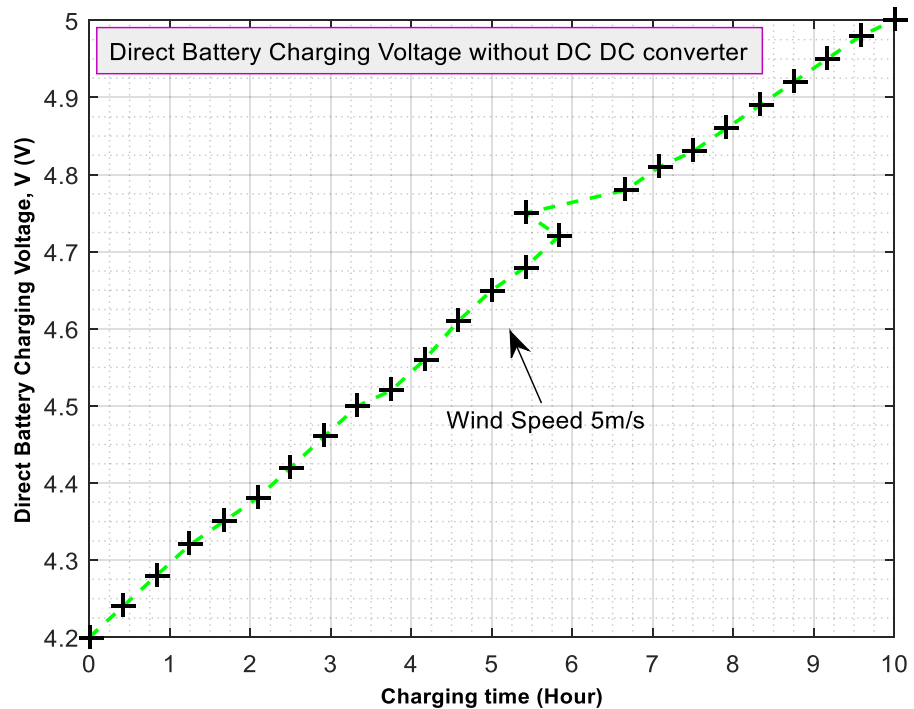


Figure 4.47: Battery Charging Voltage with respect to time for 5m/s Wind Speed (without converter)

Efficiency Comparison

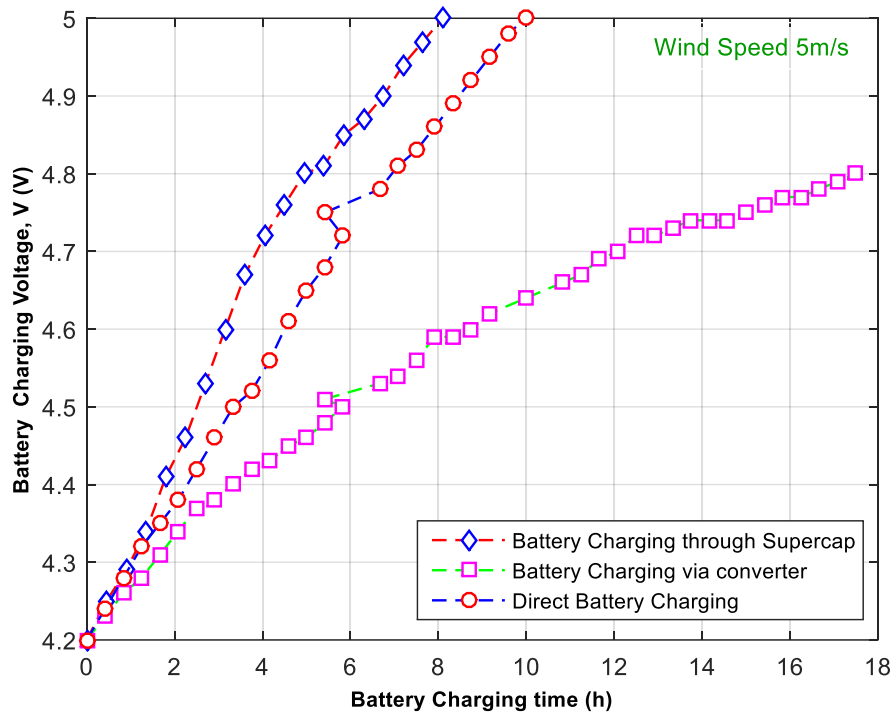


Figure 4.48: Battery Charging Voltage under 3 cases in respect with time at a fixed Wind Speed of 5m/s

Figure 4.48 indicates the comparison between all the 3 cases. ‘Case C’ was taken as a reference point while comparing. It was found out that charging through supercapacitors was 19% more efficient (Case A) than direct charging without converter (Case C). Supercap battery charging is also 133% more efficient than direct charging with a converter although charging through conduction was not successful as it failed to go beyond 4.8V; technically making ‘Case B’ as incompetent to work in 5m/s. That makes ‘Case 2’ being unworthy in low wind speed situation.

Summary

Table 4.9 and 4.10 recall the finding of this section in brief.

Table 4.9: Charging Battery (from 4.2V to 5V) through Supercap at 5m/s Wind Speed

Supercap Charging Cycle	:	25 mnts
Supercap Discharging Cycle	:	2 mnts
Number of Complete Cycle	:	18
Maximum Supercap Charging Current	:	30mA
Maximum Supercap Discharging Current	:	18.5mA
Time duration	:	8.1 hours

Table 4.10: Efficiency Comparison among Case A, Case B and Case C at 5m/s

Battery Charging Voltage (4.2V-5V)	Efficiency (%)	Reference Point:
Case A (Energy Harvesting)	: 19%	<u>Case C- Direct Charging</u> <u>Without converter</u>
Case B (Charging with Converter)	: Incompetent	

4.6.2. Part 2: For wind Speed = 4m/s

Case A: Energy Harvesting through Supercap

Same procedure from earlier section was followed and results were graphically plotted for analysis. Following figures are the details of charging process. It is noteworthy mentioning that both the Supercap discharge voltage and discharge current were same as the previous value. This is because while Supercap bank discharged its charge to the battery, the turbine system was made isolated through the MOSFET switch. Therefore, wind speed cannot make any impact on the discharging half cycle. Consequently, in all the three cases, the discharge voltage and current amount in respect to time were the same. Here, figure 49 and figure 50 show the charging voltage and current graph in respect with time. For The discharging details, section 4.5.1 may be reviewed as both of the cases, the data will be same.

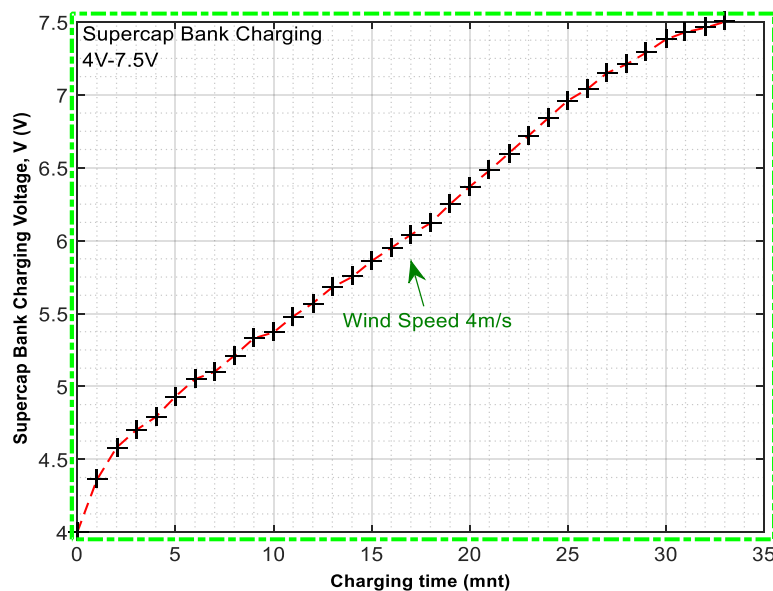


Figure 4.49: 'Supercap Charging Voltage' vs 'Time' at Wind Speed 4m/s

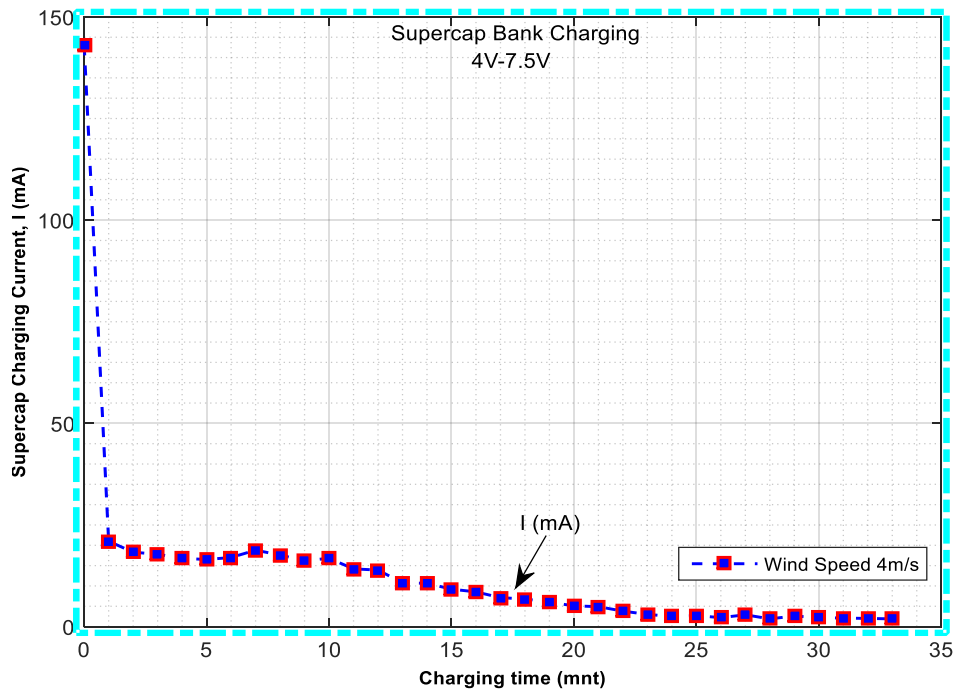


Figure 4.50: 'Supercap Charging Current' vs 'Time' at Wind Speed 4m/s

At this point, 35 minutes were required to charge up the Supercap bank. Adding the discharging cycle time which was 2mnts, the complete cycle duration was then 37 minutes. The starting current was 145mA which took a rapid fall in the next second, bringing the current down to 22mA. As for the inertia of the turbine, understandably the charging current at first was very high but that could not be misinterpreted as the actual current. The real current started from 22mA followed by a gradual decrease that ended up at 2.5mA. Therefore, the pick current could be considered as 22mA. Figure 4.51 displays the complete cycle process which basically was the charging and discharging cycle of 37 minutes.

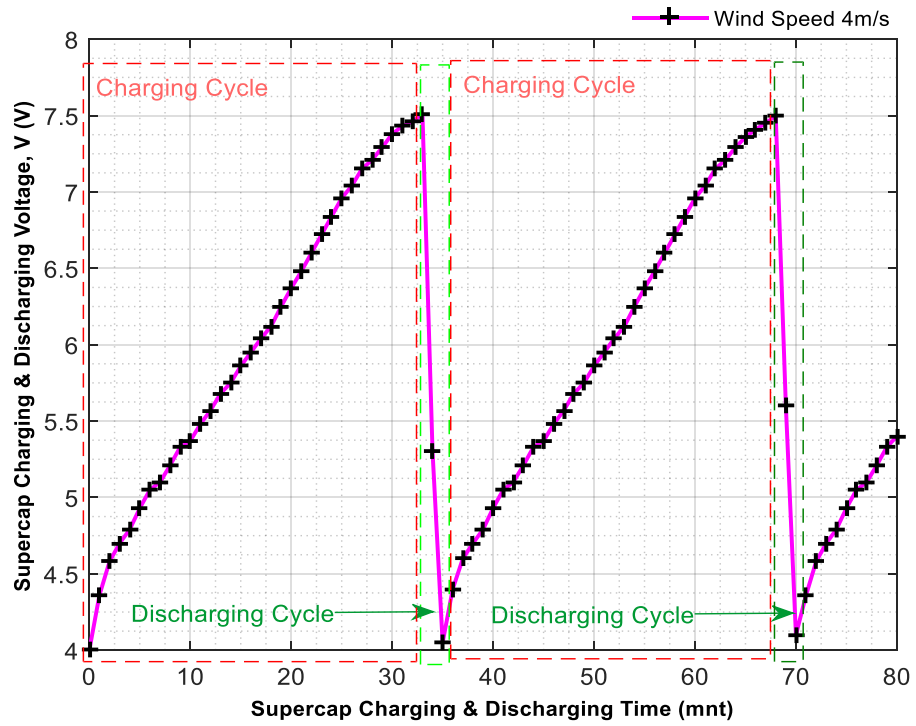


Figure 4.51: Supercap Charging & Discharging Voltage in respect of time at Wind Speed 4m/s

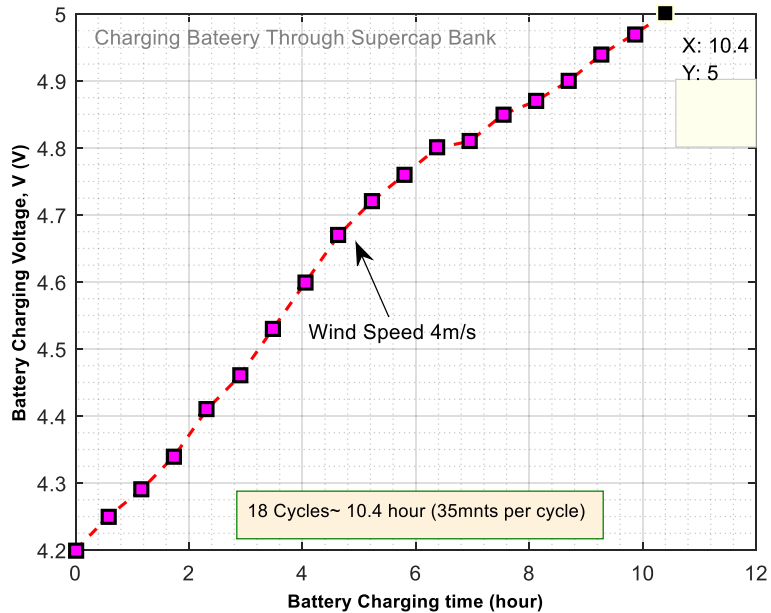


Figure 4.52: Battery Charging Voltage with respect to time for 4m/s Wind Speed

Again 18 cycles were needed to charge up the Supercap bank from 4.8V to 5V but in this time one cycle consisted of 37 minutes which in total made the system took 10.4 hours of charging time. Figure 4.52 above represents the battery voltage charging up to 5V in 10.4 hours.

Case B: Energy Harvesting without Supercap (with converter)

According to figure 4.53, it took 18.75 hours to reach its maximum value of 4.54V.

After that the increase of the voltage was so less with respect to time, the value was not taken in consideration. Therefore, this charging system was incapable to charge up the device at 4m/s.

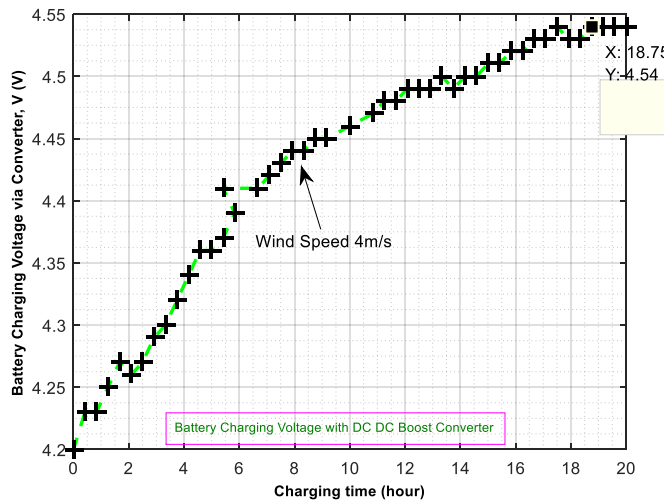


Figure 4.53: Battery Charging Voltage with respect to time for 4m/s Wind Speed (with converter)

Case C: Energy Harvesting without Supercap (without converter)

'Case C' took 15 hours to finish the task. Figure 4.54 is showing the battery charging voltage in respect to time.

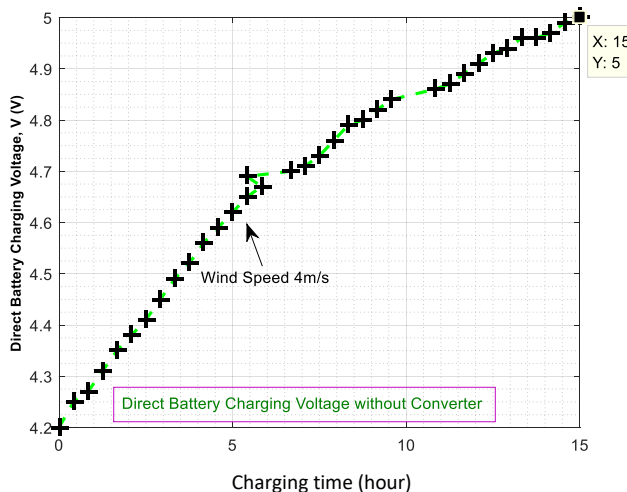


Figure 4.54: Battery Charging Voltage with respect to time for 4m/s Wind Speed (without converter)

Efficiency Comparison

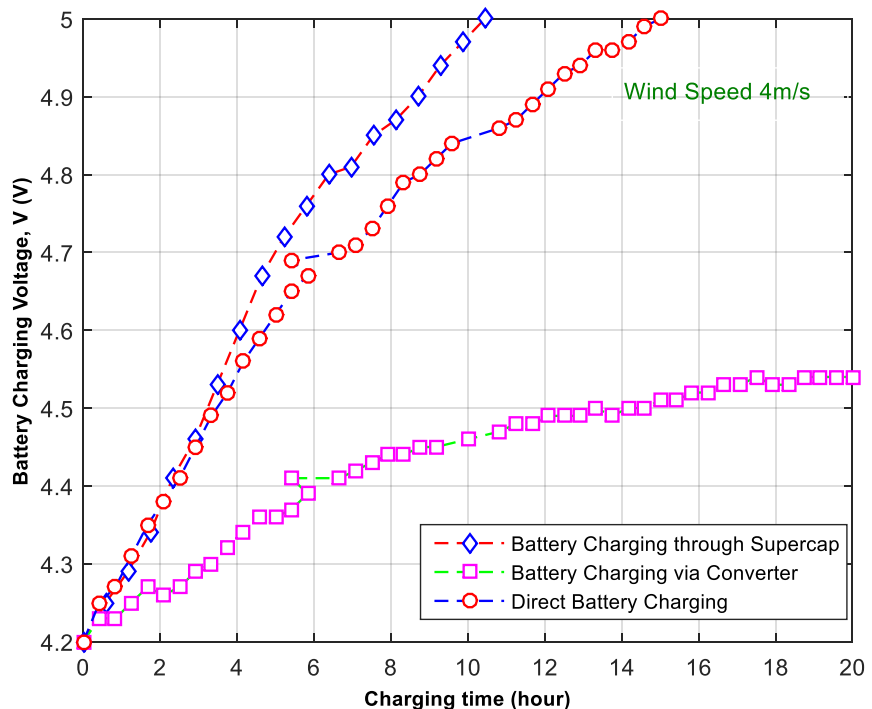


Figure 4.55: Battery Charging Voltage under 3 cases in respect with time at a fixed Wind Speed of 45m/s

Figure 4.54 illustrates the comparison among the 3 cases at wind speed 4m/s. Again, 'Case C' was taken as a reference point while comparing. It was calculated that charging through Supercapac was 31% more efficient than direct charging without converter. Supercap battery charging was stopped at 4.54V for direct charging with a converter indicating the system unable to produce enough voltage in low wind speed to charge up the battery with converter. That makes case 2 being unworthy in low wind speed situation as expected.

Summary

Table 4.11 and 4.12 recapitulate the result of this section in brief.

Table 4.11: Charging Battery (from 4.2V to 5V) through Supercap at 4m/s Wind Speed

Supercap Charging Cycle	:	35 mnts
Supercap Discharging Cycle	:	2 mnts
Number of Complete Cycle	:	18
Maximum Supercap Charging Current	:	22mA
Maximum Supercap Discharging Current	:	18.5mA
Time duration	:	10.4 hours

Table 4.12: Efficiency Comparison among Case A, Case B and Case C at 4m/s

Battery Charging Voltage (4.2V-5V)	Efficiency (%)	Reference Point:
Case A (Energy Harvesting)	: 31	<u>Case C- Direct Charging</u> <u>Without converter</u>
Case B (Charging with Converter)	: Incompetent	

4.6.3. Part 3: For wind Speed = 3m/s

Case A: Energy Harvesting through Supercap

Figure 4.56 and 4.57 show the charging voltage and current against time respectively.

Unlike the previous 4.5.1 and 4.5.2 section, Supercap bank could not be charged up to 7.5V. This was due to the lack of the mechanical torque, as the system was put in a very low speed of 3m/s. In low wind speed, turbine could not provide sufficient amount of mechanical power to PMSG so that it can charge up the Supercap bank to 7.5V. In order to come up with a solution, Supercap Bank charging voltage ranged was reprogrammed and lowered down to 6.8V. Even though, the Supercap Bank charging maximum voltage was set to 6.8V, due to low wind speed, it took 95 minutes to finish the charging cycle; whereas for wind speed 5m/s and 4m/s, Supercap Bank was finished charging up in 25 minutes and 35 minutes correspondingly. Hence, there was a significant delay of time observed while dealing with 3m/s wind speed. Apart from it, it can be spotted in figure 4.57 that the charging current also consequently was observed to be lower than the first two section, having a maximum current of 18mA.

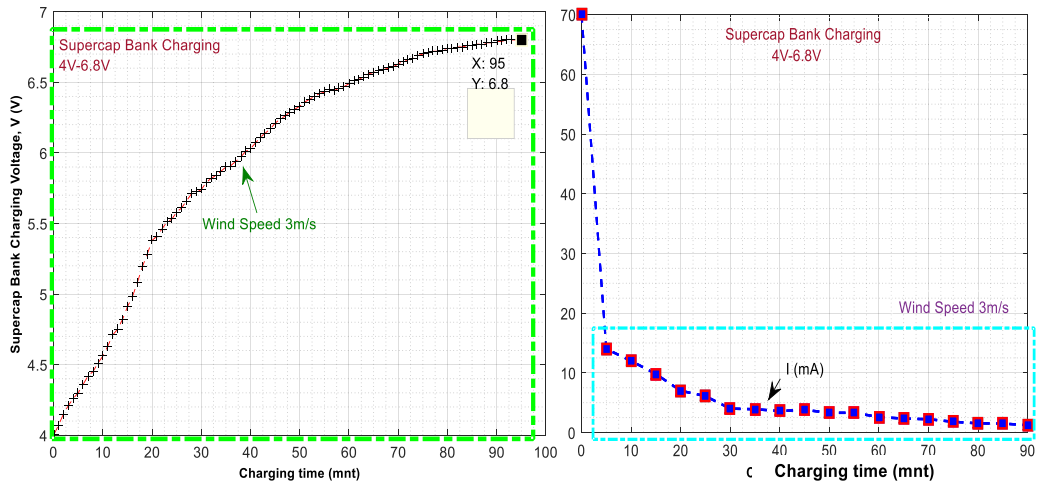


Figure 4.56: 'Supercap Charging Voltage' vs 'Time' at Wind Speed 3m/s

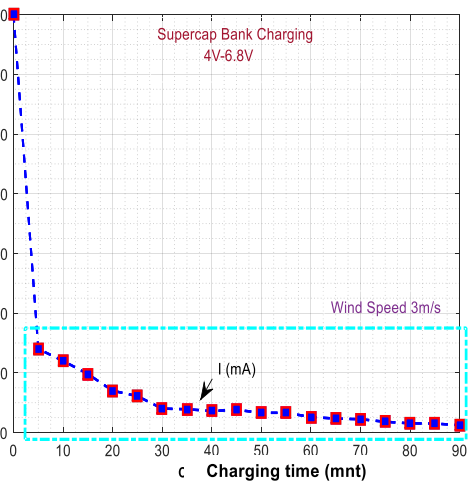


Figure 4.57: 'Supercap Charging Current' vs 'Time' at Wind Speed 3m/s

Figure 4.58 displays the complete cycle of Supercap bank charging and discharging period. Unlike the first two wind speeds, discharging process took only one minute as the Supercap voltage was no longer 7.5V. Therefore, one complete cycle in this section contains in total of 95 minutes of charging and discharging process.

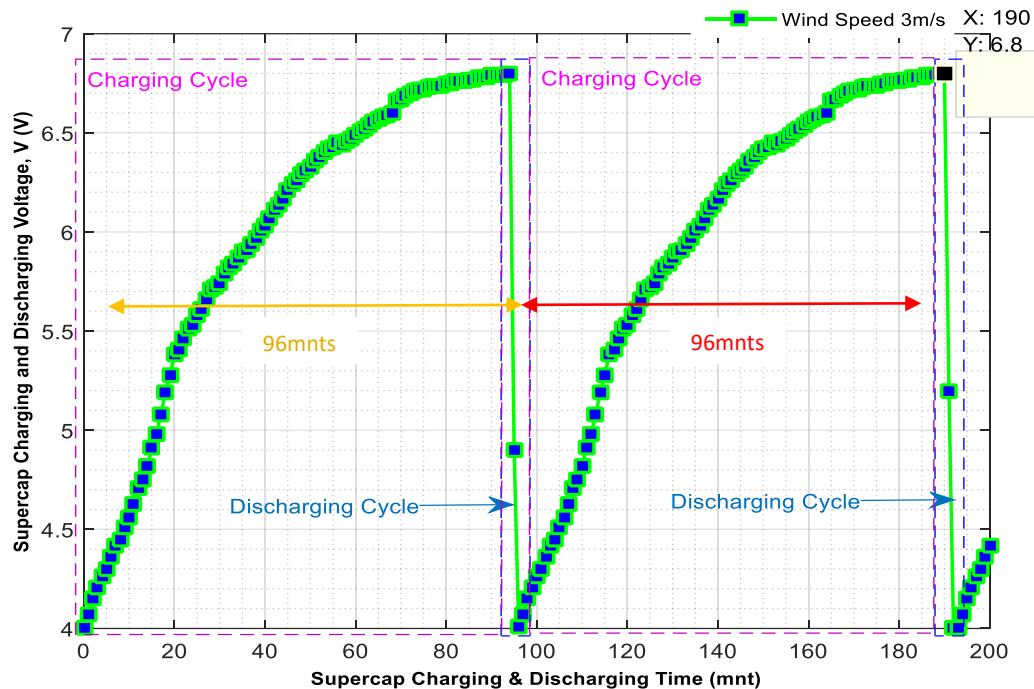


Figure 4.58: Supercap Charging & Discharging Voltage in respect of time at Wind Speed 4m/s

Figure 4.59 below points out the number of complete cycle required to charge up the Supercap Bank to 6.8V. 18 cycles were needed both in the last two sections but in this case number of cycle increased. This is because both for the last two times, the Supercap Bank was charged to 7.5V, therefore discharging process took the same number of cycle even though time duration was different. In this case, at 3m/s wind speed, generator could not charge up the Supercap bank to 7.5V but 6.8V. Consequently, while discharging, a Supercap Bank of 6.8V was discharged to the battery rather of 7.5V. Thus it ended up taking higher number of cycle (24 cycles) to finish charging.

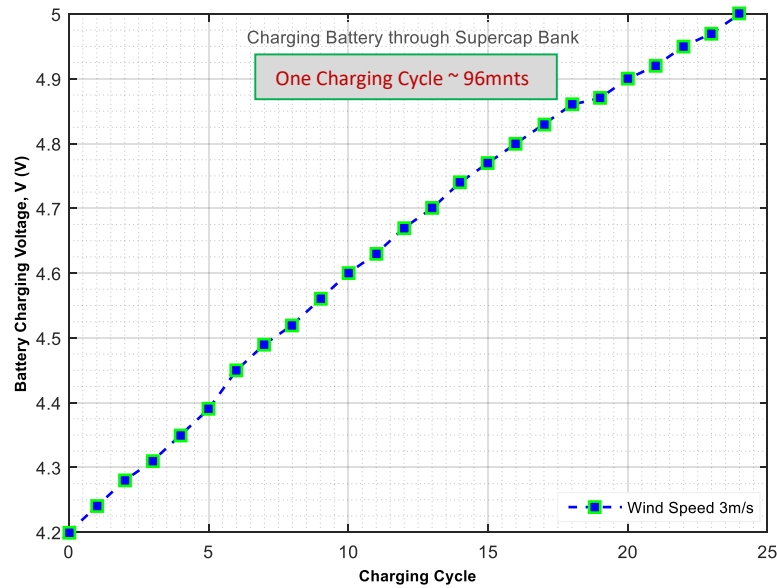


Figure 4.59: ‘Battery Charging Voltage’ vs ‘Charge Cycle’ for 3m/s Wind Speed

Figure 4.60 provides the total duration time of the charging process. It can be spotted that for a number of 24 cycles, in which each cycle was made of 95 minutes, a total duration of 38.4 hours was required to complete the battery charging process. This time period is significantly longer than the previous time of 10.4 hours which was performed at 4m/s wind speed. This is an important finding which will be discussed further on the overall comparison section.

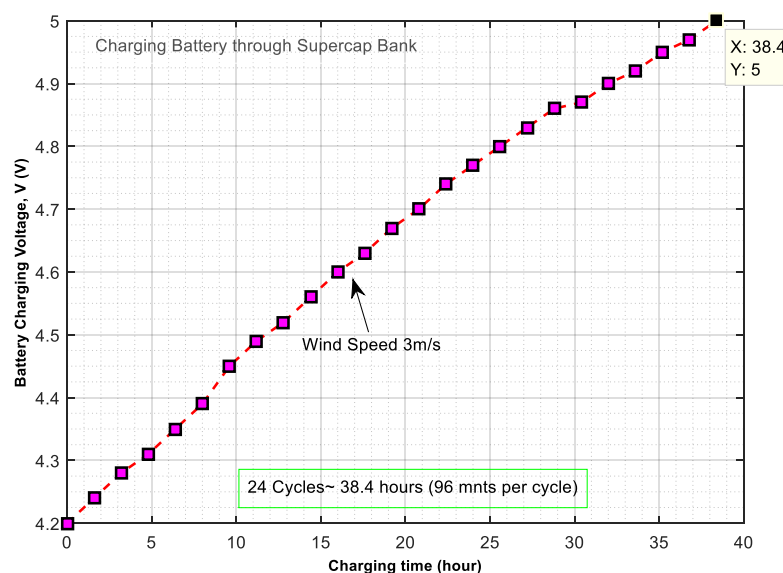


Figure 4.60: Battery Charging Voltage through Supercap with respect to time for 3m/s Wind Speed

Case B: Energy Harvesting without Supercap (with converter)

Since the system did not provide good response in wind speed of 4m/s, hence, it was expected to degrade further with even lower speed. Therefore, ‘Case B’ was not experimented in this section.

Case C: Energy Harvesting without Supercap (without converter)

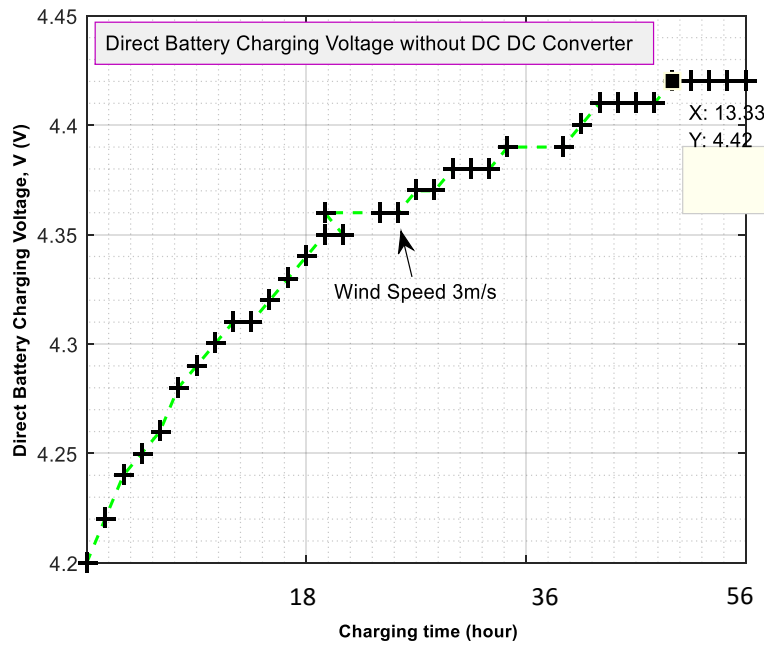


Figure 4.61: Battery Charging Voltage with respect to time for 3m/s Wind Speed (without converter)

Figure 4.61 represents the amount of time taken by the battery to get charged up from the turbine directly without the converter. As it was mentioned before, this method is not suitable for energy harvesting since for any type of battery, a constant charging cycle is required and fluctuation causes damage. Since for the sake of comparison, experiment was performed. It was observed that charging was very slow and it took nearly 53 hours to charge the battery up to 5V which surely was considerably longer than the previous charging at 4m/s where the same system needed 15 hours to charge.

Efficiency Comparison

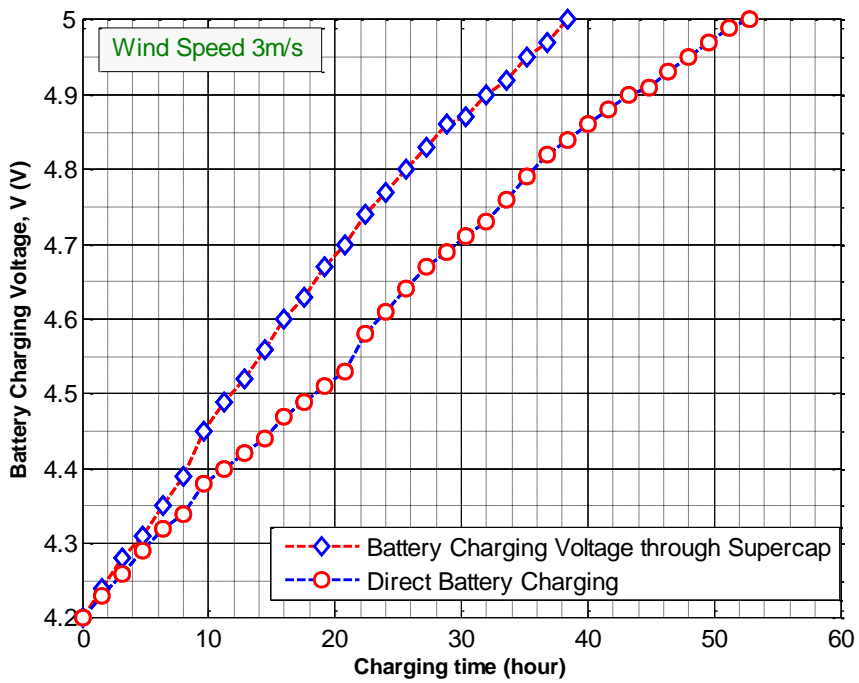


Figure 4.62: Battery Charging Voltage under 2 cases in respect with time [3m/s]

Figure 4.62 illustrates the comparison among the 3 cases at wind speed 3m/s. Again, ‘Case C’ was taken as a reference point while comparing. While ‘Case C’ required a time frame of 53 hours to complete the charging process, 38.4 hours were needed by ‘Case A’. It was calculated that charging through Supercapac was 28% more efficient than direct charging without converter. At 4m/s, Supercap battery charging was stopped at 4.54V for direct charging with a converter in the previously mentioned section. Subsequently, being unable to produce enough voltage in low wind speed to charge up the battery with converter, ‘Case B’ was not taken in consideration in this section.

Summary

Table 4.13 and 4.14 recapitulate the result of this section in brief.

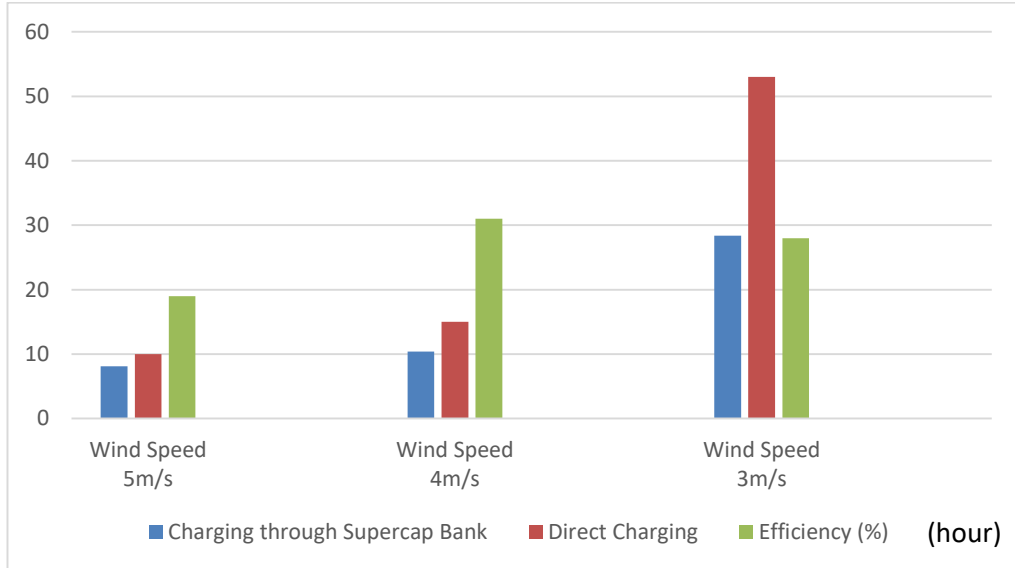
Table 4.13: Charging Battery (from 4.2V to 5V) through Supercap at 3m/s Wind Speed

Supercap Charging Cycle	:	95 mnts
Supercap Discharging Cycle	:	1 mnts
Number of Complete Cycle	:	25
Maximum Supercap Charging Current	:	18mA
Maximum Supercap Discharging Current	:	18.5mA
Time duration	:	38.4 hours

Table 4.14: Efficiency Comparison among 'Case A', 'Case B' and 'Case C' at 3m/s

Battery Charging Voltage (4.2V-5V)	Efficiency (%)	Reference Point:
Case A (Energy Harvesting)	: 28	<u>Case C- Direct Charging</u> <u>Without converter</u>
Case B (Charging with Converter)	: Incompetent	

4.6.4. Overall Summary and Efficiency comparison



Wind Speed (m/s)	Battery Charging via		Efficiency (%)
	Supercap (hr)	Direct Battery Charging Time (hr)	
5	8.1	10	19
4	10.4	15	31
3	38.4	53	28

Figure 4.63: Summary of Energy Harvesting Circuit Result for charging a 6V Lead Acid

Battery from 4.2V to5V

As shown by figure 4.63, the energy harvesting circuit data shows excellent values for all the results with very good performance overall. Change in the wind speed from 5m/s to 4m/s produces better efficiency as it goes to 31% from 19%. For a low speed of 3 m/s, where direct charging displays a poor performance, energy harvesting circuit, even though took a long time of 38.4 hours to charge up the battery, still maintains its productivity by producing an efficiency 28%. Here, the highest amount of efficiency was drawn from the system was 31%. Comparing to the Worthington's work of pulling

off 300% more efficiency with hybrid energy harvesting, it is drastically low. However, his storage system was implemented to a pump tire circuit, whereas our circuit was designed for a low wind application. As an off-grid standalone low voltage energy harvesting system, the EHC was able to provide noteworthy better efficiency in all three low wind speeds.

An important observation had been made in this experiment. At low wind speed turbine tends to slow down and stop if there is a heavy load. This is because a Permanent Magnet Synchronous Generator has an output frequency which is proportional to its armature speed. The required torque to rotate the PMSG is proportional to the electrical load. Therefore, at low wind speed, with the increase of the electric load, there is always a tendency to slow down while the mechanical input coming from the VAWT tries restore it. However, if the load is too much to handle, the mechanical speed from the turbine becomes very slow and eventually the turbine stops.

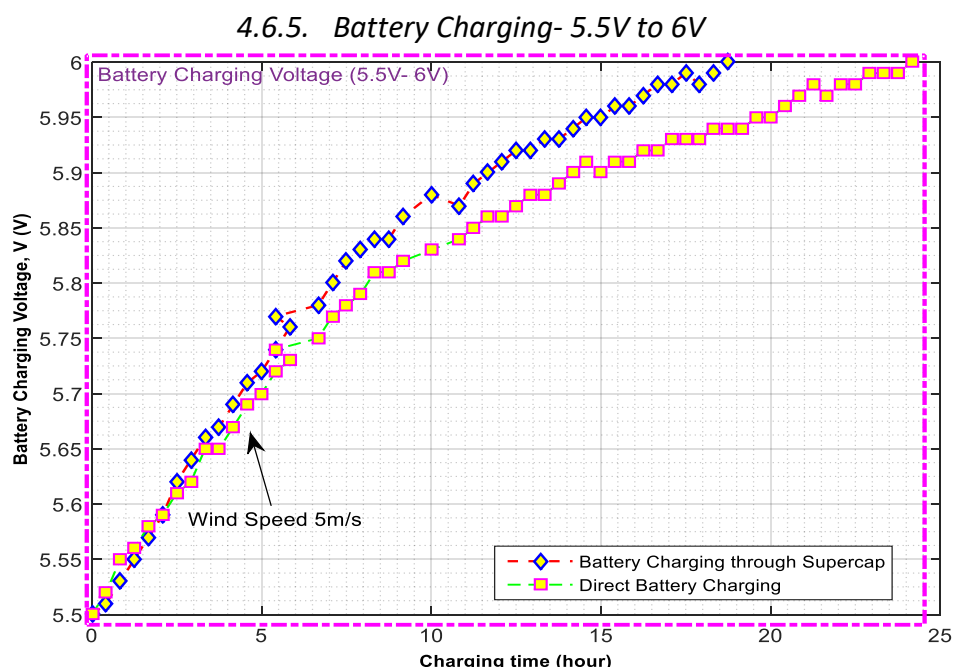


Figure 4.64: Battery Charging Voltage (5.5V to 6V] comparison with respect to time for 5m/s Wind Speed

Another experiment was conducted with and without energy harvesting circuit to charge the battery from 5V to 6V at 5m/s. Applying the energy harvesting circuit, the battery was being charged by the Supercap bank. It was observed that with the energy harvesting circuit, battery took almost 18.8 hours to finish charging whereas direct charging needed 24.2 hours. According to the experimental result, energy harvesting circuit was 22% more efficient than direct charging.

4.6.6. Theoretical Analysis of Battery charging via Supercapacitor Cycle

For wind speed = 5 m/s

Theoretical Calculation

$$\text{Energy in Supercapacitor Bank, } E_{\text{Supercap_Bank}} = \frac{1}{2}CV^2 = \frac{1}{2}8.76 \times 10.8^2 = 511 \text{ J}$$

The Peak Voltage of Supercap Bank Cycle = 10.8V,

However, the Boost Converter cannot step up voltage less than 4V. Therefore, usable Energy in the Supercapacitor Bank,

$$\begin{aligned} E_{\text{Supercap_Bank_Effective}} &= \frac{1}{2}CV_1^2 - \frac{1}{2}CV_2^2 = \frac{1}{2}C(V_1^2 - V_2^2) \\ &= \frac{1}{2}8.76 \times (10.8^2 - 4^2) = 440 \text{ J} \end{aligned}$$

Battery Rating, 6V, 3.2AH which is equivalent to 19.2Wh [A 6V 1AH can store 12Wh]

Here, 19.2 Wh \sim (19.2 \times 3600 J) \sim 69120 J

From one cycle of Supercapacitor Bank, battery can store energy up to 440 J.

Again, 440 J energy is stored into a 6V 3.2AH battery in one cycle.

Therefore, 69120 J energy can be stored into a 6V 3.2AH battery in (69120/440) or, 157 cycle.

Note: one charging cycle of Supercapacitor bank takes 27 mnts on average.

Therefore, average time required for battery charging= [(27 \times 157) /60]hr = 70.65 hr

Experimental Observation:

From section 4.6.1,

It takes 8.1 hours to charge 1V of the battery [Section 4.6.1: from 4V to 5V]. Moreover, from section 4.6.5, after 5V, it takes 18.8 hours to charge 0.5V.

Therefore, total estimated battery charging hour = $[(8.1 \times 5) + (18.8 \times 2)] \text{ hr} = 78.1 \text{ hr}$

Percentage of Error

$$\text{Percentage of Error, POE} = \frac{|70.65 - 78.1|}{70.65} \times 100 \% = 10.54\%$$

The voltage drops in boost converter and MOSFET switch are the main reasons for difference in theoretical and experimental value.

Direct Charging without Converter

The battery takes 15 hours to charge 1V from the turbine until 5V. After 5V, it takes 24.2 hours to charge 0.5V.

Therefore, average time required for battery charging = $[(15 \times 5) + (24.2 \times 2)] \text{ hr} = 123 \text{ hr}$

Efficiency of Supercap based Battery Charging Circuit

$$= \frac{|123 - 78.1|}{123} \times 100 \% = 36\%$$

Chapter 5

Conclusion

5.1. Conclusion

As a conclusion to this thesis, the achievements are reviewed in terms of research objectives. This consequently facilitates the system and results to be analyzed in terms of the percentage and degree of the research objectives that was achieved. The aim of this thesis is to provide a framework on Maglev based Vertical Axis Wind turbine and PMSG, bringing them together as a cost-effective system for low wind rural Malaysian condition, followed by the implementation of Supercap based Energy Harvesting System in it. This chapter discusses the findings in brief and co-relate the achievements with the objective of the thesis. Table 5.1 presents the summary of the results that was presented in Chapter 4.

The first research objective of the research was to simulate and analyse the performance of Vertical Axis Wind Turbine in low wind speed. Furthermore, it extends to investigate the effect of different design parameters on turbine output. With a view to accomplishing this objective, a mathematical model at first was made which later was implemented in Simulink for performance analysis. For each input parameter such as wind speed, power-coefficient, radius or height of the turbine; turbine output mechanical speed, torque and power were changed. To make sure the model gives correct value, simulation data first was compared with theoretical data. With a maximum error of 1.4%, the system was considered accurate enough. It was observed that the height and radius of the turbine was directly proportional to the power

generated from the turbine regardless the turbine radius. Next, observation made on torque produced by the wind turbine that was increased with mechanical speed until maximum torque was achieved, of which a further increase in the speed then resulted decrease in the torque. Another finding was related to blade pitch angle. The ‘Pitch Angle’ was changed to have a look at the effect on power under various TSR (Tip Speed Ratio). Result showed that with the increase of the pitch angle, turbine power and torque started to become low. At null pitch angle, turbine produces the maximum power for all cases. The simulation was carried again under different wind speed to observe the change the power with the increase of Swept Area. It was found that at high wind, a slight increase in the swept area resulted larger change in power. Therefore, any change in the radius or height will cause significant power variation at high speed and vice versa. At low wind speed of 3m/s, noteworthy change in the turbine design in terms of radius and height would be needed to generate higher current and power. The findings stated above clearly justify that the developed Simulink model of VAWT has met the first objective.

The second objective was to simulate and analysis the performance of different types of Axial Flux Permanent Magnet Synchronous Generator for low wind Vertical Axis Turbine. After building up the Simulink model in dq reference frame with Park Transformation, result showed comparison on 3 types of PMSG in terms of wind speed, pole number and turbine rotational speed. A VAWT of 1.5m radius and 2.25m height was chosen. With a nominal frequency of 60Hz, 4 pole, a 10KW 3-Phase, 5-phase and Dual Stator PMSG were put into simulation under referred design parameters. Result showed, at low wind speed, 5-phase PMSG was the most efficient

among all by producing 10W. 3-phase PMSG generated 5W whereas Dual stator produced only 2W. 5-Phase was 100% more efficient than 3-Phase. But comparing with Dual Stator, 3-Phase was 45.71% more efficient. At a relatively higher speed of 8m/s, 5-phase still holds the top but this time dual stator exceeded 3-phase with a 58% increase. Here, 3-Phase, Dual Stator and 5-phase generated 100W, 158W and 198W respectively. This pointed out that Dual Stator performed better than 3-phase in high wind. Conversely, performance of Dual Stator dropped dramatically even than of the 3-phase when wind speed became low. Therefore, for low wind speed Dual Stator cannot be used as a primary option. Coming to the Pole Pair variation, when the number of poles was fixed at 24, with a reference to 5-phase, Dual Stator was 17.78% less efficient whereas for 3-phase, it was 47.71%. While using 2 pole generator, result showed the same pattern. It is important to note that with the variation of Pole number [from 2 to 24], output power of 3-Phase, Dual Stator 5-phase increased 24%, 21.6% and 22% respectively. Both at low and high pole pair, 3-Phase exhibited maximum power reduction of more than 45% compared to 5-phase. Lastly the rotational speed of the turbine was changed. The observation followed the same pattern. But a noteworthy observation was made in the case of low rotational speed. When the rotational speed of the turbine was less than 20rad/s, generated power varied only a little. This is an important observation as it tells us that for low speed system, all the 3 types of generator configuration will not differ much in terms of power. Only few selective researches were made on the simulation comparison of 3 types of Axial Flux PMSG. Implementing all the three types of Axial Flux PMSG into VAWT was even rare. The second objective thus met with novel findings which were later used to optimize the system.

Table 5.1: Summary of results

Task	Technique	Results	Reference
Performance Analysis of VAWT	Mathematical Model, Matlab-Simulink	Theoretical Value matched with Simulation- accuracy over 98.5%.	Section 4.1, Figure 4.1-4.11
		With increase of height, both VAWT torque and power increasd regardless of swept area. But for turbine radius, MPPT was required as turbine performance decreased after MPPT point.	
		Null pitch angle provided maximum efficiency	
Performance Analysis of Axial Flux PMSG	Mathematical Model, Park Transformation, Swing Equation, Simulink	At [8m/s wind], Dual Stator- 58% more efficient; 5-Phase- 98% more efficient (reference: 3-phase PMSG).	Section 4.2.1, Figure 4.12-4.23, Table 4.1
		At [3m/s Wind], 5-phase- efficiency increased 99%, but Dual Stator reduced 45.71% efficiency compared to 3-phase.	
		Dual Stator was less efficient in low wind speed. 5-Phase outcasted other two types but for low cost and maintenance issue, 3-phase PMSG was chosen for the system.	
		With variation of Pole number [from 2 to 24], output power of 3-Phase, Dual Stator 5-phase increased 24%, 21.6% and 22% respectively which were almost same. Both at low and high pole pair, 3-Phase exhibited maximum power reduction of more than 45% compared to 5-phase	Section 4.2.2, Figure 4.24, Table 4.2
		At low VAWT rotational speed, all three types showed little variance in power if other design parameter kept same	Section 4.2.3, Figure 4.23
Optimization (Comparing with existing Rural Malaysian Model)	Low Wind speed, Maglev	Configuration 1: 3 bladed Null pitched VAWT with 2.6m Height & 1m Radius adopted to 1.5KW, 220V, 20 pole 3-phase AFPMSG. Weight 75KG	Section 4.3.1-4.3.2 Figure 4.24-4.33
		Configuration 2: 9 bladed Null pitched VAWT with 60cm Height & 14.5cmRadius adopted to 200W, 12V, 16 pole 3-phase AFSG. Weight 12.5KG	
Cost-efficiency	In comparison with existing Malaysian Model along with Weight to Power Ratio	WPR ₁ - 0.05kg/W, WPR ₂ - 0.0625. Hence, WPR ₂ ~ 20% more cost efficient Proposed System 1- 1500USD Proposed System 2- 310USD	Table 4.6
Prototype	Configuration 2	At 8 Pole configuration- exhibited Open Circuit Voltage [V] of 7, 7.5, 7.9 and 8,1 for wind speed [m/s] of 4, 5, 6 and 7 respectively	Figure 4.37

		At 4 Pole configuration- exhibited Open Circuit Voltage [V] of 5.2, 5.4, 5.8 and 5.9 for wind speed [m/s] of 4, 5, 6 and 7 respectively	Figure 4.36
Energy Harvesting Circuit (EHC)	Supercap bank, Control System, MOSFET Switching, Labview, DAQ	Battery Charging [4.2V-5V] At 5m/s- EHC 19% more efficient than direct charging At 4m/s- ECH 31% more efficient than direct charging At 3m/s- ECH 28% more efficient than direct charging	Figure 4.63
		Battery Charging [5.5V-6V] ECH 22% more efficient than direct charging [at 5m/s]	Figure 4.64

The third objective of this research was to design an optimized Maglev based VAWT system in terms of rural Malaysia that can be attached to a 3-Phase Axial Flux PMSG in rural Malaysia's perspective. This was done in two steps. First, different existing wind turbines in rural Malaysia have been studied in order to get simulation parameters. Next, with the basis of simulation results, two system configurations were selected which under different design parameters, produced sufficient amount of torque and power in low wind speed. A 3 bladed null pitched VAWT with 1m radius and 2.6m height with a 1.5KW 220V 3-Phase AFPMSG with 20 Pole was considered as optimized configuration 1 whereas a 9 bladed null pitched VAWT with 14.5cm radius and 60cm height with a 200W 12V 3-Phase AFPMSG was considered as optimized configuration 2.

The fourth objective of this research was to evaluate the developed system and compare it with current existing models in rural Malaysia in terms of cost analysis. Both the configurations then were put into the WPR, 'Weight to Power Ratio', test in order to select the performance in terms of low cost. It was found out that WPR of configuration was 0.05kg/W whereas for configuration 2, it was 0.0625 kg/W. Configuration 2, relatively was proved to be 20% more cost efficient than

configuration 1. Also, cost estimation of configuration 1 was 1500USD whereas for configuration 2, it was 310USD. Configuration 2 was the most inexpensive and economical in comparison not only with configuration 1 but also with five other existing wind turbine models in rural Malaysia. Hence, second configuration was finalized on which energy harvesting would be implemented. Also cost analysis had been made for 5 current existing wind turbine models in which our proposed system was found out to be the cheapest. Few companies then had been contacted for fabrication of the design but when they had been asked to give a datasheet of the product or an open circuit test results in low wind speed, none of them agreed to provide. Before finalizing the order, it was necessary to make sure whether the design was good enough according to the simulation value. It was important to confirm that it really could perform at low wind speed. Therefore, a prototype version was decided to be constructed in the lab with approximately the same configuration to observe the performance in low speed. The prototype was constructed with 9 bladed variable pitch VAWT with 2 PMSG pole configurations; - at first with 4 pole, then with 8 pole. The blade angle was varied to see the effect of pitch angle in output. As field testing was taken place, the turbine showed maximum power in null pitch angle which was aligned with the simulation result. Then, at 8 Pole PMSG configuration, turbine with null blade pitch angle exhibited a set of open Circuit Voltage (7V, 7.5V, 7.9V and 8.1V) for four different wind speed (4m/s, 5m/s, 6m/s and 7m/s respectively). This finding justified the optimized design configuration to be effective in low wind speed. Hence, after investigating the result from the prototype, the optimized design was finally sent for fabrication.

The final objective was to come up with an innovative efficient energy harvesting hybrid system for the optimized system. This off-grid system is supposed to charge battery through a Supercap bank in a minimal wind speed level. While waiting for the optimized system to come after fabrication, the energy harvesting system was being designed. A 10.8V Supercap bank, consisting of 4 Supercap of 2.7V, 35F each, was connected to a 6V lead acid battery via DC DC converter. The circuit was being controlled by MOSFET switching. Upon arrival of the machine, it was set-up in the laboratory and was run for fiend testing with the energy harvesting circuit. There were two parts in this experiment. For part one, 3 cases had been compared for performance analysis. ‘Case A’ showed a battery of 6V, 3.2AH, being charged from 4.2V to 5V through a DC DC converter followed by a series of 4 Supercap. ‘Case B’ and ‘Case C’ demonstrated the direct charging of the battery; where ‘Case B’ was experimented with the converter and ‘Case C’ was without converter. Investigation was carried for 3, 4 and 5 m/s wind speed. ‘Case C’ was taken as a reference. For a wind speed of 5m/s, the result showed an increase of 19% of the charging time for Case A while charging through Supercap. It took only 8.1 hours whereas direct charging without converter took 10 hours. Supercap based charging was also found to be 133% more efficient than direct battery charging with a converter. Keeping in mind, that direct charging might not be the appropriate way of charging a device since fluctuation of wind would result damaging the battery. As far as wind speed of 4m/s concerns, the energy harvesting circuit, taking only 10.4 hours to charge up the battery, again showed an excellent performance of 31% efficiency comparing with direct charging that took a straight 15 hours lap. For 3m/s, energy harvesting circuit still held the top position handsomely with 28% efficiency in comparison with direct

charging. Coming back to part 2 of the investigation, experiment was done to charge the same battery from 5V to 6V at 5m/s. Having the energy harvesting circuit being implemented in the system, the battery was being charged by the Supercap bank at first. It was found that with the energy harvesting circuit, battery took approximately 18.8 hours to finish charging whereas direct charging required 24.2 hours. In accordance with the experimental result, energy harvesting circuit was found to be 22% more efficient than direct charging. This off-grid low voltage innovative approach made the energy harvesting circuit novel in terms of design and efficiency.

To recapitulate, this research provides with an excellent novel idea of a standalone Maglev based VAWT system connected to a PMSG that can able to harvest energy via Supercap based battery charging circuit in low wind areas of rural Malaysia. Research contribution of this thesis is original and it gives an outstanding foundation for future study in energy harvesting for low wind rural areas of Malaysia.

The entire research had not been absolutely smooth all throughout and naturally it had faced few ups and downs. The limitations faced while conducting the research are listed as follow;

The limitations of the developed system and technique are listed below;

- i) Firstly, turbine blade design was not taken in consideration in the Simulation. As there was no proper mathematical model that relates turbine blade number to output torque or power, the simulation therefore did not account blade design although it could give better performance if blade number was included in the design. In addition, due to budget constrain, Finite Element Analysis could not be made possible to apply on

turbine blades. Moreover, the position of blade, cut-in angle and vibration analysis of the turbine could be done with FEA. Surely it could have given a wider research scope area on modelling and blade material could be brought into the optimization process for a better configuration.

- ii) Secondly, again due to budget constrain, while implementing the Maglev, magnet positioning in the system could not be analyzed. Generally, Computational Fluid Dynamics, CFD tool is used to analyze magnet positioning. Simulation of generator with changing friction factor could not give an exact idea on magnetic flux and force calculation for optimizing Maglev based system.
- iii) Next, 16 pole configuration could not be made possible while constructing the laboratory prototype. Instead, a maximum of 8 pole were placed in the PMSG. Yet the result was similar to the 16 pole configuration because it was seen in simulation result that at low rotational speed, effect of pole changing makes little impact in generator output.
- iv) Moreover, DC DC boost converter used in this research did not perform well according to the data sheet in its minimum range. As it was stated in the data sheet, the converter can step up voltage from as low as 2.5V, practically it could not step up voltage less than 4V. Therefore, the Supercap charging range was made from 4V-7.5V which should have been 3V-7.5V. This had a direct effect on system efficiency. Lack of enough budget could not give scope to go for an accurate low voltage range converter.

5.2. Future Work

Future work that can be an outcome from the research and analysis delivered in this thesis is going to be discussed here in brief. The potential work will be viewed from the angle of improvements that can be made to the methods, techniques and results presented. Starting from the beginning, turbine blade design and positioning is to be taken in consideration with FEA. Vibration analysis in low wind speed may also be performed. Turbine lift and drag aerodynamics may be taken in consideration to study in depth and can later be incorporated with FEA for better torque generation. No research had been conducted yet on building a mathematical model of blade number that can relate either to torque, power and wind speed. One way to do is that turbine should be tested under different number of blades and the result achieved from the experiment, a model can be proposed.

An important task that can be taken in consideration in the near future, which is to apply CFD in the magnet positioning and try to come up with few optimized designs which will give nearly 0 friction. The total number of magnet, repulsive force that it is causing, the position of them and the system weight impact can be calculated in the design. This will surely help to increase the efficiency of the system.

Conventional DC/DC Boost Converter is to be replaced with Efficient one which is specifically designed to work with voltage as low as 2-3V. This will help Supercap to discharge even more and will play a vital role while dealing with low wind. All these changes will improve the system and should make it capable of performing at 2m/s. Since most of the electronic devices operate at 12V, a second DC/DC converter may be placed to charge a 12V battery from the current 6V led Acid Battery.

Laptop should be replaced with wireless system in the future. A real time wireless monitoring interface could be made available. Embedded solutions providing wireless end-point connectivity to devices like XBEE Modules can be of use in cases like this.

6. References

1. B. Ge and F. Z. Peng, "Current balancer-based grid-connected parallel inverters for high power wind-power system," International Transactions on Electrical Energy Systems., vol. 24, no. 1, pp. 108-124, January 2014.
2. Renewable Energy Policy Network, "Global Status Report," 2015. [Online]. Available: <http://www.ren21.net/ren21activities/globalstatusreport.aspx>. [Accessed 15 March 2015].
3. World Wind Energy Association, "New Record in Worldwide Wind Installation," 5 February 2015. [Online]. Available: <http://www.wwindea.org/new-record-in-worldwide-windinstallations/>. [Accessed 15 March 2015].
4. X. S. Tang, Z. P. Qi, "Economic analysis of EDLC/battery hybrid energy storage," International Conference on Electrical Machines and System 2008, pp. 2729-2733, October 2008.
5. M. Pedram, N. Chang, Y. Kim and Y. Wang, "Hybrid electrical energy storage systems," Proceedings of the 16th ACM/IEEE International Symposium on Low Power Electronics and Design, pp. 363-368, August 2010.
6. Zaharim, S. K. Najid, A. M. Razali and K. Sopian "Wind Speed Analysis in the East Coast of Malaysia," European Journal of Scientific Research, Vol. 32, No. 2, pp. 208-215, 2009.
7. R. Bharanikumar, A. C. Yazhini and N. Kumar, "Modeling and Simulation of Wind Turbine Driven Permanent Magnet Generator with New MPPT Algorithm," Asian Power electronics journal, Vol. 4, 2012.
8. Sai PC, Yadav RS, Raj RN, Gupta GRK. Design and simulation of high efficiency counter-rotating vertical axis wind turbine arrays. International Conference and Utility Exhibition 2014 on Green Energy for Sustainable Development, 2014.
9. W. Fei and P. I. Luk, "A New Technique of Cogging Torque Suppression in Direct-Drive Permanent-Magnet Brushless Machines," IEEE Transactions on Industry Applications, Vol. 46, No.4, 2010, pp. 1332-1340. doi:[10.1109/TIA.2010.2049551](https://doi.org/10.1109/TIA.2010.2049551)
10. Hansen AD, Michalke G. Modelling and control of variable-speed multi-pole permanent magnet synchronous generator wind turbine. Wind Energy 2008.
11. Melicio R, Mendes VMF, Catalao JPS. Power converter topologies for wind energy conversion systems: Integrated modeling, control strategy and performance simulation. Renewable Energy, 2010.
12. Mohamed YA-RI. Design and implementation of a robust current-control scheme for a PMSM vector drive with a simple adaptive disturbance observer. IEEE Transactions on Industrial Electronics, 2007.
13. Wang J, Xu D, Wu B, Luo Z. A low-cost rectifier topology for variable-speed high-power PMSG wind turbines. IEEE Transactions on Power Electronics, 2011.
14. D. Almeida BR, Oliveira DS. Power converter for vertical wind energy conversion system. Power Electronics Conference, 2013.
15. Corradini ML, Ippoliti G, Orlando G. Robust control of variable-Speed wind turbines based on an aerodynamic torque observer. IEEE Transactions on Control Systems Technology, 2013.
16. Conroy JF, Watson R. Low-voltage ride-through of a full converter wind turbine with permanent magnet generator. IET Renewable Power Generation, 2007.

17. Li S, Haskew TA, Swatloski RP, Gathings W. Optimal and direct-current vector control of direct-driven PMSG wind turbines. *IEEE Transactions on Power Electronics*, 2012.
18. Wu H, Wang Z, Hu Y. Study on magnetic levitation wind turbine for vertical type and low wind speed. *Asia Pacific Power and Energy Engineering Conference*, 2010.
19. Zhang Tingting, Wang Hongxia, Dai zebing. *Structure Optimization Design for Cylindrical Vertical-axis Wind Turbines*, East China Electric Power, 2008.
20. Patel N, Uddin MN. Design and performance analysis of a magnetically levitated vertical axis wind turbine based axial flux PM generator. *7th International Conference on Electrical & Computer Engineering*, 2012.
21. Liu S, Bian Z, Li D, Zhao W. A magnetic suspended self-pitch vertical axis wind generator. *Asia Pacific Power and Energy Engineering Conference*, 2010.
22. Patel N, Uddin MN. Design and performance analysis of a magnetically levitated vertical axis wind turbine based axial flux PM generator. *7th International Conference on Electrical & Computer Engineering*, 2012.
23. A. Jha, *Wind Turbine Technology*, New York: CRC Press - Taylor & Francis Group, 2011.
24. Cooper, P. & Kennedy, O. C. Development and Analysis of a Novel Vertical Axis Wind Turbine. *Proceedings Solar 2004 - Life, The Universe and Renewables* (pp. 1-9). Perth, Australia: Australian and New Zealand Solar Energy Society (ANZSES), 2004.
25. Rogers, A., Manwell, J., & Wright, S. Wind turbine acoustic noise. University of Massachusetts at Amherst, Department of Mechanical and Industrial Engineering, 2006.
26. Annex to Pan 45 Renewable Energy Technologies, "Planning for Micro Renewables", Scottish Executive Development Department, Pan 45 Annex, 2006
27. "College of Engineering: Wind Turbines," 21 June 2010. [Online]. Available: <http://people.bu.edu/dew11/windturbine.html>. [Accessed 10 March 2014].
28. W. Tong, *Wind Power Generation and Wind Turbine Design*, Southampton: WIT Press, 2010.
29. M. Ragheb, "Vertical Axis Wind Turbines," 2014.
30. "Types of forces," 2014. [Online]. Available: <http://www.physicsclassroom.com/class/newtlaws/Lesson-2/Types-of-Forces>.
31. C. T. Crowe, D. F. Elger, B. C. Williams and J. A. Roberson, *Engineering Fluid Mechanics*, John Wiley & Sons, Inc., 2010.
32. I. Paraschivoiu, *Wind Turbine Design - with Emphasis on Darrieus Concept*, Québec: Presses internationals Polytechnique, 2009.
33. "Wind Turbine Power Output Variation with Steady Wind Speed," [Online]. Available: http://www.wind-power-program.com/turbine_characteristics.htm. [Accessed 10 March 2014].
34. P. Sabaeifard, H. Razzaghi and Forouzandeh, "Determination of Vertical Axis Wind Turbines Optimal Configuration through CFD Simulations," Singapore, 2012.
35. L. Wang, J. Wei, X.W.X. Zhang, "The development and Prospect of Offshore Wind Power Technology in the World", *IEEE World Wind Power and Energy Conference*, 2009.

36. Jinsong Kang, Zhiwen Zhang and Yongqiang, "Development and Trend of Wind Power in China," in Canada Electrical Power Conference, 2007.
37. I. Paraschivoiu, O. Trifu, and F. Saeed, " H-Darrieus Turbine with Blade Pitch Control", International Journal on Rotating Machinery, Article ID 505343, 7 pages, 2009.
38. M.H. Hsu, "Dynamic Analysis of Wind Turbine Blades Using Radial Basis Function," Advances in Acoustics and Vibration, Article ID 973591, 2011.
39. S. Eriksson, H. Bernhoff and M. Leijon, "A 225 KW Direct Driven PM Generator Adapted to a Vertical Axis Wind Turbine," Advances in Power Electronics, Article ID 239061, 7 pages, 2011.
40. M. S. Virk, Matthew C. Homola, Per J. Nicklasson, "Atmospheric icing on large wind turbine blades," International Journal of Energy and Environment, Vol. 3, Issue 1, 2012.
41. M. Luna, M. Pucci and G. Vitale, "Design of a Simple, Effective and Low Cost Micro-Wind Energy Conversion System", The Open Renewable Energy Journal, Vol. 4, 2011.
42. Li Yan, Chi Yuan, Han Yongjun, Li Shengmao and Tagawa Kotaro, "Numerical simulation of icing on static flow field around blade aerofoil for vertical axis wind turbine," International Journal of Agric. & Biol. Eng. Vol. 4, No.3, September 2011.
43. M. Arifujjaman, "Modelling and Simulation of Grid Connected Permanent Magnet Generator (PMG)- based Small Wind Energy Conversion System," The Open Renewable Energy Journal, Vol. 4, 2011.
44. M. Arifujjaman, M.T. Iqbal and J.E. Quacoe, "Development of an Isolated Small Wind Turbine Emulator," The open Renewable Energy Journal, Vol. 4, 2011.
45. C. Nemes, F. Munteanu, "Development of Reliability Model for Wind Farm Power Generation," Advances in Electrical and Computer Engineering, Vol. 10, November 2010.
46. "Wind Turbines Theory - The Betz Equation and Optimal Rotor Tip Speed Ratio," [Online]. Available: <http://www.intechopen.com/books/fundamental-and-advanced-topics-in-wind-power/wind-turbines-theory-the-betz-equation-and-optimal-rotor-tipspeed-ratio>. [Accessed 11 September 2014].
47. M. Ragheb, "Optimal Tip Speed Ratio," 15 April 2011. [Online]. Available: <http://mragheb.com/NPRE%20475%20Wind%20Power%20Systems/Optimal%20Rot%20Tip%20Speed%20Ratio.pdf>. [Accessed 5 February 2014].
48. A. Hemami, Wind Turbine Technology, New York: Cengage Learning, 2012.
49. T. Burton, N. Jenkins, D. Sharpe and E. Bossanyi, Wind Energy Handbook - Second Edition, West Sussex: John Wiley & Sons, Ltd, 2011.
50. P. Schubel and R. Crossley, "Wind Turbine Blade Design," Energies, vol. 5, no. 9, pp. 3425-3449, 2012.
51. A. Hemami, Wind Turbine Technology, New York: Cengage Learning, 2012.
52. "Pitch Systems of the Future - under all climatic conditions," [Online]. Available: http://www.fsenergy.dk/dyn/files/basic_sections/61-file/wind.pdf. [Accessed 20 March 2014].
53. Raju. A.B., Fernandes B.G., Kishore C., "Modelling and simulation of a grid connected variable speed wind energy conversion system with low cost power converters" Renewable energy & power Quality Journal, No.1, 2003.

54. Bharanikumar R., Yazhini A.C., Kumar N., "Modelling and simulation of wind turbine driven permanent magnet generator with new MPPT algorithm" Asian Power electronics journal, Vol.4, 2004.
55. Siegfried Heier, "Grid Integration of Wind Energy Conversion systems," John Wiley & Sons Ltd, 1998.
56. A. Parviaien, M. Niemelä, J. Pyrhönen, 2003Analytical, 2D FEM and 3D FEM Modeling of PM Axial Flux Machine, Proceedings of 10th Power Electronics and Applications Conference, 9-07581-506-9France, September 2003.
57. A. Miller, E. Muljadi, and D. S. Zinger, "A variable speed wind turbine power control," IEEE Trans on. Energy Conv., vol. 12, no. 2, pp.181-186, 1997.
58. T. Wildi, Electrical Machines, Drives and Power Systems (6th Edition). Sperika Enterprises Ltd and Pearson Education, Inc., 2006
59. A. R. Hambley, Electrical Engineering, Principles and Applications, 5.ed. Pearson Education, Inc, 2011.
60. Chalmers, B.J.; Wu, W.; Spooner, E. "An axial-flux PM for a gearless wind energy system." IEEE Trans. Energy Conv. 1999.
61. Sadeghierad, M.; Darabi, A.; Lesani, H.; Monsef, H. Rotor yoke thickness of coreless high-speed axial-flux permanent magnet generator. IEEE Trans. Magn. 2009.
62. Chaar, L.E.; Lamont, L.A.; Elzein, N. Wind energy technology-industrial update. In Proceedings of the IEEE Power and Energy Society General Meeting, Detroit, MI, USA, 24–29 July 2011.
63. Chan, T.F.; Lai, L.L.; Xie, S. Field computation for an axial flux permanent-magnet synchronous generator. IEEE Trans. Energy Convers, 2009.
64. J. Santiago, H. Bernhoff. "Comparison between axial and radial flux PM coreless machines for flywheel energy storage. Journal of Electrical System. 2010.
65. Caricchi, F.; Maradei, F.; de Donato, G.; Capponi, F.G. Axial-flux permanent magnet generator for induction heating gensets. IEEE Trans. Ind. Electron. 2009.
66. M. Aydin, S. Husang, and T. A. Lipo, "Optimum design and 3D finite element analysis of non-slotted and slotted internal rotor type axial flux PM disc machines", Power Engineering Society Summer Meeting, pp. 1409-1416, 2001.
67. F. Caricchi, F. Crescimbini, O. Honorati, and E. Santini, "Performance evaluation of an axial flux PM generator", Proceedings of International Conference on Electrical Machines (ICEM), pp. 761-765, 1992.
68. R. J. Hill-Cottingham, P. C. Coles, J. F. Eastham, F. Profumo, A. Tenconi, G. Gianolio, "Multi-disc axial flux stratospheric propeller drive", Proc. of IEEE IAS Annual Meeting Conference Record 2001, vol. 3, pp. 1634-1639, 2001.
69. H. Weh, H. Hoffman, and J. Landrath, "New permanent magnet excited synchronous machine with high efficiency at low speeds, Institut für Elektrische Maschinen, Antriebe und Bahnen, Technische Universität Braunschweig, 1989.
70. Y.Y. Xia, J.E. Fletcher, S.J. Finney, K.H. Ahmed, B.W. Williams. "Torque ripple analysis and reduction for wind energy conversion systems using uncontrolled rectifier and boost converter." IET Renewable Power Generatio. 2011.
71. C.Y. Hsiao, S.N. Yeh, J.C. Hwang. "Design of High Performance Permanent-Magnet Wind Generator." Energies. 2014.
72. Ming Yin; Gengyin Li; Ming Zhou; Chengyong Zhao. "Modeling of the Wind Turbine with a Permanent Magnet Synchronous Generator for Integration," Power

- Engineering Society General Meeting, 2007. IEEE, vol., no., pp.1-6, 24-28 June 2007.
73. Cristian Busca, Ana-Irina Stan, Tiberiu Stanciu and Daniel Ioan Stroe.“Control of Permanent Magnet Synchronous of large wind turbines”. Denmark: Departament of Energy Technology: Aalborg University, November 2010.
 74. A New Technique of Cogging Torque Suppression in Direct-Drive Permanent-Magnet Brushless Machines, Fei, W, Luk, P. I, IEEE Transactions on Industry Applications, July-Aug. 2010.
 75. R.S. Semken, Polikarpova, P. Nen. "Direct drive permanent magnet generators for high-power wind turbines: benefits and limiting factors," Renewable Power Generation, IET, January 2012.
 76. H. Li and Z. Chen, "Overview of different wind generator systems and their comparisons," IEEE Renewable Power Generation, Vol. 2, No. 2, 2007, pp. 123-138.
 77. H. Li and Z. Chen, —Overview of different wind generator systems and their comparisons, IET Renewable Power Generation, vol. 2, pp. 123-138, 2008.
 78. L. H. Hansen, L. Helle, F. Blaabjerg et al., —Conceptual survey of generators and power electronics for wind turbines, Riso National Laboratory Technical Report, Riso-R-1205(EN) Roskilde, Denmark, December 2001.
 79. Y. Shankir, —Review of wind turbines' drive systems and why gearless direct drive, in Proc. RCREEE Wind Energy Building Capacity Program – Stage 2, Rabat, Tangier, March 29–April 2, 2010.
 80. H. Polinder and J. Morren, —Developments in wind turbine generator systems, Electrics, Hammamet, 2005.
 81. I. Boldea, The Electric Generators Handbook — Variable Speed Generators, Taylor & Francis, 2006.
 82. Rajveer Mittal, K.S.Sandhu and D.K.Jain “An Overview of Some Important Issues Related to Wind Energy Conversion System” International Journal of Environmental Science and Development, Vol. 1, No. 4, pp 351-363, October 2010.
 83. F. Blaabjerg, Z. Chen, R. Teodorescu, F. Iov, “ Power Electronics in wind Turbine Systems” Aalborg University, Institute of Energy Technology IEEE- IPEMC 2006.
 84. Jamal A. Baroudi, Venkata Dinavahi, Andrew M. Knight “A review of power converter Topologies for wind generators”, Department of Electrical and Computer Engineering, University of Alberta, Edmonton, AB., Canada.pp1-17,2006.
 85. M. Singh V. Khadkikar A. Chandra “Grid synchronization with harmonics and reactive power compensation capability of a permanent magnet synchronous generator-based variable speed wind energy conversion system” Published in IET Power Electronics, vol 4, pp 122-130, 2011.
 86. T. Christen, M. W. Carlen, “Theory of Ragone plots.” Journal of Power Sources, December, 2000.
 87. M. Pedram, N. Chang, Y. Kim and Y. Wang, “Hybrid electrical energy storage systems,” Proceedings of the 16th ACM/IEEE International Symposium On Low Power Electronics and Design, pp. 363-368, August 2010.
 88. J. R. Miller, “Introduction to electrochemical capacitor technology,” IEEE Electrical Insulation Magazine, vol. 26, no. 4, pp. 40-47, July 2010.
 89. Y. C. Zhang, X. Shen and H. Liang, “Study of supercapacitor in the application of power electronics,” WSEAS Transactions on Circuits and Systems, June 2009.

90. D. Linzen, S. Buller, E. Karden and R. W. D. Doncker, "analysis and evaluation of charge balancing circuits on performance, reliability, and lifetime of supercapacitor systems," IEEE Transactions on Industry Applications, vol. 41, no. 5, pp. 1135-1141, September 2005.
91. W. Qiao, W. Zhou, J. M. Aller, and R. G. Harley, "Wind speed estimation based sensorless output maximization control for a wind turbine driving a DFIG," IEEE Trans. Power Electron., vol. 23, no. 3, pp. 1156–1169, May 2008.
92. W. Qiao, G. K. Venayagamoorthy, and R. G. Harley, "Real-time implementation of a STATCOM on a wind farm equipped with doubly fed induction generators," IEEE Trans. Ind. Appl., vol. 45, no. 1, pp. 98–107, Jan./Feb. 2009.
93. L. Qu, W. Qiao. "Constant Power Control of DFIG Wind Turbines with Supercapacitor Energy Storage." IEEE TRANSACTIONS ON INDUSTRY APPLICATIONS, 2011.
94. H. Babazadeh, W. Gao and X. Wang, "controller design for a hybrid energy storage system enabling longer battery life in wind turbine generators" North American Power Symposium (NAPS), pp. 1-7, August 2011.
95. S. Park, Y. Kim and N. Chang, "hybrid energy storage systems and battery management for electric vehicles," 50th ACM/IEEE Design Automation Conference (DAC), pp. 1-6, May 2013.
96. A. Ostadi, M. Kazerani and S. K. Chen, "Hybrid energy storage system (HESS) in vehicular applications- a review on interfacing battery and ultra-capacitor units," IEEE Transportation Electrification Conference and Expo (ITEC), pp. 1-7, June 2013.
97. E. L. Worthington, "Piezoelectric energy harvesting: Enhancing power output by device optimisation and circuit techniques," PhD thesis, School of Applied Sciences, Cranfield University, 2010.
98. L. Solero, Lidozzi, A and Pomilio, J.A., "Design of multiple-input power converter for hybrid vehicles," Power Electronics, IEEE Transactions, vol. 20, no. 5, pp. 1007 - 1016, September 2005.
99. G. Nielson and Emadi, A., "Hybrid energy storage systems for high-performance hybrid electric vehicles," in Vehicle Power and Propulsion Conference (VPPC), 2011 IEEE, Chicago, IL, September 2011.
100. Glavin, M.E., Chan, P.K.W., Armstrong, S and Hurley, W.G, "A standalone photovoltaic supercapacitor battery hybrid energy storage system," in Power Electronics and Motion Control Conference, 2008. EPE-PEMC 2008. 13th, Poznan, September 2008.
101. Glavin, M.E and Hurley, W.G, "Ultracapacitor/ battery hybrid for solar energy storage," in Universities Power Engineering Conference, 2007 42nd International, Brighton, September 2007.
102. M.A. Tankari, M.B. Camara, B. Dakyo, C. Nichita, "Ultracapacitors and Batteries Integration for Power Fluctuations mitigation in Wind-PV-Diesel Hybrid System", International Journal of Renewable Energy Research, Vol. 1, No. 2, pp. 86-95, 2011.
103. C. Abbey, G. Joos, "Supercapacitor Energy Storage for Wind Energy Applications", IEEE Transactions on Industry Application, Vol. 43, No. 3, June 2007.
104. L. Qu, W. Qiao, "Constant Power Control of DFIG Wind Turbines with Supercapacitor Energy Storage", IEEE Transactions on Industry Applications, Vol. 47, No. 1, February 2011.

105. E. L. Worthington, "Piezoelectric energy harvesting: Enhancing power output by device optimisation and circuit techniques," PhD thesis, School of Applied Sciences, Cranfield University, 2010.
106. W. Li and G. Joos, "A Power Electronic Interface for a Battery Supercapacitor Hybrid Energy Storage System for Wind Applications", IEEE Transactions on Energy Conv, Vol. 2, 2008.
107. C. V. Aravind, Rajparthiban, Rajprasad and Y. V. Wong "A Novel Magnetic Levitation Assisted Vertical Axis Wind Turbine- design and Procedure," IEEE Colloquium on Signal Processing and its Applications, Melacca, Ma-laysia CSPA 2012
108. J A.M. De Broe, S. Drouilllet and V. Oevorglan, "A Peak Power Tracker for Small Wind Turbines in Battery Charging Applications," IEEE Transactions on Energy Conv., Vol. 14, No. 4, Dec. 1999.
109. J. D. M. Whaley, W. L. Soongand and N. Ertugrul, "In-vestigation of Switched-Mode Rectifier for Control of Small-Scale Wind Turbines," Intl' Conference Proceed. of IEEE-IAS Annual Meeting, Vol. 4, 2005.
110. S. Belakehal, H. Benalla and A. Bentounsi, "Power Maximization of Small Wind System using Permanent magnet Synchronous Generator" Revue des energies Renouvelables, Vol. 12, No. 2, 2009.
111. J. G. Slootweg, H. Pollnder and W. L. Kling, "Repre-senting Wind Turbine Electrical Generating Systems in Fundamental Frequency Simulations," IEEE Trans. Energy Convr, Vol. 18, No. 4, Dec. 2003.
112. A. G. Westlake, J. R. Bumby and E. Spooner, "Damping the Power-angle Oscillations of a Permanent Magnet Synchronous Generator with Particular to Wind Applications," Proc. Ekct. Power Appl., Vol. 143, No. 3, May 1996.
113. Barote L., Clotea L.: MPTT control of a variable - speed wind turbine, Bulletin of the Transilvania University of Brasov, vol. 13, series A1, ISSN 123-9631, Brasov, Romania, pp. 195-201, 2006.
114. Rolan A., Luna A., Vazquez G., Aguilar D., Azevedo G., "Modelling of a variable speed wind turbine with a permanent magnet synchronous generator" IEEE international symposium on industrial electronics, 2009.
115. D. W. Novotny and T. A. Lipo, Vector control and dynamics of AC drives. Oxford: Clarendon, 1996.
116. M. Yin, G. Li, Ming Zhou, Chengyong Zhao, 2007 "Modeling of the Wind Turbine with a Permanent Magnet Synchronous Generator for Integration". Power Engineering Society General Meeting, IEEE, 2007.
117. E. Muljadi, C.P. Butterfield, Yih-Huei Wan, 1998 "Axial Flux, Modular, Permanent-Magnet Generator with a Toroidal Winding for Wind Turbine Applications" Industry Applications Conference, 1998.
118. Lusu Guo, and Leila Parsa, "Model Reference Adaptive Control of Five-Phase IPM Motors Based on Neural Network", 2011.
119. Fei Yu, Xiaofeng Zhang, Suhua Wang, "Five-phase Permanent Magnet Synchronous Motor Vector Control Based on Harmonic Eliminating Space Vector Modulation", Industry Applications Conference, 1998.

120. M. T. Mohammad, J. E. Fletcher, and N. A. Hassanain, "Novel Five-Phase Permanent Magnet Generator Systems for Wind Turbine Applications", IEEE international symposium on industrial electronics, 2004.
121. B. Zhang, H. Bai, S. D. Pekarek, W. Eversman, R. Krefta, G. Holbrook D. Buening, "Comparison of 3-, 5-, and 6-Phase Machines for Automotive Charging Applications", Power Engineering Society General Meeting, 2003.
122. M. Pedram, N. Chang, Y. Kim and Y. Wang, "Hybrid electrical energy storage systems, "Proceedings of the 16th ACM/IEEE International Symposium On Low Power Electronics And Design, pp. 363-368, August 2010.
123. S. A. Khan, R. Rajkumar, CV Aravind, "Performance Analysis of a 20 pole 1.5KW 3-Phase PMSG for low speed VAWT", Energy and Power Engineering, 2013.
124. R. Bharanikumar, A. C. Yazhini and N. Kumar, "Model-ing and Simulation of Wind Turbine Driven Permanent Magnet Generator with New MPPT Algorithm," Asian Power electronics journal, Vol. 4, 2012.
125. W. Fei and P. I. Luk, "A New Technique of Cogging Torque Suppression in Direct-Drive Permanent-Magnet Brushless Machines," IEEE Transactions on Industry Applications, Vol. 46, No.4, 2010.
126. S. Belakehal, H. Benalla and A. Bentounsi, "Power Maximization of Small Wind System using Permanent Magnet Synchronous Generator" Revue des energies Renouvelables, Vol. 12, No. 2 ,2009.
127. C. Busca, A. Stan, T. Stanciu and D. I. Stroe "Control of Permanent Magnet Synchronous of Large Wind Tur-bines," Denmark : Department of Energy Technology: Aalborg University, November 2010.
128. A. Hossain, A.k.M. Iqbal, A. Rahman. Design and Development of a 1/3 Scale Vertical Axis Wind Turbine for Electrical Power Generation, Journal of Urban and Environmental Engineering, pp 53-60, 2007.
129. A. Albani, A.Z. Ibrahim, Preliminary Development of Prototype of Savonius Wind Turbine for Application in Low Wind Speed in Kuala Terengganu, Malaysia, International Journal of Scientific and Technology Research, Vol-2, May 2013.
130. A.S.M.F. Aljen, A. Maimum, Low Speed Vertical Axis Current Turbine for Electrification of Remote Areas in Malaysia, Recent Advances in Renewable Energy Sources, 2015.
131. Z.A.Darus, N.A.Hashim, Potential of Wind Energy in Sustainable Development of Resort Island In Malaysia: A Case Study of Pulau Perenthian, Journal of Mathematical Methods, Computational Techniques, Non-Linear Systems, Intelligent Systems, ISBN: 1790-2769, 2007.
132. I. Daut, M. Irwanto, Suwarno, Y.M Irwan, N. Gomesh, N.S. Ahmad; Potential of Wind Speed for Wind Power Generation in Perlis, Northern Malaysia; TELKOMNIKA, Vol. 9, pp 575-582, Malaysia, December 2011.
133. M. Yin, G. Y. Li, M. Zhou and C. Y. Zhao, "Modeling of the Wind Turbine with a Permanent Magnet Synchro-nous Generator for Integration," Power Engineering So-ciety General Meeting, 2007.
134. K. Tan and S. Islam, "Optimum Control Strategies in Energy Conversion of PMSG Wind Turbine System without Mechanical Sensors," Energy Conversion, IEEE Transactions on, Vol. 19, No. 2, June 2007.
135. NASA, "Priorities in Space Science Enabled by Nuclear Power and Propulsion," National Academies Press, 2008.

136. Mollenhauer, Klaus, Tschöke, Helmut, "Handbook of Digital Engines," Springer, 2010.
137. K. Yazawa, A. Shakouri, "Cost-effective waste heat recovery using thermoelectric system", Birck and NCN Publications, 2012.
138. LT103 Data Sheet, Available[online]: <http://cds.linear.com/docs/en/datasheet/lt103.pdf>. [Accessed 12 December 2015]
139. [Online]. Available: <http://www.electronics-lab.com/tag/current-sense/>. [Accessed 5 January 2016].
140. W. X. Y. Yang, "Design of high-side current sense amplifier with ultra-wide ICMR," Circuits and Systems, 2009. MWSCAS '09. 52nd IEEE International Midwest Symposium , pp. 5-8, 2009.
141. S. Z. H. H. C. I. C. W. Lai, "High gain amplification of low-side current sensing shunt resistor," Power Engineering Conference, 2008. AUPEC '08. Australasian Universities, pp. 1-5, 2008.
142. Interface an LCD with an Arduino," 16 April 2015. [Online]. Available: <http://www.allaboutcircuits.com/projects/interface-an-lcd-with-an-arduino/>. [Accessed 1 February 2016]
143. NASA, "Priorities in Space Science Enabled by Nuclear Power and Propulsion," National Academies Press, 2008.
144. Mollenhauer, Klaus, Tschöke, Helmut, "Handbook of Digital Engines," Springer, 2010.
145. K. Yazawa, A. Shakouri, "Cost-effective waste heat recovery using thermoelectric system", Birck and NCN Publications, 2012.
146. S. A. Khan, R. Rajkumar, CV Aravind, "Performance Analysis of a 20 pole 1.5KW 3-Phase PMSG for low speed VAWT", Energy and Power Engineering, 2013.
147. R. Bharanikumar, A. C. Yazhini and N. Kumar, "Model-ing and Simulation of Wind Turbine Driven Permanent Magnet Generator with New MPPT Algorithm," Asian Power electronics journal, Vol. 4, 2012.
148. W. Fei and P. I. Luk, "A New Technique of Cogging Torque Suppression in Direct-Drive Permanent-Magnet Brushless Machines," IEEE Transactions on Industry Applications, Vol. 46, No.4, 2010.
149. S. Belakehal, H. Benalla and A. Bentounsi, "Power Maximization of Small Wind System using Permanent Magnet Synchronous Generator" Revue des energies Renouvelables, Vol. 12, No. 2 ,2009.
150. C. Busca, A. Stan, T. Stanciu and D. I. Stroe "Control of Permanent Magnet Synchronous of Large Wind Tur-bines," Denmark: Department of Energy Technology: Aalborg University, November 2010.
151. M. Yin, G. Y. Li, M. Zhou and C. Y. Zhao, "Modeling of the Wind Turbine with a Permanent Magnet Synchro-nous Generator for Integration," Power Engineering So-ciety General Meeting, 2007.
152. K. Tan and S. Islam, "Optimum Control Strategies in Energy Conversion of PMSG Wind Turbine System without Mechanical Sensors," Energy Conversion, IEEE Transactions on, Vol. 19, No. 2, June 2007.

Appendix

Journal 1

Energy and Power Engineering, 2013, 5, 423-428
doi:10.4236/epe.2013.54B082 Published Online July 2013 (<http://www.scirp.org/journal/epe>)



Performance analysis of 20 Pole 1.5 KW Three Phase Permanent Magnet Synchronous Generator for low Speed Vertical Axis Wind Turbine*

Shahrukh Adnan Khan¹, Rajprasad K. Rajkumar¹, Rajparthiban K. Rajkumar¹, Aravind CV²

¹Faculty of Engineering, University of Nottingham Malaysia Campus, Jalan Broga, Semenyih, Malaysia

²School of Engineering, Taylor's University, Selangor, Malaysia

Email: kecx1msa@nottingham.edu.my, Rajprasad.Rajkumar@nottingham.edu.my,
Rajparthiban.Rajkumar@nottingham.edu.my aravindcv@ieee.org

Received April, 2013

ABSTRACT

This paper gives performance analysis of a three phase Permanent Magnet Synchronous Generator (PMSG) connected to a Vertical Axis Wind Turbine (VAWT). Low speed wind condition (less than 5 m/s) is taken in consideration and the entire simulation is carried in Matlab/Simulink environment. The rated power for the generator is fixed at 1.5 KW and number of pole at 20. It is observed under low wind speed of 6 m/s, a turbine having approximately 1 m of radius and 2.6 m of height develops 150 Nm mechanical torque that can generate power up to 1.5 KW. The generator is designed using modeling tool and is fabricated. The fabricated generator is tested in the laboratory with the simulation result for the error analysis. The range of error is about 5%-27% for the same output power value. The limitations and possible causes for error are presented and discussed.

Keywords: Vertical Axis Wind Turbine; Three Phase Multi-pole permanent Magnet Synchronous Generator; Low Wind Speed; Modeling; Performance Analysis

1. Introduction

Various countries worldwide are aware of the fact that the past and current trends of energy system are not sustainable and a solution needs to be drawn to secure the world energy from a drastic falling. One of the sources that can replace the current trend is surely wind energy which greatly depends on the availability of the wind resource. Areas found around the equatorial regions tend to have low wind speeds. For example, Malaysia currently has an average wind speed of 2-3 m/s, with higher wind velocity in the east coast of west Malaysia [1]. For a typical horizontal axis wind turbine to run and generate power, a wind speed of at least 5 m/s is required [2]. A speed that is less than 5 m/s is not sufficient to turn the turbine. Another predicament is that these regions face unsteady multi-directional winds making HAWT totally incompatible in such areas. The vertical axis wind turbine (VAWT) on the other hand is appropriate for such regions due to its ability to capture wind energy at any direction. Also, the use neodymium magnets for suspension at the bottom surface assist attaining zero friction, which helps counter the low wind speed problem [2].

Conventional generators can be replaced with Permanent Magnet Synchronous Generator (PMSG) using multi-

pole stator arrangement. The multi-pole stator arrangement can be configured to generate high voltage at low revolution, and high current at faster speeds. The stator is designed to produce negligible cogging torque therefore causing the generator to start up and cut-in at low speeds to produce high current [3]. One significant advantage of PMSG, is that it is much lighter, smaller in size, and uses less constructional material so lowering cost and hub size [2][3]. Although a number of researches in the area of VAWT and PMSG are carried through separately, few attempts were taken to build a system together that work more efficiently at low wind speed. Moreover, there is a significant lack of research to find an optimal multi-pole PMSG for a VAWT with a fixed swept area which is realistic to work in those low wind speed countries. The main objective of this paper is to simulate and investigate the response of a permanent synchronous generator of a vertical wind turbine under different operating scenario through in Matlab/ Simulink environment.

2. Methodology

The equations of VAWT and PMSG are implemented in SIMULINK and a graphical user interface is developed to aid users in designing the VAWT. For the modeling

part, at first the turbine section is designed. The radius, wind speed, the swept area, the power coefficients and pitch angles are made as variables. After designing the turbine, simulation is performed and the data is compared with the analytical design value to ensure the accuracy of the turbine design. Later, with the changing parameters, the torque and the power output values are observed and optimal design parameters are derived. The simulation of PMSG is carried for different values of mechanical torque and speed for the pre selected values from the simulation and lastly the load voltage, current and power are measured for evaluation. The generator design is developed and is experimentally tested and compared with the simulation data. Figure 1 show the methodology used in this approach.

3. Modelling

3.1. Design of VAWT

The design of VAWT derived from the work stated in [5-12].

The aerodynamic power P_m of the turbine is given by the Equation 1.

$$P_m = C_p (\lambda) \frac{1}{2} \rho A U_w^3 \quad (1)$$

Here, ρ is the air density in (kg/m^3) at normal temperature, A is the area covered by the wind turbine rotor in (m^2) , U_w is the wind speed in (m s^{-1}) , C_p is the power coefficient of the wind turbine and λ is the tip-speed ratio and is related to the rotor speed (ω_m in rad s^{-1}) in as in Equation 2.

$$\lambda = \frac{\omega_m R}{U_w} C_p \quad (2)$$

$$A = 2RH \quad (3)$$

where R is turbine radius in (m), H is the turbine height in (m). The power coefficient C_p is given as a function of ϵ (pitch angle of the turbine) and λ (the tip-speed ratio). The value of C_p can only go as high as 0.59 according to the Betz law [6, 7]. The mechanical torque is related with mechanical power by Equation 4.

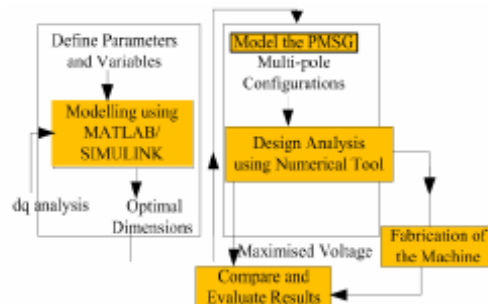


Figure 1. Methodology used in this design.

$$T_m = \frac{P_m}{\omega_m} \quad (4)$$

Figure 2 shows the modeling and design of the turbine. For computation of the power coefficient, maximum power coefficient is at null pitch angle is 0.4412 [1]. Taking the value of C_p as 0.4412, air density as 1.225, the above mentioned equations are used to calculate the swept area, mechanical power from the turbine and mechanical torque generated from it. Wind speed, radius and the height of the turbines are varied in the simulation to get optimal torque and power.

3.2. Design of the Three Phases PMSG

Axial Flux Permanent Magnet (AFPM) motor with its magnetic flux propagating at an axial direction from the magnets and are best suited for low wind speed [4-5] [12]. In comparison to the transverse flux design the axial flux design offers high torque and power density. Therefore the AFPM is considered for the development of this research work. The entire simulation is designed in terms of park transformation analysis that is a vector representation of three phase ac circuit models into a dq reference coordinates [10-13] as shown in Figure 3.

The park transform equation is given below:

$$\begin{bmatrix} f_q \\ f_d \\ f_0 \end{bmatrix} = [T_{dq0}] \begin{bmatrix} f_a \\ f_b \\ f_c \end{bmatrix} \quad (5)$$

Here, f can be current, voltage or flux .

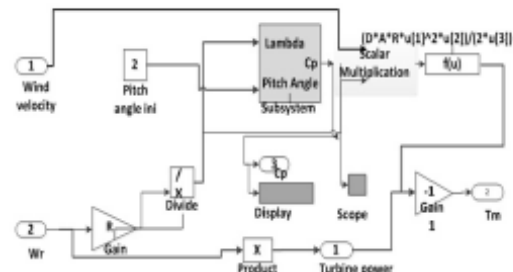


Figure 2. Modeling of turbine.

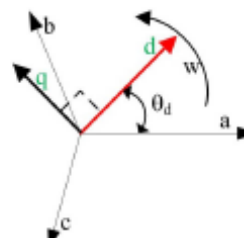


Figure 3. Park transform for generators.

T_{dq0} is given by Equation 6.

$$\begin{bmatrix} T_{dq0} (Q_q) \end{bmatrix} = \frac{2}{\pi} \begin{bmatrix} \cos \theta_q & \cos(\theta_q - \frac{\pi}{2}) & \cos(\theta_q + \frac{\pi}{2}) \\ -\sin \theta_q & -\sin(\theta_q - \frac{\pi}{2}) & -\sin(\theta_q + \frac{\pi}{2}) \\ \frac{1}{2} & \frac{1}{2} & \frac{1}{2} \end{bmatrix} \quad (6)$$

Here, θ_q is the angular position. The coupling element between turbine and generator is described with Swing's equation which is stated at Equation 7 and Equation 8.

$$\frac{d^2\theta}{dt^2} = T_m - T_e = T_a \quad (7)$$

$$T_a = \frac{dW_e}{dt} \quad (8)$$

Here, J is the total moment of inertia of the rotor mass in kgm^2 , T_m is the mechanical torque in Nm, T_e is the electrical torque output of the generator in Nm, W_e is the mechanical speed of the rotor in (rpm) and θ is the angular position of the rotor in (rad). Voltage of PMSM in the d-q axis is then expressed as in Equation 9 - Equation 10.

$$V_q = -(r + pL_q)i_q - w_e L_d i_d + w_q \lambda_m \quad (9)$$

$$V_d = -(r + pL_d)i_d - w_e L_q i_q \quad (10)$$

From the above assertions, the dynamic electrical model is shown as in Equation 11 - Equation 13.

$$\frac{di_d}{dt} = \frac{1}{L_{qs} + L_{ds}}(-R_d i_q - w_e (L_{ds} + L_{qs}) i_d + \lambda_0) + U_d \quad (11)$$

$$L_d = L_{ds} + L_{dk} \quad (12)$$

$$L_q = L_{qs} + L_{kq} \quad (13)$$

Here, L_d , L_q and L_{ds} , L_{qs} are the inductances and leakage inductances (H) on the d axis and q axis respectively. i_d , i_q and U_q , U_d are the stator currents and voltages corresponding to the d-axis and q-axis. R_d is stator resistance (Ω), λ_0 is the magnetic flux linkage (Wb). Here,

$$w_q = p\omega_m \quad (14)$$

Here, p is the number of poles [12]. The dq frame current is mentioned as follows [13]:

$$\frac{di_d}{dt} = \frac{-R_d i_d}{L_d} + \frac{w_e L_q i_q}{L_d} + \frac{U_d}{L_d} \quad (15)$$

$$\frac{di_q}{dt} = \frac{-R_d i_q}{L_q} + \frac{w_e L_d i_d}{L_q} + \frac{w_e \lambda_0}{L_q} + \frac{U_q}{L_q} \quad (16)$$

Figure 4 shows the equivalent circuit for dq axis where as Figure 5 represents the block diagram of three phase PMSM which is designed in Simulink.

The electromagnetic torque for generator [12]:

$$T_q = 1.5 p (L_d - L_q) i_d i_q + i_q \lambda_0 \quad (17)$$

The stator resistance is taken as 14Ω ; inductance of both dq axes is used as 0.8 mH ; flux linkage established by magnet is 0.175 Wb and mass inertia is considered to be 0.089 kg/m^2 . The design is for 10 pole pairs and the friction factor is neglected. The rated power at load is considered to be 1.4 KW . An AC-DC rectifier is connected at the load terminal of the generator to convert the voltage and current to DC value. The inside subsystem part of the generator is given as in Figure 6. Table 1 gives the values of parameters used in the design. The optimal parameter for the generator is used for numerical analysis. Figure 7(a) show the design of the generator Figure 7(b) shows the fabricated generator.

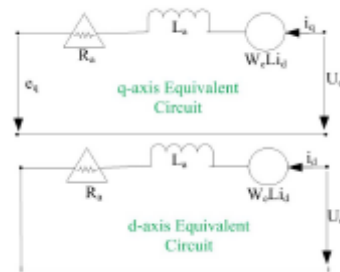


Figure 4. Equivalent q-axis and d-axis representation.

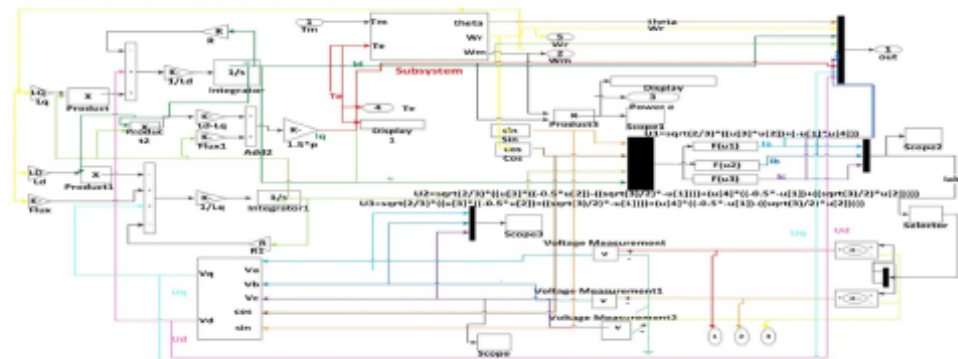


Figure 5. Modeling in Matlab/Simulink (Generator Part I).

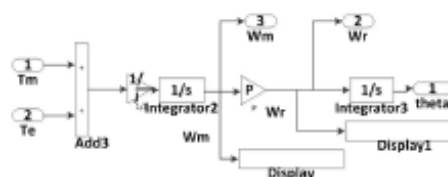


Figure 6. Subsystem (Generator Part II).

Table 1. Design Parameter.

Model	Parameter Name	Value
VAWT	Air Density	1.225 kg/m ³
	Pitch Angle	0
	Power Coefficient	0.4412
	Wind Speed	2 m/s-7 m/s
	Turbine Height	1.6 m-2.6 m
	Turbine Radius	1.6 m-2.6 m
	Stator Phase Resistance	14 ohm
PMG	Inductance (d,q)	0.8 mH
	Flux Linkage	0.175 V.s
	Inertia	0.089 J
	Pole Pair	10
	Rated Power	1.5 KW
Nominal Frequency		50Hz

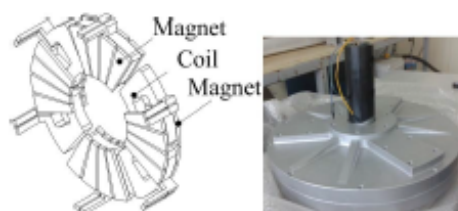


Figure 7. PMSG at optimal values.

4. Results and Discussion

4.1. Case 1 (Simulation of Turbine)

In this part, simulation is performed to get torque and power for different values of radius and height keeping one parameter fixed at a time and compared with analytical values to verify the accuracy of design. Figure 8 shows the analytical and simulation comparison of mechanical torque for different swept areas while varying the radius of the turbine. The height is fixed at 2m. As it can be seen from Figure 7, analytical and simulation results are much closer to each other. This proves that the design of the turbine created in modeling is appropriate to work with. After taking consideration of different val-

ues of turbine radius and height, it is observed from Figure 9 that at low wind speed, 0.8 m-1.2 m radius would be suitable for producing higher output power. However, the radius of the turbine is taken to be a fixed value of 1m. From Figure 10, it can be observed that the height between 2 m to 2.8 m is suitable to produce better output power. Therefore, the height of it is fixed at 2.6 m.

4.2. Case 2 (PMG connected to VAWT)

The stator resistance, inductance at dq frame, flux linkage, mass inertia and pole pairs are varied and a set of realistic parameter values are fixed (given in Table 1) in which the voltage and current were satisfactory to produce power. The power is increased with the increase in the number of pole and for practical consideration the

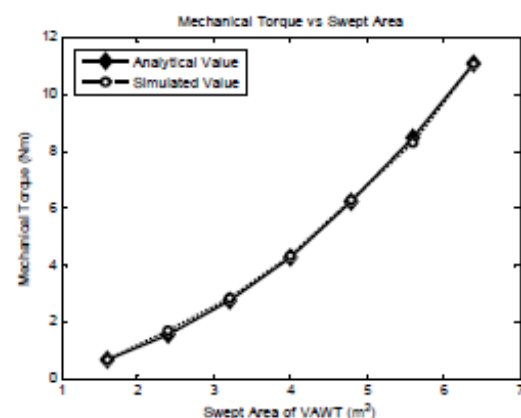


Figure 8. Mechanical Torque- Swept Area curve.

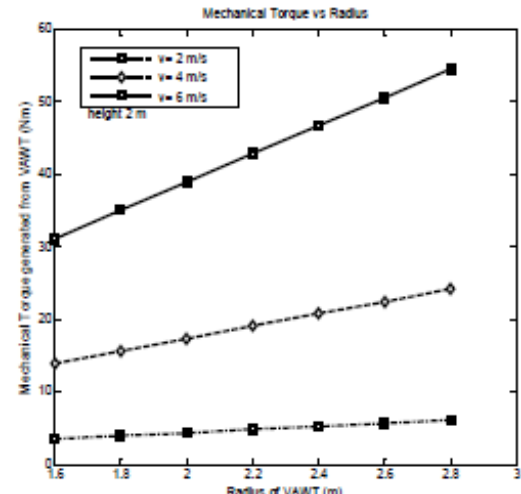


Figure 9. Torque generated for different radius.

number of pole pair is fixed at 10. Figure 11 evolved by changing the mechanical torque for different wind speed and keeping the generator parameter fixed at optimal value. The load power is measured to make sure that the generator is able to produce adequate output power for a range of torque at low wind speed.

4.3. Case 3 (Hardware Testing)

The developed generator is experimentally tested at laboratory and the results are compared with that of the simulation value. Figure 12 - Figure 14 shows theoretical and experimental comparisons for a fixed wind speed of 6 m/s. Wind speed is taken as high value in order to investigate the difference in value accurately.

The experimental values are quite identical with simulation indicating the accuracy of the simulation design. The simulation power values for different speed and mechanical torque are higher than experimental values. This is due to power loss for friction factor as it is neglected in the simulation.

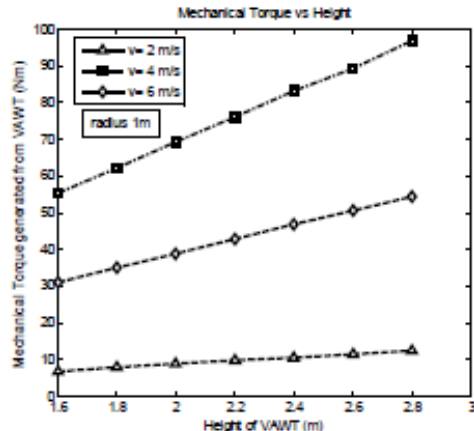


Figure 10. Torque generated for different heights.

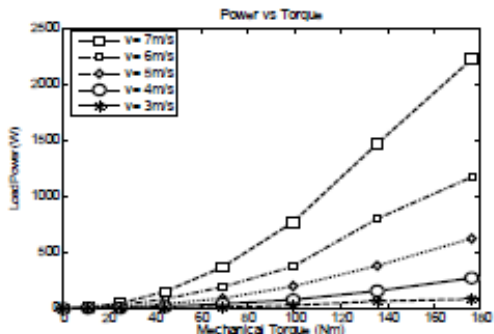


Figure 11. Graph of Power values at the load for different mechanical torque.

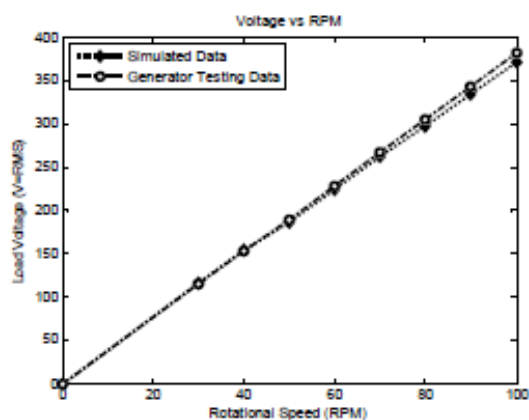


Figure 12. Voltage- Rotational Speed (RPM) curve.

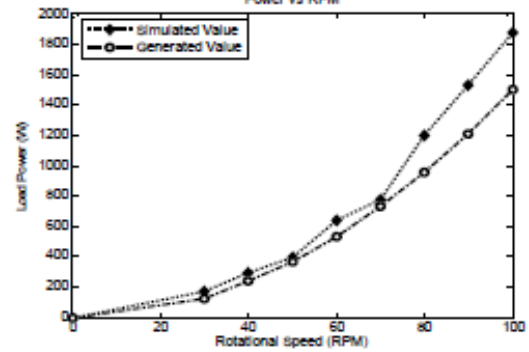


Figure 13. Power- Rotational Speed (RPM) curve.

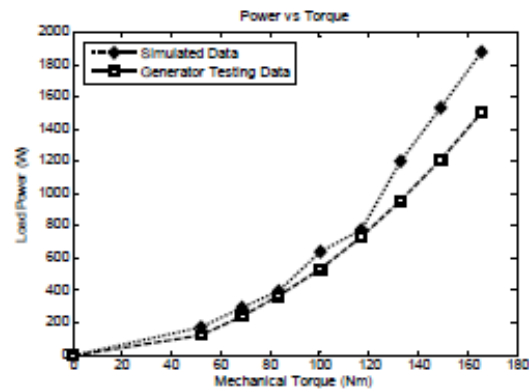


Figure 14. Power- Torque curve.

5. Conclusions

An optimal system is built for low level wind speed. The VAWT simulation produces torque and power with an estimated error of ion ranging from 0.05%-10% according to Table 2. After running several stages of simulation,

the swept area is

Table 2. Error Estimation of VAWT.

Swept Area [m ²]	Mechanical Torque [Nm]		Error [%]
	Theoretical	Simulation	
1.6	0.68	0.7	2.9
2.4	1.557	1.7	9.18
3.2	2.76	2.84	2.9
4	4.29	4.324	0.8
4.8	6.226	6.3	1.18
5.6	8.474	8.3	2.05
6.4	11.069	11.074	0.05

Table 3. Error Estimation of PMSG.

Mechanical Torque(Nm)	Load Power		Error (%)
	Simulation	Experimental	
52	148	126	14.90
68.6	284	240	15.49
83.4	416	367	11.81
100.2	586	534	8.81
116.9	817	733	10.23
132.9	1004	956	4.79
149.2	1262	1209	4.19
165.8	1878	1500	20.13

fixed at 5.2 m² having fixed the radius and height of the turbine to 1 m and 2.6 m respectively. For the generator part, the simulation data is gathered for different values of torque from the turbine; the design is built in CFD and sent to a manufacturing company. Upon arrival, the generator is tested and load voltage and power were measured for different set of values of RPM and Torque. As it can be seen in Table 3, there were differences while calculating the error (5%- 27%) for load power. It is due to the friction factor and stator inductance difference. This VAWT with PMSG can make a significant impact for low level wind situation in which Malaysia and so many other countries stand.

6. Acknowledgements

The project is funded by the Ministry of Higher Education (MOHE) of Malaysia under the ERGS grant.

REFERENCES

- [1] Zaharim, S. K. Najid, A. M. Razali and K. Sopian "Wind Speed Analysis in the East Coast of Malaysia," *European Journal of Scientific Research*, Vol. 32, No. 2, 2009, pp. 208-215.
- [2] R. Bharanikumar, A. C. Yazhini and N. Kumar, "Modeling and Simulation of Wind Turbine Driven Permanent magnet Generator with New MPPT Algorithm," *Asian Power electronics journal*, Vol. 4, 2012.
- [3] W. Fei and P. I. Luk, "A New Technique of Cogging Torque Suppression in Direct-Drive Permanent-Magnet Brushless Machines," *IEEE Transactions on Industry Applications*, Vol. 46, No.4, 2010, pp. 1332-1340. [doi:10.1109/TIA.2010.2049551](https://doi.org/10.1109/TIA.2010.2049551)
- [4] P. C. Krause, O. Wasynszuk and S. D. Sudho, "Analysis of Electric Machinery and Drive Systems," Wiley & Sons, 2002. [doi:10.1109/9780470544167](https://doi.org/10.1109/9780470544167)
- [5] C. V. Aravind, Rajparthiban, Rajprasad and Y. V. Wong "A Novel Magnetic Levitation Assisted Vertical Axis Wind Turbine design and Procedure," *IEEE Colloquium on Signal Processing and its Applications*, Melacca, Malaysia CSPA 2012
- [6] J.A.M. De Broe, S. Drouillet and V. Oevorglan, "A Peak power Tracker for Small Wind Turbines in Battery Charging Applications," *IEEE Transactions on Energy Conv.*, Vol. 14, No. 4, Dec. 1999, pp. 1630-1635. [doi:10.1109/60.815116](https://doi.org/10.1109/60.815116)
- [7] J. D. M. Whaley, W. L. Soongand and N. Ertugrul, "Investigation of Switched-Mode Rectifier for Control of Small-Scale Wind Turbines," *Intl' Conference Proceed. of IEEE-LAS Annual Meeting*, Vol. 4, 2005, pp. 2849-2856.
- [8] S. Belakehal, H. Benalla and A. Bentoussi, "Power Maximization of Small Wind System using Permanent magnet Synchronous Generator" *Revue des energies Renouvelables*, Vol. 12, No. 2, 2009, pp. 307-319.
- [9] J. G. Slootweg, H. Pollinder and W. L. Kling, "Representing Wind Turbine Electrical Generating Systems in Fundamental Frequency Simulations," *IEEE Trans. Energy Conv.*, Vol. 18, No. 4, Dec. 2003, pp. 516-524.
- [10] A. G. Westlake, J. R. Bumby and E. Spooner, "Damping the Power-angle Oscillations of a Permanent Magnet Synchronous Generator with Particular to Wind Applications," *Proc. Ekct. Power Appl.*, Vol. 143, No. 3, May1996, pp. 269-280. [doi:10.1049/ip-epa:19960285](https://doi.org/10.1049/ip-epa:19960285)
- [11] C. Busca, A. Stan, T. Stanciu and D. I. Stroe "Control of Permanent Magnet Synchronous of Large Wind Turbines," Denmark : Department of Energy Technology: Aalborg University, November 2010, *Industrial Electronics (ISIE)*, pp. 3871-3876.
- [12] M. Yin, G. Y. Li, M. Zhou and C. Y. Zhao, "Modeling of the Wind Turbine with a Permanent Magnet Synchronous Generator for Integration," *Power Engineering Society General Meeting*, 2007, pp.1-6.
- [13] K. Tan and S. Islam, "Optimum Control Strategies in Energy Conversion of PMSG Wind Turbine System without Mechanical Sensors," *Energy Conversion, IEEE Transactions on*, Vol. 19, No. 2, June 2007, pp. 392- 399. [doi:10.1109/TEC.2004.827038](https://doi.org/10.1109/TEC.2004.827038)

Optimization of Multi-pole Three Phase Permanent Magnet Synchronous Generator for low speed Vertical Axis Wind Turbine

Md. Shahrukh Adnan Khan^{1,a}, Rajprasad K. Rajkumar^{2,b},
Rajparthiban K. Rajkumar^{3,c}, CV Aravind^{4,d}

^{1,2,3}University of Nottingham Malaysia Campus, Jalan Broga 43500, Semenyih, Selangor, Malaysia

⁴School of Engineering, Taylors University, Selangor, Malaysia

^{a,b,c}kecx1msa@nottingham.edu.my, ^daravindcv@ieee.org

Keywords: Modelling, Optimization, Three Phase Permanent Magnet Synchronous Generator, Low Wind Speed, Vertical Axis Wind Turbine

Abstract: This paper focuses on developing an optimal system of Vertical Axis Wind Turbine (VAWT) for low wind speed. After studying the performance analysis of the turbine parameters for speeds less than 5 m/s, a realistic model was designed in Matlab/ Simulink that could produce suitable torque for low wind condition. The Multi-pole Axial Flux Permanent Magnet Synchronous Generator (PMSG) had been proven to be a good choice for this optimal design as it performed well enough to generate sufficient amount of voltage and power. The turbine design parameters such as the radius, height and wind speed were varied to observe the change in generator output voltage and power and based on that an optimal design for Permanent Magnet Synchronous Generator was proposed in this paper. The simulation results were tested with an actual Permanent Magnet Synchronous Generator in laboratory applying the optimized turbine parameters and were compared accordingly for error calculation. Lastly, future possibility of improvement and the limitations had been proposed to develop the system further.

Introduction

It is a matter of fact that the trends of energy system are not sustainable and a superior solution is required in order to protect the world energy from diminishing. Surely, wind energy is one of the promising sources in this aspect but this energy very much relies on the accessibility of the wind resource. Many countries do not have an average wind speed more than 5m/s, for example Malaysia; thus making the horizontal axis wind turbine (HAWT)[1]. Furthermore, multidirectional wind is another problem while taking in consideration the incapability of HAWT to handle it. The vertical axis wind turbine (VAWT) on the other hand is appropriate for such regions being capable of catching wind from all directions. On the other hand, lacking of DC field, use of strong neodymium magnets make the Permanent Magnet Synchronous Generator a perfect match with VAWT. Furthermore, it is light in weight, smaller in comparison with other generators which makes it the best suited considering low wind speed environments [2][3]. A lot of research in the area of VAWT and PMSG had been done already. Yet, a small number of efforts were taken to construct a system jointly. To recapitulate, there is a considerable need of research to be done finding the best possible realistic multi-pole PMSG arrangements that can work with VAWT for a specific swept area for low wind level cases. The aim of this paper is to look into the behaviours of a PMSG connected to a VAWT under various changing parameters using Matlab/Simulink.

Methodology

At first, the mathematical formulas of VAWT and PMSG had been put into the design in SIMULINK for both VAWT and PMSG. As far as the turbine concerns, radius, wind speed, area, the power coefficients and pitch angles were made to be the variables where as turbine mechanical speed, output torque and power were taken as turbine output. Next, three phase PMSG was designed and simulation was performed for different values of turbine mechanical torque and RPM. Load voltage, current and power were taken as the output of the generator.

Modelling and design

The aerodynamic equations of VAWT are given by the equation 1, 2, 3 and 4 stated below [2]-[4]:

$$P_m = C_p(\lambda) \frac{1}{2} \rho A U_w^3 \quad (1), \quad \lambda = \frac{\omega_m R}{U_w} C_p \quad (2), \quad T_m = \frac{P_m}{\omega_m} \quad (3), \quad A = 2RH \quad (4)$$

Here, A is the turbine rotor cover area in meter square (m^2), ρ is the air density that is 1.225 kg/m^3 at normal temperature, U_w is the wind speed in meter per second ($m s^{-1}$), C_p is the power coefficient of the wind turbine and λ is the tip-speed ratio, ω_m is the rotor angular speed in rad s^{-1} , R is turbine radius in meter (m), H is turbine height in meter (m), C_p is power coefficient and θ is pitch angle of the. The maximum value of C_p is 0.59 as per Betz law. For, VAWT, the pitch angle is nearly 0. therefore at null pitch angle, the maximum power coefficient is 0.4412 [3]-[5]. The design of turbine in simulink is given in figure 1.

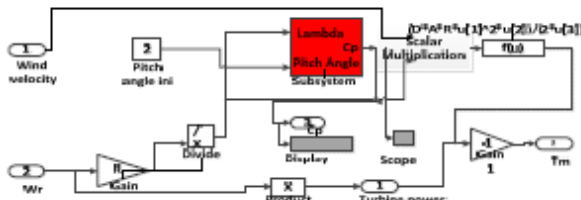


Fig. 1. Modelling of turbine

There are three kinds of PMSM namely Radial Flux, Axial Flux and Transverse Flux. Among them, Axial Flux exerts high torque and power density values making it appropriate for low wind speed applications. Thus Axial Flux was taken in consideration. The simulation for the generator was made using park transformation analysis taking dq reference coordinates (equation 5 and 6) [5][6].

$$\begin{bmatrix} f_q \\ f_d \\ f_0 \end{bmatrix} = [T_{q0}] \begin{bmatrix} f_a \\ f_b \\ f_c \end{bmatrix} \quad (5), \quad [T_{q0}(Q_q)] = \frac{2}{3} \begin{bmatrix} \cos \theta_q & \cos(\theta_q - \frac{2\pi}{3}) & \cos(\theta_q + \frac{2\pi}{3}) \\ -\sin \theta_q & -\sin(\theta_q - \frac{2\pi}{3}) & -\sin(\theta_q + \frac{2\pi}{3}) \\ \frac{1}{2} & \frac{1}{2} & \frac{1}{2} \end{bmatrix} \quad (6)$$

Here, f is treated either as current (I) or voltage (V) or flux(λ) and θ_q is the angular position of the rotor. Next, Swing equation defines the coupling element between the turbine and the generator (equation 8 and 9). The d-q axis Voltages (V_d and V_q), electromagnetic torque and electrical rotating speed are expressed as follows [5]-[8] (equation 10, 11, 12 and 13 respectively):

$$J \frac{d^2 \theta}{dt^2} = T_m - T_e = T_a \quad (8), \quad T_a = \frac{dw_e}{dt} \quad (9), \quad V_q = -(r + pL_q)i_q - w_e L_d i_d + w_e \lambda_m \quad (10).$$

$$V_d = -(r + pL_d)i_d - w_e L_q i_q \quad (11), \quad T_e = 1.5p((L_d - L_q)i_d i_q + i_q \lambda_0) \quad (12), \quad w_e = pw_m \quad (13)$$

Here, T_m is mechanical torque in Nm, w_e is the mechanical speed of the rotor, θ is the angular position of the rotor in radian, J is rotor moment inertia in kg m^2 and T_e is the generator output electrical torque in Nm. L_d , L_q and L_{dq} , L_{dq} are the inductances and leakage inductances (H); i_d , i_q and U_d , U_q are the stator currents and voltages respectively with reference to d and q axis. λ_0 is magnetic flux in Weba (Wb), R_s is stator resistance in ohms (Ω), W_e is electrical rotating speed (rad/s) of the generator and Here, p is the number of poles. Figure 2 and 3 shows the design of PMSM in simulink. An AC-DC rectifier was put at generator load terminal to get the DC power reading. Figure 4 refers to the equivalent circuit for dq axis:

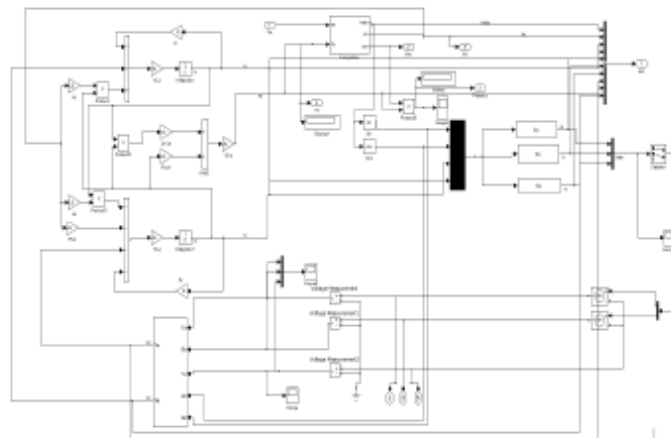


Fig. 2. Modelling (Generator Part I)

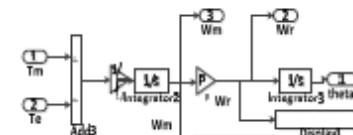


Fig. 3. Subsystem (Generator Part II)

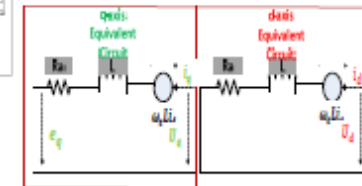


Fig. 4. Q and D axis equivalent circuit respectively

After varying the parameters, the stator resistance of the PMSG was taken as 15Ω ; the inductance was taken as $0.8mH$; the flux linkage of magnet was 0.175 Wb and mass inertia was considered to be 0.089 kg/m^2 . It was observed that at an increase number of pole pair, the power generated was high but considering a realistic model, number of pole pair was chosen as 10.

Result and Discussion

A. Optimization of VAWT for low wind speed: After designing the turbine, simulation was performed to get the mechanical torque and power from the turbine for different values of radius and height keeping one fixed at a time.

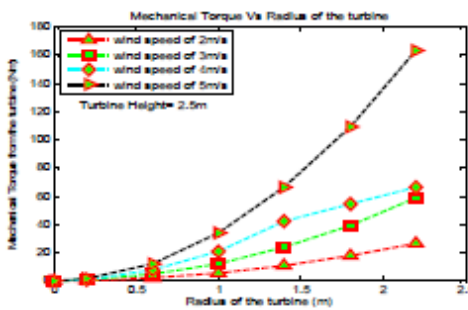


Fig 5: Torque generated for different radius values of VAWT

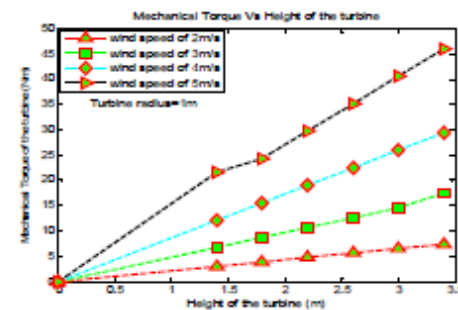


Fig 6: Torque generated for different heights of VAWT

To get the optimal turbine design parameters, 2 cases had been taken for consideration. The 1st one was to vary the radius keeping the height fixed and the 2nd one was the opposite of it. In both cases, the mechanical torque was obtained to get the best match (Figure 7 and 8). After taking consideration of different values of turbine radius and height, it could be seen that at low speed, 0.8m-1.2m radius could be suitable for producing higher power and proper torque. Yet again, to have a realistic system, the radius of the turbine has been decided to fix at 1m. Following the same concept, the height between 2m-2.8m were suitable enough to produce good power and torque. Therefore, with respect to the turbine radius, the height of it was fixed at 2.6m.

B. Optimization of PMSG for VAWT: The stator resistance, inductance at dq frame, flux linkage, mass inertia and pole pairs were varied and a set of realistic values were fixed to produce a good amount of power. Fig. 7 and 8 show the load voltage and power for different swept areas for low wind speed. Fig. 9 was gained by changing the mechanical torque keeping the generator parameter fixed at optimal value.

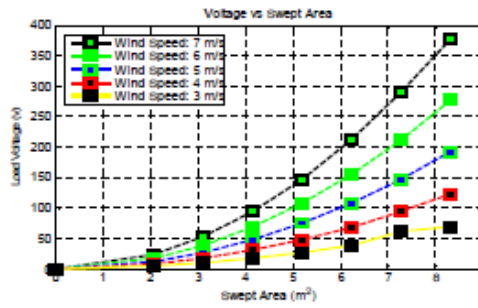


Fig. 7: Load Voltage at the generator terminal for different swept areas of the turbine

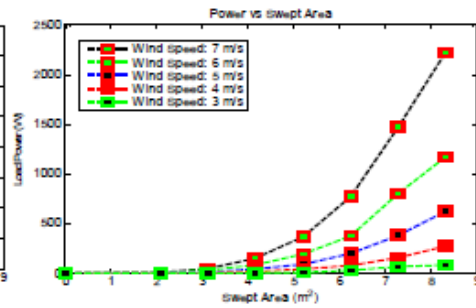


Fig. 8: Output Power at the generator terminal for different swept areas of the turbine

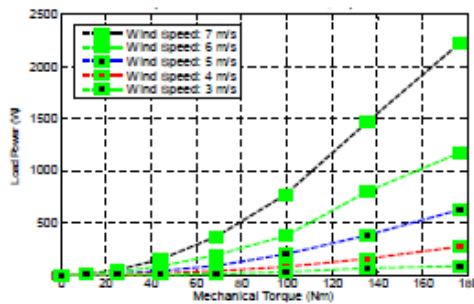


Fig. 9. Graph of Power values at the load for different mechanical torque from VAWT

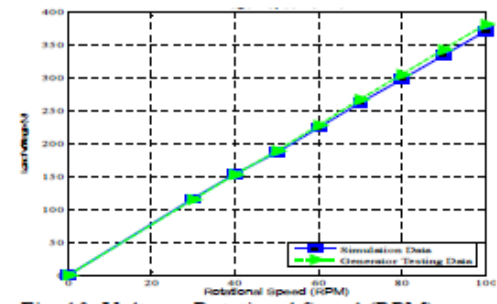


Fig. 10. Voltage- Rotational Speed (RPM) curve

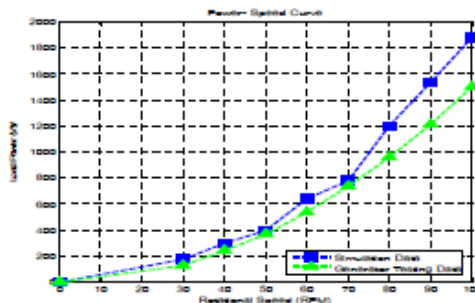


Fig. 11. Power- Rotational Speed (RPM) curve

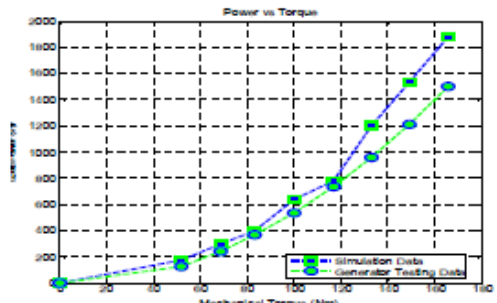


Fig. 12. Power- Torque curve

The simulation data were tested for a 1.5KW PMSG and were compared with a PMSG generator setting-up at the laboratory. The stator resistance was fixed at 14 ohm and the pole pair was set to be 10 as per the laboratory generator specification. Fig. 12, 13 and 14 show theoretical and experimental comparisons for a fixed wind speed of 6 m/s. Wind speed was taken as high value in order to investigate the differences clearly. Referring to figure 10, 11 and 12, the experimental values are quite identical with simulation indicating the accuracy of the simulation design. The simulation power values for different RPM and mechanical torque were higher than experimental values. It was due to power loss for friction factor as it was neglected in the simulation.

C. *Further Work:* For VAWT, number of blade could be varied up to 5 to analyse the effects of it. Emphasis will be put to come up with a new equation related to the number of blades, power and torque. The next step will be implementing the magnetic levitation (Maglev) in Vertical Axis

Wind Turbine (VAWT). Using very powerful neodymium magnets, the VAWT can be levitated without the use of bearing, which will reduce frictional losses and lower start up speed.

Conclusion:

To recapitulate, the paper presented an optimization of PMSG based VAWT for low wind speed condition. The modelling and design were carried through in Matlab/Simulink. It was concluded after the turbine simulation that a range of 0.8m-1.2m for radius and 2m-3m for height of the turbine were adequate to generate good amount of mechanical torque. Next, the generator was put on test on the simulation and with the above mentioned specification of the turbine; it had produced suitable power and voltage. It produced up to 1.8KW of power for a mechanical torque of 165Nm. But with the same configuration, the laboratory generator was able to produce around 1.5KW of power. The reason for the difference could be the change in friction factor and dq inductance in the simulink design. But at low torque, less than 100Nm, the difference in load power was very negligible which showed the accuracy of the system. This optimal system can play a significant role for low level wind situation.

Acknowledgements

The project is funded by Ministry of Higher Education (MOHE) of Malaysia under the ERGS grant.

References

- [1] Wind Speed Analysis in the East Coast of Malaysia, Azami Zaharim, Siti Khadijah Najid, Ahmad Mahir Razali and Kamaruzzaman Sopian(UKM) European Journal of Scientific Research, ISSN 1450 216X Vol.32 No.2 (2009), pp.208-215.
- [2] Bharanikumar R., Yazhini A.C., Kumar N., "Modelling and simulation of wind turbine driven permanent magnet generator with new MPPT algorithm" Asian Power electronics journal, Vol.4 (2012).
- [3] Belakehal S., Benalla H., and Bentounsi A. "Power maximization of small wind system using permanent magnet synchronous generator" Revue des energies Renouvelables Vol.12 N°2 (2009) 307-319.
- [4] J. G. Slootweg, H. Pollinder and W. L. Kling, "Representing wind turbine electrical generating systems In fundamental frequency simulations", IEEE Trans. Energy Conversion, vol. 18,no. 4, Dec. 2003, pp. 516-524.
- [5] Ming Yin; Gengyin Li; Ming Zhou; Chengyong Zhao; , "Modeling of the Wind Turbine with a Permanent Magnet Synchronous Generator for Integration," Power Engineering Society General Meeting, 2007. IEEE , vol. , no. , pp.1-6, 24-28 June 2007.
- [6] Cristian Busca, Ana-Irina Stan, Tiberiu Stanciu and Daniel Ioan Stroe."Control of Permanent Magnet Synchronous of large wind turbines". Denmark : Departament of Energy Technology: Aalborg University, November 2010, Industrial Electronics (ISIE), ieee, pp. 3871 – 3876.
- [7] A New Technique of Cogging Torque Suppression in Direct-Drive Permanent-Magnet Brushless Machines, Fei, W, Luk, P. I, IEEE Transactions on Industry Applications , Issue Date: July-Aug. 2010.
- [8] Semken, R.S.; Polikarpova, M.; Ro_ytta_, P.; Alexandrova, J.; Pyrho_nen, J.; Nerg, J.; Mikkola, A.; Backman, J.; , "Direct drive permanent magnet generators for high-power wind turbines: benefits and limiting factors," Renewable Power Generation, IET , vol.6, no.1, pp.1-8, January 2012

Applied Mechanics and Materials Vol. 446-447 (2014) pp 709-715
Online available since 2013/Nov/08 at www.scientific.net
© (2014) Trans Tech Publications, Switzerland
doi:10.4028/www.scientific.net/AMM.446-447.709

A Comparative Analysis of Three-phase, Multi-phase and Dual Stator Axial Flux Permanent Magnet Synchronous Generator for Vertical Axis Wind Turbine

Md. Shahrukh Adnan Khan^{1,a}, Rajprasad K. Rajkumar^{2,b},
Rajparthiban K. Rajkumar^{3,c}, CV Aravind^{4,d}

^{1,2,3}University of Nottingham Malaysia Campus, Jalan Broga 43500, Semenyih, Selangor, Malaysia

⁴School of Engineering, Taylors University, Selangor, Malaysia

^{a,b,c}kecx1msa@nottingham.edu.my, ^daravindcv@ieee.org

Keywords: Modelling, Optimization, Three Phase Permanent Magnet Synchronous Generator, Low Wind Speed, Vertical Axis Wind Turbine

Abstract: In this paper, the performances of all the three kinds of Axial type Multi-Pole Permanent Magnet Synchronous Generators (PMSG) namely 'Three-phase', 'Multi-phase' or 'Five Phase' and 'Double Stator' fixed in Vertical Axis Wind Turbine (VAWT) were investigated and compared in order to get an optimal system. 'MATLAB/Simulink' had been used to model and simulate the wind turbine system together with all the three types Permanent Magnet Generators. It was observed from the result that with the increasing number of pole in both low and high wind speed, the five phase generator produced more power than the other two generators. In general, it was observed that the responses of the Multi-phase generator at both high and low speed wind showed promising aspect towards the system followed by Dual Stator. But with the change of the variables such as wind velocity, turbine height, radius, area together with the generator pole pairs and stator resistance, the optimum system should be chosen by considering the trade-off between different configurations which were firmly analyzed and described in this paper.

Introduction

Wind power is one of the promising sectors of renewable energy but it greatly depends on the accessibility of the wind resource. As far as low wind condition applies, VAWT is the only choice with the added advantage of catching wind from multi direction. On the other hand, lacking of DC field, use of strong neodymium magnets, light in weight, smaller in size make PMSG is a perfect match for VAWT [1][2]. It is possible to design the stator in such a way that it can generate insignificant cogging torque allowing the generator to have a low speed start up and generate high current [2]. Radial Flux, Axial Flux and Transverse Flux are the three types of PMSG. Among them, Axial Flux exerts high torque and power density values making it appropriate for low wind speed applications[2][3]. In this paper, the performances of all the three kinds of axial "Permanent Magnet Synchronous Generators (PMSG)" namely 'Three-phase', 'Multi-phase' and 'Double Stator' with high pole pairs fixed in Vertical Axis Wind Turbine (VAWT) were investigated and compared in order to get an optimal system. Regarding PMSG, there is an obvious lack of research in the sector of 'Vertical Axis Wind Turbine', in particular when all three Multi-phase, Dual stator and Three-phase Permanent magnet Synchronous Generators are concerned. 'Matlab/Simulink' had been used to model and simulate the wind turbine system together with all the three types Permanent Magnet Generators. The investigation had been made mostly for low wind speed although adequate analysis had been carried through for high wind speed as well.

Literature Review Vertical Axis Wind Turbine: The aerodynamics of the turbine is given by the equations (1)-(4) stated below [1][2][3]:

$$P_m = C_p(\lambda) \frac{1}{2} \rho A U_w^3 \quad (1); \quad \lambda = \frac{\omega_m R}{U_w} C_p \quad (2); \quad T_m = \frac{P_m}{\omega_m} \quad (3); \quad A = 2RH \quad (4)$$

Here, A is the turbine rotor cover area in meter square (m^2), ρ is the air density that is 1.225 kg/m^3 at normal temperature, U_w is the wind speed in meter per second ($m s^{-1}$), C_p is the power coefficient of

the wind turbine and λ is the tip-speed ratio, ω_m is the rotor angular speed in rads^{-1} , R is turbine radius in meter (m), H is turbine height in meter (m), C_p is power coefficient and ϕ is pitch angle of the. The maximum value of C_p is 0.59 as per Betz law [6-7]. For, VAWT, the pitch angle is nearly 0, therefore at null pitch angle, the maximum power coefficient is 0.4412 [2][3].

Permanent Magnet Synchronous Generator

Three Phase Permanent Magnet Synchronous Generator: The analysis of the three phase permanent magnet synchronous generator was done using a quadrature dq equivalent circuit reference frame, in which the q-axis is 90° ahead of the d-axis with respect to the direction of rotation. Voltage, current and electromagnetic torque for a PMSG in the d-q axis synchronous rotational frame are then expressed as following (equation 5-11) [2][3]:

$$V_q = -(r + pL_q)i_q - w_e L_d i_d + w_e \lambda_0 \quad (5); \quad V_d = -(r + pL_d)i_d - w_e L_q i_q \quad (6); \quad L_d = L_{d0} + L_{lq} \& L_q = L_{q0} + L_{ld} \quad (7)$$

$$\frac{di_d}{dt} = \frac{-R_s i_d + w_e L_q i_q + U_d}{L_d} \quad (8); \quad \frac{di_q}{dt} = \frac{-R_s i_q + w_e L_d i_d + w_e + U_d}{L_q} \quad (9);$$

$$w_e = pw_m \quad (10); \quad T_e = 1.5p((L_d - L_q)i_d i_q + i_q \lambda_0) \quad (11)$$

Here, L_d , L_q and L_{ld} , L_{lq} are the inductances and leakage inductances (H) respectively; i_q , i_d and U_d , U_q are the stator currents and voltages; R_s is the stator resistance in ohms(Ω); λ_0 is the magnetic flux in Weber (Wb); w_e is the electrical rotating speed (rad/s); p is the number of poles and T_e indicates the electromagnetic torque. The figure 1.1 shows the equivalent circuit for d and q axis.

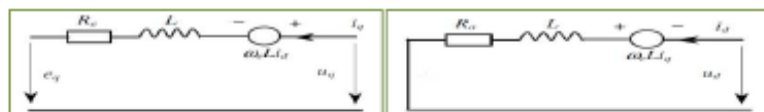


Fig. 1.1: Q and D axis equivalent circuit respectively

Multi-phase or 5 phase permanent magnet generator: The multi-phase has more slots on its stator to occupy more than 3 phase windings [4]. It is known to offer a more power density and better efficiency. The mathematical model includes a multiple-reference-frame. The transformation is given in equation (12). The electromagnetic torque of the generator is given by equation (13) where P_n is the number of poles [4][5].

$$T(\theta) = \frac{2}{5} \begin{vmatrix} \cos \theta & \cos(\theta - \frac{2\pi}{5}) & \cos(\theta - \frac{4\pi}{5}) & \cos(\theta + \frac{2\pi}{5}) & \cos(\theta - \frac{2\pi}{5}) \\ -\sin \theta & -\sin(\theta - \frac{2\pi}{5}) & -\sin(\theta - \frac{4\pi}{5}) & -\sin(\theta + \frac{4\pi}{5}) & -\sin(\theta + \frac{2\pi}{5}) \\ \cos 3\theta & \cos 3(\theta - \frac{2\pi}{5}) & \cos 3(\theta - \frac{4\pi}{5}) & \cos 3(\theta + \frac{4\pi}{5}) & \sin(\theta + \frac{2\pi}{5}) \\ -\sin 3\theta & -\sin 3(\theta - \frac{2\pi}{5}) & -\sin 3(\theta - \frac{4\pi}{5}) & -\sin 3(\theta + \frac{4\pi}{5}) & -\sin 3(\theta + \frac{2\pi}{5}) \\ \frac{1}{2} & \frac{1}{2} & \frac{1}{2} & \frac{1}{2} & \frac{1}{2} \end{vmatrix} \quad (12)$$

$$T_c = \frac{5}{2} P_n (\lambda i_q + \lambda i_{q2}) \quad (13)$$

Double stator permanent magnet generator: As the name implies, it has two stators operating with one rotor. It is much preferable to a single stator construction due to its high torque rating [6]. The dual stator configuration is to have two sets of three phase stator windings. All the physical parameters of the two windings will be made the same for the analysis. Equations (24)-Equation (21) are voltage equations to 1st and 2nd set of three phase winding respectively where $usd1$, $usd2$, $usq1$, $usq2$, $isd1$, $isd2$, $isq1$, $isq2$ are the voltages and currents of two sets winding respectively, R_s

is the stator resistance, L_{sd} and L_{sq} are the inductance components in the d - and q - axis, Ψ_f is rotor flux produced by permanent magnet and ω_s is the rotor electrical angular speed [6].

$$\begin{aligned} u_{sd1} &= -Rj_{sd1} - L_{sd} \frac{di_{sd1}}{dt} + \omega_f L_{sq} j_{sq1} \quad (14); \\ u_{sd1} &= -Rj_{sd1} - L_{sd} \frac{di_{sd1}}{dt} + \omega_f L_{sq} j_{sq1} \quad (15); \\ u_{sd1} &= -Rj_{sd1} - L_{sd} \frac{di_{sd1}}{dt} + \omega_f L_{sq} j_{sq1} \quad (16); \\ u_{sd1} &= -Rj_{sd1} - L_{sd} \frac{di_{sd1}}{dt} + \omega_f L_{sq} j_{sq1} \quad (17); \\ u_{sq1} &= -Rj_{sq1} - L_{sq} \frac{di_{sq1}}{dt} - \omega_f L_{sd} j_{sd1} + \omega_f \Psi_f \quad (18); \\ u_{sd2} &= -Rj_{sd2} - L_{sd} \frac{di_{sd2}}{dt} + \omega_f L_{sq} j_{sq2} \quad (19); \\ u_{sq2} &= -Rj_{sq2} - L_{sq} \frac{di_{sq2}}{dt} - \omega_f L_{sd} j_{sd2} + \omega_f \Psi_f \quad (20); \\ T_e &= \frac{3p_a}{2} [-\Psi_f (i_{sq1} + i_{sq2}) + (L_{sd} - L_{sq})(i_{sd1} j_{sq1} + i_{sd2} j_{sq2})] \quad (21) \end{aligned}$$

Methodology:

The entire simulation was designed in terms of park transformation analysis. Park transform is a vector representation of AC circuit (three phase) models in a dq reference coordinates which is given (equation 22 and 23) below where f can be current (I), voltage (V) or flux(λ) [7].

$$\begin{bmatrix} f_q \\ f_d \\ f_0 \end{bmatrix} = [T_{qd0}] \begin{bmatrix} f_a \\ f_b \\ f_c \end{bmatrix} \quad (22); \quad [T_{qd0}(Q_q)] = \frac{2}{3} \begin{bmatrix} \cos \theta_q & \cos(\theta_q - \frac{2\pi}{3}) & \cos(\theta_q + \frac{2\pi}{3}) \\ -\sin \theta_q & -\sin(\theta_q - \frac{2\pi}{3}) & -\sin(\theta_q + \frac{2\pi}{3}) \\ \frac{1}{2} & \frac{1}{2} & \frac{1}{2} \end{bmatrix} \quad (23)$$

Swings Equation: Swings equation portrays the physical features of a turbine and explains how a common drive shaft of the turbine drives the generator rotor. It serves as the coupling element between the turbine and the generator. The swing's equation is provided in equation (16) followed by equation (17) [9]. Here, J is the total moment of inertia of the rotor mass in kgm^2 , T_m is the mechanical torque supplied by the turbine in Nm, T_e is the electrical torque output of the generator in Nm, W_e is the mechanical speed of the rotor, θ is the angular position of the rotor in radian, Methodology used in this paper is shown in a flowchart in figure 2.1 [7].

$$J \frac{d^2\theta}{dt^2} = T_m - T_e = T_a \quad (24) \quad \text{And} \quad T_a = \frac{dW_e}{dt} \quad (25)$$

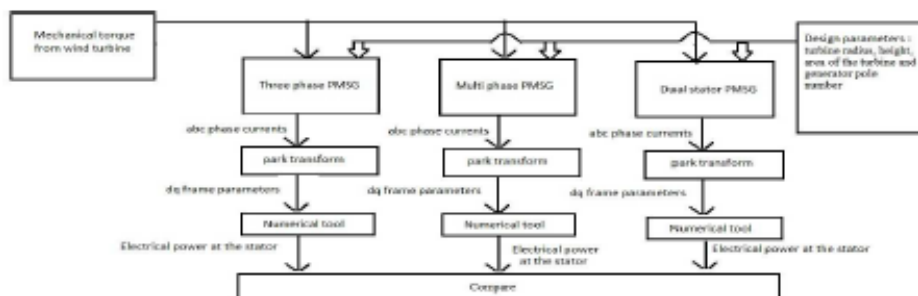


Fig. 2.1 Methodology

Modeling and Design

Table 3.1 shows different parameters of the PMSG. The load on the generator was fixed at 500KW. Fig. 3.1, 3.2 and 3.3 are simulink designs for 3-Phase, Multi-Phase and Dual-Stator PMSG. Here, wind speed was varied as external input and turbine radius, height, area and generator pole number were changed one by one keeping the others fixed. Rotational speed, torque and mechanical power

from the turbine had been achieved, tabulated and graphically analyzed. On the other hand the voltage and current drawn by the generator were also collected for further analysis. The number of poles had been varied from 2 to 42 to observe the impact in all the three kinds of generators.

Table 3.1 Below shows different parameters of the PMSG

Parameter Value	Three phase PMSG	Multi phase PMSG	Dual stator PMSG
Stator Resistance R_s	0.435 Ω	0.435 Ω	0.435 Ω
Stator Inductance	0.199 H	0.199 H	0.199 H
Flux linkage λ	0.07 Wb	0.07 Wb	0.07 Wb
Mass Inertia	0.089 kgm^2	0.089 kgm^2	0.089 kgm^2

For the 3 Phase PMSG, The mechanical torque from the wind turbine serves as an input to the swing's equation subsystem (Fig. 3.1). The dq reference currents I_d and I_q were structured base on equations mentioned above earlier and the electrical rotating speed was used in those equations. The theta from the swings equation was used for $dq-abc$ transformation of the currents. The abc current was then fed to a load. The voltage across each phase of the load was acquired and then converted to V_d and V_q to be fed back into the I_d and I_q formulation design inside a closed loop operation. Similarly for 5 Phase PMSG model, the mechanical torque from the wind turbine went to the swing's equation subsystem. The $abcde$ currents were fed to a load that is situated outside the mask model. The voltage across each phase of the load was acquired using voltage measurement blocks, the value of which was then converted to $dqd2q2$ reference frames to be fed back into the currents formulation design (Fig. 3.2). Next, design of Dual Stator is identical to that of the 3 Phase. But in this case, two stators share one rotor. The $abcdef$ current was fed to the load and the voltage across each phase of the load was converted to V_d and V_q to be fed back into the I_d and I_q formulation design for each of the stator sets (Fig. 3.3).

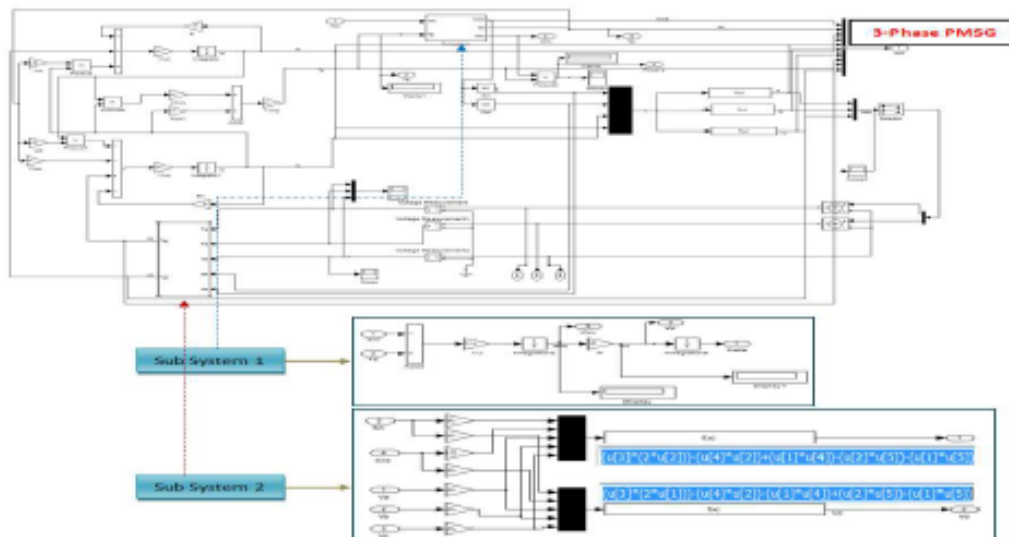


Fig. 3.1: MATLAB simulink block diagram for 3 phase PMSG

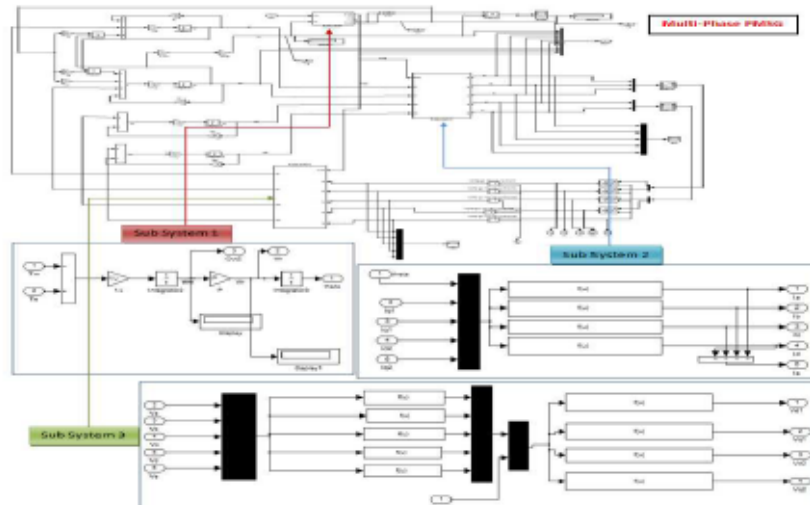


Fig. 3.2: MATLAB simulink block diagram for multiphase PMSG

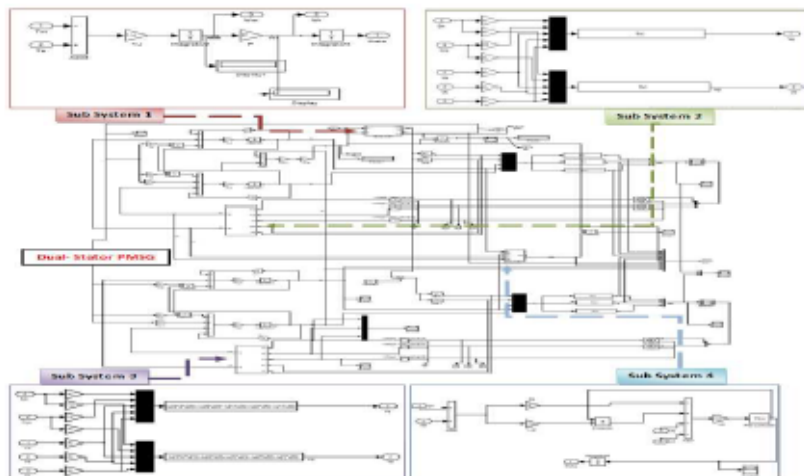


Fig. 3.3: MATLAB simulink block diagram for dual stator PMSG

Result and discussion

Setting the wind speed to 8m/s, the Fig. 4.1- 4.3 below show the amount of current produce where as Fig. 4.4-4.6 provide the electromagnetic output power of it.

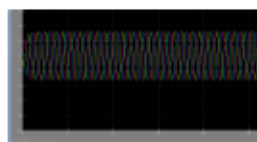


Fig. 4.1: Three phase PMSG current (Peak 3.5A) at 8m/s

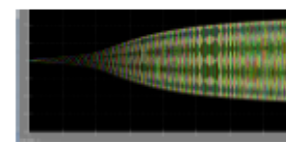


Fig. 4.2: Multi phase PMSG current (Peak 13A) at 8m/s

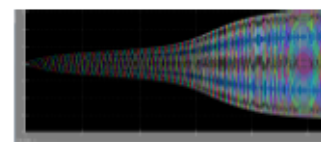


Fig. 4.3: Dual stator PMSG current (Peak 7A) at 8m/s

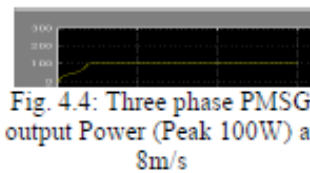


Fig. 4.4: Three phase PMSG output Power (Peak 100W) at 8m/s

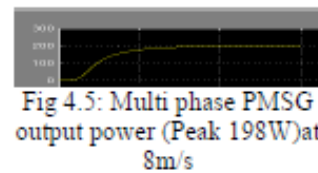


Fig. 4.5: Multi phase PMSG output power (Peak 198W) at 8m/s

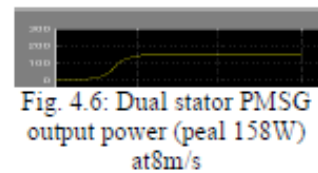


Fig. 4.6: Dual stator PMSG output power (peak 158W) at 8m/s

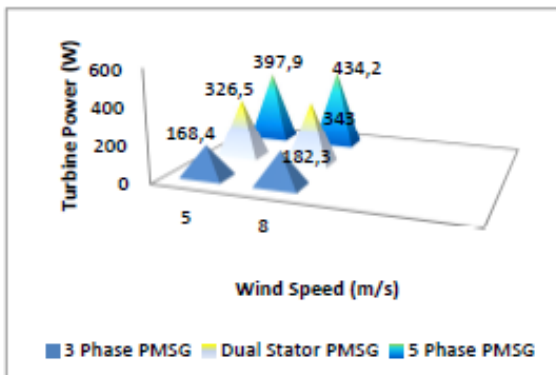


Fig. 4.7: Turbine power at Different Wind Speed for all 3 generators.

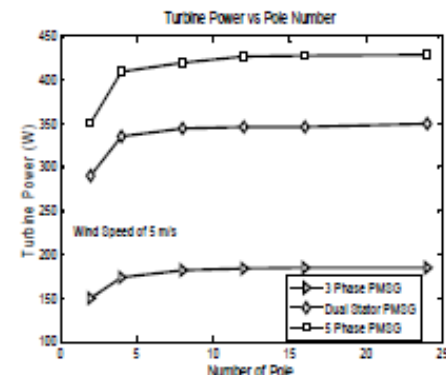


Fig. 4.8: Number of Pole vs Turbine Power for 3 Phase, 5 Phase and Dual Stator PMSG

An optimal wind speed of 8 m/s was considered for all three types of PMSG. After running the simulation, time offset versus current was plotted. It was observed from Fig. 4.1, 4.2 and 4.3 that current from 3 Phase PMSG reached the peak at 3.5 A whereas as multiphase showed 13A and dual stator achieved 7 A. Next, time offset versus electric output power at the generator end was plotted. From Fig. 4.4, Fig. 4.5, Fig. 4.6, it could be seen that 3 Phase reached around 100 W whereas as multiphase and dual stator achieved 200 W and 150 W respectively. Fig. 4.7 shows the output pick power for all the three generators for different wind speed. Again it was clear from the observation that 5 Phase drew the most amount of power for both the speeds, followed by the dual stator. Therefore even if wind speed is varied, keeping all other parameter's constant, here too we can jump into similar conclusion that, multiphase performs the best.

Table 4.1 PMSG Output Power comparison at Different Wind Speed

PMSG Types	Wind speed	
	5 m/s	8 m/s
	Turbine Power (W) (reference-5 Phase) [Reference 5 Phase Pmsg]	
Dual stator PMSG	17.96% reduction	21% reduction
3 phase PMSG	48.42% reduction	46.85% reduction

Table 4.2 PMSG Output Power comparison after changing the Wind Speed

PMSG Types	Turbine power reduction due to the change in wind speed from 8 m/s to 5 m/s
5 phase PMSG	8.36% reduction
Dual stator PMSG	4.81% reduction
3 phase PMSG	7.62% reduction

By analyzing table 4.1, it could be clear that for 5 m/s wind speed, turbine power of dual stator PMSG reduces 17.96% compared to 5 phase PMSG; whereas for 3 phase PMSG, the turbine power reduces 48.42%. Considering wind speed of 8 m/s, turbine power dropped down 21% for dual stator PMSG with respect to 5 Phase PMSG. 46.85% turbine power reduction was observed in the case of 3 Phase PMSG. Next, wind speed was fixed at 8 m/s and turbine power was measured (table 4.2). It was viewed that turbine power had reduced to 8.36 %, 4.81% and 7.62% for 5 Phase, Dual Stator and 3 Phase respectively. If higher number of poles were taken in consideration (Fig. 4.8), it could be monitored that with the increase of pole number, 5 Phase PMSG responded the most with getting high power values followed by Dual Stator and 3 Phase respectively. According to table 4.3, when the number of poles was fixed at 24, turbine power reduced 17.78% from 5 Phase to dual stator for

same configuration. For same number of poles, turbine power dropped down 45.71% for 3 Phase PMSG with respect to 5 Phase. While using 2 pole generator, 17.14% reduction in turbine power was noticed for dual stator as far as 5 Phase is concerned. Lastly, 3 phase PMSG's turbine power reduced remarkably, 48.28%.

Table 4.3 PMSG Output Power comparison for minimum and maximum number of pole

PMSG Types	Number of poles	
	24	2
	Turbine power (W) [Reference 5 phase PMSG]	
Dual stator PMSG	17.78% reduction	17.14% reduction
3 phase PMSG	45.71% reduction	48.28% reduction

Conclusion

An optimal system for VAWT was created using MATLAB/ simulink based on 3 Phase PMSG, Multiphase PMSG and Dual Stator PMSG. Wind speed, turbine height and radius were treated as primary input. Parameters such as turbine mechanical torque, generator pole number, stator resistance, and inductance were varied. In both low and high wind conditions, it was concluded that multiphase PMSG drew the highest amount of power for VAWT followed by Dual stator. 3 Phase PMSG's power was lowest as expected. The research will play a significant role for choosing optimal system for VAWT under low wind speed. Impact of change of blade and applying Magnetic Levitation to VAWT should be investigated for all three types of generators in future.

Acknowledgement

This project has been funded by the Ministry of Higher Education (MOHE) of Malaysia and we are grateful for their kind support and help.

REFERENCES

- [1] Wind Speed Analysis in the East Coast of Malaysia, Azami Zaharim, Siti Khadijah Najid, Ahmad Mahir Razali and Kamaruzzaman Sopian(UKM) European Journal of Scientific Research, ISSN 1450 216X Vol.32 No.2 (2009), pp.208-215.
- [2] Bharanikumar R., Yazhini A.C., Kumar N., "Modelling and simulation of wind turbine driven permanent magnet generator with new MPPT algorithm" Asian Power electronics journal, Vol.4 (2012).
- [3] Belakehal S., Benalla H., and Bentoussi A. "Power maximization of small wind system using permanent magnet synchronous generator" Revue des energies Renouvelables Vol.12 N°2 (2009) 307-319.
- [4] Hamid A. Toliyat, Ruhe Shi, and Huangsheng Xu, "A DSP-Based Vector Control of Five-Phase Synchronous Reluctance Motor," IEEE Trans. on Industry Applications, Vol. 4, No. 2, pp. 432-437, Jul./Aug. 2000.
- [5] L. Parsa, H. Toliyat and A. Goodarzi, "Five-Phase Interior Permanent Magnet Motor with Low Torque Pulsation" IEEE Transactions on Industry Applications, Volume 43, Jan-Feb. 2007, pp. 40 - 46.
- [6] Jiawen Li, Heng Nian, Yipeng Song, "Dual Stator Windings PMSG Fed by Half-Controlled Converters for Wind Power Application" IEEE Electrical Machines and Systems (ICEMS) conference 2011, pp. 1-6, 2011
- [7] Ming Yin; Gengyin Li; Ming Zhou; Chengyong Zhao; , "Modeling of the Wind Turbine with a Permanent Magnet Synchronous Generator for Integration," Power Engineering Society General Meeting, 2007. IEEE , vol., no., pp.1-6, 24-28 June 2007.

Journal 4

Applied Mechanics and Materials Vol. 492 (2014) pp 113-117
Online available since 2014/Jan/09 at www.scientific.net
© (2014) Trans Tech Publications, Switzerland
doi:10.4028/www.scientific.net/AMM.492.113

Optimization of Multi-Pole Permanent Magnet Synchronous Generator based 8 Blade Magnetically Levitated Variable Pitch Low Speed Vertical Axis Wind Turbine

Md. Shahrukh Adnan Khan^{1,a}, Rajprasad K. Rajkumar^{2,b},
Rajparthiban K. Rajkumar^{3,c}, CV Aravind^{4,d}

^{1,2,3}University of Nottingham Malaysia Campus, Jalan Broga 43500, Semenyih, Selangor, Malaysia

⁴School of Engineering, Taylors University, Selangor, Malaysia

^{a,b,c}kecx1msa@nottingham.edu.my, ^daravindcv@ieee.org

Keywords: Lab Prototype Three Phase Permanent Magnet Synchronous Generator, Low Wind Speed, Modeling, Design, Vertical Axis Wind Turbine.

Abstract: The paper presents a new Vertical Axis Wind Turbine (VAWT) design by using magnetic levitation (Maglev) and Permanent Magnet Synchronous Generator (PMSG). A lab prototype of VAWT was built which was run at low wind speed of around 3 to 5 meter per second. The bearing was replaced by Neodymium Magnet to avoid the friction which in turns reduces the losses and increase the efficiency. A Prototype version of PMSG was built which could generate voltage from the turbine even in low rotational speed. Suitable turbine blade angle was also determined using trial and error method.

Introduction

Magnetic Levitation (MAGLEV) Vertical Axis Wind Turbine (VAWT) is a new concept and is assumed to be implemented in the next generation wind turbines. It has a potential of generating power at very low wind speed. The main purpose of this project is creating a prototype version of Maglev-VAWT working with permanent magnet synchronous generator (PMSG). These wind turbine system ability to operate in both high and low speed conditions [1][2]. This design is levitated via maglev (magnetic levitation) vertically on a rotor shaft unlike the design of traditional horizontal axis wind turbine. This maglev technology, which will be serves as a useful replacement for ball bearings used on the conventional wind turbine reducing friction loss to almost as negligible to null. This maglev levitation will be used between the rotating shaft of the turbine blades and the base of the whole wind turbine system.

A. Literature Review

The aerodynamic power P_m of the turbine is given by the Equation 1[2].

$$P_m = C_p(\lambda) \frac{1}{2} \rho A U_w^3 \quad (1); \quad \lambda = \frac{\omega_m R}{U_w} C_p \quad (2); \quad A = 2RH \quad (3); \quad T_m = \frac{P_m}{\omega_m} \quad (4)$$

Here, in Equation (1), ρ is the air density in (kg/m^3) at normal temperature, A is the area covered by the wind turbine rotor in (m^2) , U_w is the wind speed in (m s^{-1}) , C_p is the power coefficient of the wind turbine and λ is the tip-speed ratio and is related to the rotor speed (ω_m in rads^{-1}) in as in Equation 2 [2][3]. In Equation (2) and (3), R is turbine radius in (m) , H is the turbine height in (m) . The power coefficient C_p is given as a function of ϕ (pitch angle of the turbine) and λ (the tip-speed ratio) [2][3]. The value of C_p can only go as high as 0.59 according to the Betz law. The mechanical torque is related with mechanical power by Equation (4). For computation of the power coefficient, maximum power coefficient is at null pitch angle is 0.4412 [2][3][4]. Taking the value of C_p as 0.4412, air density as 1.225, the above mentioned equations are used to calculate the swept area, mechanical power from the turbine and mechanical torque generated from it. Wind speed, radius and the height of the turbines are varied in the simulation to get optimal torque and power [5][6][7].

Methodology

Two standing fans were used to give wind speed to the wind turbine. While the wind turbine was spinning, the generator used to produce an AC output voltage which was measured by multimeter. The set-up included a rotary encoder kit (RE08A) followed by NI-USB 6212 Driver which was connected to a laptop. The rotary encoder kit had a 5V power supply from NI-USB 6212 Driver while NI-USB 6212 Driver had power supply from laptop/computer. RE08A is a rotary encoder kit which can convert the data of rotary motion into a series of electrical pulses which is read by controller. When one specific end of the turbine detects one rotation of the turbine, the LED sensor will be turned off and the signal will be sent to NI-DAQ driver which is used for data acquisition (DAQ). LAB View Signal express 2011 program collects the signal from NI-DAQ driver and gives a digital input. The RPM then be calculated from the interval of two complete rotations of the turbine. The system was then experimented with some other parameters, giving different speed of wind turbine for rotating and different angle of blades. All the reading were taken down and recorded.

Modeling and Design

Fig. 4 shows the sequence for data collection procedure, the algorithm for the collaboration of DAQ and Labview. Fig. 3.2 explains the overall working process of the laboratory set-up in-brief. Angular Speed of the turbine was measured from Equation (5) and (6); the data was taken from the Rotary Encoder Kit sensor (Fig. 3.3) which passed the signal to DAQ (Fig. 3.4).

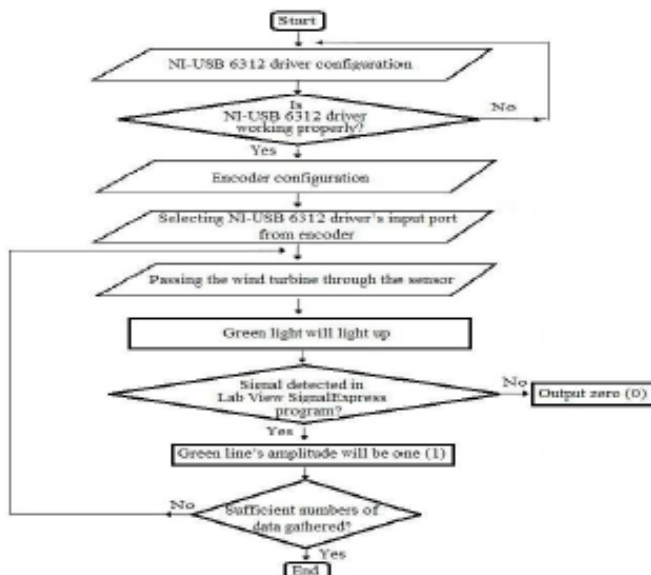


Fig 3.1 Flowchart for data collection procedure

$$\frac{rev}{s} = \frac{\text{number of wind turbine revolution}}{\text{time interval}} \quad (5); \quad \text{angular velocity, RPM} = \frac{rev}{s} * 60 \quad (6)$$

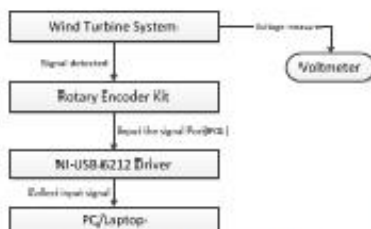


Fig. 3.2 Overall hardware setup for the system



Figure 3.3 Rotary Encoder Kit (sensor)

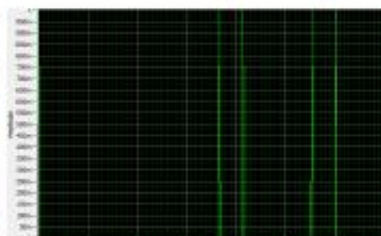


Fig. 3.4 Time interval recording

B. Wind blade design- A variable Pitch angle: The concept of design for the wind blade is implied with eight half-oval shape blades. All the blades direction could be changed to different angles. It was observed carefully whether the change of pitch angel affects the output torque and power. The design of the blade was suited to the small wind turbine. The following Fig. 3.5, 3.6 and 3.7 are showing the blade chord length, radius, pitch angle control and positioning.

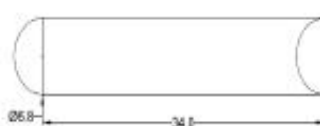


Figure 3.5 Blade design parameter



Figure 3.6 Wind Turbine



Figure 3.7 Blade angle control

C. Generator Design- Three Phase Permanent Magnet:

Synchronous Generator was used for the system. The magnetic poles were varied from 4 to 8 poles and they were attached to a stainless steel casing. Figure 3.8, 3.9 and 3.10 show the arrangements of the magnetic poles attached to the casing.

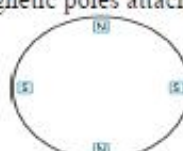


Figure 3.8 Arrangement of 4 poles of permanent magnet

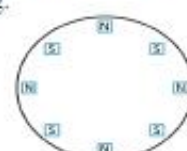


Figure 3.9 Arrangement of 8 poles of permanent magnet

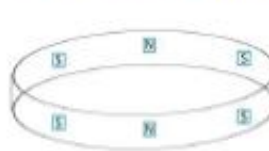


Figure 3.10 Side view of the generator

D. Neodymium Magnet: The Neodymium NX8CC-N42 Magnets from K&J were used for the magnetic levitation. These magnets were Nickel plated to enhance and protect the magnet itself. Two magnets having the same poles were faced to each other to create a repelling force, thus can levitate the whole turbine without attaching it with the shaft which reduced the friction loss of the system. Fig. 3.11 and 3.12 show the magnet placements in the shaft of VAWT.

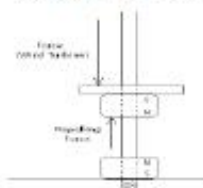


Figure 3.11 MAGLEV arrangements



Figure 3.12 Maglev implementation



Figure 3.13 Generator



Figure 3.14 Overall hardware setup

Result and Discussion

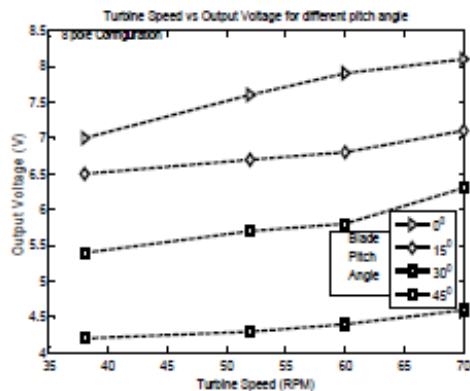


Fig. 5.1: Turbine speed Vs Generator output voltage for 0° , 15° , 30° and 45° blade angle.
(8 pole)

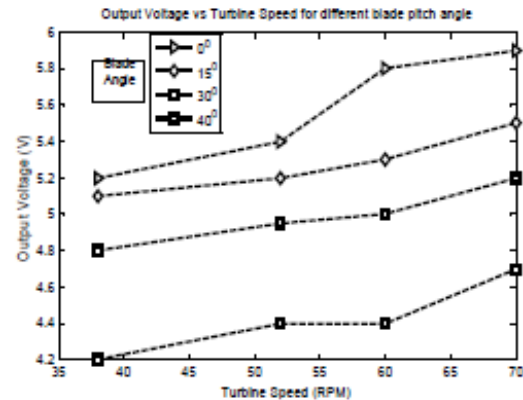


Fig. 5.2: Permanent magnet's turbine speed Vs output voltage for 0° , 15° , 30° and 45° blade angle.
(4 pole)

For the 8 pole generator, blade angle was first kept 0° . From a general perspective, we can say that, if we keep the blade angle 0° , it will cut maximum wind, thus it will rotate at a higher speed and produce larger voltage. On the other hand, when the blade angle is 90° , it will cut minimum wind and will produce minimum voltage. Referring Fig. 5.1, for 0° blade angle, produced voltage was 7V at 38 rpm. Output voltage dropped down to 6.5 V when the blade angle was changed to 15° keeping the turbine speed same. Output voltage was around 5.5 V and 4.2 V for 30° and 45° blade angle respectively, which clearly show the reduction in voltage with respect to increasing blade angle. Secondly, from the graph mentioned above, if 52 rpm was considered as the turbine speed, it could be observed that generated output voltage was 7.5 V for 0° blade angle. Then the voltage reduced to 6.6 V for 15° blade angle. Voltage came down to 5.6 V for 30° and 4.3 V for 45° blade angle. Output voltage followed the sequence 8 V, 6.7 V, 5.7 V and 4.4 V when blade angle was changed sequentially 0° , 15° , 30° and 45° . Here turbine speed was set to 60 rpm. And finally when the turbine was being rotated at 70 rpm speed with the 8 pole permanent magnet configuration, more than 8V was produced with 0° blade angle orientation. Increasing the blade angle to 15° reduced the generated voltage to 7.1 V. 6.3 V was generated for 30° blade angle, which dropped down to 4.6 V as soon as we increased the blade angle to 45° . For 8 pole permanent magnet generator, output voltage is maximum when the blade angle is null for all turbine speed. Generated output voltage starts to reduce when we start to increase the blade angle, keeping the turbine speed same. As we increase the blade angle, the output voltage reduces and vice versa. Next 2 pole pair permanent magnet generator was being experimented. Observations supported the basic concept observed in the case of 4 pole pair generator. But here we get lower output voltage compared to 4 pole pair generator for the similar conditions. When the turbine speed was 38 rpm, output voltage was 5.2 V for 0° blade angle. Increasing the blade angle to 15° , 30° and 45° reduces the output voltage to 5.1 V, 4.8 V and 4.2 V respectively. These values were higher for 4 pole pair generator at the same turbine speed. For all turbine speeds null blade angle provided the highest output voltage. As we increased the blade angle, generated voltage started to reduce.

Conclusion

This paper shows the overall wind turbine system design; constructing the system to optimization and future suggestion. Vertical Axis Wind Turbine was selected over Horizontal Axis Wind Turbine, because wind generally flows horizontally which will give more wind speed to VAWT than HAWT. Magnetic levitation was used to minimize friction. The wind turbine was designed thoughtfully with 8 half-oval shaped (position changeable) blades which were made of plastics. Turbine shaft was made of wood. Thin weight turbine was designed considering the low wind speed. Two permanent magnet

generators were designed, one is 2 pole pair another is 4 pole pair. When the VAWT was rotating in the wind, the voltage generated by the voltage was measured by an AC multimeter. Another set of hardware was also connected with the turbine. The purpose of it was to convert the turbine's number of rotations to angular velocity. In order to accomplish this goal, we required a rotary encoder kit (RE08A) and a Data Acquisition device (NI-USB 6212 Driver). The NI-USB 6212 Driver was connected with a laptop/PC from where it got its power supply, whereas, the rotary kit RE08A was connected with the DAQ device from where it would get its necessary 5 V power supply. The rotary kit was not directly connected with the wind turbine, but when the turbine rotates, it would cut the rotary device's signal and thus the device would be able to measure the rotation. The DAQ device acquired the data and sent it to the computer. The computer showed it in presentable format using LAB View Signalexpress 2011 program. Next, wind speed to the turbine was varied using two stand fans. The wind turbine was designed such a way that, blade angle was changeable manually. Thus wind speed, blade angle and number of poles were changed one at a time, keeping the other two fixed and the output voltage generated by the generator was recorded each time. By analyzing all the recorded values, it was concluded that, greater turbine speed, smaller pitch angle, higher number of poles and less friction force give maximum voltage for the generator.

References

- [1] Zaharim, S. K. Najaid, A. M. Razali and K. Sopian "Wind Speed Analysis in the East Coast of Malaysia," *European Journal of Scientific Research*, Vol. 32, No. 2, 2009, pp. 208-215.
- [2] R. Bharanikumar, A. C. Yazhini and N. Kumar, "Modelling and Simulation of Wind Turbine Driven Permanent magnet Generator with New MPPT Algorithm," *Asian Power electronics journal*, Vol. 4, 2012.
- [3] W. Fei and P. I. Luk, "A New Technique of Cogging Torque Suppression in Direct-Drive Permanent-Magnet Brushless Machines," *IEEE Transactions on Industry Applications*, Vol. 46, No.4, 2010, pp. 1332-1340. doi:10.1109/TIA.2010.2049551
- [4] P. C. Krause, O. Wasynczuk and S. D. Sudho. "Analysis of Electric Machinery and Drive Systems," Wiley & Sons, 2002. doi:10.1109/9780470544167
- [5] C. V. Aravind, Rajparthiban, Rajprasad and Y. V. Wong "A Novel Magnetic Levitation Assisted Vertical Axis Wind Turbine- design and Procedure," *IEEE Colloquium on Signal Processing and its Applications*, Melacca, Malaysia CSPA 2012
- [6] S. Belakehal, H. Benalla and A. Bentoussi, "Power Maximization of Small Wind System using Permanent magnet Synchronous Generator" *Revue des energies Renouvelables*, Vol. 12, No. 2, 2009, pp. 307-319.
- [7] M. Yin, G. Y. Li, M. Zhou and C. Y. Zhao, "Modeling of the Wind Turbine with a Permanent Magnet Synchronous Generator for Integration," *Power Engineering Society General Meeting*, 2007, pp.1-6.

Journal 5

(Status- accepted in International Journal of Control Theory and Applications, ISSN : 0974-5572)

A NOVEL APPROACH TOWARDS INTRODUCING SUPERCAPACITOR BASED BATTERY CHARGING CIRCUIT IN ENERGY HARVESTING FOR AN OFF-GRID LOW VOLTAGE MAGLEV VERTICAL AXIS WIND TURBINE

MD Shahrukh A. K.* , Rajprasad K. R. ** , Aravind CV*** , Wong. Y.W.***

Abstract: This paper gives performance analysis of a novel Supercap (Supercapacitor) based energy harvesting battery charging device operated by a Maglev (Magnetic Levitation) VAWT (Vertical Axis Wind Turbine). A 200W PMSG (Permanent Magnet Synchronous Generator) was adopted into the system. A 9 bladed hybrid VAWT, with a radius of 15.5cm and a height of 60cm, was driven at a fixed wind speed of 5m/s. The rated power (W), voltage (V) and diameter (cm) of PMSG were 200, 12 and 16 respectively. Data Acquisition, NIUSB-6009, was used interfacing with Labview software to collect the reading from sensors. 3 cases have been compared for performance analysis. ‘Case A’ showed a battery of 6V, 3.2AH, being charged from 4.2V to 5V through a DC DC converter followed by a series of 4 Supercapacitors (2.7V, 35F). ‘Case B’ and ‘Case C’ demonstrated the direct charging of the battery; where ‘Case B’ was experimented with the converter and ‘Case C’ was without converter. Taking ‘Case C’ as a reference, the result showed an increase of 21% of the charging time while charging through Supercapacitor. Case A, Supercap based charging, was also found to be 133% more efficient than direct battery charging with a converter. For a low voltage small VAWT system, this novel energy harvesting circuit could bring a significant improvement that can help off-grid areas where on-grid system is not approachable.

Keywords: Supercapacitor, Energy Harvesting, Off-grid, Maglev VAWT, Low Voltage.

1. INTRODUCTION

Wind energy is emerging in different number of locations expanding in Africa, Asia, and Latin America [1]. Figure 1 gives an idea of total wind power capacity from 2004 to 2014 [2]. Wind energy produces 370GW out of 657 GW from total renewable power at the end of 2014 which is 56% of the total renewable power excluding hydro energy. In addition, total wind energy capacity in the world has increased from 318 GW (end of 2013) to 370 GW (end of 2014) with a boost of 16%. With the increase of wind global power capacity, plentiful researches in the field of wind energy harvesting have been conducted frequently. However, many of the current options have their own limitations such as require wider area to install, difficult to implement in rural area, high costing, real time maintenance and so on. Moreover, for rural areas, there is not ample opportunity to set-up grid turbine. This situation is also

* **Research Assistant (PhD)**, Dept. of Electrical & Electronic, Faculty of Engineering, University of Nottingham, 43500 UNMC, Jalan Broga, Semenyih, Selangor, Malaysia, E-mail; kecx1msa@nottingham.edu.my

** **Associate Professor**, Dept. of Electrical & Electronic, Faculty of Engineering, University of Nottingham, 43500 UNMC, Jalan Broga, Semenyih Selangor, Malaysia, E-mail; Rajprasad.Rajkumar@nottingham.edu.my

*** **Senior Lecturer**, School of Engineering, Taylor’s University, Selangor, Malaysia Taylor’s, Selangor, Malaysia, E-mail; aravindcv@ieee.org

true for turbine with low voltage output [3] [4]. A need of an alternative way to harvest energy, therefore, is required where it is easily accessible and available. This brings up the idea and interest of harvest energy through Super Capacitor based hybrid system for low voltage output turbines. Current environment demand to have small, autonomous and energy harvesting in wind power for off grid low voltage system.

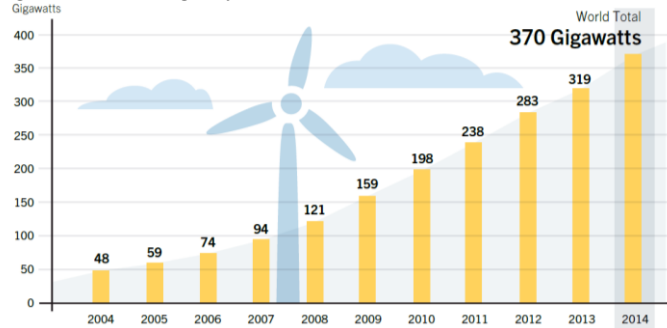


Figure 1 – Wind Global Power Capacity from 2004 to 2014[2]

In order for wind turbines to harvest energy, there is still lack of research being done. Earlier studies showed that Maglev VAWT adapted to a PMSG is a good choice for multi-directional, low wind speed areas [5] and therefore were put into the system. Next, hybrid energy harvesting circuit was brought into the experiment and efficiency was tested in compared with standard system. The objective of this paper is to incorporate a novel design of a Supercap based energy harvesting system that can provide power source from Maglev VAWT for charging batteries for off-grid energy storage.

2. SYSTEM FLOWCHART

The entire system can be divided into four parts. The 1st part consists of the Maglev VAWT and its Permanent Magnet generator. Second part deals with the energy harvesting circuit with the combination of battery and supercap.

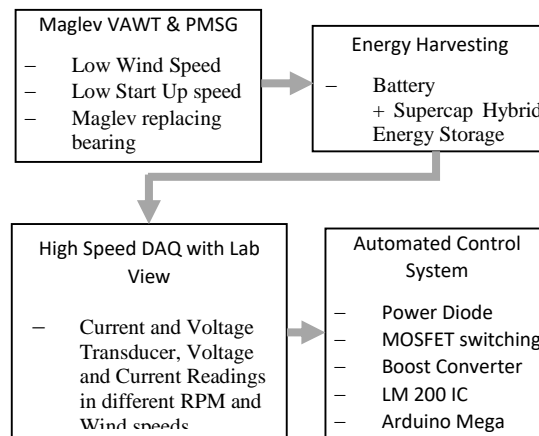


Figure 2: Overall System Flowchart

The 3rd and 4th parts basically act like a bridge between the first two parts. Figure 2 illustrates the overall system flowchart.

3. METHODOLOGY

This design of VAWT uses magnetic levitation concept, making it gearless and lightweight resulting in significant reduction in friction and start-up speed. The concept was taken from previous work in the year of 2013, where a 1.5KW PMSG was adopted to a Maglev VAWT for

performance analysis for low wind speed [5]. Having taken consideration of the multi-phase, three phase and dual stator, as per the comparative analysis result from 2014 [6], 3 Phase PMSG has been chosen to incorporate with the system [6]. Generated charges are to be stored in a lead acid battery. The charges are not constant as it varies even with a little change of wind [8]. Thus, The DC DC boost converter was applied after the Supercap. This concept was used by *Ottman and Hofman* in 2002 [7]. It provides constant current supply to charge the battery lengthening the life cycle of the battery [9] [10]. Since supercapacitors are able to hold charges for a long time; hence, it will not deplete its charges comparing to normal capacitors [11][12]. An efficiency comparison is shown between direct charging and through super capacitor bank charging. ‘Arduino Uno’ has been implemented to control the charging and discharging circuit through mosfet switches. The pick Supercap charging voltage was fixed as 7.5V whereas the lowest discharging voltage was set as 4V.

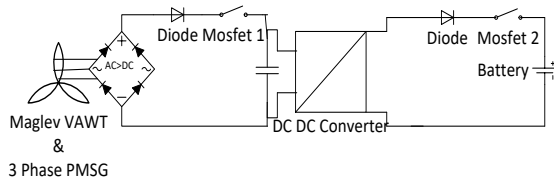


Figure 3: Schematic Diagram of the proposed system

When the supercaps being charged by the generator, Mosfet 1 becomes close circuit and Mosfet 2 becomes open. On the contrary, when supercapacitors discharge through battery, Mosfet 2 becomes open and Mosfet 1 becomes close. DAQ was used interfacing with LabVIEW based GUI for data acquisition for data collection. For testing the efficiency of the proposed system, the battery, being charged from 4.2V to 5V through supercapacitor, has been compared with the direct charging.

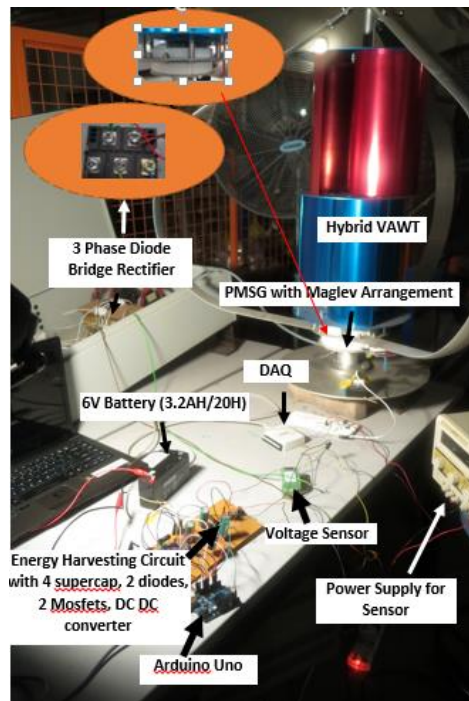


Figure 4: Experimental set-up

4. EXPERIMENTAL SET-UP

A. Maglev VAWT adopted to PMSG

A 200W PMSG has been attached to a 9 bladed hybrid Maglev VAWT. The turbine is constructed with a combine approach of the Darrieus and Savonius technology.

B. Energy Harvesting through Supercapacitor

Four supercapacitors, 2.7V each, have been combined in series to make a total of 10.8V. The turbine is supposed to charge the supercap through a diode. A Mosfet is placed in between as a switch to control charging and discharging time (Figure 5). A 6V battery is supposed to be charged from the supercapacitor (Case A), direct charging via converter (Case B), and direct charging without converter (Case C).

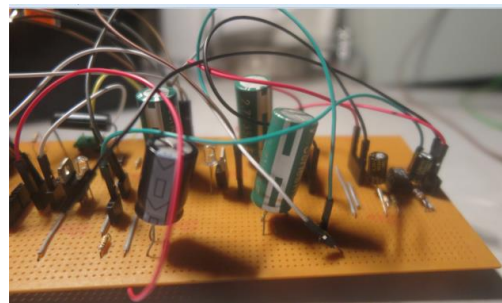


Figure 5: Arrangement of Supercapacitor, DC DC converter. Diodes and Mosfets

C. Power Electronics

Two Diodes have been placed in the circuit to prevent back flow of the voltage. One is placed before the supercapacitor and another is after the DC-DC converter. The DC-DC converter has been adjusted to produce an output voltage of 7.3V.

D. Data Acquisition (DAQ), Labview and Sensors

DC Voltage sensor is used to measure the voltage across the Supercapacitor and battery whereas DC Current sensor is used for measuring current going into Supercapacitor while charging and coming from the Supercapacitor while discharging. The DAQ, NIUSB-6009, is interfaced with the lab view software. The sensors connected to the DAQ pass the readings to the labview from where the data are collected.

E. System Parameter

The experiment has been run with the following system parameters.

Table 1: System Parameter

VAWT			
	Wind Speed	:	5 m/s
	Height	:	60 cm
	Radius	:	14.5 cm
	Number of blade	:	9
PMSG			
	Phase	:	3-Phase

	Rated Power	:	200W
	Rated Voltage	:	12V
	Diameter	:	16cm
Top net weight		:	12.5kg
Energy Harvesting			
	Battery Details	:	6V, 3.2AH/20H
	Supercap details	:	2.7V, 35F
	Number of Supercap	:	4
	Series Voltage	:	10.8V
	Pick Charging Voltage	:	7.5V
	Lowest Discharge Voltage	:	4V
	Battery Charging range	:	4.2V-5V
Power Electronics	DC DC Converter Output	:	7.3V
	Mosfet 1	:	a.'Open' when supercap charging b.'close' when supercap discharging
	Mosfet 2	:	Vice versa

5. RESULTS AND DISCUSSIONS

5.1. Case A: Energy Harvesting through Supercap

First, battery was charged through supercapacitor. Supercapacitors being charged by the generator discharged to battery. One entire charging and discharging process was considered as one cycle. For a wind speed of 5 m/s, 18 cycle was needed to charge the battery from 4.2V to 5V. Each cycle was for 25mmts in which charging of supercap took 23 minutes on average whereas discharging took only 2minutes.

Figure 6 and 7 show the charging and discharging voltage with respect to time. The increase of the battery voltage per cycle is shown in figure 8. 18 cycles here indicate 7.5 hours of total charging process of the battery.

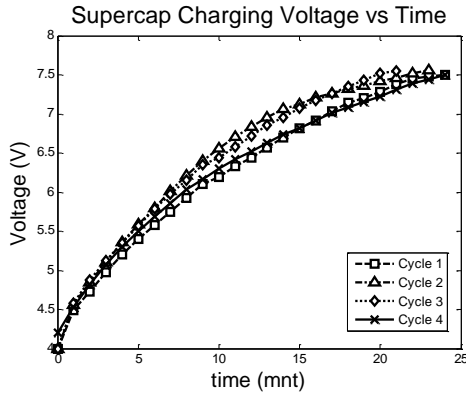


Figure 6: Supercapacitor Charging Voltage with respect to time

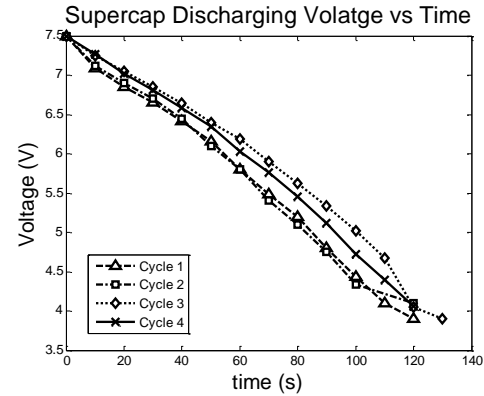


Figure 7: Supercapacitor discharging Voltage with respect to time

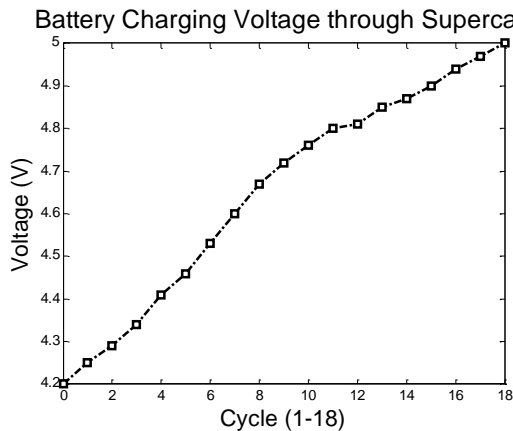


Figure 8: Battery Charging Voltage though supercap for 18 cycle (7.5 hours)

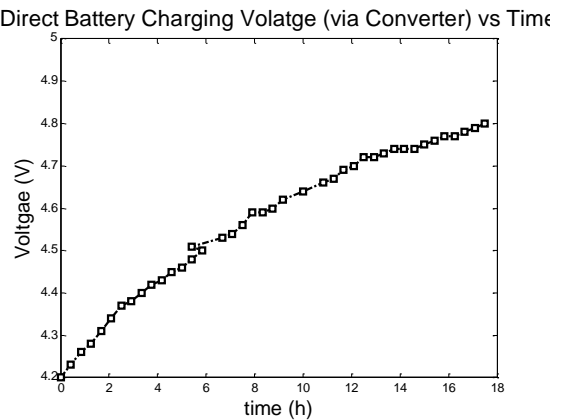


Figure 9: Direct battery charging voltage via converter with respect to time

5.2. Case B: Energy Harvesting without Supercap (with converter)

In this part, without the use of supercapacitors, turbine was fed to charge the battery through the converter. According to figure 9, it took almost 17.5 hours to reach its maximum value of 4.8V. After that the increase of the voltage was so less with respect to time, the value was not taken in consideration.

5.3. Case B: Energy Harvesting without Supercap (without converter)

Last section takes the converter out and connects the turbine directly with the battery. As it can be observed from figure 10, this approach took less time (9.5 hours) than the second approach (direct charging via converter). However, the generator output voltage fluctuates and battery needs a steady constant voltage for charging up. Therefore this method is not recommended and applying this method for a longer period will result damaging of the battery. Still results were gathered for the sake of comparison.

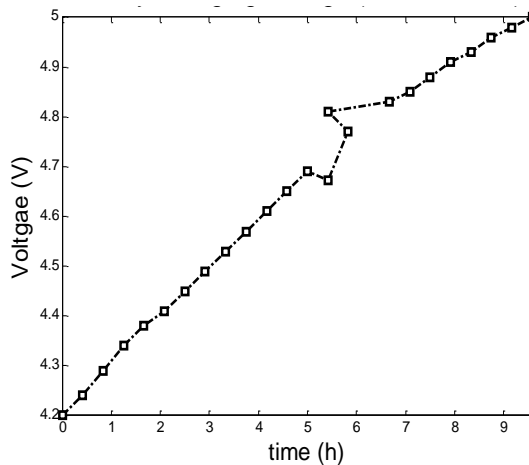


Figure 10: Direct battery charging voltage without convert with respect to time

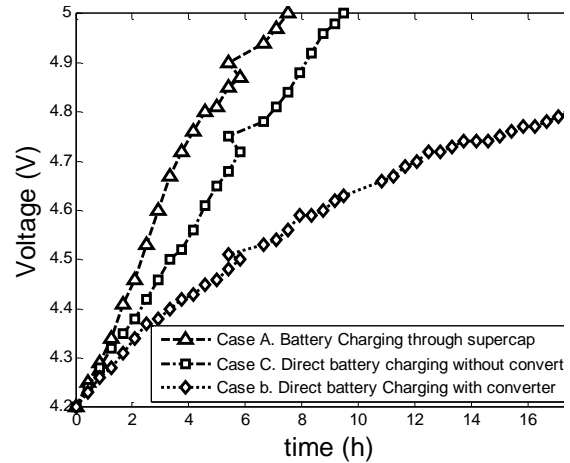


Figure 11: Battery Charging Voltage under 3 cases in respect with time

5.4. Efficiency Comparison

Figure 11 indicates the comparison between all the 3 cases. ‘Case C’ was taken as a reference point while comparing. It was found out that charging through supercapacitors was 21% more efficient than direct charging without converter. Supercap battery charging is also 133% more efficient than direct charging with a converter. That makes case 2 being unworthy in low wind speed situation.

6. FUTURE WORK AND CONCLUSION

There is vast scope to extend this work further and come out with potential results. This surely can bring a revolutionary change in low voltage turbine off-grid system. As for example, wind speed can be made lower while experimenting and data should be collected for low wind speed areas. Also, converter and switching configurations should be varied in order to observe the effect on the charging system. To recapitulate, for a low voltage turbine output system, this kind of hybrid supercap based battery charging device could bring a radical change for off-grid technology. With efficiency over 21% than the unconventional direct battery charging, makes the proposed system worthy of consideration. The conventional energy harvesting battery charging circuit through a DC DC converter just failed to catch up the charging speed. To conclude, the supercap based emery harvesting hybrid circuit for battery charging has shown remarkable results with our proposed Maglev PMSG based VAWT and thus more research and further study should be conducted in order for its betterment.

7. REFERENCE

1. World Wind Energy Association, "New Record in Worldwide Wind Installation," 5 February 2015. [Online]. Available: <http://www.wwindea.org/new-record-in-worldwide-windinstallations/>. [Accessed 15 March 2015].
2. Renewable Energy Policy Network, "Global Status Report," 2015. [Online]. Available: <http://www.ren21.net/ren21activities/globalstatusreport.aspx>. [Accessed 15 March 2015].

3. X. S. Tang, Z. P. Qi, “Economic analysis of EDLC/battery hybrid energy storage,” International Conference on Electrical Machines and System 2008, pp. 2729-2733, October 2008.
4. M. Pedram, N. Chang, Y. Kim and Y. Wang, “Hybrid electrical energy storage systems,” Proceedings of the 16th ACM/IEEE International Symposium on Low Power Electronics and Design, pp. 363-368, August 2010.
5. Md Shahrukh A. Khan, Rajprasad K. R., C. Aravind, “Performance analysis of 20 Pole 1.5 KW Three Phase Permanent Magnet Synchronous Generator for low Speed Vertical Axis Wind Turbine”, Energy and Power Engineering, (2013), pp. 423-428.
6. K. A. Md Shahrukh, R. K. Rajprasad, R.K. Rajparthiban., C. Aravind, “A Comparative Analysis of Three- phase, Multi-phase and Dual Stator Axial Flux Permanent Magnet Synchronous Generator for Vertical Axis Wind Turbine”, Applied Mechanics and Materials Vols. 446-447 (2014) pp 709-715.
7. G. K. Ottman, H. F. Hofmann, A. C. Bhatt and G. A. Lesieutre, “Adaptive piezoelectric energy harvesting circuit for wireless remote power supply,” IEEE Transactions on Power Electronics, vol. 17, no. 5, pp. 669-676, September 2002.
8. E. L. Worthington, “Piezoelectric energy harvesting: Enhancing power output by device optimisation and circuit techniques,” PhD thesis, School of Applied Sciences, Cranfield University, 2010.
9. J. R. Miller, “Introduction to electrochemical capacitor technology,” IEEE Electrical Insulation Magazine, vol. 26, no. 4, pp. 40-47, July 2010.
10. Y. C. Zhang, X. Shen and H. Liang, “Study of supercapacitor in the application of power electronics,” WSEAS Transactions on Circuits and Systems, vol. 8, no. 6, pp. 508-517, June 2009.
11. S. Park, Y. Kim and N. Chang, “hybrid energy storage systems and battery management for electric vehicles,” 50th ACM/IEEE Design Automation Conference (DAC), pp. 1-6, May 2013.
12. A. Ostadi, M. Kazerani and S. K. Chen, “Hybrid energy storage system (HESS) in vehicular applications- a review on interfacing battery and ultra-capacitor units,” IEEE Transportation Electrification Conference and Expo (ITEC), pp. 1-7, June 2013.

Journal 6

Cost Effective Design Fabrication of a Low Voltage Vertical Axis Wind Turbine

Shahrukh Adnan K.¹, Rajprasad K.R.², Aravind C.V.³ and Wong Y.W.⁴

ABSTRACT

This paper applied Weight to Power Ratio into two different Permanent Magnet Synchronous Generator based Vertical Axis Wind Turbines and found out the relative cost-efficient model. Both the models were developed in Matlab Simulink under various parameters and were in low voltage range. Before sending the cost-effective design out of the two Simulink model, the chosen design was implemented and a prototype version of it was built in the lab to make sure the turbine produces enough torque and falls in to the low voltage open circuit region. After getting satisfactory result, the design was sent for fabrication. Upon arrival, the turbine was set-up in the laboratory and was performed open circuit analysis and comparison was made between the manufactured design and the prototype. It was found out at the high wind speed range, error estimated was also high. Reason was found out and suggestion was made to develop the model further.

Keywords: Cost-efficiency, Vertical Axis Wind Turbine, Weight to Power Ratio, Permanent Magnet Synchronous Generator, Low Voltage, Prototype

1. INTRODUCTION

Recent revolutionary advances in technology are creating better future for countries with low wind speeds like Malaysia and also changing the face in wind technology. The first known specific windmill, Pneumatics, was said to be found in the 1st century BC by Hero of Alexandria [1-2]. Time goes even earlier to 500 B.C. when People first used wind power to propel the boats in Nile opposite to river current [3-4]. Wind power technology has been developing since then and each era brings us closer to perfection. Coming back to 21st century, numerous projects regarding this sector have been funded and many a researcher are getting interested to develop the wind power technology to further extension. The low speed kind, Vertical Axis Wind Turbine (VAWT) with its ability to function from multi directional wind angle is getting popular with low average speed countries like Malaysia [5]. Government as well as private companies are coming forward to sponsor these low speed turbines. In order to bring a project in the industry-efficiency, environment friendliness and cost-efficiency are one of the most important factors to cover. But these has been a lack of finding a cost-effective technique that can compare the newly invented current model to the old ones. This paper finds a solution to this problem by applying a relative comparison and finding out the relative cost-efficient model from the two products. It took one comparative old model of Permanent Magnet Synchronous Generator (PMSG) based VAWT which was experimented in 2013[6] and it was compared with another simulated model. The comparatively cost-efficient model was built as a prototype which was later sent for fabrication after getting satisfactory open circuit voltage result.

¹ Research Assistant (PhD), Dept. of Electrical & Electronic, Faculty of Engineering, University of Nottingham, 43500 UNMC, Jalan Broga, Semenyih, Selangor, Malaysia, Email: kcc1msa@nottingham.edu.my

² Associate Professor, Dept. of Electrical & Electronic, Faculty of Engineering, University of Nottingham, 43500 UNMC, Jalan Broga, Semenyih Selangor, Malaysia, Email: Rajprasad.Rajkumar@nottingham.edu.my

³ Senior Lecturer, School of Engineering, Taylor's University, Selangor, Malaysia Taylor's, Selangor, Malaysia, Email: aravindcv@ieee.org

⁴ Assistant Professor, Dept. of Electrical & Electronic, Faculty of Engineering, University of Nottingham, 43500 UNMC, Jalan Broga, Semenyih Selangor, Malaysia, Email: YeeWan.Wong@nottingham.edu.my

2. COST EFFICIENCY COMPARISON-WPR

This section discussed the two system configuration in brief and came up with a low cost system which was then sent for fabrication. A simple but effective “Weight to Power Ratio” (WPR) technique was used here. “Weight to Power Ratio” is commonly applied to power sources in order to find out the relative cost effective but yet efficient unit or design being compared to a second unit or design. It simultaneously represents efficiency and cost-effectiveness together and indicates which design is better in terms of percentage. [7][8]. It is important to note that this model tells a relative cost effective scenario in terms of “Kg/W” or “m³/s”. It is a measurement of relative cost-effective performance of any engine, motor, generator or power source. It is also used as a measurement of efficiency of a system as a whole, in here, which is the weight (m) of the entire system (PMSG adopted to VAWT) being divided by the PMSG rated output power (P). It is noteworthy to mention that in “Weight to Power Ratio”, “Weight” in this context means “Mass” (m). Weight is the colloquial term often used instead of mass and since then “Weight to Power Ratio” has been conventionally used. [7-10]

2.1. Physical Interpretation

$$WPR = \frac{m}{P} \quad (1)$$

$$\begin{aligned} - \frac{m}{\left(\frac{W}{t}\right)} &= \frac{m}{\left(\frac{FS}{t}\right)} = \frac{m}{\left(\frac{ma \cdot S}{t}\right)} = \frac{m \cdot t}{m \cdot a \cdot S} = \frac{m \cdot t}{m \cdot \frac{v}{t} \cdot S} \\ &= \frac{m \cdot t^2}{m \cdot v \cdot S} = \frac{m \cdot t^2}{\left(m \cdot \frac{S}{t} \cdot S\right)} = \frac{t^2}{S^2} \\ - \frac{\text{kg}}{W} &= m \cdot t^2 / m^2 \end{aligned}$$

$$\text{Efficiency, } \eta = \frac{WPR_i - WPR_f}{WPR_i} \times 100\%$$

After applying the cost effective technique in the two configurations achieved from the simulation, the better model, in terms of low costing, was sent for fabrication. An earlier work in 2013 [6][11], a 1.5kW 20 Pole PMSG based maglev 3-bladed VAWT was analysed for low wind speed. The configuration of the system from previous work was compared with the current model for relative cost-efficiency. The current system was developed under Matlab Simulation under various wind parameters and described previously in the same year of 2016 [12]. Following are the configuration details.

Table 2.2 illustrates the “Weight to Power Ratio of the two design configuration. It is clear that the smaller design version is 20% cost effective relative to the first design due to its small weight scale. Also, this 200W, 12V 9 bladed rated system much compact comparing to the 1.5kW, 220V, 3 bladed turbine. As far as low wind and low torque concern, the voltage and power output will also be very low as per the simulation data. Therefore it was decided to send current configuration for fabrication.

3. PROTOTYPE CONFIGURATION AND FIELD TESTING

A Chinese Company namely “JN Wind Power Technology Development Co LTD” was chosen for design fabrication. The company was requested to put Maglev in the system. They had also been asked to

Table 1
System Design Configuration

<i>VAWT</i>		<i>Current System</i>	<i>Previous system</i>
PMSG	Height	60 cm	2.6m
	Radius	14.5 cm	1m
	Number of Blade	9	3
	Pitch Angle	0	0
	Power Co-efficient	0.4412	0.44
	Phase	3-Phase	3-Phase
PMG	Type	Axial Flux	Axial Flux
	Rated Power	200W	1500W
	Rated Voltage	12V	220V
	Pole Pair	8	10
	Diameter	16cm	55.5cm
	Top net weight	12.5kg	75kg

Table 2
Weight to Power Ratio

Weight to Power Ratio 1, WPR ₁	:	0.05 Kg/W
Weight to Power Ratio 2, WPR ₂	:	0.0625 Kg/W
Cost Efficiency	:	20%

provide a data sheet for the system but generally data sheets were to be provided only after fabrication, not before that. Therefore, before ordering from the Chinese Company, in order to be assured that the design would work well in low wind speed, a lab prototype was built similar to the current design configuration. The idea was to go for fabrication only if the lab prototype indicated good pattern of result.

3.1. VAWT & PMSG Design and Set-up

The design of VAWT included eight blades as aerofoil (1). The length of the blade, that was also the height of the turbine, was 60cm, the aerofoil chord diameter was 6.5cm and the radius of the turbine was 14.5cm matching the current configuration which was being investigated. The PMSG used was taken from the fan motor. The only difference between prototype and current simulation model was the pole number. Unlike the current 8 pole pairs, the prototype PMSG was made with 4 pole pair.

Figure 2 shows the laboratory set-up where the prototype was experimented with external fans and open circuit voltage was measured by a multimeter.

3.2. Prototype Field Testing

Figure 3 focuses the generator open circuit voltage at null pitch angle. Furthermore, at the lowest wind speed of 4m/s, the generator was still able to produce an open circuit voltage of 7V (figure 3). It was not possible to make a 16 pole configuration for the prototype but even with 8 pole configuration it showed good result overall. Therefore, it was decided that the prototype system made was good enough to produce low voltage at lower wind speeds.



Figure 1: Hardware Architecture-Design of VAWT and PMSG



Figure 2: Prototype Set-up

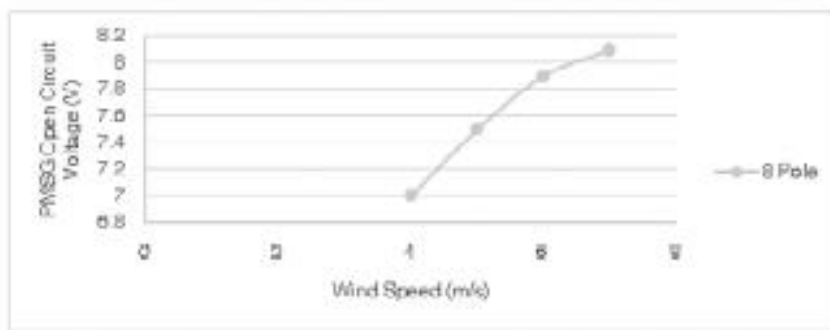


Figure 3: Prototype 3-phase 8 Pole PMSG Open Circuit Voltage for various wind speeds

4. FABRICATION AND FIELD RESULT

The design was then sent for fabrication and upon arrival, it was set-up in the lab and tested for open circuit voltage. Figure 4 shows the fabricated PMSG based VAWT with the cost-effective optimal design parameters.

The system was tested at the Research Building of the Engineering faculty of University of Nottingham Malaysia Campus. The open circuit voltage found was recorded and compared with the prototype design. The wind speeds were varied in the same range as the prototype and the findings are shown in figure 5. It was found that the developed design performed significantly better, particularly at high wind speed. At low wind such as 4m/s, the open circuit voltage different was only 0.5V and estimated error was only 7.7%. But

it can be observed that with the increase amount of wind speed, error started to increase as well. At maximum wind speed of 7m/s, 26% error was estimated. After analysis, it was clear that the difference was due to the pole pair number. The manufactured model basically had 8 pole pairs whereas the prototype built only had 4. Therefore, the factory made design showed better performance at high wind speed.

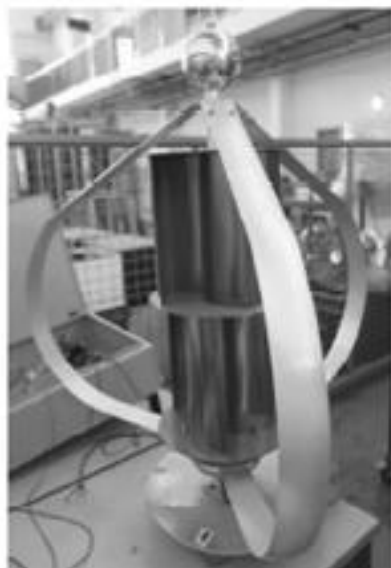


Figure 4: VAWT upon arrival

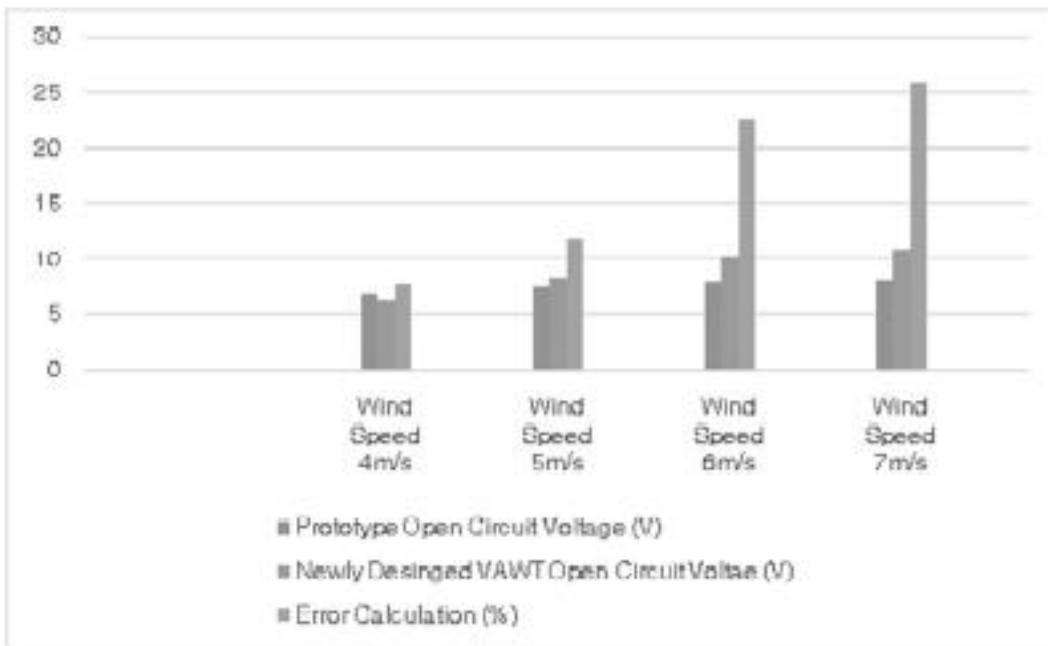


Figure 5: Open Circuit Voltage Comparison and Error Estimation

Wind Speed (m/s)	Prototype Open Circuit Voltage (V)	Newly Designed VAWT Open Circuit Voltage (V)	Estimation of Error(%)
4	7	6.5	7.7
5	7.5	8.5	11.8
6	7.9	10.2	22.6
7	8.1	11	26

5. CONCLUSION

To recapitulate, the paper contributed a new approach towards measuring relative cost-efficiency of different wind power models. One earlier model of 1.5KW PMSG based 3-bladed VAWT was taken for evaluation and it was compared with another model of 200W PMSG based hybrid VAWT. Both model was tested and developed in Matlab Simulink. After comparison by applying Weight to Power Ratio, the newer and smaller version of VAWT was found to be cost-effective. Afterwards, a laboratory prototype of the developed smaller version of VAWT was built to test the open circuit performance in order to confirm low voltage performance. Having accomplished satisfactory performance, the model was sent for fabrication and upon arrival tested for error calculation. Lastly, analysis was done and it was found out the prototype voltage performance error was significantly high at higher wind speed. It was found out due to the limitation of matching the high number of pole, the prototype was built with 8 poles only whereas the proposed system consisted of 16. Due to the insufficient amount of pole number, the prototype was unable to produce enough voltage compared to the manufactured model and thereby causing the estimated error to be high. In short, method used in this paper could be useful to further research model and could give us a relative idea in cost-efficiency.

REFERENCE

- [1] A.L. Rogers J.F. Manwell, J.G. McGowan. Wind Energy Explained – Theory, Design and Application. John Wiley and Sons Ltd., second edition, 2009.
- [2] World Wind Energy Association, "New Record in Worldwide Wind Installation," 5 February 2015. [Online]. Available: <http://www.wwindea.org/new-record-in-worldwide-windinstallations/>. [Accessed 15 March 2015].
- [3] S.M. Muyeen, Junji Tamura, T. Murata, Stability Augmentation of a Grid-connected Wind Farm, Springer-Verlag London Limited, 2009.
- [4] MD Shahrukh A. Khan, R. Rajkumar, Rajparthiban K., CV Aravind, "Optimization of Multi-Pole Permanent Magnet Synchronous Generator based 8 Blade Magnetically Levitated Variable Pitch Low Speed Vertical Axis Wind Turbine", Applied Mechanics and Materials, Vol. 492, pp. 113-117, 2014.
- [5] K. A. MdShahrukh, R. K. Rajprasad, R.K. Rajparthiban., C. Aravind, "A Comparative Analysis of Three-phase, Multi-phase and Dual Stator Axial Flux Permanent Magnet Synchronous Generator for Vertical Axis Wind Turbine", Applied Mechanics and Materials Vols. 446-447 (2014) pp. 709-715.
- [6] MdShahrukh A. Khan, Rajprasad K. R., C. Aravind, "Performance analysis of 20 Pole 1.5 KW Three Phase Permanent Magnet Synchronous Generator for low Speed Vertical Axis Wind Turbine", Energy and Power Engineering, (2013), pp. 423-428.
- [7] NASA, "Priorities in Space Science Enabled by Nuclear Power and Propulsion," National Academies Press, 2008, ISBN: 0309100119
- [8] Mollenhauer, Klaus, Tischke, Helmut, "Handbook of Digital Engines," Springer, 2010.
- [9] K. Yazawa, A. Shakouri, "Cost-effective waste heat recovery using thermoelectric system", Birck and NCN Publications, 2012, p. 1199.
- [10] Aravind C. V., M. Norhisam, M. H. Marhaban, and I. Aris, "Analytical design of double rotor switched reluctance motor using optimal pole arc values," International Review in Electrical and Electronics, Vol. 7, No. 1, 3314-3324, Feb. 2012.
- [11] MD Shahrukh A. Khan, R. Rajkumar, Rajparthiban K., CV Aravind, "Optimization of Multi-pole Three Phase Permanent Magnet Synchronous Generator for low speed Vertical Axis Wind Turbine", Applied Mechanics and Materials, Vol. 446-447, pp. 704-708, 2014.

Comprehensive Review on the Wind Energy Technology

Shahrukh Adnan K.¹, Rajprasad K.R.², Aravind C.V.³, Wong Y.W.⁴,
Selima Shahnaz Geo.⁵ and Low Jay See⁶

ABSTRACT

This paper presents a comprehensive review on the wind energy technology in the past two decades. It presents some of the most important literatures of wind energy technology in the way it is used for energy harvesting. The emphasis is placed on reviewing literature in wind power history and wind turbine types which have been developed gradually over time. The beginning of wind technology followed by a steady yet progressive expansion of wind industry is given in the chronological order.

Keywords: Wind Power History, Vertical Axis Wind Turbine, Classification, Turbine Generator.

1. INTRODUCTION

Wind energy is one of the oldest ways for energy solutions through mechanical means of control. The highly unreliable wind speed and the deep fluctuations in the conversion mechanisms push a biggest challenge in the energy conversion. Also the dynamic nature of production of energy rather like the static way of energy conversion in solar energy makes wind to be second next source than the solar technology. The choice of new types of power control strategy the development of electromechanical devices read the interest on this technology in the past decade. In order to look into the road map of the wind energy technology start from the initial days to the state of art today makes an interesting journey. The main idea of this paper is to get the overview of the gradual development towards wind power technology that has happened over years. At the same times, all the work that have been carried through in recent years along with the ancient time have been reviewed in brief in a sequential manner. This paper gives a clear idea on the preliminary stage of wind energy followed by its gradual progress and perfection together with the latest innovation and research work carried by the scientists and engineers.

1.1. Before 18th Century

Coming to the 1st use of wind power, history goes back to 500 B.C. People used wind power to propel the boats in Nile opposite to river current [1]. The first known specific windmill, Pneumatics, was

¹ Research Assistant (PhD), Dept. of Electrical & Electronic, Faculty of Engineering, University of Nottingham, 43500 UNMC, Jalan Broga, Semenyih, Selangor, Malaysia, Email: kcc1msa@nottingham.edu.my

² Associate Professor, Dept. of Electrical & Electronic, Faculty of Engineering, University of Nottingham, 43500 UNMC, Jalan Broga, Semenyih Selangor, Malaysia, Email: Rajprasad.Rajkumar@nottingham.edu.my

³ Senior Lecturer, School of Engineering, Taylor's University, Selangor, Malaysia, Taylor's, Selangor, Malaysia, Email: aravindcv@ieee.org

⁴ Assistant Professor, Dept. of Electrical & Electronic, Faculty of Engineering, University of Nottingham, 43500 UNMC, Jalan Broga, Semenyih Selangor, Malaysia, Email: YeeWan.Wong@nottingham.edu.my

⁵ Deputy General Manager (Geologist), Data Management Division, BAPEX (Bangladesh Petroleum Exploration & Production Company Limited), PetroBangla (Bangladesh Oil, Gas & Mineral Corporation), Ministry of Power, Energy and Mineral Resources, 4 Kawran Bazar C/A, Dhaka-1215, Bangladesh, Email: Selima.shahnaz_geologist@yahoo.com

⁶ Research Assistant (PhD), Dept. of Electrical & Electronic, Faculty of Engineering, University of Nottingham, 43500 UNMC, Jalan Broga, Semenyih, Selangor, Malaysia, Email: kcc2jys@nottingham.edu.my

illustrated in the 1st century BC by Hero of Alexandria [2]. The purpose of creating it was to grind the corn. Although a figure (Figure 1) of the invention can be found, the existence of it has not well been established.

Vertical axis windmills were found in China in 13th century where as it was found long back in Persia around 900 AD. Along with the sailing concept, idea of wind turbine got developed gradually with the need of pumping water for irrigation; for example the ancient irrigation system of the island of Crete. This windmill (Figure 2) was used to rotate around its vertical axis. Nowadays, such a configuration is known as Savonius rotor. [3-4].

In European countries, the windmills first started to appear in the 12th century [3]. Although the design was changed, the primary purpose was still the same—grinding corn and pumping water. The turbines were used to be mounted on a house facing along with the wind direction. Those windmills were horizontal in nature. Starting from the year of 1700, the windmills found in Europe were improvised and developed with twisting blades (Figure 3) whereas a different configuration was developed in the United States (Figure 4). It was a multi-bladed windmill mostly recognized as fan mills [5]. It was given a nickname as ‘Pumping Jack’ as it was used mainly for pumping water. Over 6 million fan mills were built in the US before the starting of 19th century. Before the industrial revolution, windmills were one of the major energy sources [7].



Figure 1: Pneumatic Windmill by Hero of Alexandria
(1st Century BC)



Figure 2: Persian VAWT (900AD)



Figure 3: Dutch Windmill



Figure 4: American Pumping Jack

2. FROM THE YEAR BETWEEN 1800 TO 1900

In need of pumping water, followed by electricity, modern wind power technology was first explored. From 1850 onwards, windmills were being developed in large areas with a view to pumping waters [3]. The early farm windmills were made by woods which were extinct gradually except in the museum [3]. Figure 5 gave us an idea of those ancient historical windmills. The turbine picture was taken in Texas at J.B. Buchanan's firm. In 1880s, in order to develop medium sized wind plant with a view to achieving pumping and electricity demand on dairy industries, a Royal Commission was set up in Denmark. Later a company namely "Lykkegaard Company" brought the one kind of wind machine in the market in commercial basis. Those machines came with four blades. Later on, in the beginning of 20th century, hundreds of machines were manufactured [7].

In the year of 1888, a windmill was built to produce electricity by a person named Brush. That was the 1st automatic wind turbine that used to produce electricity [8]. It was constructed with a wooden rotor having a diameter of 17cm which was connected to DC generator via a gear box (step up) having a ratio of 50:1. In a strong wind situation, it used to produce 12kW. The problems of it were the giant size and the low rotational speed which was inefficient. It was operated nearly for 20 years [8]. In that time another wind turbine was built around in 1891 though it was experimental. It was built by Poullaour in Denmark which was driving a dynamo [9]. He conducted vast research on this field in 1890 and he made the baseline configuration of today's modern Horizontal Axis Wind Turbine [10].

From the year 1900 onwards, all of the windmills had multi blade system having an average of 3-5 m in diameter [7]. The prime time of farm windmills was the year between 1930s and 1940s in which they reached its pick [7]. In that period of time, no more wood was used rather than metal with multi-bladed vanes [7]. Around 6 million farms were in operation on that time to pump water for residential use together with water for livestock. Different countries such as Australia, Africa, Canada, United States, and Argentina were making use of them [7]. But due to in demand of less expensive machine, those farms started to exploit replaced by modern design wind turbines. In the beginning of the 20th century, a new idea came up in different countries. It was called Wind Chargers (Figure 6) [11]. It was quite popular in United States. Because of the high expense of transmission line and the huge distance to cover from isolated location to generating plant, some companies started constructing stand-alone wind system having a rotor of propeller type consisting of maximum 3 blades. The generated electricity was stored in battery. Those batteries, called wet-cell, were made off with lead-acid and it used to require great maintenance care for longevity [8-11]. These machines differ a lot from the earlier windmills. Those windmills used to have multiple large number



Figure 5: Historical farm windmills at J. B. Buchanan farm. Location: Spearman Texas



Figure 6: Wind Charger (100 W, DC, with flap air brakes). Location: USDA-ARS wind test station, Bushland, Texas

of blades used to pump water of low volume. In capable of generating electricity because of slow rotational speed due to large number of blades, these wind chargers grew popularity but became outdated in 1940s and 1950s since electricity was made available in very cheap rate in United States from rural electric cooperatives [3]. Starting from this time, wind turbines were thought of being used in utility. Therefore different types of designs and structure were brought into the market.

Focusing on different points of angles on how to deal with the wind energy, several shapes of blades were innovated with two kinds of turbine: one is horizontal axis wind turbine (axis of the rotor is horizontal) and another is vertical axis wind turbine (axis of the rotor is vertical) [3]. Though the concepts and partial implementation of both of them were brought up before, combined studies with advantages and disadvantages had been started. In 1926, a horizontal axis wind turbine having four blades was constructed by Flettner. It provided 30KW of rated power with a wind speed of 10 m/s. Meanwhile a guy named Madras came up with an idea of mounting vertical rotating cylinders on railroad cars. He proposed the Magnus Effect to drive the cylinder travelling around a circular track. The generator on the other hand was planned to be constructed on the axels of the car. The proposal turned into a prototype in 1933 but due to the inconclusive result, the idea was abandoned [3]. In the year of 1927, G. Darrieus built a rotor. His machine blades were similar to jumping rope. In 1931, he proposed a design using lift to produce torque around a vertical axis [11]. Darrieus patented the design of his rotor and it was known as Troposkien.

Meanwhile, Savonius discovered a rotor of S-shaped in Finland. It was built with two half of a cylinder and the distance between them was smaller than the diameter. This basically became the starting point of VAWTs [10-11]. Both of the machines of Savonius and Darrieus were designed with straight vertical blades and those two are called the main two types of modern vertical axis wind turbine [3]. Between 1940 and 1950, the two major achievements were made in terms of wind power history. The first revolution was the design of 3 blades wind turbine structure and the second was to introduce AC generator replacing DC [8]. The other one took place after the occurrence of revolution in USSR (Union of Soviet Socialist Republics), in Crimea, successful construction of 100KW wind machine prototype had been taken place between 1935 and 1953. It played importance for developing industrialization and agriculture. It was inter-connected in parallel with a conventional station. For the next 15 years further research had been carried through and around 30 prototypes with successful series production were achieved with a rated power of 30KW [7]. Meanwhile in USA, from 1939 to 1945, design and operation had been being taken place and finally at Vermont, engineers came up with the largest machine available that time. It had a diameter of 53m and the rated power was 1250KW. It gave a moderate performance for a brief period of time in a routing generation station [7]. The research and scope did not go further because of the World War II.

3. BETWEEN 1950 TO 1999

After the 2nd world war, the main research and analysis was focused in Europe. According to the DIWA which is Danish Wind Industry Association, the first modern wind turbine was built by engineer Johannes Juul in Denmark in 1956. It came with electromechanical yawing system. It was a three blades upwind turbine that used to have an asynchronous generator[3]. It had a rated power of 200KW and was called as "Gedser Wind Turbine" [6]. Built with a concept of horizontal axis, it was connected to a there phase AC power grid. Looking at the case history in United Kingdom, a national wind power committee was brought up in 1948 and continued till 1958. The committee worked with "Electrical Research Association" of United Kingdom. The main supervisor of the project was Lake E.W. A vast research regarding sites, building prototypes and wind survey had been carried through. One prototype had been installed at CostaHill by the supervision of John Brown Company in 1955 having a diameter of 15m and having a rated power of 100KW with a wind speed of 16m/s. It was connected with a power grid which mainly ran in diesel. It was established in a remote side of Northern having high wind that blocked the development of mechanical features of it and ended up failing to be proven as reliable and ended up failing to be proven as reliable. The



Figure 7 (a): Darrieus concept



Figure 7 (b): FloWind turbine AT Tehachapi Pass

other one was located at St. Albans built by Enfield which was a low speed site. It was designed by Frenchman Adreau. It had a rated power of 100KW with a wind speed of 13m/s. The hollow blades and the rotation (while the blades were rotating, the air flowed through air turbine) made the turbine unique in nature [3]. Under British Electricity Authority (BEA), it failed to get permission for further innovation and was sent to Algeria where it was implemented successfully by a local company. However the system turned out to be inefficient and did not go further [7].

In this period of time, in 1970s, there was a great concern regarding the decrease of fossil fuel and limited resources which led to many researchers and surveys. The crisis of oil in the year between 1973 and 1979 also was added into the flow. As a result several wind power technologies were invented and the power capacity increased to 100KW and furthermore from 1980s, turbines with MW power was started to be designed [8]. It was also the time when European Countries first had the idea to put wind turbine into the sea [6]. In that period of time, around in 1980, Danish industry came up with "Riisager Wind Turbine". Having almost the same concept as the Gester Wind Turbine, this one was built by used car parts which were very cheap and reasonable in price. It became very popular in numerous private households [12].

Coming back to VAWT again, in 1980s, Sandia National Laboratory (SNL) started a vast research with a 17 m high Darrieus's turbine [13]. FloWind purchased the design and implemented numerous amount of it in the United States (Figure 7) and became the most successful VAWT manufacturer [2] [14]. Next, Dr. Peter Musgrove proposed H-type VAWT with straight blades which was known as H-type rotor. Mc Donnell took his concept and built a 40 kW H-rotor (Figure 8.1) [14]. Since, Darrieus patented his design, MC Donnell had to change the shape of the rotor and therefore he took the H-type motor concept to build a different shape of VAWT.

Fascinatingly in this period of time, VAWT concept began to spread in Europe. In Denmark, Riso invented their own H-rotor having a capacity of 15KW (Figure 8.2) [14]. In Canada, Eole had a 3.5 MW VAWT operated from 1987 to 1993. They had to shut it down as it was too costly in terms of bearings and maintenance [15]. Eole's was the biggest VAWT built in that period of time and also the last VAWT milestone of the early generation. After that, the research and study of VAWT stopped for a while but the development of HAWTs continued.

From the beginning of 1990s, wind energy has gained acknowledgement of one of the vital renewable sources. In the year of 1993, asynchronous generator in wind turbines was being started slowly changing to synchronous generator [16]. In the mid of 1990s, wind turbine was being started to build in offshore because of the strong wind in the high sea [17]. Although the technical difficulty and installation cost are higher in offshore, other conditions and cases stay in the favour of it comparing to onshore wind power energy.

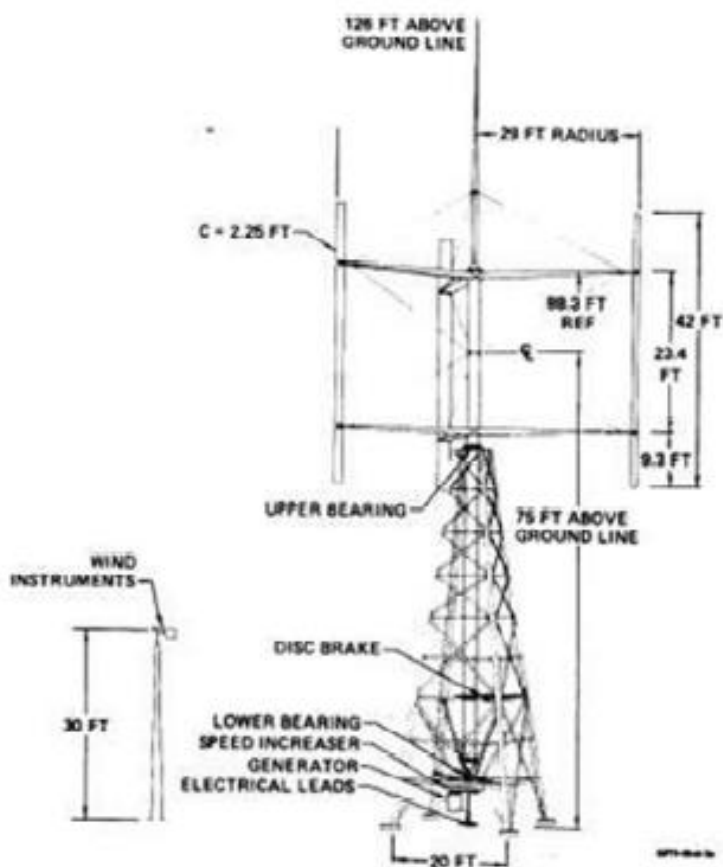


Figure 8 (a): MC Donell's 40KW Design

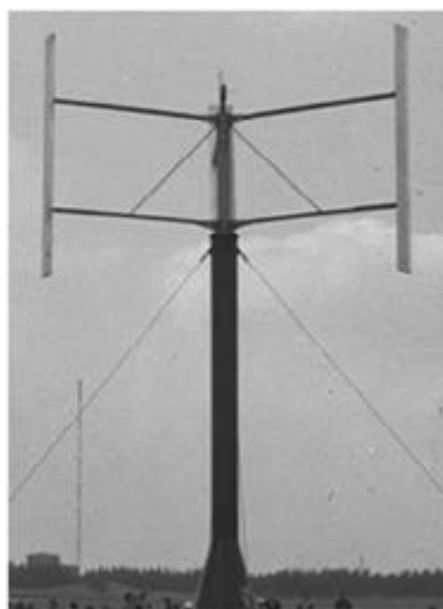


Figure 8 (b): Riso's 15KW Design

Firstly, wind speed is almost 25% greater than of onshore. Secondly, frame of tower is lower comparing to onshore; therefore it can face greater speed. Moreover the roughness is also less in sea level [6].

Although some European countries tried to develop a thought of spreading wind energy at sea level at 1970s, not much of progression took place that time except for couple of prototypes being tested [6]. The first country to build offshore wind turbine successfully in the middle of the sea was Denmark in the year of 1991. From 1991 to 1997, Denmark, Netherland and Sweden performed couple of prototype based wind turbine operations in deep sea [6]. Requiring less land area, less noise pollution, no greenhouse gas emission with an addition of great environmental protection, the offshore wind energy were getting popular among the European countries. By the end of 20th century, around 50 countries were running wind turbines generating approximately 17500 MW of electricity. More than 70% of this electricity was generated by the European countries. In 1999, Germany, Spain and Denmark being the leading countries produced an overall power of 7675MW which was almost 80% of the entire production of wind energy in Europe [18].

4. CONCLUSION: 21STCENTURY AND PRESENT SITUATION

Although there are a lot of activities going on towards the offshore wind energy, the development process was still very slow. But from the beginning of 21st century, the offshore deep blue wind technology has gained new inspiration. From the starting of 21st century, within 6 years of time, 21 offshore plants had been built in different countries namely Denmark, Sweden, Ireland, Germany and Netherlands [19]. By the end of 2006, installed capacity of offshore project in the entire world reached 798.2 MW [19]. Around time there were couple of famous projects which have to be mentioned-East China Bridge in Shanghai generating electricity of around 100MW, Shanghai FengxianNanhui Offshore Wind Power and Cixi Wind Power at sea in Zhejiang. European countries, America and other countries such as China also have been progressing firmly. China had constructed 59 wind farms by 2005 including 1883 turbine generator. They produced 1266 MW of Power in 2005 making sure to be one of the top 10 global wind energy producers [20]. The Northern side of the world has good wind energy but still development of wind power has not yet been observed that much due to couple of major problems until 2011. Among them, icing on the turbine blade is the main obstacle. In average 20% power loss occurred annually due to this problem. To overcome it, not much of steps were taken. In 2011, Muhammad S. Virk, Matthew C. Homola, Per J. Nicklasson from Narvik University College carried out a numerical study on a horizontal axis wind turbine (5MW) about the atmospheric ice accretion. The result was achieved using Computational Fluid Dynamics. For both of the conditions of rime and glaze ice, five different sections in the blades were taken into consideration for numerical analysis. Moreover, several atmospheric temperatures were used to simulate the rate and shape of accreted ice. The result indicated that both the blade size and relative section velocity of the blade affected ice growth. Near the root section, the icing was less. In the blade section, from centre to top, significant change in icing was noticed with the variation in atmospheric temperature. Furthermore, the result also proved that the icing could be managed by optimizing the geometric design parameters [21]. In recent years, Micro-Wind Energy has made a lot of impact due to its low speed operation along with low power applications resulting cost reduction and simplicity. For example, Massimiliano, Marcello and Giampaolo from Italy designed a simple, effective and low cost Micro-Wind Energy Conversion System in 2011 that gathered several attentions. It used a Permanent Magnet Synchronous Generator, boost converted, and Voltage Oriented Controller were used. The system performed a reliable operation at the maximum power. It also showed a promising quick response with variable wind speeds. It had low losses and almost zero reactive power exchanged with the power grid.

In comparison with a conventional wind turbine of same maximum power range and with the same average wind speed, it could generate twice the energy produced by the generator [22]. With view of the facts stated above, it could easily be predicted that the renewable energy like wind power is taking over the fossil fuel gradually and we are looking towards the world where green energy dominate on large scale.

This paper provided the history of wind power in brief starting from the ancient timethat ends with modern era. At present, numerous projects on wind turbine are being implemented each day. This paper would certainly be a great source of information for those projects for further development.

REFERENCE

- [1] S.M. Muyeen, Junji Tamura, T. Murata, Stability Augmentation of a Grid-connected Wind Farm, Springer-Verlag London Limited, 2009.
- [2] A.L. Rogers J.F. Manwell, J.G. McGowan. Wind Energy Explained—Theory, Design and Application. John Wiley and Sons Ltd., second edition, 2009.
- [3] V. Nelson, Wind Energy Renewable Energy and the Environment, Taylor and Francis Group, LLC, United States of America, 2009.
- [4] D. Zafirakis John K. Kalassis. The wind energy revolution: A short review of a long history. *Renewable Energy*, 36: 1887–1901, 2011.
- [5] Nick Jenkins Tony Burton, David Sharpe. Wind Energy-Handbook. John Wiley and Sons Ltd., first edition, 2001.
- [6] L. Wang, J. Wei, X.W.X. Zhang, "The development and Prospect of Offshore Wind Power Technology in the World"
- [7] D.F. Warne and P.G. Calnan, "Generation of Electricity from the Wind", *IEEE Reviews*, Vol. 124, No. 11r, November 2007, pp. 963-985.
- [8] C. Wang, L. Wang, L. Shi and Y. Ni, "A survey on Wind Power Technologies in Power System," *IEEE Conference*, 2007.
- [9] Jin-song Kang, Zhiwen Zhang and Yongqiang, "Development and Trend of Wind Power in China," in Canada Electrical Power Conference, 2007, pp. 330-335
- [10] Nick Jenkins Tony Burton, David Sharpe. Wind Energy-Handbook. John Wiley and Sons Ltd., first edition, 2001.
- [11] G.J.M. Darrieus. Turbine having its rotating shaft transverse to the flow of the current, 1931.
- [12] L.H. Hansen, F. Blaabjerg, H.C. Christensen, U. Lindhard and K. Eskildsen, "Generators and Power Electronic Technology for Wind Turbine" The 27th Annual Conference of the IEEE Industrial Electronic Society, 2001, pp. 2000-2005
- [13] James H. Strickland. The darrieus turbine: A performance prediction model using multiple steam tube model. Technical report, Sandia National Laboratories, 1975.
- [14] Paul Gipe. Photos of vertical axis wind turbines by paulgipe. Website (31st January 2014), 2014. URL <http://www.windworks.org/cms/index.php?id=219>.
- [15] Thomas D. Ashwill Herbert J. Sutherland, Dale E. Berg. A retrospective of vawt technology. Technical report, Sandia National Laboratories, 2012.
- [16] L.H. Hansen, F. Blaabjerg, H.C. Christensen, U. Lindhard and K. Eskildsen, "Generators and Power Electronic Technology for Wind Turbine" The 27th Annual Conference of the IEEE Industrial Electronic Society, 2001, pp. 2000-2005
- [17] I. Erlich and F. Shewarega, "Interaction of Large Wind Power Generation Plants with the Power System," First International Power and Energy Conference PECon, Putrajaya, Malaysia, November 28-29, 2006, pp. 12-18.
- [18] Nikos Hatziyargyriou and ArthurosZervos, "Wind Power Development in Europe," *IEEE*, Vol. 89, No. 12, December 2001 pp. 1765
- [19] Zaharin, S. K. Nadjid, A. M. Razali and K. Sopian "Wind Speed Analysis in the East Coast of Malaysia," *European Journal of Scientific Research*, Vol. 32, No. 2, 2009, pp. 208-215.
- [20] Jin-song Kang, Zhiwen Zhang and Yongqiang, "Development and Trend of Wind Power in China," in Canada Electrical Power Conference, 2007, pp. 330-335
- [21] M. S. Virk, Mathew C. Homola, Per J. Nicklasson, "Atmospheric icing on large wind turbine blades," *International Journal of Energy and Environment*, Vol. 3, Issue 1, 2012, pp. 1-8.
- [22] Li Yan, Chi Yuan, Han Yongjun, Li Shengmao and Tagawa Kotaro, "Numerical simulation of icing on static flow field around blade airfoil for vertical axis wind turbine," *International Journal of Agric. & Biol. Eng.* Vol. 4, No. 3, September 2011, pp. 41-47.

Feasibility Study of a Novel 6V Supercapacitor based Energy Harvesting Circuit Integrated with Vertical Axis Wind Turbine for Low Wind Areas

MD Shahrukh Adnan Khan*, R. K. Rajkumar**, CV Aravind***, Y. W. Wong***

* Department of Electrical & Electronic Engineering, Faculty of Engineering, University of Nottingham Malaysia Campus, Jalan Broga, Semenyih, Selangor-43500

** Department of Electrical & Electronic Engineering, Faculty of Engineering, University of Nottingham Malaysia Campus, Jalan Broga, Semenyih, Selangor-43500

*** Department of Electrical & Electronic Engineering, Faculty of Engineering, University of Nottingham Malaysia Campus, Jalan Broga, Semenyih, Selangor-43500

**** School of Engineering, Taylor's University, Selangor, Malaysia

(kecxlmsa@nottingham.edu.my, Rajprasad.Rajkumar@nottingham.edu.my, aravindcv@ieee.org, YewWan.Wong@nottingham.edu.my)

[†] Corresponding Author; MD Shahrukh Adnan Khan, University of Nottingham Malaysia Campus, Jalan Broga, Semenyih, Selangor-43500, Tel: +60107779012, Fax: +60389248017, kecxlmsa@nottingham.edu.my

Received: 16.05.2016 Accepted: 23.07.2016

Abstract- This paper provides a platform for a novel innovative approach towards an off-grid Supercapacitor based battery charging and hybrid energy harvesting system for low wind speed Vertical Axis Wind Turbine (VAWT). A 3-Phase Permanent Magnet Synchronous Generator (PMSG) was chosen for its low maintenance cost, light weight and less complicated design. Simulation studies was carried out to obtain an optimized design and a 200W 12V 16 Pole PMSG attached to a VAWT of 14.5m radius and 60cm of height was sent for fabrication with Maglev implementation (Magnetic Levitation). Upon arrival, the optimized system is implemented into the energy harvesting circuit and field testing is carried to observe the performance. Under wind speed range of 3-5m/s, the energy harvesting circuit showed better efficiency in charging battery in all aspects comparing to direct charging of battery regardless of with or without converter. Based on analysis and results carried out in this paper, all feasibility studies and information were successfully provided for future work.

Keywords: Energy Harvesting; Supercapacitor; Battery Charging; Low Wind; Vertical Axis Wind Turbine.

1. Introduction

A burning concern of the 21st century is that conventional energy sources are depleting. Thus, it has become a necessity to find alternative power generating sources. Having considered the speedy development of electronic devices, the need for power has never been greater. Each day, people spend more time on electronics but are often found to be in difficult situations with limited battery charge. Wind power can be an alternate renewable energy source to this problem. Wind energy research in Malaysia is still in the early stage and

not many researches have been conducted on off-grid wind energy harvesting device for low wind speed [1] [2]. Although crude oil and natural gas are the leading energy sources in Malaysia, studies estimate that fossil fuels will only be supplying energy to mankind till 2088 [1][3]. As a main part of renewable energy, wind power is emerging as a strong alternative source to fossil fuels [4]. By utilizing the wind energy, countries like Malaysia demand to have a standalone system to charge up their small scale electronic devices in a greener way.

The average wind speed of Malaysia is less than 5m/s and more commonly in the range of 2-3m/s, which is not favorable to Horizontal Axis Turbine [5-6]. Therefore, Vertical Axis Wind Turbine (VAWT), capable of working at multidirectional low wind speed [6], could be used. In addition, use of powerful neodymium magnets instead of DC field, light weight and smaller size make the Permanent Magnet Synchronous Generator (PMSG) a good match for VAWT [7]. Implementing wind power and connecting it to grid system is not possible for most of the rural areas in Malaysia. Therefore, these places require an off-grid energy harvesting turbine being able to work in low wind. But there has been a lack of research in the field of small scale low voltage wind turbine when it comes to low wind off-grid standalone system. Previous work in the field of 'PMSG adopted Maglev VAWT' and 'energy harvesting' was mostly carried out on separate field. For example, in 2008, Lei created a power electronic interface for a Battery Supercapacitor Hybrid Energy Storage System which was of MW power range and meant for grid connection [8]. Tankari and Camara, in 2011, integrated ultracapacitor and batteries with wind-PV hybrid system but the PMSG used was of 4.5KW [9]. Abbey and Joos proposed Supercapacitor Energy Storage for Wind Energy Applications. Again they used a 1MW doubly fed induction generator for simulation and the system was built for grid connection [10]. Similar work was also done by L. QU and W. Qiao [11].

This paper fills up the gap in research providing an off-grid standalone energy harvesting circuit (EHC) incorporated with 3-Phase PMSG adopted to Maglev VAWT that can perform in low wind speeds. This research works with an off-grid VAWT which makes the system easier to implement in rural places and areas where grid system has not yet been available. Having compared with previous models, in which Tankari used a 4.5KW PMSG [9], Abbey as well as L. QU used a 1MW induction generator [10-11]; this VAWT adopts a 200W small scale PMSG making it as a portable standalone system. Also areas with low wind does not require a system that includes a generator of Mega Watt range. Coming back to the energy harvesting circuit, this investigation discovers a

novel hybrid circuit with a combination of a battery and supercapacitor bank. Hybrid energy harvesting technology is not new. In 2010, Worthington proposed a novel circuit that combines the Synchronous Switched Harvesting technique which was connected to a load capacitor directly to harvest energy [12]. This allowed the capacitor to act as a reservoir that would be disconnected when fully charged and then would discharge to a load. The circuit was connected with a charge pump tire circuit [12]. Experiment results showed that this idea was capable of harvesting three times more amount of energy compared to the usual bridge rectifier circuit. However, this idea has not yet been implemented into off-grid wind energy sector. Although Lee [8] implemented a hybrid energy harvesting storage in 2008 for wind power application, it was meant for grid connection and again was of high power range. Hence, it was impossible for the energy storage system to be implemented for off-grid system. Our study brings the supercapacitor based hybrid energy harvesting for first time into the off-grid low wind power application. A supercapacitor bank is used in our experiment that charges up from the turbine and discharges through the battery with the use of power electronics. As far as low wind speed is concerned, a 6V battery is used for energy harvesting. A full phase complete system analysis was made, starting from optimization of the design, followed by design fabrication, field testing and lastly efficiency analysis.

2. Methodology

At first, simulation was carried out for small scale low speed VAWT with the adaptation of 3-Phase PMSG into the system. The optimized system design configuration, supported by the Matlab Simulink modelling, was then sent for fabrication. In the meantime, Energy Harvesting Circuit (EHC) was configured and upon arrival of the turbine, EHC was implemented into VAWT. The control strategies were made by the use of power MOSFET switching and system was brought into the field for testing. While the system was operational, data were collected from the Labview interface through DAQ and result was analyzed to find out the efficiency of the system. Figure 2.1 shows the data process flow of the system.

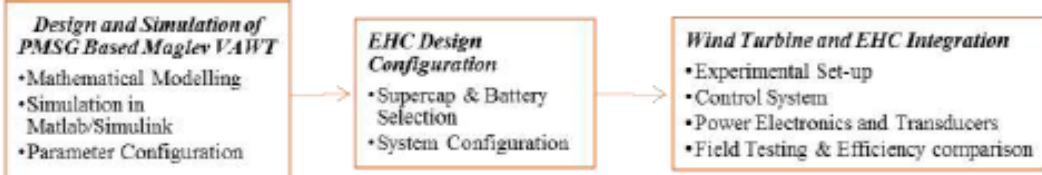
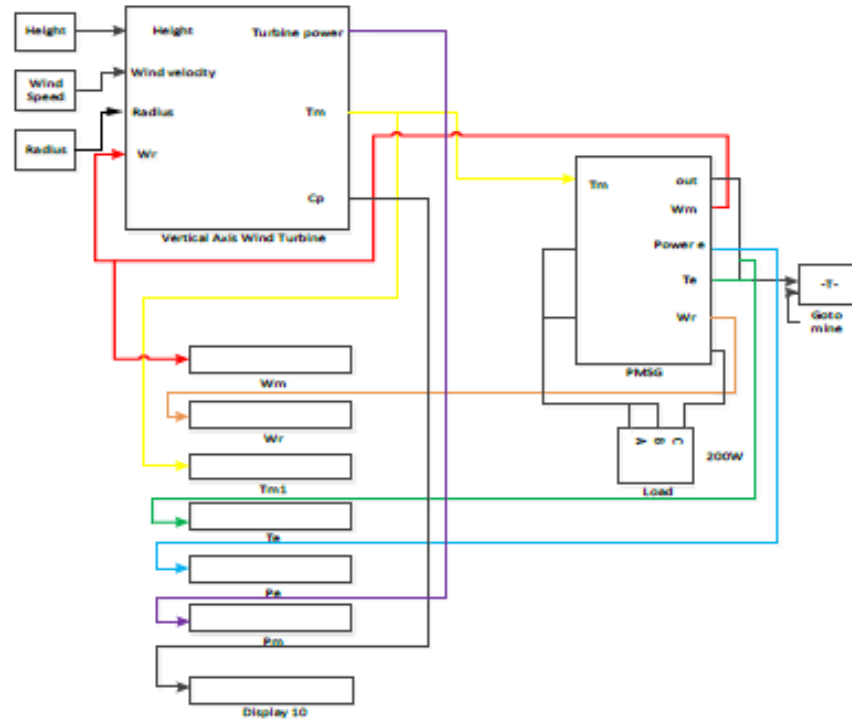
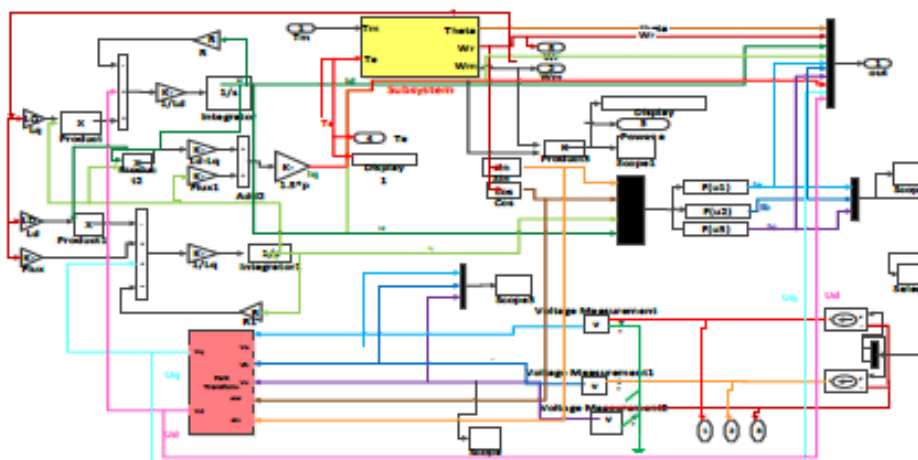


Fig. 2.1: Data Process Flow of the System



(a)



(b)

Fig. 3.1: (a) Simulink Modelling of PMSG adopted VAWT, (b) Simulink Modelling of PMSG subsystem

3. Design and Simulation of PMSG based Maglev VAWT

3.1. Modelling

The mathematical equations of VAWT was given as follows [13-16].

$$P_m = Cp \frac{1}{2} \rho A V_w^3 \quad (3.1), \quad \lambda = \frac{\omega_m^2}{V_w} Cp \quad (3.2),$$

$$T_m = \frac{P_m}{\omega_m} \quad (3.3), \quad A = 2RH \quad (3.4)$$

Introducing the equation parameter where A indicates the rotor cover area of VAWT in (m^2), ρ is the air density in (Kg/m^3), V_w is the wind speed in (m/s), Cp stands for Power Coefficient of VAWT, λ is the tip-speed ratio, ω_m is the rotor angular speed in ($rads^{-1}$), R is the radius of VAWT in (m) and H is the height of VAWT in (m). Tip speed ratio, λ , is the ratio of the rotor speed of the turbine to the wind stream velocity. The basic design parameters of the turbine were the radius, height and wind speed. The maximum value of Cp (0.48) is achieved for Pitch Angle, $\beta = 0$ degree, therefore the blade pitch angle was set to 0 [6]. The modelling of the 3-Phase PMSG was done with dq equivalent circuit reference frame. Voltage, current and electromagnetic torque for a PMSG in the d-q axis frame had then been expressed as following (equation 3.5-3.8) [17-19]:

$$V_q = -(r + pL_q)i_q - w_e L_d i_d + w_e \lambda_n, \quad (3.5)$$

$$V_d = -(r + pL_d)i_d - w_e L_q i_q$$

$$L_d = L_{dd} + L_{bb}, \quad L_q = L_{qf} + L_b \quad (3.6)$$

$$\frac{di_d}{dt} = \frac{-R_i_d + w_e L_d i_q + U_d}{L_d}, \quad (3.7)$$

$$\frac{di_q}{dt} = \frac{-R_i_q + w_e L_d i_d + w_e + U_d}{L_q} + \lambda_0 \quad (3.8)$$

$$w_e = p\omega_m \quad (3.9)$$

Here, L_d , L_q and L_{dd} , L_{bb} are the inductances and leakage inductances of d and q axis respectively; i_d , i_q and U_d , U_q are the stator currents and voltages; R_s is the stator resistance in ohms (Ω); λ_0 is the magnetic flux in Weber (Wb); W_e is the electrical rotating speed (rad/s); p is the number of poles and T_e indicates the electromagnetic torque. Having implemented the equations in the Matlab/Simulink, the Fig. 3.1 and 3.2 represent the block diagram of Simulink modelling. The stator resistance of the PMSG was taken as 15 Ω ; the inductance as 0.8mH; the flux linkage of magnet was 0.175 Wb and mass inertia was considered to be 0.089 kg/m². Research had been made on previous works conducted in this field and for the

sake of simulation these values were taken as a standard basis [6] [14] [17].

3.2. Simulation Analysis

Figure 3.3 and 3.4 display the mechanical torque generated for different height and radius respectively under various wind speeds. While running the simulation for turbine torque under different heights, radius was fixed at 0.2m. In such way, the swept area will vary with only the change of the turbine height. As it can be seen, the low torque generated in the low wind (2m/s-5m/s) was improved with the gradual increase of the height from 0.4m onwards. Similarly, from figure 3.4, it can be spotted the low torque generated in the low wind (2m/s-5m/s) was getting better with the increase of the radius from 0.2m onwards. Therefore, for an optimized design, turbine height was fixed at 60cm whereas the radius was set as 15cm.

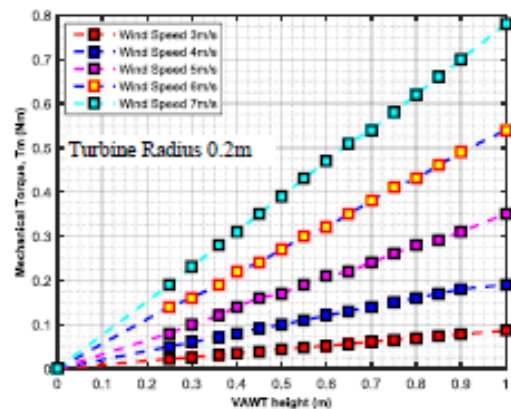


Fig. 3.3: Mechanical Torque generated for different heights under different wind speeds

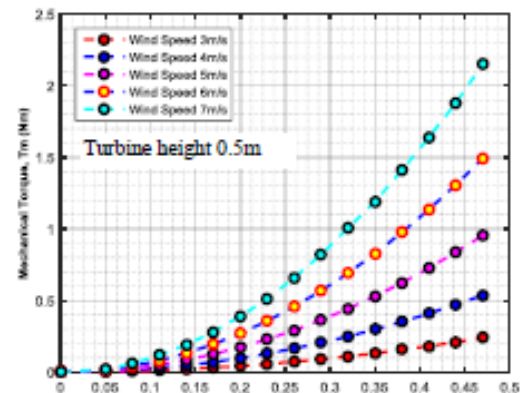


Fig. 3.4: Mechanical Torque generated for different heights under different wind speeds

Figure 3.5 illustrates the effect of turbine torque on generator output power on various pole pairs. Here, the generator power jumped from 548W to 3.6KW with changing pole pair (8 to 18). At low torque range such as at 5Nm, generator power increased from 6.6W to 24W for the same change in Pole Pair. Thus, number of pole plays a vital role in generator performance regardless wind speed. Result shows for low torque, the rated power from the generator could maximum be 500W. Therefore, a rated power of 200W was fixed as the generator output. The pole pair was decided to be 8 for a realistic system. Coming to the friction factor, it basically represents the friction in the bearing while being rotated with relative to the shaft. Since Maglev reduces the friction to in the bearing by levitating the system with the repulsive force of the magnets, a minimal of friction factor hence may represent the Maglev implementation in the system.

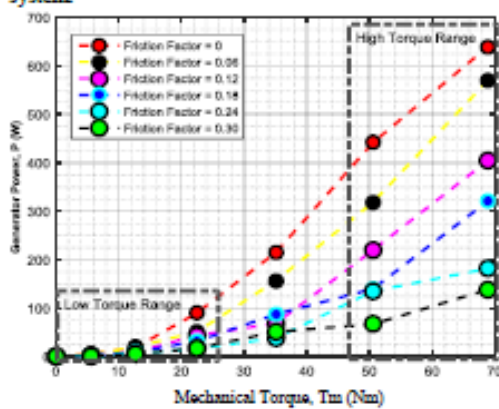


Fig. 3.5: Generator Power vs Mechanical Torque for different Friction Factor

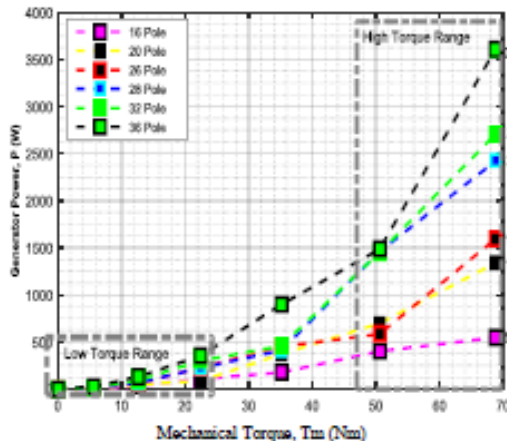


Fig. 3.6: Generator Power vs Mechanical Torque under Various Pole Number

Figure 3.6 demonstrates that a 0.3 reduction in the friction factor increases the output power from 1.32W to 5.45W at a mechanical torque of 5Nm. As Maglev makes noteworthy improvement in efficiency, it was decided to be implemented in the system.

After analyzing the results from simulation, a 200W 12V 16 Pole PMSG adopted to a VAWT of 14.5m radius and 60cm of height was sent for fabrication with Maglev.

4. EHC Design Configuration

At this stage, Battery and Supercap were combined to create a hybrid system. Voltage coming from PMSG is not constant, wind dependent and may fluctuate. Therefore a combination of Supercapacitor and battery is needed to be employed as battery needs a constant charging voltage.

Upon arrival, the turbine was tested and PMSG open circuit voltage ranged from 3.5V to 8V for low wind speed configuration. It was decided to use a 6V (3.2AH/20HR) lead-acid battery for charging. Considering all the facts, lead-acid battery remained as the best choice [20]. A Supercapacitor bank were to be placed before the battery which would be charged up by the turbine and subsequently would be discharged through the battery. To form a Supercapacitor bank, four Supercapacitors of 35F each with voltage rating of 2.7 V, were placed in a series connection. Thus a 10.8V Supercapacitor bank with 8.75F was assembled.

5. Wind Turbine and EHC Integration

Figure 5.1 shows the architecture of the overall system.

5.1. Control Strategy

In this system, two N-channel MOSFETs namely, P36NF06L, with the aid of Arduino UNO microprocessor, were used to create the switching. Even though MOSFET 3 does not have any role in the control system, it was put in the circuit if battery needed to discharge to the load manually. Figure 5.2 shows the flowchart of the control architecture of the system. Until the battery was charged up to its desired voltage, the charging and discharging process would be continued. Here, current and voltage transducer were used to measure the Supercapacitor and battery rating. A rotary encoder was used for turbine rotational speed whereas anemometer for wind speed. All the signals were passed through the DAQ to the Labview interface.

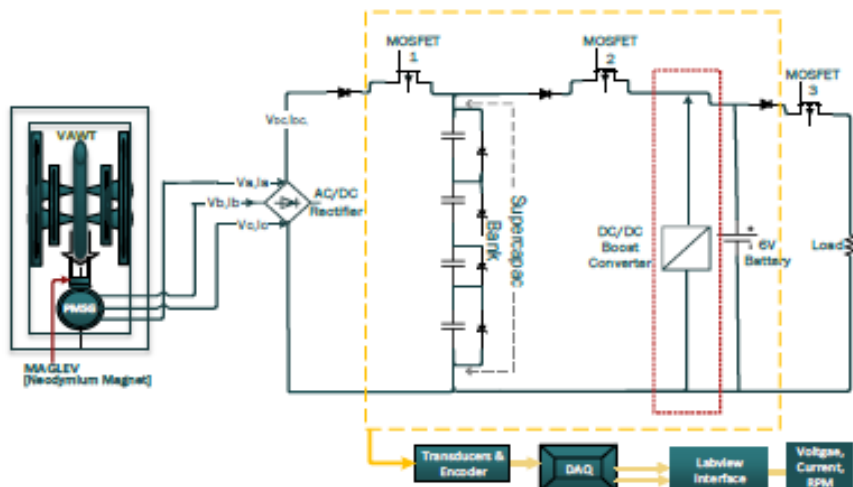


Fig. 5.1: Schematic Diagram of System Architecture of Energy Harvesting system

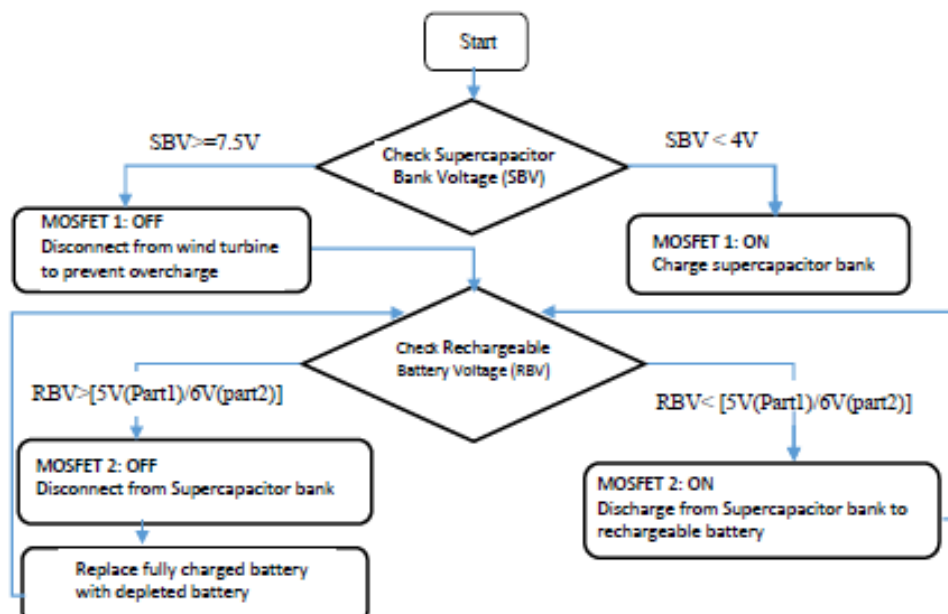


Fig. 5.2: Flow Chart of Energy Harvesting Control Architecture

5.2. Experimental Set-up

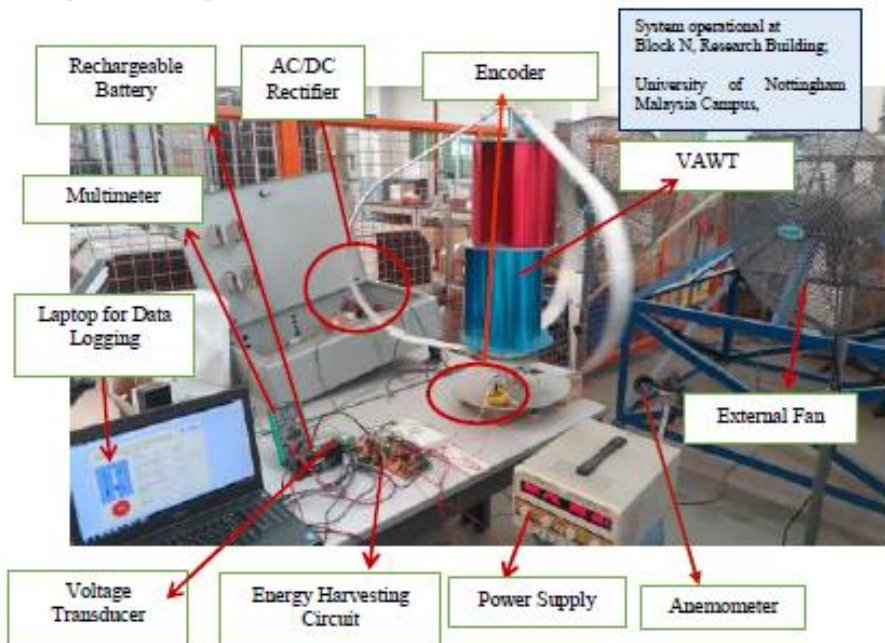


Fig. 5.3: Experimental Setup for the Integrated System

Figure 5.3 and 5.4 illustrate the experimental set-up and the EHC of the integrated system respectively.



Fig. 5.4: Energy Harvesting Circuit Built on Stripboard

5.3. Experimental Result

For better understanding, results have been divided into two parts. First part includes 3 cases of battery charging performance in which battery was charged up to 5V from 4.2V. 1st case shows battery charging by EHC, 2nd case describes battery charging with converter whereas last one shows direct battery charging without converter. Second part of this section deals with the complete charging analysis which is given in the later part of the result.

5.3.1. Battery Charging From 4.2V to 5V

For wind Speed = 5m/s

In the 1st case, battery was charged through Supercapacitor. Supercap, being charged by the generator, discharged to battery. One entire charging and discharging

process was considered as one cycle. For a wind speed of 5 m/s, 18 cycle was needed to charge the battery from 4.2V to 5V. Each cycle was for 27 minutes in which charging of Supercap took 25 minutes on average whereas discharging took 2 minutes. 18 cycles, therefore, indicate 7.5 hours of total charging process of the battery. Figure 5.5 (A) indicates the Supercap readings while charging and discharging whereas Fig. 5.5 (B) provides the EHC efficiency comparison.

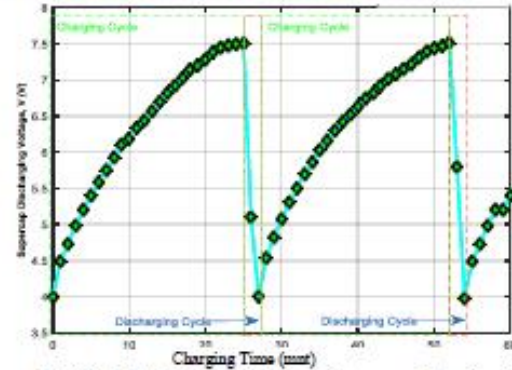


Fig. 5.5 [A]: For wind speed 5m/s- Supercap Charging & Discharging Complete Cycle

Without the use of Supercap, turbine was fed to charge the battery through the converter which was Case B. According to fig. 5.5 [B], it took almost 17.5 hours to reach its maximum value of 4.8V. After that the increase of the voltage was so less with respect to time, the value was not taken in consideration. Case C connects the turbine directly with the battery. This approach took less time (10 hours) than case B (direct charging via converter). However, the generator output voltage fluctuates and battery needs a steady constant voltage for charging up. Therefore this method is not recommended and applying this method for a longer period will result damaging of the battery. Still results were gathered for the sake of comparison and data was graphically displayed.

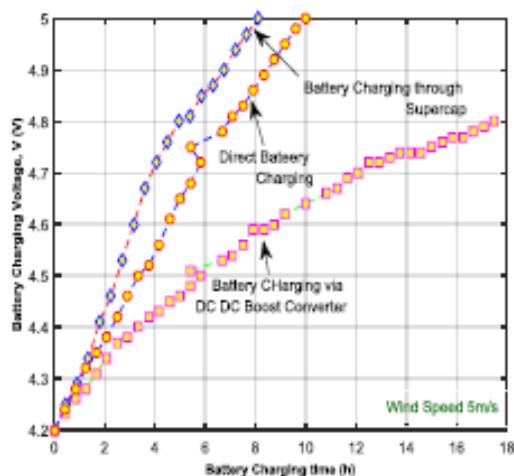


Fig. 5.5 [B]: For wind speed 5m/s- EHC Efficiency

Comparing all the 3 cases in 5m/s wind speed, 'Case C' was taken as a reference point. It was found out that charging through Supercap was 21% more efficient than direct charging without converter. Charging through converter was not successful as it failed to go beyond 4.8V. Therefore Case 2, technically, was considered as incompetent to work in 5m/s wind speed.

For wind Speed = 4m/s

At this stage, in Case A, one cycle was consisted of 37 minutes. Hence, it took 10.4 hours of charging time for 18 cycles (Fig. 5.6[A]). According to Fig. 5.6[B], Case B was incapable to charge the device at 4m/s. 'Case C' took 15 hours to finish the task. It was found out charging through Supercap was 31% more efficient than direct charging without the boost converter.

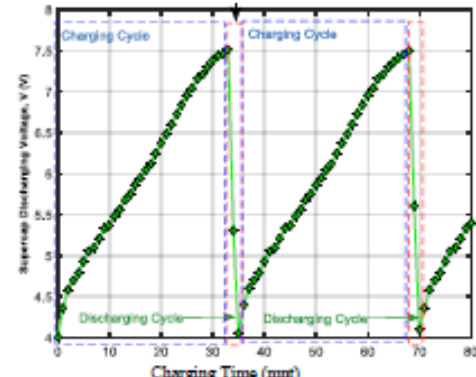


Figure 5.6 [A]: For wind speed 4m/s- Supercap Charging & Discharging Complete Cycle

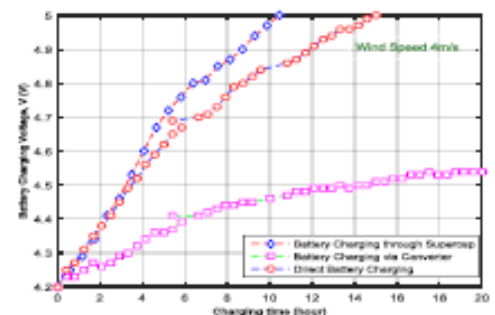


Fig. 5.6 [B]: For wind speed 4m/s- EHC Efficiency

For wind Speed = 3m/s

Unlike the previous experiments, Supercapacitor bank could not be charged up to 7.5V. This was due to the lack of the mechanical torque, as the system was put in a very low speed of 3m/s. In order to come up with a solution, Supercapacitor Bank charging voltage limit was reconfigured and lowered down to 6.8V. It took 95 minutes to finish the charging cycle. Also it ended up taking higher number of cycle (24 cycles) to finish charging.

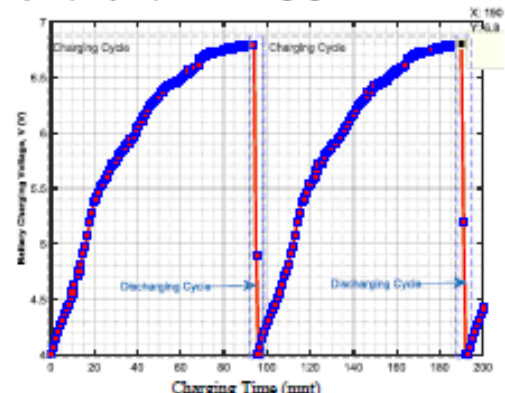


Fig. 5.7 [A]: For wind speed 3m/s- Supercap Charging & Discharging Complete Cycle

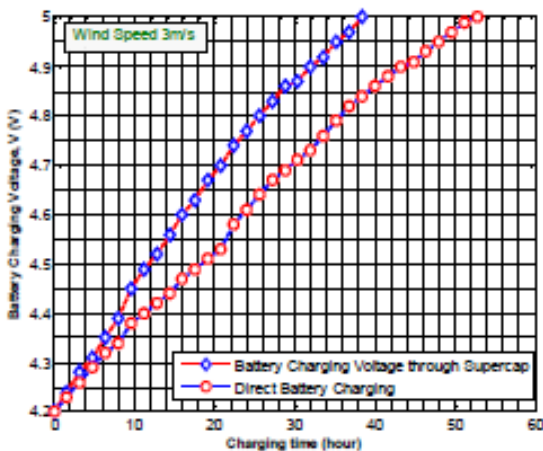


Fig. 5.7 [B]: For wind speed 4m/s- EHC Efficiency

Figure 5.7[A] displays the complete cycle of Supercapacitor bank and the charging and discharging period of it. For a number of 24 cycles, in which each cycle was made of 95 minutes, a total duration of 38.4 hours was required to complete the entire battery charging process. It is important to note that 'Case B' was not experimented in this section because of its poor performance in the earlier stage. For case C, it took nearly 53 hours to charge the battery up to 5V which surely was considerably longer than the previous charging. It was calculated and concluded that charging through Supercapacitor was 28% more efficient than direct charging without converter (Fig. 5.7 [B]).

Overall Summary and Efficiency comparison

The Energy harvesting circuit (EHC) shows excellent values for each of the different wind speed case with good performance overall. Change in the wind speed from 5m/s to 4m/s produces better efficiency as it goes to 31% from 19%. For a low speed of 3 m/s, EHC, even though took a long time of 38.4 hours to charge up the battery, still maintains its productivity by producing an efficiency 28%. Table 5.1 shows the summary of the result in this section.

Table 5.1. Summary of efficiency comparison for battery charging from 4.2V to 5V

Wind Speed (m/s)	Battery Charging via Supercap (hr)	Direct Battery Charging Time (hr)	Efficiency (%)
5	8.1	10	19
4	10.4	15	31
3	38.4	53	28

5.3.2. Battery Charging- 5.5V to 6V

After charging the battery from 4.2V to 5V, another experiment was conducted to charge battery from 5V to 6V at 5m/s. Figure 5.8 shows that with EHC, battery took almost 18.8 hours to finish charging whereas direct charging needed 24.2 hours. Hence, EHC was 22% more efficient than direct charging.

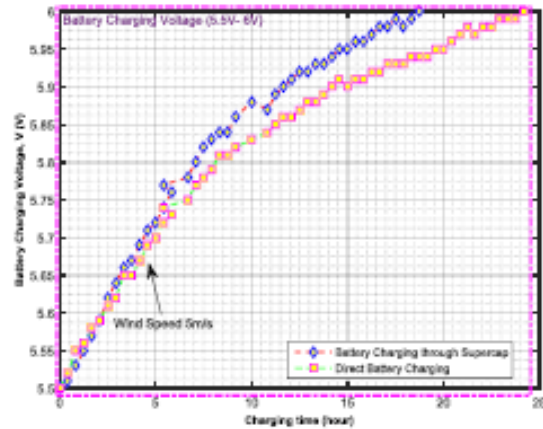


Fig. 5.8: Battery Charging Voltage [5.5V to 6V] comparison with respect to time

6. Conclusion

To conclude, this paper provides a platform for a novel innovative approach towards an off-grid energy harvesting system for Maglev VAWT. A complete simulation analysis was done for 3-Phase PMSG adopted to VAWT. With the variation of design parameters under low wind speeds, an optimized system of a 200W 12V 16 Pole PMSG attached to Maglev VAWT of 14.5m radius and 60cm of height was fabricated. Upon arrival, the optimized system was integrated with a 6V EHC. A 10.8V Supercapacitor bank with 8.75F capacitance was used in the ECH. While operational, EHC showed better efficiency in charging battery in all aspects comparing to direct charging of battery regardless of with or without converter. The highest amount of efficiency was drawn from the system was 31%. Comparing to the Worthington's work of pulling off 300% more efficiency with hybrid energy harvesting, it is drastically low. However, his storage system was implemented to a pump tire circuit, whereas our circuit was designed for a low wind application. As an off-grid standalone low voltage energy harvesting system, the EHC was able to provide noteworthy better efficiency in all three low wind speeds.

There were some issues and limitations encountered during this research. Firstly, turbine blade design was not taken in consideration in the simulation. As there was no

proper mathematical model for a hybrid VAWT which would relate turbine blade number to output torque or power, the simulation therefore did not account blade design. Moreover, DC DC boost converter used in this research did not perform well according to the data sheet in the minimum range. As it was stated in the data sheet, the converter should be able to step up voltage from as low as 2.5V; practically it could not step up any amount of voltage less than 4V. Therefore the Supercap charging range was made from 4V-7.5V which should have been 3V-7.5V. This had a direct effect on system efficiency. Future works which can be outcomes from the research are quite a few. Apart from improving the converter, an important task that can be taken in consideration in the near future is to apply CFD (Computational Fluid Dynamics) in the magnet positioning and try to come up with few optimized designs which will give nearly zero friction. In addition, Finite Element Analysis could be made possible to apply on turbine blades. These will surely help to increase the efficiency of the system. A real time wireless monitoring interface could be made available. Embedded solutions, providing wireless endpoint connectivity to devices like XBEE Modules, can be of use.

To recapitulate, sufficient groundwork and results had been laid out in this paper to deliver the necessary development and framework for further improvements. For rural areas in countries like Malaysia where grid connection is not always available, this standalone system can make a difference for using small scale electronic devices.

Acknowledgements

Authors would like to thank Ministry of Education Malaysia to fund their research project.

References

- [1] M. Z. Ibrahim, K. H. Yong, M. Ismail, A. Albani, "Wind Speed Modelling for Malaysia", International Journal of Renewable Energy Research, vol. 2, No. 4, 2014.
- [2] K. Sopian, M. Othman, B. Yatim, W. Daud, "Future directions in Malaysian environment friendly renewable energy technologies research and development", ISESC Science and Technology Vision, Vol. 1, pp. 30 – 36, 2005.
- [3] H. C. Ong, T. M. Mahlia, and H. H. Masjuki, "A review on energy scenario sustainable energy in Malaysia", Renewable and Sustainable Energy Reviews, Vol. 15, pp. 639 – 647, 2011.
- [4] L. Zhang, G. Barakat, A. Yassine, "Deterministic Optimization and Cost Analysis of Hybrid PV/Wind/Battery/Diesel Power System", International Journal of Renewable Energy Research, Vol.2, No.4, 2012.
- [5] Zaharim, S. K. Najid, A. M. Razali, K. Sopian, "Wind Speed Analysis in the East Coast of Malaysia," European Journal of Scientific Research, Vol. 32, No. 2, pp. 208-215, 2009,
- [6] MD S. A. Khan, R. Rajkumar, Rajparthiban K., CV Aravind, "Optimization of Multi-pole Three Phase Permanent Magnet Synchronous Generator for low speed Vertical Axis Wind Turbine", Applied Mechanics and Materials, Vol. 446-447, pp 704-708, 2014.
- [7] R. Bharanikumar, A.C. Yazhini, N. Kumar, "Modelling and simulation of wind turbine driven permanent magnet generator with new MPPT algorithm" Asian Power electronics journal, Vol.4, 2012.
- [8] W. Li and G. Joos, "A Power Electronic Interface for a Battery Supercapacitor Hybrid Energy Storage System for Wind Applications", IEEE Transactions on Energy Conv, Vol. 2, 2008.
- [9] M.A. Tankari, M.B. Camara, B. Dakyo, C. Nichita, "Ultracapacitors and Batteries Integration for Power Fluctuations mitigation in Wind-PV-Diesel Hybrid System", International Journal of Renewable Energy Research, Vol. 1, No. 2, pp. 86-95, 2011.
- [10] C. Abbey, G. Joos, "Supercapacitor Energy Storage for Wind Energy Applications", IEEE Transactions on Industry Application, Vol. 43, No. 3, June 2007.
- [11] L. Qu, W. Qiao, "Constant Power Control of DFIG Wind Turbines with Supercapacitor Energy Storage", IEEE Transactions on Industry Applications, Vol. 47, No. 1, February 2011.
- [12] E. L. Worthington, "Piezoelectric energy harvesting: Enhancing power output by device optimisation and circuit techniques," PhD thesis, School of Applied Sciences, Cranfield University, 2010.
- [13] D. Broe, S. Drouillet, V. Oevorglan, "A Peak power Tracker for Small Wind Turbines in Battery Charging Applications," IEEE Transactions on Energy Conv., Vol. 14, No. 4, pp. 1630-1635, Dec. 1999.
- [14] K.MD. Shahrukh, R. Rajkumar, CV Aravind, "Performance analysis of 20 Pole 1.5 KW Three Phase Permanent Magnet Synchronous Generator for low Speed Vertical Axix Wind Turbine", Journal of Energy and Power Engineering, Vol. 5, pp. 423-428, July 2013.
- [15] A. M. Eid, M. A. Salam, M. T. A. Rahman, "Vertical Axis Wind Turbine Modelling and Performance with Axial Flux Permanent Magnet Synchronous Generator for Battery Charging Application", IEEE Power Systems Conference, Vol. 1, pp. 162-166, 21 December 2006.
- [16] J. G. Slootweg, H. Pollinder, W. L. Kling, "Repre-senting Wind Turbine Electrical Generating Systems in Fundamental Frequency Simulations," IEEE Transaction of Energy Convt, Vol. 18, No. 4, pp. 516-524, Dec. 2003.



A LABVIEW based Real Time GUI for Switched Controlled Energy Harvesting Circuit for Wind Power Application

Journal:	<i>IETE Journal of Research</i>
Manuscript ID:	TIJR-2016-1196
Manuscript Type:	Original Article
Date Submitted by the Author:	12-Aug-2016
Complete List of Authors:	K. MD , Shahrukh; University of Nottingham, Electrical and Electronic Engineering R K, Rajkumar; University of Nottingham, Electrical and Electronics Engineering Aravind, C.V; Taylor's University, Electrical and Electronics Engineering Y.W, Wong; University of Nottingham
Keywords:	Graphical User Interface (GUI), LABVIEW, Real Time Monitoring, Energy Harvesting, Wind Energy
Abstract:	This paper developed a universal Real Time Graphical User Interface for wind powered Energy Harvesting Circuit. The proposed GUI was built in LABVIEW with NIUSB 621 DAQ that synchronized the data to perform real-time analysis through the use of power electronics. A hybrid Vertical Axis Wind Turbine adopted to a 200W Permanent Magnet Synchronous Generator was used for incorporating the Supercapacitor based battery charging energy harvesting system. The GUI displayed the real time energy harvesting output readings both graphically and digitally along with wind speed and angular velocity of the turbine. The model was built in such a way so that it could be used as a universal GUI for wind energy harvesting with minimal adjustment.

SCHOLARONE™
Manuscripts

URL: <https://mc.manuscriptcentral.com/tijr> E-mail: mgeditor.iete@gmail.com

A LABVIEW based Real Time GUI for Switched Controlled Energy Harvesting Circuit for Wind Power Application

K. MD Shahrukh, R. K. Rajkumar, Aravind C.V, and Y. W. Wong

K. MD Shahrukh is a Research Assistant, Department of Electrical and Electronic Engineering, University of Nottingham, Jalan Broga, Selangor, 43500, Malaysia (corresponding author to provide phone: +60107779012; fax: +60389248017; e-mail: kexlma@nottingham.edu.my). R. K. Rajkumar., is with the University of Nottingham, Jalan Broga, Selangor, 43500, Malaysia (e-mail: Rajprasad.Rajkumar@nottingham.edu.my). Aravind C.V. is with the School of Engineering, Taylor's University Malaysia (e-mail: aravindcv@sees.org). Y. W. Wong is with the University of Nottingham, Jalan Broga, Selangor, 43500, Malaysia (e-mail: YeeWan.Wong@nottingham.edu.my).

ABSTRACT

This paper developed a universal Real Time Graphical User Interface for wind powered Energy Harvesting Circuit. The proposed GUI was built in LABVIEW with NIUSB 621 DAQ that synchronized the data to perform real-time analysis through the use of power electronics. A hybrid Vertical Axis Wind Turbine adopted to a 200W Permanent Magnet Synchronous Generator was used for incorporating the Supercapacitor based battery charging energy harvesting system. The GUI displayed the real time energy harvesting output readings both graphically and digitally along with wind speed and angular velocity of the turbine. The model was built in such a way so that it could be used as a universal GUI for wind energy harvesting with minimal adjustment.

Keywords:

Graphical User Interface (GUI), LABVIEW, Real Time Monitoring, Energy Harvesting, Wind Energy

1. INTRODUCTION

Numerous countries worldwide are conscious about the fact that the past and current trends of energy system are not sustainable and a solution needs to be drawn to protect the world energy from a drastic falling. In order to search for an alternating source, the world is turning towards renewable energy. Wind power is the next promising source along with hydro and solar. Wind energy is gaining more interest each year [1]. Asia captured the largest market of wind power for the last few years. China, followed by the United States and Germany is leading from front [2][3]. Wind energy has generated more than 20% of electricity in quite a few countries including Denmark, Nicaragua, Portugal and Spain. Moreover, World Wind Energy Association (WWEA) reported that wind production in China increased considerably by adding another 23.3 GW at year 2014 followed by Germany and USA [3]. However, most of the researches on wind power were focused more on grid-connected system [4][5]. In 2013, a 1.5KW Permanent Magnet Synchronous Generator (PMSG) based standalone Vertical Axis Wind Turbine (VAWT) developed was too heavy and bulky in size for small-scale off-grid system [6]. In 2014, a laboratory prototype of 300W PMSG based 8 bladed VAWT to observe the off-grid performance of small scale VAWT system is designed and developed [7]. In 2016, a small scale VAWT adapted to PMSG was fabricated in order to incorporate the system with battery charging energy harvesting circuit [8].

This paper describes the real time output characteristic of the turbine which is incorporated with a 6V battery charging Energy Harvesting Circuit (EHC). The readings are to be displayed in a Graphical User Interface (GUI) developed in LABVIEW. A Hybrid Vertical Axis Wind Turbine (VAWT) attached to Permanent Magnet Synchronous Generator (PMSG) is used for incorporating the EHC system.

2. REAL TIME MONITORING SYSTEMS

Few works were done before in wind energy sector regarding real time monitoring system. An atmospheric wind profiler that could able to measure atmospheric horizontal and vertical winds is developed in [9]. An interface in LABVIEW to measure wind speed, direction, pressure and temperature in real time is presented in [10]-[11]. A wind turbine emulator using LABVIEW that displayed the static and dynamic characteristics of a typical wind turbine is presented in [12]. A real time monitoring of wind power with environmental issues was presented in [13]. A wind turbine emulator for multiple power plants is introduced [14]. But the system was too complex and it was improvised with advanced FPGA controller system which was also designed in LABVIEW. Consequently a digital subsystem with programmable computer and transducer to record frequency distribution of wind direction in separate sector is developed [15]. No significant graphical user interface has yet to be built for off-grid wind Energy Harvesting Circuit (EHC).

However energy harvesting through renewable sources is not a new idea. Babazadeh [16] invented a hybrid energy storage system for a PMSG wind turbine with a large variable wind speed between 6 m/s to 21 m/s. The system helped to smoothen and regulate the output. Currently available electric vehicle (EV) such as Tesla Model S, Toyota Prius and Chevrolet Volt use battery banks for energy storage. The average urban driving patterns cause rapid discharging of battery banks when accelerating. This results reduction in the battery bank lifespan, thus supercapacitors are beneficial in this case. Since supercapacitors are able to charge and discharge at a fast rate, it can provide a boost of power during acceleration and absorbs power during regenerative braking [17][18]. Battery and supercapacitors are used together to form a hybrid energy storage system. For instance, Lei (2008) proposed a power electronic interface for a Battery Supercapacitor Hybrid Energy Storage System. The interface was developed for grid connection which was in Mega Watt power range [19]. Worthington (2010) developed a novel SSHI (synchronized switch harvesting on inductor) technique that could be connected to a load capacitor directly to harvest energy. Experiment results showed that this idea is capable of harvesting three times more amount of energy compared to the usual bridge rectifier circuit [20]. This paper introduces a novel approach of bringing energy harvesting into wind power technology and delivers a standard and user friendly LABVIEW based GUI real time monitoring for switched controlled wind energy harvesting system.

3. Hardware Design

a. Energy Harvesting Circuit

Figure 1 shows the configuration of the VAWT along with PMSG used in this experiment.

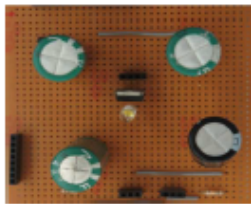


Figure 1 Supercapacitors on Stripboard

In this experiment, battery and Supercapacitors (Supercap) are used together to form a hybrid system. Battery has higher Equivalent Series Resistance (ESR) comparing to Supercap which results in high internal loss, thus less efficient compared to Supercap [21][22][23]. In addition voltage coming from the generator of turbine is not constant, wind dependent and may fluctuate. Therefore a combination of Supercap and battery is needed to be employed. Moreover, it can be observed from Table 1 that the highest open circuit voltage ranges from 3.5V to 8V for low wind speed configuration. As far as low voltage concerns, for batter selection, two choices were there; either to work with a battery 6V or 12V.

Since the open circuit voltage range was low, it was decided to use a 6V battery for charging. A Supercap bank was to be placed before the battery which would be charged up by taking the voltage generated from the turbine and subsequently would be discharged through the battery. Since the battery needed a constant voltage for charging up, the system required a DC DC boost converter in between the Supercap Bank and Battery that would give a constant stepped up voltage to the battery. As a part of the hybrid energy harvesting, Supercap were used to store the charges initially generated by the turbine. To form a Supercap bank, four Supercap of 35F each, manufactured by Cooper Bussmann with voltage rating of 2.7 V were placed in a series connection (figure 3.1). When four Supercap are linked in series, total operating voltage, V_t and total capacitance, C_{total} were calculated as follow:

$$V_t = 10.8V \quad \& \quad C_{total} = \frac{1}{\frac{1}{C_1} + \frac{1}{C_2} + \frac{1}{C_3} + \frac{1}{C_4}} = 8.76F$$

As a result, a Supercap bank with 8.76F capacitance and voltage rating of 10.8V were assembled. Although there were a few better batteries found in the research but they were excluded from the list due to the cost-effectiveness and maintenance difficulties. For example, as a result of additional protection circuit requirement, Li-Ion batteries was omitted; even though have high efficiency and cycle life [16] [17]. Considering all the facts, because of having the optimum characteristics, lead-acid battery remained as the best choice. Throughout this project, a 6 V (3.2AH/20HR), 3 cells, lead-acid battery (Figure 3.2), manufactured by Yokohama, was chosen.

Table 1: VAWT Configuration

<i>VAWT</i>	Wind Speed range	:	3-5 m/s
	Height	:	60 cm
	Radius	:	14.5 cm
	Number of blade	:	9
<i>PMSG</i>	Phase	:	3-Phase
	Rated Power	:	200W
	Rated Voltage	:	12V
	Diameter	:	16cm
<i>Top net weight</i>	Entire System	:	12.5kg
<i>Generator Performance</i>	PMSG Open Circuit Analysis	:	8.0V (Case A) 6.5V (Case B) 3.5V (Case C)

m = meter, s = second, W = Watt; Case A indicates 5m/s wind speed, Case B indicates 4m/s wind speed and Case C indicates 3m/s wind speed.

b. DC DC Boost Converter

A DC DC Boost Converter was used in the system to give a constant voltage of 7.5V to the 6V battery. The "LT1303" micro-power step-up high efficiency DC/DC converter was chosen as they were ideal for use in small, low-voltage battery operated systems. An adjustable version of it is LT1303 which can supply an output voltage up to 25V. The schematic diagram of LT1303 converter is shown in Figure 2.

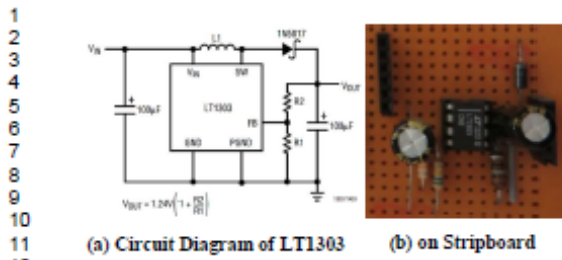


Figure 2 DC-DC Converter

Since the constant charge cycle of the battery ranges from 7.4V-7.5V, it was therefore set to 8.18V. The voltage was expected to drop down a little, therefore the output at DC DC converter was set as little high. By setting the $R_1 = 100k$ and $R_2 = 560k$, the output voltage can be calculated as shown below.

$$V_{OUT} = 1.24 \left(1 + \frac{560k}{100k}\right) = 8.18 \text{ V}$$

Current monitoring is a fundamental technique in many electronics systems. For a high-side current sensing circuit, a sense resistor is placed on the high side, located in between the supply voltage and load. For a low-side sensing, a sense resistor is placed on the low-side, which is connected to the load and grounded on the other side [24] [25].

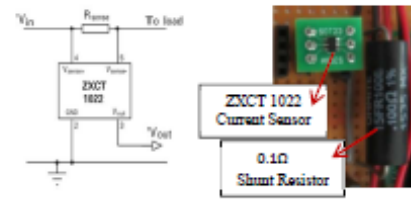


Figure 3 Current Sensing Circuit

A high-side current sensing is preferred if the generated current from the wind turbine is basically the measured current flowing through the load. Therefore, for the energy harvesting circuit, a high-side current sensor was chosen. Here, a low offset high-side current monitor, namely ZXCT 1022, was used to read the value of current. The circuit diagram and the stripboard form are shown in Figure 3. It is noteworthy to remark that value of R_{sense} was set to the 0.1Ω and $Vout$ was connected to the analog input pin of the Arduino microprocessor. To measure the rotational speed of the wind turbine, a rotary encoder (Figure 4) was used for this project. It was installed at the base of the turbine. It could sense the rotation and send the signal to LABVIEW through DAQ. It sent logic high whenever the marked turbine blade cuts

through the encoder; or else logic low. To count the number of logic high per minute, counter was used in LABVIEW.



Figure 4 Rotary encoder

4. SYSTEM LAYOUT

A novel design of a small vertical axis wind turbine (VAWT) has been used to charge batteries for energy storage. This design of VAWT uses magnetic levitation concept, making it gearless and lightweight which result in significant reduction in friction and start-up wind speed. The charges generated are desired to be stored in a 6V lead acid battery. The charges generated from the turbine are not constant because it depends highly on the wind speed. Therefore, Supercapacitor bank followed by a boost converter is used to provide a constant current supply to charge the battery through discharging the Supercapacitor; thereby, able to lengthen the life cycle of the battery. Since Supercapacitors are able to hold charges for a long time, hence it will not deplete its charges comparing to normal capacitors. A control system using Arduino is implemented to control the charging and discharging circuit so that the system is able to perform efficiently. Encoder, current and voltage transducers are to provide real time monitoring data. DAQ interfaced the laptop through LABVIEW based GUI for data acquisition. Figure 5 provides the system layout of the entire experiment.

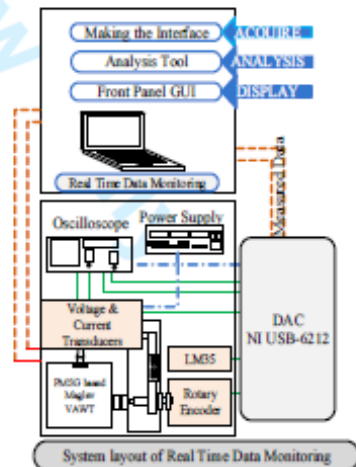


Figure 5 Layout of the entire system

5. CONTROL SYSTEM

5.1 Switching Configuration

In this harvesting system, switch plays a vital role. Two N-channel MOSFETs, P36NF06L, programmed by Arduino UNO, were used here (Figure 6) to create the switching condition in energy harvesting circuit. A LED was placed in parallel to the gate-source pin of the MOSFET for testing purpose.

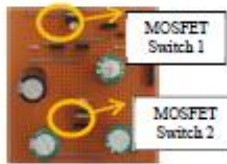
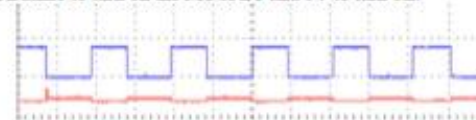
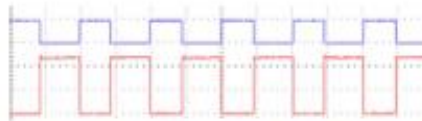


Figure 6 Configuration of Switching Circuit on Stripboard

To control the charging and discharging algorithm of the supercapacitors bank and rechargeable battery, two N-channel MOSFETs were used to act as a switching circuit in this project. In order to verify the suitability and validity of the use of N-channel MOSFET several tests had been carried out (Figure 7). When a PWM pulse with amplitude of 1V was connected to the gate to source; the MOSFET was off. On the other hand, when a 4.8V PWM pulse was applied to the gate to source, it can be seen from figure that the MOSFET was switched on. In this project, a 5V PWM was used from Arduino to turn on the MOSFET and 0V to turn off.



(a) Analysis of MOSFET off using Oscilloscope



(b) Analysis of MOSFET on using Oscilloscope

Figure 7 Switching configuration

5.2 Case 1 Charging supercapacitor from the turbine circuit

This condition occurs when, V_{Supercap} was less than 4V MOSFET 1 was turned on so that the wind turbine could charge up the supercapacitor bank. In this period of time, MOSFET 2 was turned off which basically isolated the battery from the Supercap. Figure 8 shows the schematic diagram of the system circuit at condition 1. Here, V_a-c and I_a-c are the AC voltage and current coming from the 3-Phase PMSG.

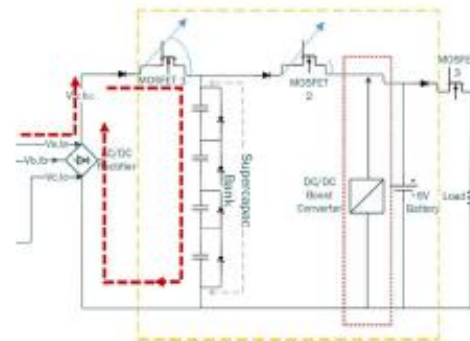


Figure 8 Case 1

5.3 Case 2 Discharging supercapacitor bank to rechargeable battery

This condition occurs when V_{Supercap} is greater or equal to 7.5V, MOSFET 1 then was turned off to prevent overcharging from the wind turbine, while MOSFET 2 was turned on (Figure 9). At this point of time, the rechargeable battery was charged up to the battery rated voltage, 6V. MOSFET 1 would be switched on again as soon as the voltage of supercapacitor dropped to 4V.

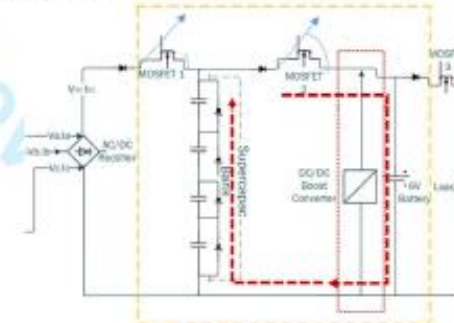


Figure 9 Case 2

Until the battery was charged up to 6V, the charging and discharging process is continued. Two LEDs are put aligned with the bias voltage. To indicate its logic high close circuit status, LED would light on whenever the MOSFET was turned on and vice versa. Figure 10 shows the energy harvesting circuit on stripboard.

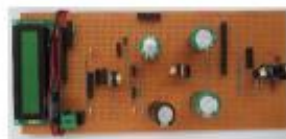
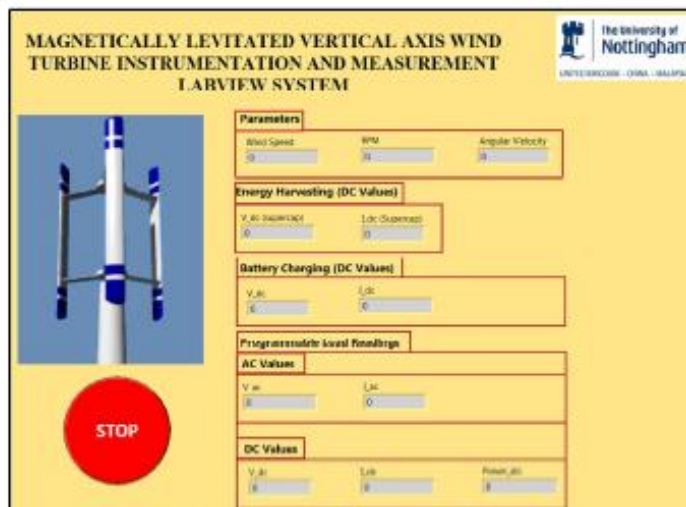


Figure 10 EHC on stripboard

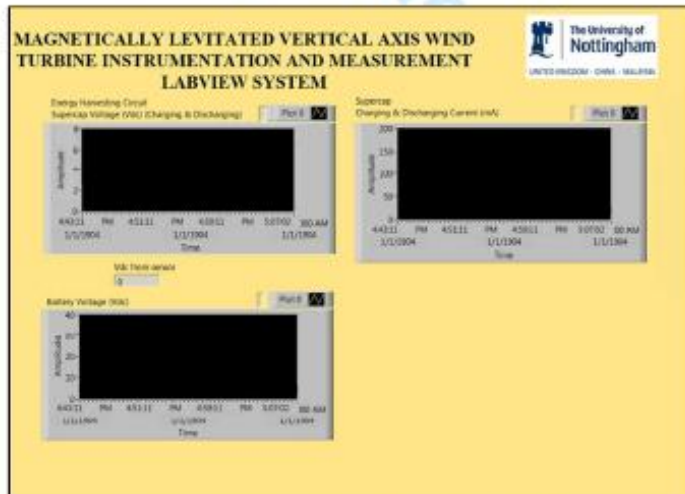
1 4. LABVIEW BASED GRAPHICAL USER
 2 INTERFACE
 3

4 The Graphical User Interface (GUI) for this project was
 5 created using LABVIEW. A user friendly GUI enabled the
 6 user to be able to monitor and analyze data. The front panel of
 7 developed LABVIEW GUI is shown in Figure 11 and Figure
 8 12 respectively whereas Figure 13 shows the block diagram of
 9 LABVIEW interface.
 10

Programmable load reading was the additional feature for further use. The data from the graph could also be exported to Excel. This enabled user to keep track and acknowledge the current status of the system. The experiment was carried out at the University of Nottingham Malaysia Campus, located in Jalan Broga, Semenyih. The research is performed at the Research Building, N block. Figure 14 displays the experimental set-up of the system.



33 Figure 11 Developed Front Panel of LABVIEW GUI- Part 1
 34



35 Figure 12 Developed Front Panel of LABVIEW GUI- Part 2
 36

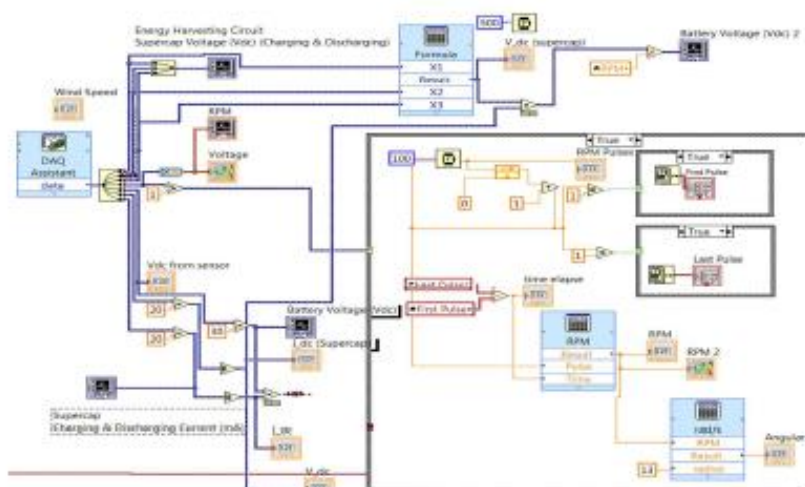


Figure 13 Back Panel of Developed LABVIEW GUI

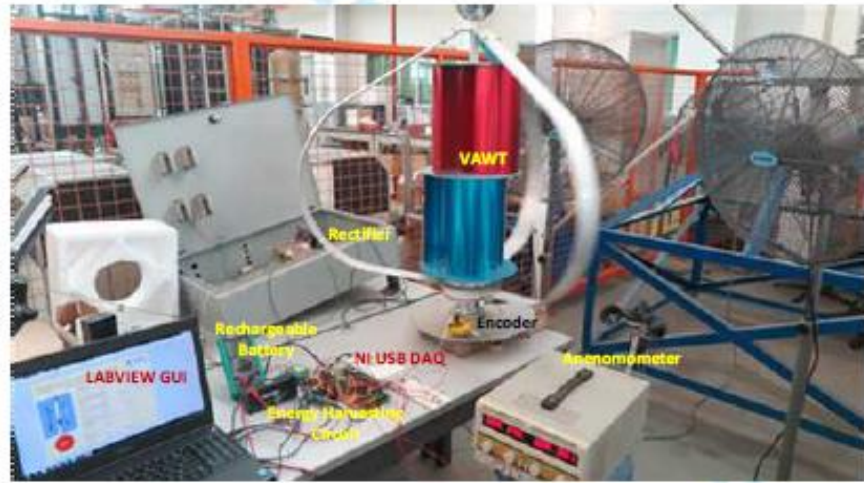


Figure 14 Experimental Set-up

1

2

3

5. RESULTS

4

5

6

7

8

9

10

11

12

13

14

15

16

17

18

19

20

21

22

23

24

25

26

27

28

29

30

31

Figure 15 and Figure 16 here show the LABVIEW GUI while the system was operational. Figure 15 gives the digital reading of energy harvesting Supercapacitor bank and battery charging values for a fixed wind speeds and angular velocity. On the other hand, Figure 16 provides the graphical analysis of Supercap bank current and Voltage reading along with battery charging progress. Data was imported directly in excel and analyzed for efficiency comparison (Figure 17).

For a wind speed of 5m/s, the result showed an increase of 19% of the charging time while charging through the Supercap. It took only 8.1 hours whereas direct charging without converter took 10 hours. For wind speed 4m/s, the energy harvesting circuit, taking only 10.4 hours to charge up the battery, again showed an excellent performance of 31% efficiency. For 3m/s, energy harvesting circuit still held the top position handsomely with 28% efficiency

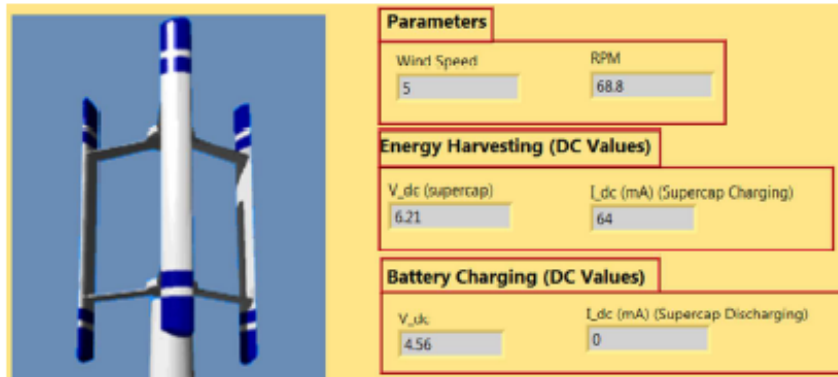


Figure 15 LABVIEW GUI Reading at operation- Part 1

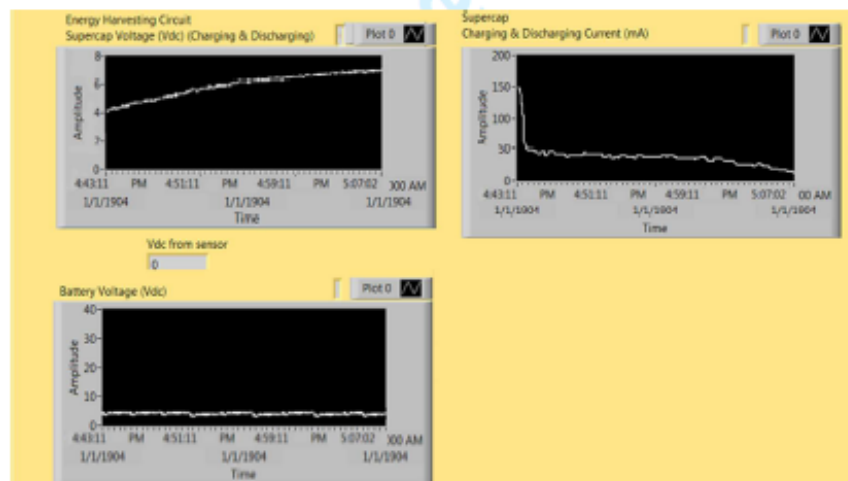


Figure 16 LABVIEW GUI Graph at operation- Part 2

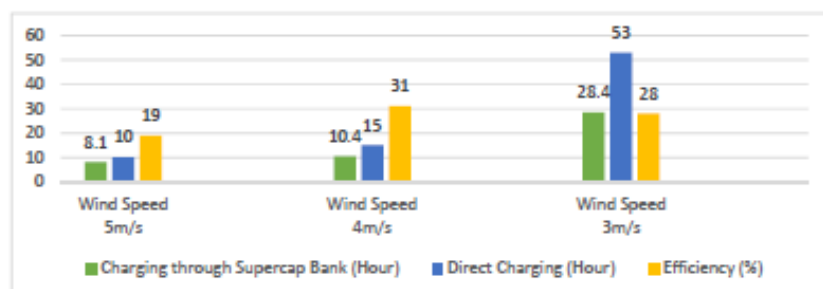


Figure 17 EHC efficiency comparison

6. CONCLUSION

As a conclusion to this paper, the aim of this experiment was to provide a LABVIEW based GUI that can work with a standalone off-grid wind turbine incorporated with energy harvesting circuit. The proposed interface provides an easy, less complicated access to energy harvesting data without much difficulty. There is vast scope to extend this work further. The GUI developed in the LABVIEW is universal and can be integrated with any sort of energy harvesting with a minimal adjustment. This surely can bring a revolutionary change for real time data monitoring for off-grid wind power application and can be a replacement of SCADA (Supervisory Control and Data Acquisition) for small scale real time system.

REFERENCES

- M. Balat, 'A Review of Modern Wind Turbine Technology', Energy Sources, Part A: Recovery, Utilization, and Environmental Effects, Vol. 31, pp. 1561-1572, 2009.
- Renewable Energy Policy Network, "Global Status Report," 2015. [Online]. Available: <http://www.ren21.net/ren21/activities/globalstatusreport.aspx>. [Accessed 15 March 2015].
- World Wind Energy Association, "New Record in Worldwide Wind Installation," 5 February 2015. [Online]. Available: <http://www.wwindea.org/new-record-in-worldwide-windinstallations/>. [Accessed 15 March 2015].
- S.M. Muyeen, Junji Tamura, T. Murata, Stability Augmentation of a Grid-connected Wind Farm, Springer-Verlag London Limited, 2009.
- M. Arifujaman, "Modelling and Simulation of Grid Connected Permanent Magnet Generator (PMG)- based Small Wind Energy Conversion System," The Open Renewable Energy Journal, Vol. 4, 2011, pp. 13-18.
- MD Shahrkhan A. Khan, R. Rajkumar, Rajparthiban K., CV Aravind, 'Performance analysis of 20 Pole 1.5 KW Three Phase Permanent Magnet Synchronous Generator for low Speed Vertical Axis Wind Turbine', Journal of Energy and Power Engineering, Vol. 5, pp. 423-428, July 2013.
- MD Shahrkhan A. Khan, R. Rajkumar, Rajparthiban K., CV Aravind, 'Optimization of Multi-Pole Permanent Magnet Synchronous Generator based 8 Blade Magnetically Levitated Variable Pitch Low Speed Vertical Axis Wind Turbine', Applied Mechanics and Materials, Vol. 492, pp 113-117, 2014.
- MD Shahrkhan A. Khan, R. Rajkumar, CV Aravind, Wong, Y.W, 'A Novel Approach towards Introducing Supercapacitor based Battery Charging Circuit in Energy Harvesting for an off-grid low voltage Maglev Vertical Axis Wind Turbine', International Journal of Control Theory and Applications, Vol. 9, pp. 369-375, 2016.
- B. Madhu, G. Beena, J. Thomas, S. Dhan, S. Omkar, S.C. Garg, M. R. Khanna, 'A Phased Array Acoustic Wind Profiler for Remote Atmospheric Wind Measurement', IETE Journal of Research, Vol. 57, pp.190-193, 2011.
- V. Aiswarya, N. K. Prakash, 'Wind turbine instrumentation system using LABVIEW', IEEE Global Humanitarian Technology Conference: South Asia Satellite, pp. 218-222, 2013.
- L. Bayon, J. M. Garu, M. M. Ruiz, P.M. Saurez, 'Real-time optimization of wind farms and fixed-head pumped-storage hydro-plants', International Journal of Computer Mathematics, Vol. 90, pp. 2147-2160, 2013.
- N. C. Sahoo, A. S. Satpathy, N. K. Kishore, B. Venkatesh, 'DC motor-based wind turbine emulator using LABVIEW for wind energy conversion system laboratory setup', International Journal of Electrical Engineering Education, Vol. 50, pp. 111, 2013.
- S. Zheng, X. Xiong, J. Vause, J. Liu, 'Real-time measurement of wind environment comfort in urban areas by Environmental Internet of Things', International Journal of Sustainable Development & World Ecology, Vol. 20, pp. 254-260, 2013.
- M. Topor, 'Wind Turbine Emulator Development Using LABVIEW FPGA', International Journal of Emerging Research and Technology, Vol. 3, pp. 13-21, 2015.
- C. W. Joshi, N. A. Ingle, N.B. Jathar, 'A Digital Subsystem to Record Sectorwise Frequency Distribution of Wind Direction', IETE Journal of Research, Vol. 17, pp. 296-300, 2015.
- T. Christen, M. W. Carlen, "Theory of Ragone plots," December, 2000, Journal of Power Sources.
- H. Babazadeh, W. Gao and X. Wang, "controller design for a hybrid energy storage system enabling longer battery life in wind turbine generators" North American Power Symposium (NAPS), pp. 1-7, August 2011.

- 1 18. S. Park, Y. Kim and N. Chang, "hybrid energy storage
2 systems and battery management for electric vehicles,"
3 50th ACM/IEEE Design Automation Conference (DAC),
4 pp. 1-6, May 2013.
5 19. A. Ostadi, M. Kazerani and S. K. Chen, "Hybrid energy
6 storage system (HESS) in vehicular applications- a review
7 on interfacing battery and ultra-capacitor units," IEEE
8 Transportation Electrification Conference and Expo
9 (ITEC), pp. 1-7, June 2013.
10 20. W. Li and G. Joos, "A Power Electronic Interface for a
11 Battery Supercapacitor Hybrid Energy Storage System for
12 Wind Applications", *IEEE Transactions on Energy Conv*,
13 Vol. 2, 2008.
14 21. E. L. Worthington, "Piezoelectric energy harvesting:
15 Enhancing power output by device optimisation and circuit
16 techniques," PhD thesis, School of Applied Sciences,
17 Cranfield University, 2010.
18 22. M. Pedram, N. Chang, Y. Kim and Y. Wang, "Hybrid
19 Electrical Energy Storage Systems," Proceeding of The
20 16th ACM/IEEE International Symposium on Low Power
21 Electronics and Design, pp. 363-368, August, 2010.
22 23. J. R. Miller, "Introduction to electrochemical capacitor
23 technology," *IEEE Electrical Insulation Magazine*, vol. 26,
24 no. 4, pp. 40-47, July 2010.
25 24. W. X. Y. Yang, "Design of high-side current sense
26 amplifier with ultra-wide ICMR," *Circuits and Systems,*
27 2009. MWSCAS '09. 52nd IEEE International Midwest
28 Symposium , pp. 5-8, 2009.
29 25. S. Z. H. C. I. C. W. Lai, "High gain amplification of
30 low-side current sensing shunt resistor," *Power*
31 Engineering Conference, 2008. AUPEC '08. Australasian
32 Universities, pp. 1-5, 2008.

About Author's



MD Shahrukh Adnan Khan graduated (2011) from University of Nottingham with 1st class (Hons) in Electrical and Electronic Engineering. He got Enhanced High Achievers Scholarship throughout his Bachelor degree. In the same year, as the only student of the department, he was awarded with the prestigious 'Dean Scholarship' to pursue his PhD. He is currently serving as a Research Assistant (PhD) at the University of Nottingham. His research area includes renewable energy, low wind power application, energy harvesting and optical fiber communication.



R. Rajkumar received the Master's and PhD degree from the Department of Electrical and Electronic Engineering, Faculty of

Engineering, University of Nottingham, Malaysia Campus, in 2005 and 2010 respectively. He is currently an associate professor in the same university. His main interest is in using the Support Vector Machine to predict failures in oil and gas pipelines.



Aravind C.V. received his PhD from the University Putra Malaysia in 2013. He is a chartered engineer registered with the IET UK since 2013. He is currently attached with the School of Engineering, Taylor's University, Malaysia since 2011. His main research interests is of energy efficient energy conversions system for renewables. He is member of IEEE, IET and a frequent speaker in international meetings.



Wong Yee Wan achieved her PhD in the year 2011 from the University of Nottingham Malaysia Campus. She is now working as an assistant professor in the same university. Her research interest is in image processing, artificial intelligence (AI), and implementing AI in power system.

Simulation data

For wind speed = 4 m/s

Case1 :

Turbine Radius (m)	Turbine Height (m)	Swept Area (m ²)	Mechanical Power from the turbine, P _m (w)	Mechanical generated from the turbine, T _m (Nm)	Torque
0.4	2	1.6	27.67	2.76	
0.6	2	2.4	41.51	6.23	
0.8	2	3.2	55.34	11.07	
1	2	4	69.18	17.3	
1.2	2	4.8	83.02	24.93	
1.4	2	5.6	96.85	33.86	
1.6	2	6.4	110.7	44.28	

Case 2:

Turbine Radius (m)	Turbine Height (m)	Swept Area (m ²)	Mechanical Power from the turbine, P _m (w)	Mechanical Torque generated from the turbine, T _m (Nm)
1	1.6	3.2	55.34	13.84
1	1.8	3.6	62.26	15.57
1	2	4	69.18	17.3
1	2.2	4.4	76	19.02
1	2.4	4.8	83.2	20.75
1	2.6	5.2	89.3	22.4
1	2.8	5.6	96.85	24.21

For wind speed = 2 m/s

Case1 :

Turbine Radius (m)	Turbine Height (m)	Swept Area (m ²)	Mechanical Power from the turbine, P _m (w)	Mechanical generated from the turbine, T _m (Nm)	Torque
0.4	2	1.6	3.5	0.7	
0.6	2	2.4	5.2	1.6	
0.8	2	3.2	7	2.8	
1	2	4	8.74	4.324	
1.2	2	4.8	10.38	6.24	
1.4	2	5.6	12.11	8.466	
1.6	2	6.4	13.8	11.07	

Case 2:

Turbine Radius (m)	Turbine Height (m)	Swept Area (m ²)	Mechanical Power from the turbine, P _m (w)	Mechanical Torque generated from the turbine, T _m (Nm)
1	1.6	3.2	6.9	3.5
1	1.8	3.6	7.8	3.9

1	2	4	8.7	4.3
1	2.2	4.4	9.5	4.8
1	2.4	4.8	10.38	5.189
1	2.6	5.2	11.24	5.621
1	2.8	5.6	12.11	6.053

7.2.2. Comparing the Simulation Data with theoretical value:

(Data given here only for Wind Speed at 2 m/s):

For wind speed = 2 m/s

Case 3 :

Turbine Radius (m)	Turbine Height (m)	Swept Area (m ²)	Mechanical Power from the turbine, P _m (w)	Mechanical generated from the turbine, T _m (Nm)
0.4	2	1.6	3.47	1.79
0.6	2	2.4	5.43	2.76
0.8	2	3.2	7.22	3.74
1	2	4	8.88	4.132
1.2	2	4.8	10.12	5.32
1.4	2	5.6	12.41	6.113
1.6	2	6.4	13.8	6.76

Case 4:

Turbine Radius (m)	Turbine Height (m)	Swept Area (m ²)	Mechanical Power from the turbine, P _m (w)	Mechanical Torque generated from the turbine, T _m (Nm)
1	1.6	3.2	6.77	3.34
1	1.8	3.6	7.81	3.76
1	2	4	8.84	4.28
1	2.2	4.4	9.67	4.63
1	2.4	4.8	10.45	5.21
1	2.6	5.2	11.48	5.79
1	2.8	5.6	12.39	6.22

1. Generator Parameter testing in SimPower:

The PowerSim toolbox in the Matlab is used to simulate the generator parameter for different mechanical torque (T_m) from the turbine to get maximum voltage and power.

Parameter 1: Pole Pair

For Pole Pair 8,

T _m (Nm)	V _{rms} (v)	I _{rms} (A)	P (W)
68.86	240.913	0.75802	547.8561079
50.59	176.990	0.75590	401.3637482
35.13	122.896	0.47694	175.8455227
22.48	78.6310	0.45495	107.3211784

For Pole Pair 10,

T _m (Nm)	V _{rms} (V)	I _{rms} (A)	P(W)
68.86	294.512	1.51605	1339.489691
50.59	216.376	1.07410	697.234373
35.13	150.261	0.82237	370.7133603
22.48	96.1674	0.29613	85.43683868

For Pole Pair 16,

Torque	Vrms(V)	Irms(A)	P=(W)
68.86	425.61	2.1206	2707.699084
50.59	315.30	1.5330	1450.094613
35.13	218.99	0.6961	457.3582471
22.48	140.14	0.7148	300.576065
12.65	78.843	0.3931	92.9927836
5.621	35.037	0.1697	17.84577478

For Pole Pair 18,

Torque	Vrms(V)	Irms(A)	P=(W)
68.86	464.07	2.5944	3612.016328
50.59	340.97	1.4509	1484.240068
35.13	236.81	1.2621	896.7119489
22.48	151.53	0.7757	352.6374136
12.65	85.277	0.5114	130.8474797
5.621	37.894	0.2110	23.98734408

12.65	44.2582	0.26446	35.11366348
5.621	19.6648	0.11200	6.607782737

For Pole Pair 12,

Tm(Nm)	Vrms(V)	Irms(A)	P=(W)
68.86	344.081	1.54575	1595.592003
50.59	252.793	0.77004	583.9874509
35.13	175.576	0.85631	451.0456011
22.48	112.360	0.67267	226.746704
12.65	63.2159	0.32194	61.05690107
5.621	28.0936	0.11575	9.755888618

For Pole Pair 14,

Torque	Vrms(V)	Irms(A)	P=(W)
68.86	389.053	2.07537	2422.30196
50.59	285.886	1.70060	1458.540225
35.13	198.486	0.68724	409.226344
22.48	127.068	0.58747	223.9464353
12.65	71.4891	0.30405	65.21075074
5.621	31.7635	0.17168	16.36017779

Parameter 2: Friction Factor

For Friction Factor 0,

Tm (Nm)	Vrms(V)	Irms(A)	P=(W)
68.86	216.871	0.98218	639.0217064
50.59	159.383	0.92419	441.9051757
35.13	110.663	0.64906	215.4811579
22.48	70.7820	0.42462	90.1668044
12.65	39.8458	0.15464	18.48597206
5.621	17.7061	0.10267	5.453816604

For Friction Factor 0.06,

Tm (Nm)	Vrms(V)	Irms(V)	P=(W)
68.86	184.344	1.02955	569.3797207
50.59	135.412	0.78418	318.5663601
35.13	94.0461	0.55628	156.9496603
22.48	60.1753	0.28327	51.13757082
12.65	33.8566	0.1986	20.17462495
5.621	15.047	0.0944	4.261401734

For Friction Factor 0.12,

Tm (Nm)	Vrms(V)	Irms(A)	P=(W)
68.86	158.11	0.85207	404.1647519
50.59	116.178	0.63187	220.231944
35.13	80.6816	0.28362	68.6495817

For Friction Factor 0.18,

Tm (Nm)	Vrms(V)	Irms(A)	P=(W)
68.86	136.897	0.78053	320.6077493
50.59	100.515	0.46644	140.1621183
35.13	69.8246	0.41187	87.60280522

22.48	51.6122	0.28362	43.91527579		22.48	44.6251	0.23237	31.80097744
12.65	29.0482	0.10719	9.341771175		12.65	25.1446	0.12331	9.227996993
5.621	12.9048	0.04911	1.902872747		5.621	11.1729	0.06256	2.079951893

For Friction Factor 0.24,

Tm (Nm)	Vrms(V)	Irms(A)	P=(W)
68.86	119.572	0.38672	138.7238457
50.59	87.8235	0.51308	135.1818728
35.13	60.9956	0.21498	38.70129129
22.48	39.3267	0.14114	16.52719699
12.65	21.9695	0.08813	5.851816238
5.621	9.75817	0.58542	1.71378587

For Friction Factor 0.30,

Tm (Nm)	Vrms(V)	Irms(A)	P=(W)
68.86	105.359	0.57383	181.3737287
50.59	77.4284	0.28827	67.11383724
35.13	53.7403	0.31896	51.38078548
22.48	34.34	0.16689	17.21889026
12.65	19.3537	0.09762	5.669804247
5.621	8.59851	0.05136	1.324249399

Parameter 3: Stator Resistance

For Stator Resistance 5 Ohm,

Tm (Nm)	Vrms(V)	Irms(A)	P(W)
68.86	162.211	0.95743	465.9203364
50.59	119.148	0.70181	250.8591865
35.13	82.7322	0.47546	118.0084634
22.48	52.9557	0.28482	45.24940588
12.65	29.7977	0.17098	15.28447116
5.621	13.2442	0.06196	2.462012071

For Stator Resistance 13 Ohm,

Tm (Nm)	Vrms(V)	Irms(A)	P(W)
68.86	155.07	0.86762	403.6293916
50.59	113.916	0.68267	233.2933846
35.13	79.1260	0.43961	104.3543465
22.48	50.6364	0.28001	42.53715586
12.65	28.4896	0.16511	14.11184317
5.621	12.6573	0.05852	2.222148621

For Stator Resistance 21 Ohm,

Tm (Nm)	Vrms(V)	Irms(A)	P(W)
68.86	191.203	0.76439	438.4620097
50.59	109.178	0.65337	214.0025046
35.13	75.8025	0.40454	91.99544447
22.48	62.4239	0.27414	51.34021871
12.65	27.2945	0.15945	13.05670043
5.621	12.127	0.05540	2.015849664

For Stator Resistance 29 Ohm,

Tm (Nm)	Vrms(V)	Irms(A)	P(W)
68.86	142.624	0.65598	280.6810185
50.59	104.794	0.61773	194.2050049
35.13	72.7619	0.37102	80.98899837
22.48	46.5492	0.26757	37.36582468
12.65	26.1985	0.15400	12.10446716
5.621	11.6390	0.05258	1.836230519

For Stator Resistance 37 Ohm,

Tm (Nm)	Vrms(V)	Irms(A)	P(W)
68.86	137.038	0.54773	225.180539
50.59	100.693	0.57863	174.7922325
35.13	69.9335	0.33945	71.2093658
22.48	44.7461	0.26057	34.97869089
12.65	25.1803	0.14877	11.23873156
5.621	11.1865	0.05002	1.678929702

For Stator Resistance 45 Ohm,

Tm (Nm)	Vrms(V)	Irms(A)	P(W)
68.86	131.947	0.44371	175.6406188
50.59	96.9452	0.53783	156.4203901
35.13	67.3242	0.30971	62.55416979
22.48	43.0773	0.25335	32.74208199
12.65	24.2398	0.14382	10.4590286
5.621	10.7693	0.04768	1.540696351

Parameter: Inductance

For Inductance 0.8H,

Tm (Nm)	Vrms(V)	Irms(A)	P(W)
68.86	25.1053	0.14121	10.63422896
50.59	24.5598	0.08327	6.129933572
35.13	23.3489	0.12428	8.687728631
22.48	20.5204	0.25339	15.59709815
12.65	12.8697	0.07372	2.847444614
5.621	10.1689	0.06526	1.990733482

For Inductance 0.08H,

Tm (Nm)	Vrms	Irms	P(W)
68.86	113.739	0.75449	257.3653363
50.59	95.0366	0.60407	172.2301834
35.13	71.9846	0.44452	96.00433136
22.48	48.502	0.25117	36.54545294
12.65	27.9875	0.15804	13.26944951
5.621	12.5584	0.06025	2.268972319

For Inductance 8mH,

Tm (Nm)	Vrms(V)	Irms(A)	P(W)
68.86	25.1023	0.14121	10.63422896
50.59	24.5508	0.08327	6.129933572
35.13	23.3489	0.12408	8.687728631
22.48	20.5204	0.25339	15.59709815
12.65	12.8697	0.07372	2.847444614
5.621	10.1689	0.06526	1.990733482

For Inductance 0.8mH,

Tm (Nm)	Vrms	Irms	P(W)
68.86	113.709	0.7544	257.3653363
50.59	95.0366	0.60407	172.2301834
35.13	71.9846	0.44452	96.00433136
22.48	48.5002	0.25117	36.54545294
12.65	27.9875	0.15804	13.26944951
5.621	12.5584	0.06025	2.268972319

For Inductance 0.8H,

Tm (Nm)	Vrms(V)	Irms(A)	P(W)
68.86	153.726	0.86975	401.1106933
50.59	113.138	0.67734	229.9004095
35.13	78.6313	0.43963	103.701549
22.48	50.3324	0.27729	41.86531998
12.65	28.3344	0.16398	13.93861684
5.621	12.5939	0.05836	2.203228308

For Inductance 0.08H,

Tm (Nm)	Vrms(V)	Irms(A)	P(W)3
68.86	154.225	0.85567	395.8590926
50.59	113.353	0.6795	231.0528366
35.13	78.7014	0.43518	102.7430006
22.48	50.3603	0.27931	42.20934258
12.65	28.3344	0.16444	13.97468053
5.621	12.5969	0.05811	2.195480809

For Parameter: Intertia (Kg/m²)

For Inertia 0.01 Kg/m²,

Tm (Nm)	Vrms(V)	Irms(A)	P(W)
68.86	287.865	1.72535	1490.014578
50.59	211.497	0.69157	438.788116
35.13	146.865	0.87969	387.5756337
22.48	93.9759	0.32644	92.02172498
12.65	52.8929	0.31722	50.34510562
5.621	23.5045	0.07149	5.040942685

For Inertia 0.04 Kg/m²,

Tm (Nm)	Vrms(V)	Irms(A)	P(W)
68.86	235.822	1.40857	996.5171132
50.59	173.242	0.93904	488.0493608
35.13	120.28	0.46726	168.6063539
22.48	77.0046	0.43303	100.0374587
12.65	43.3178	0.25595	33.26481802
5.621	19.2473	0.11352	6.557423771

For Inertia 0.07 Kg/m²,

For Inertia 0.1 Kg/m²,

Tm (Nm)	Vrms(V)	Irms(A)	P(W)		Tm (Nm)	Vrms(V)	Irms(A)	P(W)
68.86	179.397	1.06272	571.9776205		68.86	142.484	0.71847	307.09189
50.59	131.806	0.58991	233.1349515		50.59	104.658	0.51556	161.8633045
35.13	91.5009	0.27419	75.27342374		35.13	72.6927	0.43198	94.03296355
22.48	58.5702	0.19444	34.13075613		22.48	46.5193	0.19427	27.14463763
12.65	32.9556	0.10961	10.82304959		12.65	28.3304	0.16475	13.98069115
5.621	14.6442	0.07595	3.299166278		5.621	11.6302	0.06922	2.429547099

For Inertia 0.13 Kg/m²,

Tm (Nm)	Vrms(V)	Irms(A)	P(W)
68.86	117.667	0.64062	226.0420955
50.59	86.4098	0.43895	113.7764922
35.13	60.0123	0.29697	53.45639479
22.48	38.4034	0.21934	25.24648773
12.65	21.6099	0.12853	8.333871844
5.621	9.60262	0.0374	1.072908478

For Inertia 0.15 Kg/m²,

Torque	Vrms(V)	Irms(A)	P(W)
68.86	105.282	0.61632	194.6755939
50.59	77.3582	0.24695	57.32122942
35.13	53.7125	0.31532	50.80682047
22.48	34.3729	0.19602	20.21242567
12.65	19.3396	0.10052	5.833866894
5.621	8.59143	0.0486	1.250987994

Parameter: Flux Linkage (λ)

Torque	Vrms(V)	Irms(A)	P(W)
68.86	44.7109	0.26682	35.75725082
50.59	32.8442	0.16565	16.30426272
35.13	22.8148	0.13564	9.208793625
22.48	34.3729	0.19012	20.21242567
12.65	8.21666	0.04015	1.109615082
5.621	3.64943	0.01143	0.130756443

For Flux Linkage 0.05 λ

Torque	Vrms(V)	Irms(A)	P(W)
68.86	216.801	1.15966	754.2504665
50.59	113.33	0.67956	231.0768821
35.13	110.596	0.61219	203.1205759
22.48	70.7807	0.39716	84.34087266
12.65	39.8371	0.12573	15.1248951

For Inertia 0.15 λ ,

Torque	Vrms(V)	Irms(A)	P(W)
68.86	132.799	0.63686	253.703886
50.59	97.5106	0.43251	126.5325719
35.13	67.7341	0.24005	48.78199314
22.48	43.3389	0.25994	33.77756685
12.65	24.3885	0.14619	10.68348241
5.621	10.8405	0.0445	1.503901845

For Inertia 0.35 λ ,

Torque	Vrms(V)	Irms(A)	P(W)
68.86	294.528	1.23883	1094.582994
50.59	216.378	1.26573	821.6257588
35.13	150.266	0.66901	301.6070348
22.48	96.1674	0.57694	166.4467924
12.65	54.1083	0.30916	50.27460427

5.621	17.6990	0.09491	5	5.282682822		5.621	24.0416	0.13943	10.0573929
-------	---------	---------	---	-------------	--	-------	---------	---------	------------

For Flux Linkage 0.45λ

Torque	Vrms(V)	Irms(A)	P(W)
68.86	363.951	2.18356	2384.136128
50.59	267.430	0.82803	664.3210417
35.13	185.688	1.11370	620.4043994
22.48	118.795	0.37583	133.940569
12.65	66.8646	0.40126	80.48155964
5.621	29.7129	0.08952	7.979751052

For Inertia 0.50λ ,

Torque	Vrms(V)	Irms(A)	P(W)
68.86	395.131	1.81561	2151.70067
50.59	290.348	0.98922	861.6606267
35.13	201.591	0.86975	526.0195891
22.48	128.975	0.5396	208.3230356
12.65	72.6206	0.23005	50.12883147
5.621	32.2582	0.16098	15.56128047

WIND SPEED 4

w= 20	h	r=0.2	area	TM	PM
		0.25	0.1	0.08	1.73
		0.3	0.12	0.1	2.07
		0.36	0.144	0.12	2.49
		0.4	0.16	0.14	2.77
		0.45	0.18	0.16	3.11
		0.5	0.2	0.17	3.46
		0.55	0.22	0.19	3.8
		0.6	0.24	0.21	4.15
		0.65	0.26	0.22	4.5
		0.7	0.28	0.24	4.84
		0.75	0.3	0.26	5.19
		0.8	0.32	0.28	5.53
		0.85	0.34	0.29	5.88
		0.9	0.36	0.31	6.22
		1	0.4	0.35	6.91

WIND SPEED= 3

w= 15	h	r=0.2	area	TM	PM
		0.25	0.1	0.05	0.73
		0.3	0.12	0.06	0.88
		0.36	0.144	0.07	1.05
		0.4	0.16	0.08	1.17
		0.45	0.18	0.09	1.31
		0.5	0.2	0.1	1.46
		0.55	0.22	0.11	1.61
		0.6	0.24	0.12	1.75
		0.65	0.26	0.13	1.9
		0.7	0.28	0.14	2.04
		0.75	0.3	0.15	2.19
		0.8	0.32	0.16	2.33

				0.85	0.2	0.34	0.17	2.49
				0.9	0.2	0.36	0.18	2.63
				1	0.2	0.4	0.19	2.91
WIND SPEED= 5		w= 25	h	r=0.2	area	TM	PM	
				0.25	0.2	0.1	0.14	3.38
				0.3	0.2	0.12	0.16	4.05
				0.36	0.2	0.144	0.19	4.96
				0.4	0.2	0.16	0.22	5.41
				0.45	0.2	0.18	0.24	6.08
				0.5	0.2	0.2	0.27	6.76
				0.55	0.2	0.22	0.3	7.43
				0.6	0.2	0.24	0.32	8.11
				0.65	0.2	0.26	0.35	8.78
				0.7	0.2	0.28	0.38	9.46
				0.75	0.2	0.3	0.41	10.13
				0.8	0.2	0.32	0.43	10.91
				0.85	0.2	0.34	0.46	11.48
				0.9	0.2	0.36	0.49	12.16
				1	0.2	0.4	0.54	13.51
WIND SPEED 4		2	w= 10	h	r=0.2	area	TM	PM
				0.25	0.2	0.1	0.022	0.22
				0.3	0.2	0.12	0.026	0.26
				0.36	0.2	0.144	0.031	0.31
				0.4	0.2	0.16	0.035	0.35
				0.45	0.2	0.18	0.039	0.39
				0.5	0.2	0.2	0.043	0.43
				0.55	0.2	0.22	0.048	0.48
				0.6	0.2	0.24	0.052	0.52
				0.65	0.2	0.26	0.056	0.56
				0.7	0.2	0.28	0.061	0.61
				0.75	0.2	0.3	0.065	0.65
				0.8	0.2	0.32	0.069	0.69
				0.85	0.2	0.34	0.074	0.74
				0.9	0.2	0.36	0.078	0.78
				1	0.2	0.4	0.086	0.86
WIND SPEED 4		6	w= 30	h	r=0.2	area	TM	PM
				0.25	0.2	0.1	0.19	5.84
				0.3	0.2	0.12	0.23	7.004

				0.36	0.2	0.144	0.28	8.405
				0.4	0.2	0.16	0.31	9.34
				0.45	0.2	0.18	0.35	10.51
				0.5	0.2	0.2	0.39	11.67
				0.55	0.2	0.22	0.43	12.84
				0.6	0.2	0.24	0.47	14.01
				0.65	0.2	0.26	0.51	15.18
				0.7	0.2	0.28	0.54	16.34
				0.75	0.2	0.3	0.58	17.51
				0.8	0.2	0.32	0.62	18.68
				0.85	0.2	0.34	0.66	19.85
				0.9	0.2	0.36	0.7	21.01
				1	0.2	0.4	0.78	23.35
WIND SPEED 4	7	w= 35	h	r=0.2	area	TM	PM	
				0.25	0.2	0.1	0.26	9.27
				0.3	0.2	0.12	0.32	11.12
				0.36	0.2	0.144	0.38	13.35
				0.4	0.2	0.16	0.42	14.83
				0.45	0.2	0.18	0.48	16.68
				0.5	0.2	0.2	0.53	18.54
				0.55	0.2	0.22	0.58	20.39
				0.6	0.2	0.24	0.64	22.25
				0.65	0.2	0.26	0.69	24.1
				0.7	0.2	0.28	0.74	25.95
				0.75	0.2	0.3	0.79	27.81
				0.8	0.2	0.32	0.85	29.66
				0.85	0.2	0.34	0.9	31.51
				0.9	0.2	0.36	0.95	33.37
				1	0.2	0.4	1.06	37.08

WSPID4	R	W	H	A	TM	PM
	0.05	80	0.5	0.05	0.011	0.86
	0.08	50	0.5	0.08	0.028	1.38
	0.11	36.36364	0.5	0.11	0.052	1.9
	0.14	28.57143	0.5	0.14	0.085	2.42
	0.17	23.52941	0.5	0.17	0.125	2.94
	0.2	20	0.5	0.2	0.173	3.46
	0.23	17.3913	0.5	0.23	0.229	3.98
	0.26	15.38462	0.5	0.26	0.292	4.5
	0.29	13.7931	0.5	0.29	0.364	5.02
	0.32	12.5	0.5	0.32	0.442	5.53
	0.35	11.42857	0.5	0.35	0.53	6.05

	0.38	10.52632		0.5	0.38	0.624	6.57
	0.41	9.756098		0.5	0.41	0.727	7.09
	0.44	9.090909		0.5	0.44	0.837	7.61
	0.47	8.510638		0.5	0.47	0.955	8.13
	R	W=3/M		H	A	TM	PM
	0.05	60		0.5	0.05	0.006	0.36
	0.08	37.5		0.5	0.08	0.016	0.58
	0.11	27.27273		0.5	0.11	0.029	0.8
	0.14	21.42857		0.5	0.14	0.048	1.02
	0.17	17.64706		0.5	0.17	0.07	1.24
	0.2	15		0.5	0.2	0.097	1.46
	0.23	13.04348		0.5	0.23	0.129	1.68
	0.26	11.53846		0.5	0.26	0.164	1.9
	0.29	10.34483		0.5	0.29	0.205	2.12
	0.32	9.375		0.5	0.32	0.249	2.34
	0.35	8.571429		0.5	0.35	0.298	2.55
	0.38	7.894737		0.5	0.38	0.351	2.77
	0.41	7.317073		0.5	0.41	0.409	2.99
	0.44	6.818182		0.5	0.44	0.471	3.21
	0.47	6.382979		0.5	0.47	0.537	3.43
	R	W=5/M		H	A	TM	PM
	0.05	100		0.5	0.05	0.017	1.69
	0.08	62.5		0.5	0.08	0.043	2.7
	0.11	45.45455		0.5	0.11	0.081	3.72
	0.14	35.71429		0.5	0.14	0.132	4.73
	0.17	29.41176		0.5	0.17	0.195	5.74
	0.2	25		0.5	0.2	0.27	6.76
	0.23	21.73913		0.5	0.23	0.357	7.77
	0.26	19.23077		0.5	0.26	0.457	8.78
	0.29	17.24138		0.5	0.29	0.568	9.8
	0.32	15.625		0.5	0.32	0.691	10.81
	0.35	14.28571		0.5	0.35	0.828	11.82
	0.38	13.15789		0.5	0.38	0.976	12.84
	0.41	12.19512		0.5	0.41	1.136	13.85
	0.44	11.36364		0.5	0.44	1.308	14.86
	0.47	10.6383		0.5	0.47	1.492	15.88
	R	W=2/M		H	A	TM	PM
	0.05	40		0.5	0.05	0.002	0.11

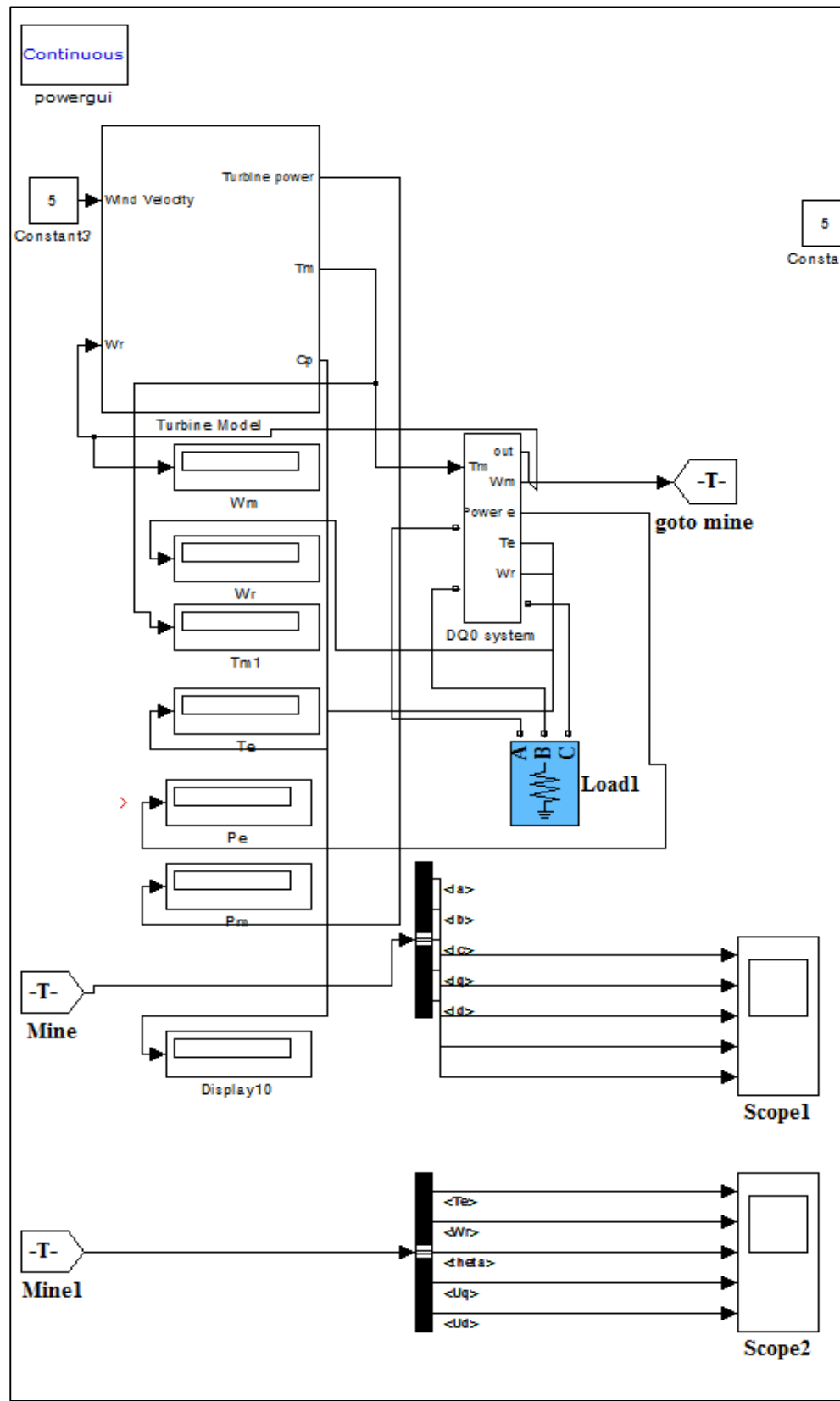
	0.08	25		0.5	0.08	0.007	0.17
	0.11	18.18182		0.5	0.11	0.013	0.24
	0.14	14.28571		0.5	0.14	0.021	0.3
	0.17	11.76471		0.5	0.17	0.031	0.37
	0.2	10		0.5	0.2	0.043	0.43
	0.23	8.695652		0.5	0.23	0.057	0.5
	0.26	7.692308		0.5	0.26	0.073	0.56
	0.29	6.896552		0.5	0.29	0.09	0.63
	0.32	6.25		0.5	0.32	0.11	0.69
	0.35	5.714286		0.5	0.35	0.13	0.76
	0.38	5.263158		0.5	0.38	0.16	0.82
	0.41	4.878049		0.5	0.41	0.18	0.89
	0.44	4.545455		0.5	0.44	0.21	0.95
	0.47	4.255319		0.5	0.47	0.24	1.02
R	W=6/M	H	A	TM	PM		
	0.05	120		0.5	0.05	0.02	2.92
	0.08	75		0.5	0.08	0.06	4.67
	0.11	54.54545		0.5	0.11	0.12	6.42
	0.14	42.85714		0.5	0.14	0.19	8.17
	0.17	35.29412		0.5	0.17	0.28	9.92
	0.2	30		0.5	0.2	0.39	11.67
	0.23	26.08696		0.5	0.23	0.51	13.43
	0.26	23.07692		0.5	0.26	0.66	15.18
	0.29	20.68966		0.5	0.29	0.82	16.93
	0.32	18.75		0.5	0.32	1.006	18.68
	0.35	17.14286		0.5	0.35	1.19	20.43
	0.38	15.78947		0.5	0.38	1.41	22.18
	0.41	14.63415		0.5	0.41	1.64	23.93
	0.44	13.63636		0.5	0.44	1.88	25.68
	0.47	12.76596		0.5	0.47	2.15	27.43
R	W=7/M	H	A	TM	PM		
	0.05	140		0.5	0.05	0.03	4.64
	0.08	87.5		0.5	0.08	0.08	7.42
	0.11	63.63636		0.5	0.11	0.16	10.2
	0.14	50		0.5	0.14	0.26	12.98
	0.17	41.17647		0.5	0.17	0.38	15.76
	0.2	35		0.5	0.2	0.53	18.54
	0.23	30.43478		0.5	0.23	0.7	21.32
	0.26	26.92308		0.5	0.26	0.9	24.1
	0.29	24.13793		0.5	0.29	1.11	26.88

	0.32	21.875		0.5	0.32	1.36	29.66
	0.35	20		0.5	0.35	1.62	32.44
	0.38	18.42105		0.5	0.38	1.91	35.22
	0.41	17.07317		0.5	0.41	2.23	38
	0.44	15.90909		0.5	0.44	2.56	40.78
	0.47	14.89362		0.5	0.47	2.93	43.56

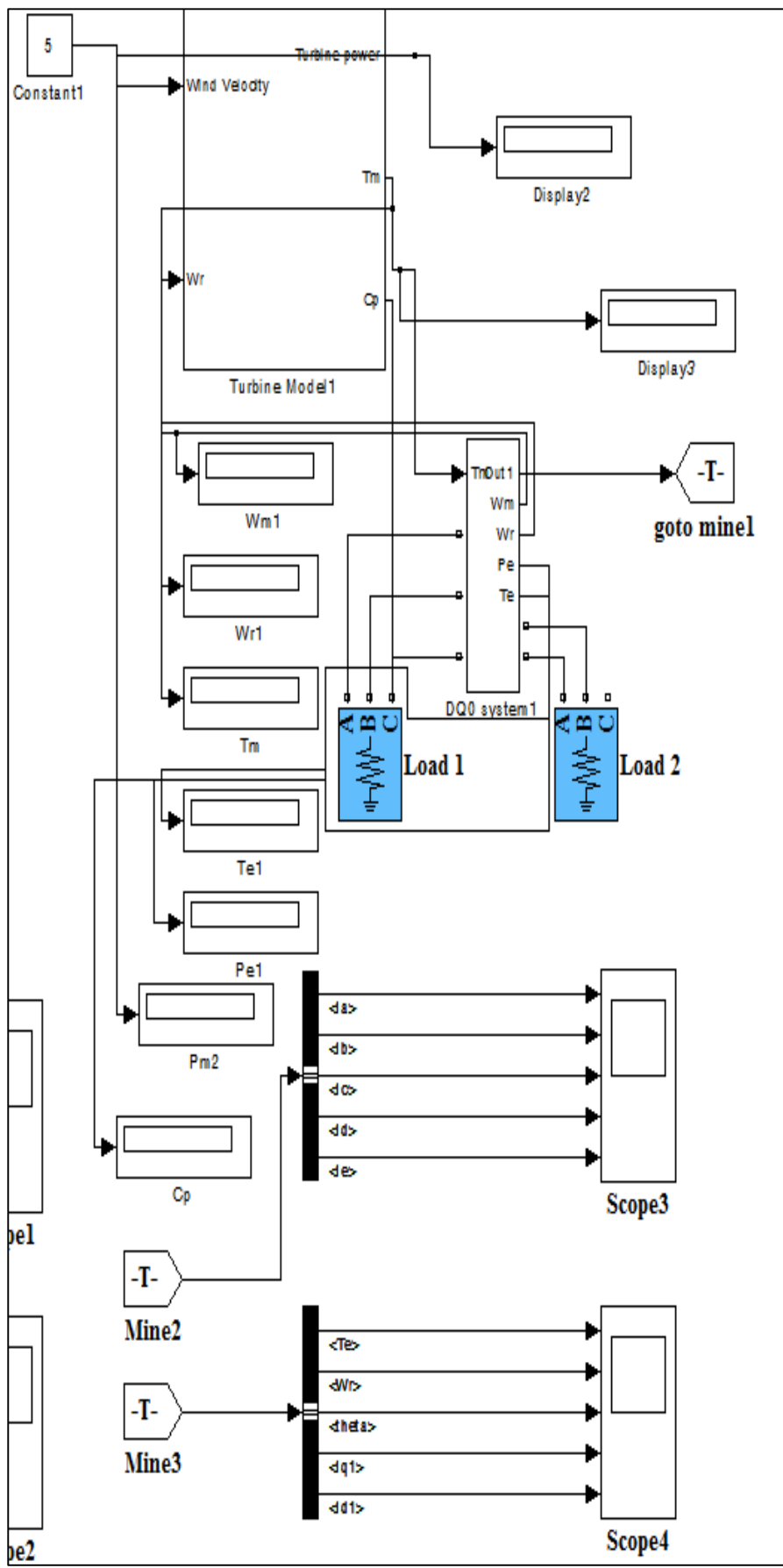
Figure 3.12

Following is the detailed zoom in 3 parts of Figure 3.12 in the Methodology Chapter

Part 1



Part 2



Part 3

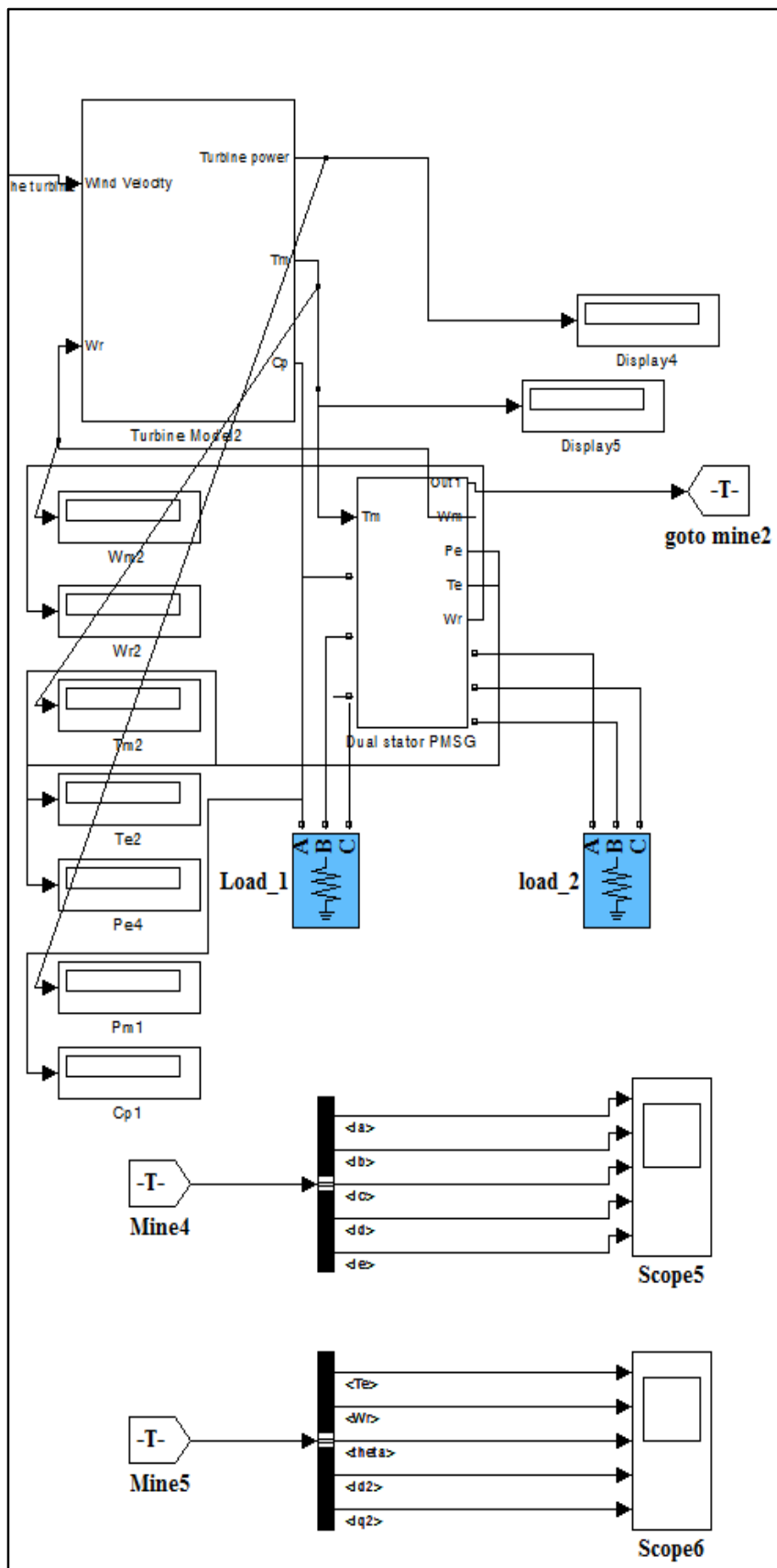
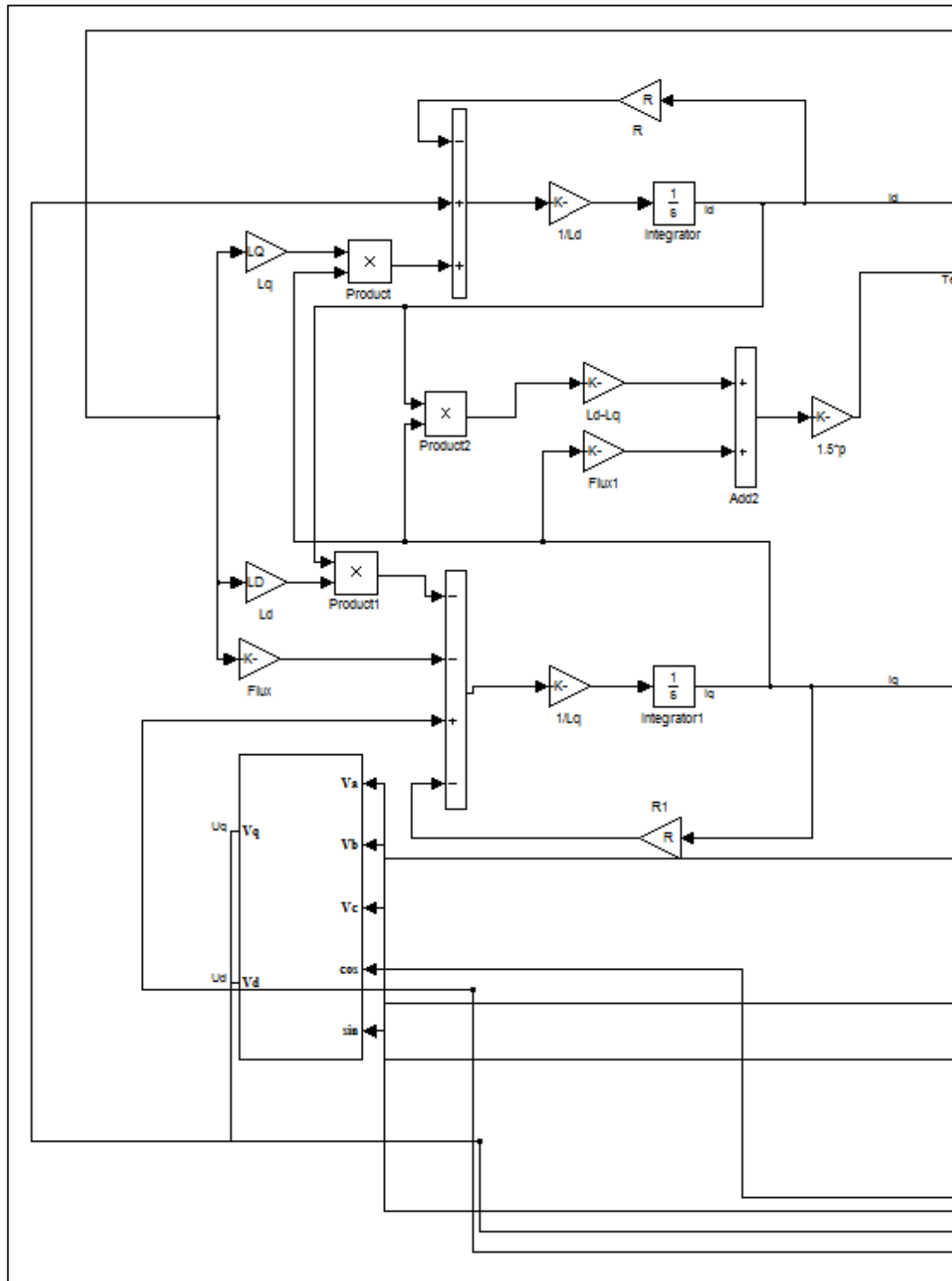


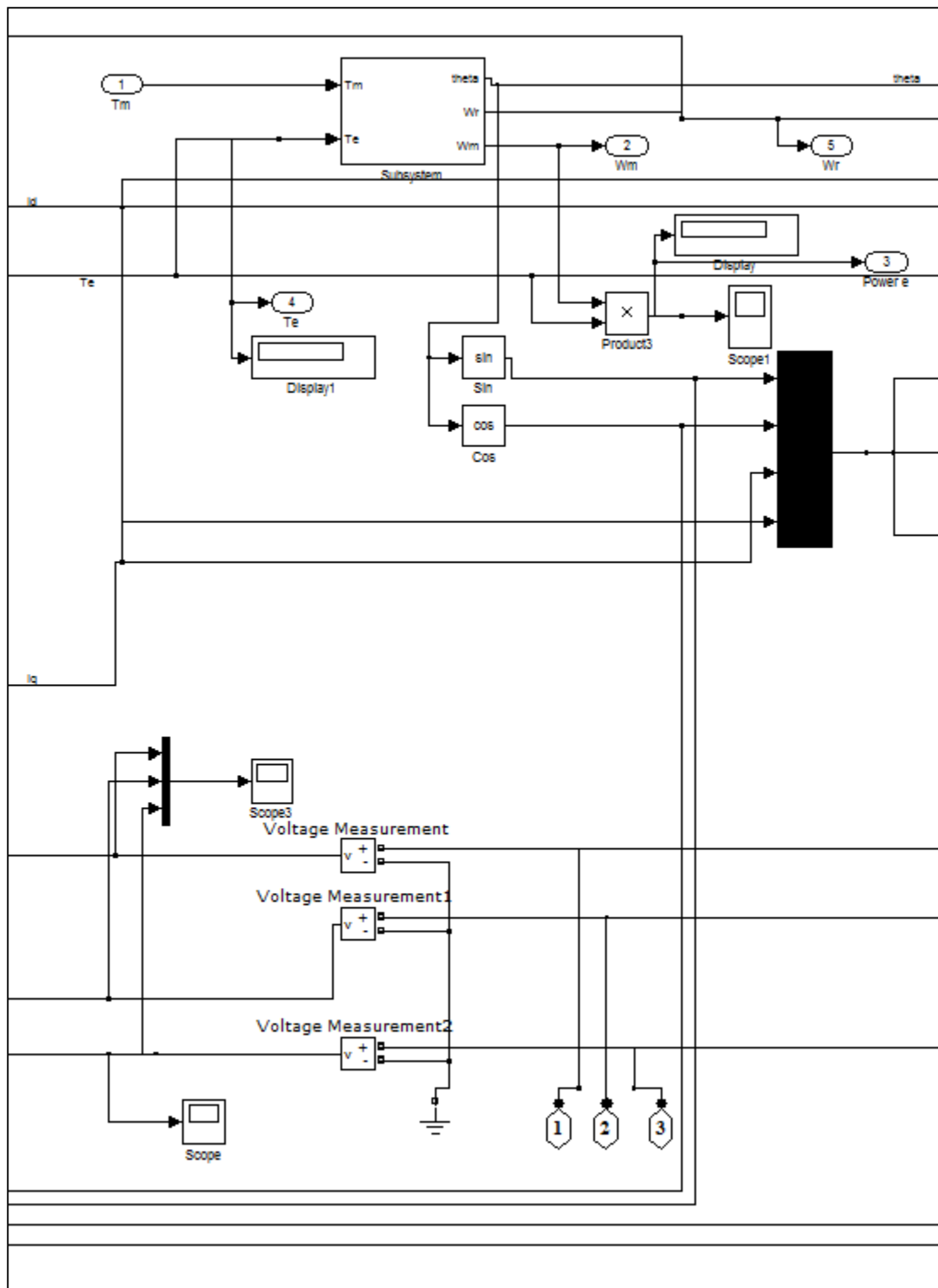
Figure 1.13- 3 Phase PMSG:

Following is the detailed zoom in 3 parts of Figure 3.13 in the Methodology Chapter

Part 1



Part 2



Part 3

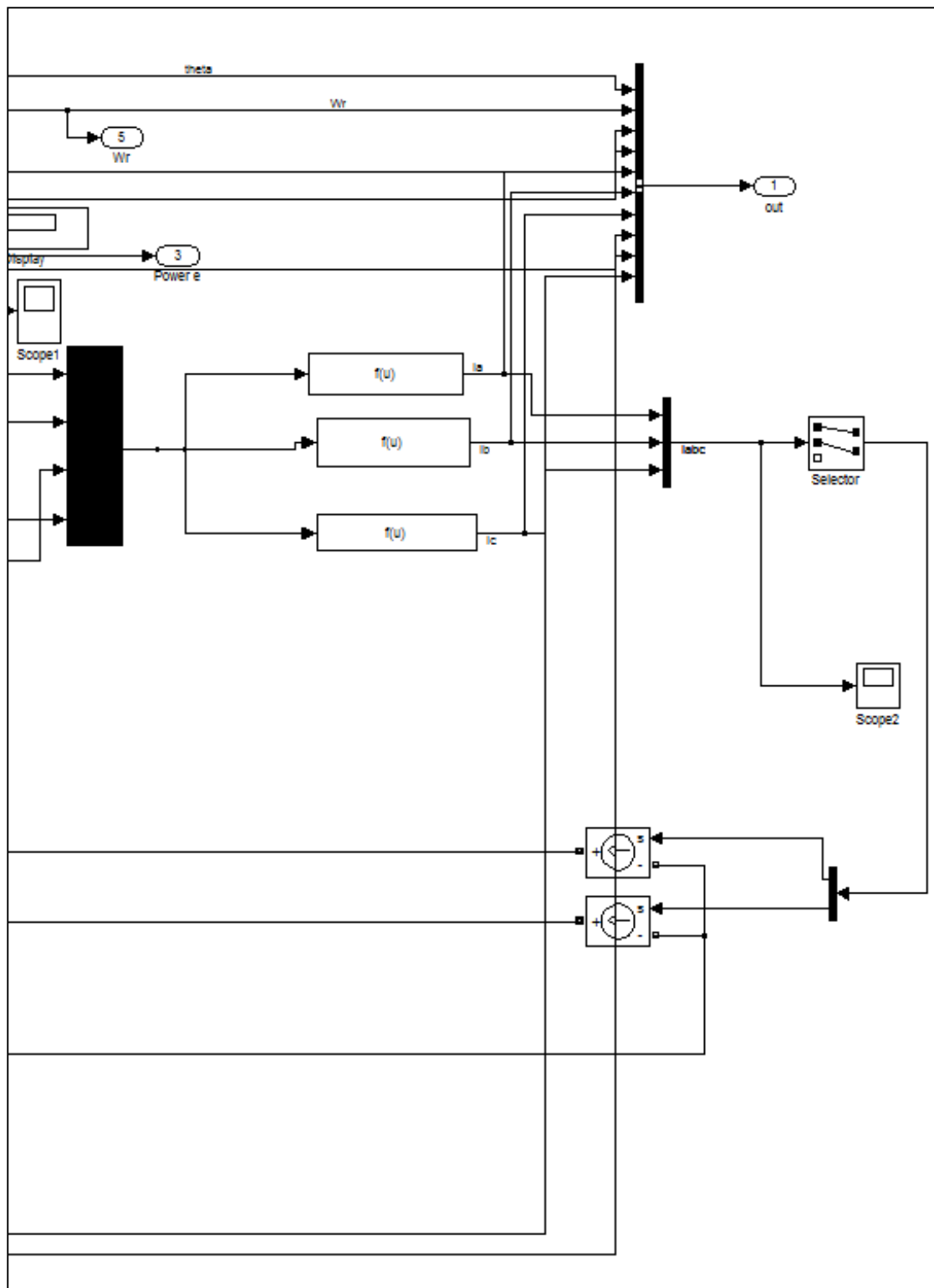
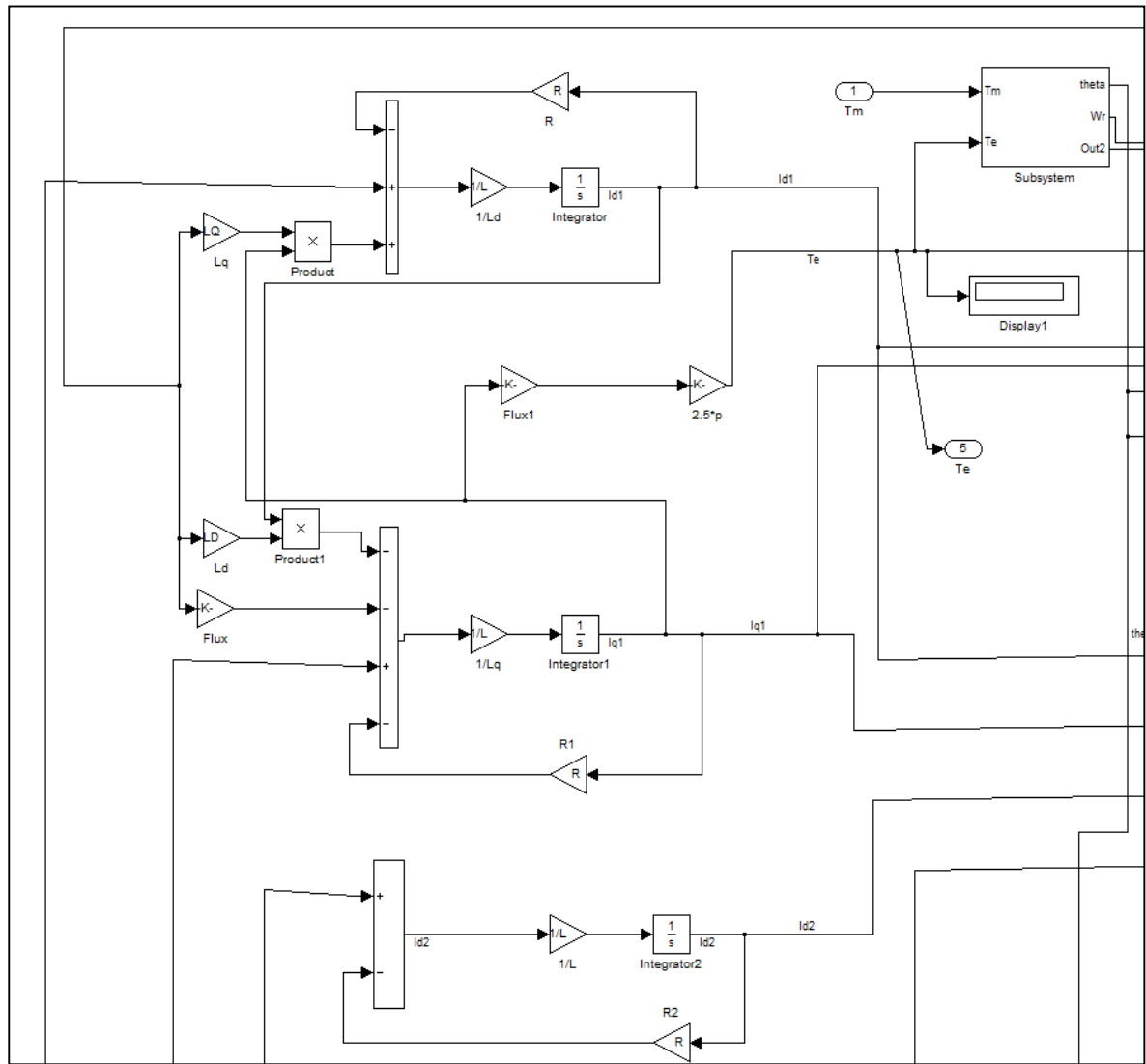


Figure 1.14- 5 Phase PMSG:

Following is the detailed zoom in 2 parts of Figure 3.14 in the Methodology Chapter

Part 1



Part 2

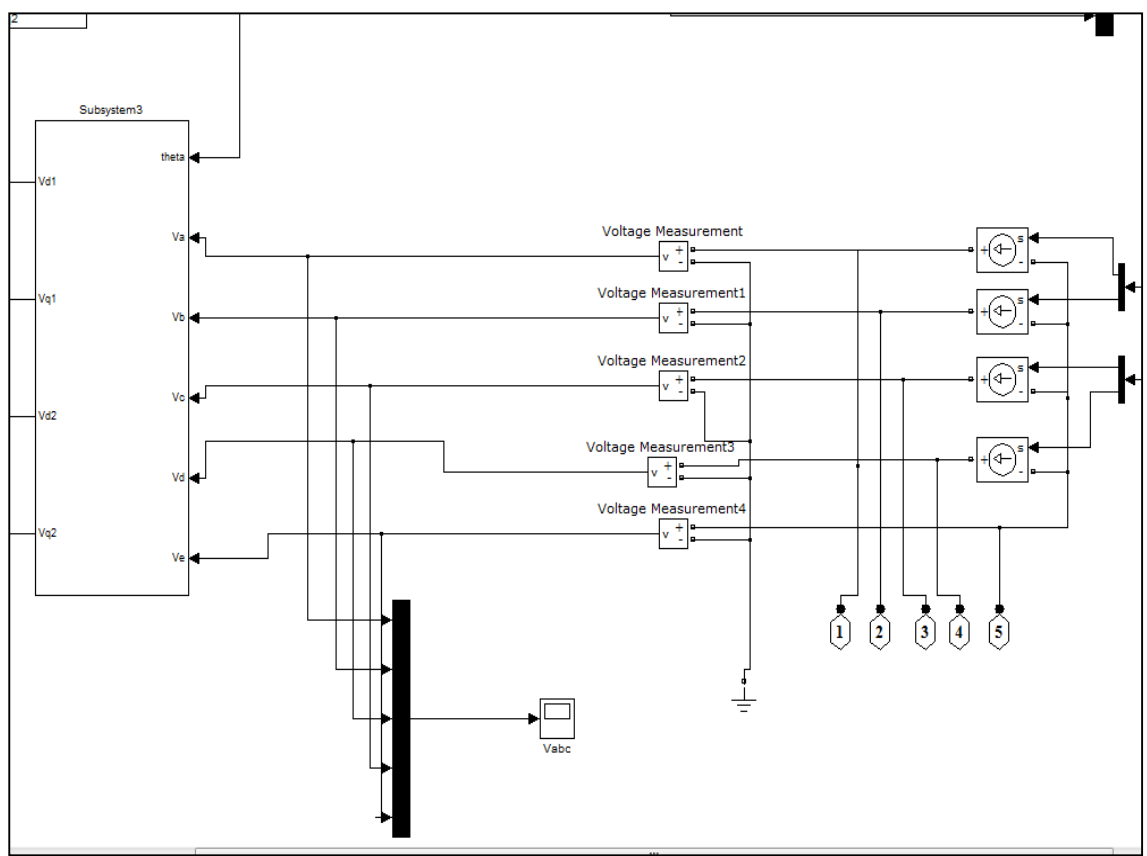
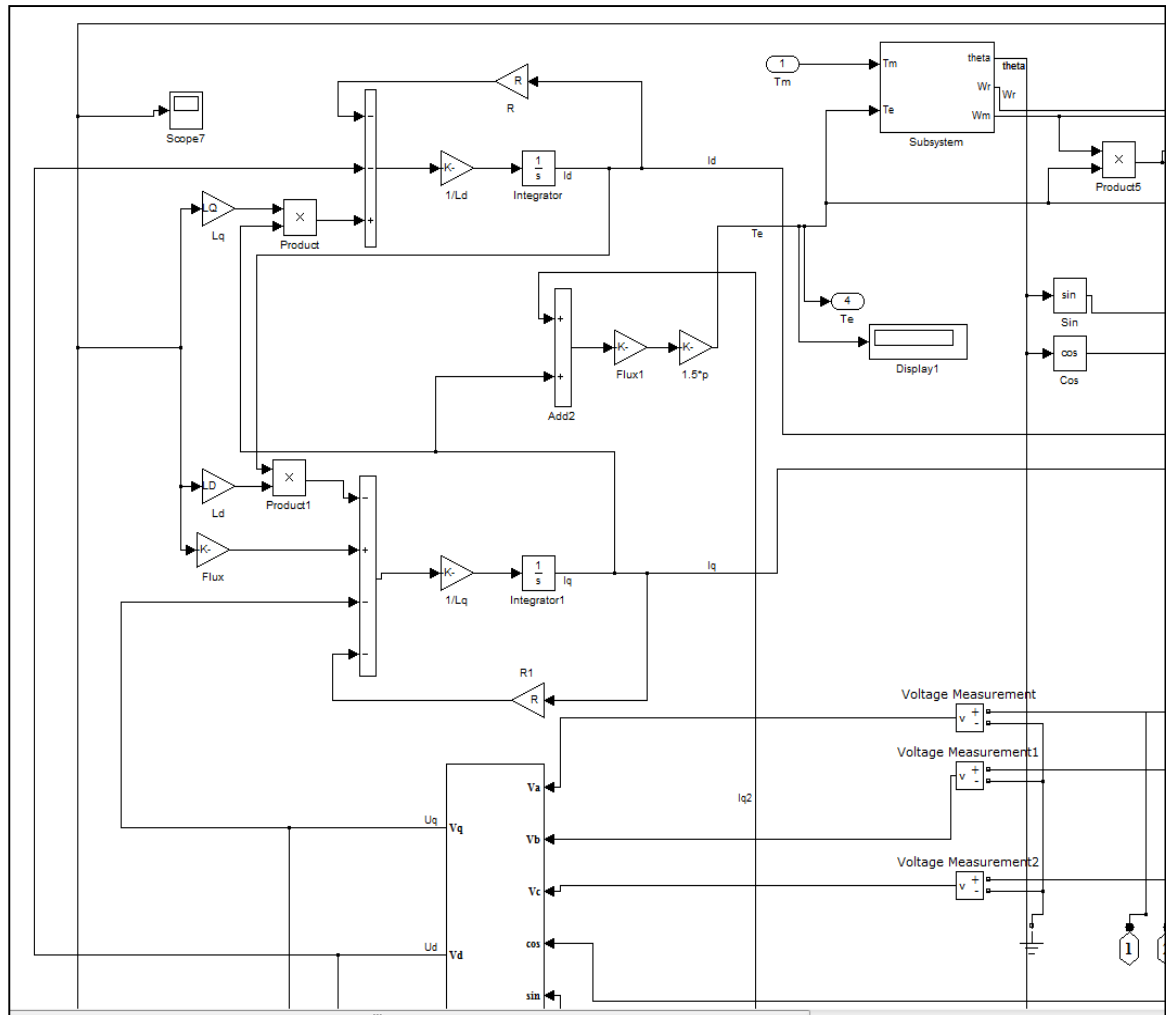


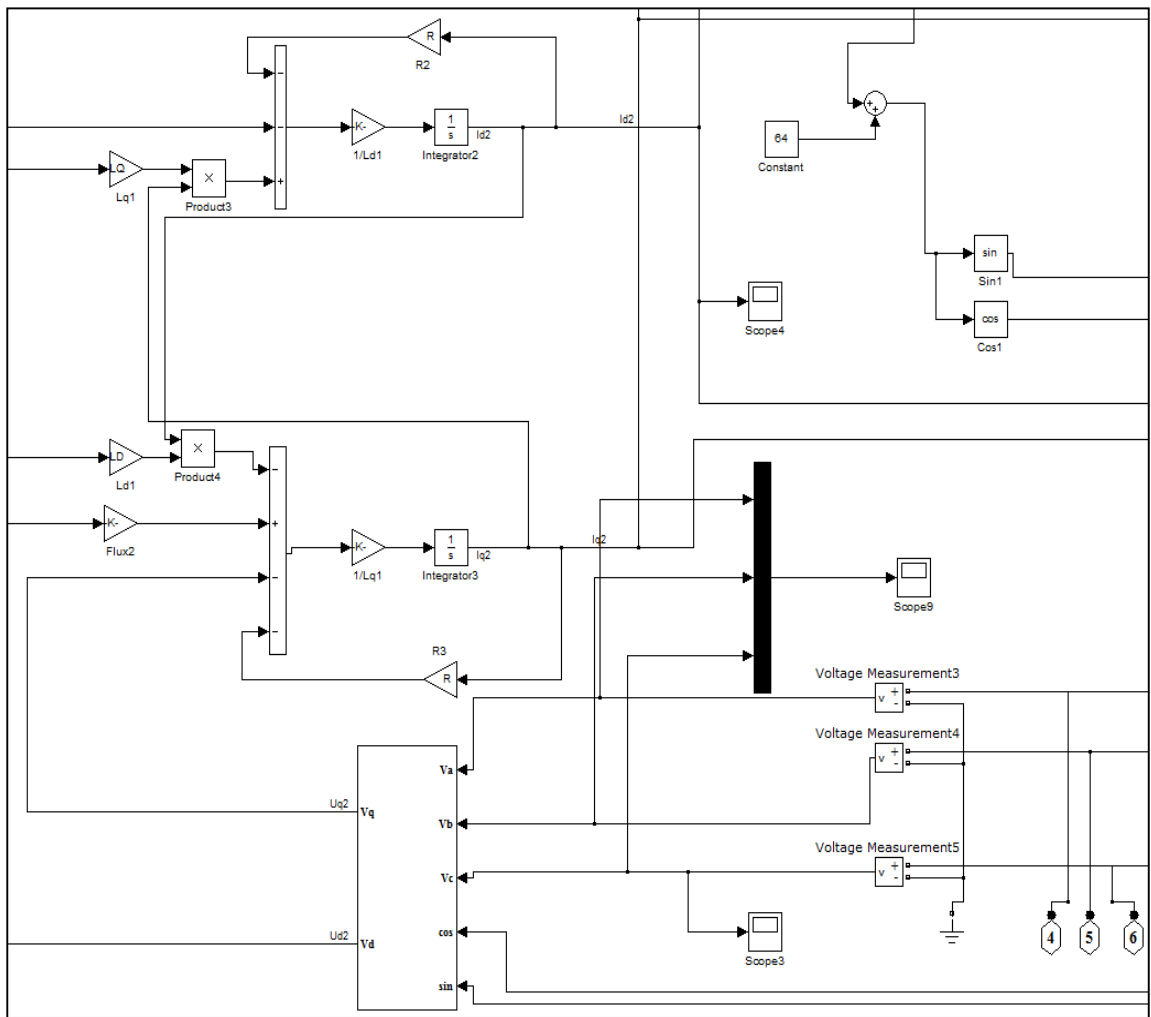
Figure 1.15- Dual Stator PMSG:

Following is the detailed zoom in 3 parts of Figure 3.15 in the Methodology Chapter

Part 1



Part 2



Part 3

